Determination of biotic and abiotic factors influencing soil structure development in a riparian system based on observational and experimental approaches

Inaugural-Dissertation
to obtain the academic degree
Doctor of Philosophy (Ph.D)
in River science
submitted to the Department of Biology, Chemistry and Pharmacy
of Freie Universität Berlin

by

ULFAH MARDHIAH

2014

This work was carried out between 2011 and 2014 under the supervision of Prof. Dr. Matthias C. Rillig in the Institute of Biology at Freie Universität Berlin, Germany, under an Erasmus Mundus Joint Doctorate Programme: Science for MAnagement of Rivers and their Tidal systems (SMART).

Supervisor: Prof. Dr. Matthias C. Rillig
Co-supervisors: Prof. Angela Gurnell
Dr. Tancredi Caruso

1st reviewer: Univ. - Prof. Dr. Matthias C. Rillig
2nd reviewer: Univ. - Prof. Dr. Klement Tockner

Date of defense: 05.03.2015

BERLIN 2014

FOREWORD

This dissertation is a cumulative work of manuscripts, either published or ready for submission from my publication list. This thesis is based on the following papers:

I. Mardhiah, U., Rillig, M.C., Gurnell, A., 2014. Reconstructing the development of sampled sites on fluvial island surfaces of the Tagliamento River, Italy, from historical sources. Earth Surface Processes and Landforms (in press).

II. Mardhiah, U., Caruso, T., Gurnell, A., Rillig, M.C., 2014. Just a matter of time: fungi and roots significantly and rapidly aggregate soil over four decades along the Tagliamento River, NE Italy. Soil Biology & Biochemistry 75: 133-142.

III. Mardhiah, U., Caruso, T., Gurnell, A., Rillig, M.C. Root and arbuscular mycorrhizal fungal hyphae contrasting effect on surface soil flow erosion: a greenhouse experiment.

ACKNOWLEDGMENTS

I'd like to thank the many nemeses of my life, but I'll keep it short (enough) as followings.

First of all, I would like to thank Prof Matthias Rillig for being my mentor and supervisor throughout these three years. Apparently, tough love is one of the best recipes to finish a PhD!

Second, I would like to send my gratitude for Prof Angela Gurnell, not just for being a great teacher, but also those time driving down in Italy mountainside during snowy and sunny days, sampling and shoveling for samples in the ground, sieving soil in the backyard, then spending the evening with heart warming food and conversations. You are so awesome.

Third, I thank Dr Tancredi Caruso who mentored me while working on the first manuscript and helped me a lot to gain academic related skills I never had before. Your moral support and trust was also one of the thing which helped me go through this whole process.

I am also grateful for the fellow lab mates and technicians in Rillig lab, especially Kriszta Valyi, Weishuang Zheng, Anika Lehmann, Dongwei Wang, Erik Verbruggen, Stavros Veresoglou, Kathryn Morris, Almut Scholtysik, Jana Mazukatow, Carlos Aguilar, Josef Kohler, Gabriele Erzigkeit, Sabine Artelt, Sabine Buchert not just for teaching me many techniques I required to go through this PhD, but also for being such awesome friends to talk to.

I am also grateful for fellow SMART PhD students, especially Prima Sekarsari, Roshni Arora, Matthew Cashman, Jean-Philippe Belliard, Simone Zen, Marco Redolfi, James Holloway, Alejandra Garcia Lugo, Francesca Pilotto, Cagri Cokdemir and Hossein Mohajeri. Thank you for sharing your skill and knowledge (Simone and Marco!), bunch of

laughter and dinners and movies and birthday celebrations, and also those days under the sun, trying to avoid work talk as best as we could (and failed) while having lunch break just beside the canal in Queen Mary's. You guys are the best. I'm gonna miss you all.

Last but not least, I would like to say thank you to the following people:

Vera Peters, thank you for sharing the first toast with me!

Anika Lehmann, for translating the summary chapter to German in a matter of hours!

My best buddies, Dian Handiani, Yusuf Pratama and Aneta Takhtamysheva. You guys have no idea how great it is to spend hours talking about anything with all of you.

My hard working partner, Rizki Rahadiyan. You have been an amazing source of energy throughout this year. Thank you for being funny, kind and patient. I'll see you soon.

My cool sister, Hanifah Siregar. More than a sister, you are one amazing buddy and a fellow fan girl of all things we love. Thanks for Figure 1 in chapter 4! Can't wait to fangirling again, together!

Susanty Z. Tamin and Rizal Siregar, my parents, to whom I dedicate this dissertation. I'm sorry I have been so busy these last few months. Thank you for everything. Including for always trusting your daughters to do whatever they want to do in life. It's funny how I ended up working on a similar topic as yours, Dad (you already knew the outcome of my work just based on years of first hand experience).

Too bad I can't include all the pop culture which contributed a lot to maintain sanity during these three years. But I have to wrap up.

This work started with a Bismillah, and I am glad to finally able to say, Alhamdulillah.

TABLE OF CONTENTS

FOREWORD i

ACKNOWLEDGMENTS ii

LIST OF TABLES v

LIST OF FIGURES viii

CHAPTER I. General Introduction 1

CHAPTER II. Soil development on fluvial islands: combining information from historical sources, field measurements and laboratory analyses 7

CHAPTER III. Just a matter of time: fungi and roots significantly and rapidly aggregate soil over four decades along the Tagliamento River, NE Italy. 62

CHAPTER IV. Root and arbuscular mycorrhizal hyphae contrasting effect on surface soil flow erosion: a greenhouse experiment 104

CHAPTER V. Summary 148

CHAPTER VI. Zusammenfassung 152

BIBLIOGRAPHIC REFERENCES 157

CONTRIBUTIONS TO PUBLICATIONS 164

APPENDIX A Supplementary Material to Chapter III 165

APPENDIX B Supplementary Material to Chapter IV 179

APPENDIX C Preliminary data set for a meta-analysis study 188

LIST OF TABLES

Table II. 1. Aerial image dates, types and sources used in the research 18

Table II. 2. Kruskal Wallis tests on % mature vegetation cover, % sparse vegetation cover and % unvegetated area estimates at all sample locations across the twelve image dates within each of the 2, 8, 12 and 40 year areas. 34

Table III.1. Linear models for each of the measured variables as a function of soil age. 78

Table III. 2. Linear models to test the effect of Soil Structure determinants on soil structural parameter. 85

Table III. S1. Linear model to test the response of soil aggregate size class 2-4 mm to soil structure determinants. 165

Table III. S2. Linear modelto test the response of soil aggregate size class 1-2 mm to soil structure determinants. 166

Table III. S3. Linear model to test the response of soil aggregate size class 0.5-1 mm to soil structure determinants. 167

Table III. S4. Linear model to test the response of soil aggregate size class 0.2-0.5 mm to soil structure determinants. 168

Table III. S5. Linear model to test the response of soil structure index, percent total WSA, to soil structure determinants. 169

Table III. S6. Linear model to test the response of soil structure index, MWD, to soil structure determinants. 170

Table III. S7. Linear model to test the response of soil structure index, fractal 171

dimension, to soil structure determinants.

Table III. S8. Correlation test results, based on the Pearson's product moment correlation test between all explanatory variables of soil structure determinants and three soil structure indices.. 172

Table III. S9. Principal Components Analysis (PCA) of soil aggregate-size classes, soil structure indices, and soil structure determinant. 174

Table IV. 1. Linear model to test the response of soil detachment rate (TS1, TS2 and TS3) through time (R1, R2, R3, R4 and R5) for each treatment. 120

Table IV. 2. Kruskal Wallis test to test the differences of treatment groups of several variables assumed to explain the variances of the soil detachment rates. 126

Table IV. 3. Linear model to test the response of soil detachment rate to soil detachment rate determinants PC1 and PC2 used as main effect. 133

Table IV. S1. Kruskal Wallis test to test the differences of soil detachment rates for each treatments at each time point. 181

Table IV. S2.a. Linear model to test the response of soil detachment rate to each of the soil detachment rate determinants used as the main effect. 182

Table IV. S2.b. Linear model to test the response of soil detachment rate to all soil detachment rate determinants used as the main effect. 183

Table IV. S3. Correlation test results based on the Pearson's product moment correlation test between all explanatory variables of soil detachment rate determinants as main effect. 185

Table IV. S4. Principal Components Analysis (PCA) of soil detachment rateand soil detachment rate determinants 186

Table S1. Overview of search engine results from data collection step for a meta-analysis investigating the potential of riparian system to store carbon. 188

Table S2. Extracted values and data from papers generated from Google scholar search to investigate the potential of riparian system in storing carbon. 189

LIST OF FIGURES

Figure II. 1. The study reach photograph (2005) and patches sampled 14

Figure II. 2. Islands at different development stages within the study reach. 15

Figure II . 3. Mean daily river water levels at the Villuzza gauge, 1982-2011. 27

Figure II. 4. Oblique photographs of a part of the study reach. 29

Figure II. 5. Dot plots illustrating the percentage cover of mature vegetation, sparse vegetation and unvegetated areas estimated from aerial images collected in 2003. 32

Figure II. 6. Dot plots illustrating the percentage cover of mature vegetation, sparse vegetation and unvegetated areas around sampling sites in the 40 year area. 37

Figure II. 7. Dot plots illustrating the percentage cover of mature vegetation, sparse vegetation and unvegetated areas around sampling sites in the 12 year area. 39

Figure II. 8. Dot plots illustrating the percentage cover of mature vegetation, sparse vegetation and unvegetated areas around sampling sites in the 8 year area. 41

Figure II. 9. Dot plots illustrating the percentage cover of mature vegetation, sparse vegetation and unvegetated areasaround sampling sites in the 2 year area. 43

Figure II. 10. Boxplots of the percentage of total nitrogen, total organic carbon , and mean weight diameter of sediment samples. 46

Figure III. 1. The study reach, Tagliamento River, Italy, photographed on 23 May 2005 locating the sampling patches within the sites of different age. 72

Figure III. 2. Response of four soil structure indices to soil age using linear models. 77

Figure III. 3. Biplots showing variable vectors and samples following Principal Components analysis (PCA) for two soil structure indices and one soil structure determinants. 84

Figure III. 4. The first two principal component analysis axes of the PCA of soil structure are used as predictor of size classes (first principal component axes (PC1) and second principal component axes (PC2)) and soil structure (PC1) indices. 87

Figure III. S1. Response of three soil aggregation indices to soil age using linear models. 176

Figure III. S2. Response of nine soil structure determinants to soil age using linear models. 177

Figure III. S3. Variogram and bubble plot showing spatial autocorrelation. 178

Figure IV. 1. Image of hydraulic flume used to measure soil detachment rates of surface soil samples. 113

Figure IV. 2. Linear model used to plot accumulative soil detachment rate through time for different treatments. 123

Figure IV. 3. Boxplots showing soil detachment rate through time from nine experiment treatments. 125

Figure IV. 4. Boxplots showing four variables responsible for explaining soil detachment rate of four levels of treatment. 127

Figure IV. 5. Linear model correlating soil detachment rate to two explanatory 129

variables.

Figure IV. 6. Biplots showing variable vectors and samples following Principal Components analysis (PCA) for soil detachment rate determinants and soil detachment rate. 132

Figure IV. 7. Linear model correlating two soil detachment rate determinants PC axis to soil detachment rate axis. 134

Figure IV. 8. Linear model correlating six soil detachment rate with soil detachment rate determinants (PC2). 135

Figure IV. S1. L inear model correlating soil detachment rate to four explanatory variables. 179

CHAPTER 1

General Introduction

Riparian system: the example of the pristine Tagliamento River

Fluvial riparian systems in their present state have been highly negatively influenced by human activities. These activities include ground water mining, stream flow diversion, damming, the establishment of physical barriers like dikes and levees which separate channels from the floodplain, harvest of fuel wood, overgrazing and conversions of floodplain into urban or agricultural areas (Stromberg, 2001; Ward *et al*., 2002; Toner and Keddy, 1997). Riparian systems are known for their high biodiversity (Arscott et al., 2000; Tockner and Stanford, 2002; Ward et al., 2002; Naiman *et al*., 1993) due to interactions with the spatial and temporal heterogeneity of the various hydrogeomorphological processes. Its dynamics involve endurance against various natural disturbances related to the geomorphology and the hydrology of the system (Junk *et al*., 1989, Naiman and Decamps, 1997; Tabacchi *et al*., 1998). The various river engineering activities and land conversion resulted in reduced stream water flow, plummeting of ground-water table, increased salinity, decrease sediment input and in the end, decreased biodiversity due to the reduced micro-habitat variability and also introduction of exotic species just to mention a few (Stromberg, 2001; Tockner and Stanford, 2002). Considering the importance of the system for disturbance regulations, water supply and waste treatment (Tockner and Stanford, 2002), this rate of decline is alarming and highlights the importance of restoring riparian systems to their natural state.

One type of landform within fluvial riparian ecosystem are fluvial islands, which are a landform elevated above and surrounded by stream-channel branches or waterways that persist sufficiently long to establish permanent vegetation (Osterkamp, 1998). This landform is in constant change, formed by avulsion, rapid and gradual channel incision, channel migration, dissection of bed sediment, deposition of bed sediment on a vegetated surface or behind a channel obstruction (Osterkamp, 1998; Gurnell *et al*., 2001; Ward *et al*., 2002). Currently more attention is given to understanding the importance of vegetative sprouting initiating island formation (Gurnell and Petts, 2002). Although it can also be found in regulated river systems, in general this landform is a signature of river system in their natural state (Gurnell and Petts, 2002). They can be stable over decadal or century times (Wyrick and Klingeman, 2011) but due to high-energy conditions this state is not permanent (Osterkamp, 1998). Islands can support biodiversity and habitat complexity (Wyrick and Klingeman, 2011) by acting as a moderator of ecological processes including influencing temperature and light regimes, producing organic detritus, routing water and sediment, structuring the physical habitat and also providing substrate for biological activities (Ward *et al*., 2002).

Our study area focused on the Flagogna reach in the pristine Tagliamento River, NE Italy. The river is identified as the last morphologically intact river corridor in the Alps, arises in the limestone Alps of northern Italy and flows 172 km into the Adriatic Sea (Ward, 1999; Tockner *et al*., 2003). The climate is alpine in the headwaters and mediterranean in the lower reaches causing a flashy flow regime (Bertoldi *et al*., 2009). The active floodplain is up to 2 km and contains numerous vegetated islands (Ward *et al*., 2002). The varied

landscape in this river, including islands, shows high turnover (ca. 30% in 3-5 years) although the relative composition of the landscape elements remain relatively constant (Edwards *et al*., 1999; Kollmann *et al*., 1999; Tockner *et al*., 2003). The river has riparian woodland bordering most of its course and encompasses reaches with patches of riparian shrubs and trees of varying size and age (Bertoldi *et al*., 2009). Along our study reach, the dominant riparian tree species is the black poplar (*Populus nigra)* although other species can also be found including *Salix alba, Salix daphnoides, Salix elaeagnos, Salix purpurea* and *Salix triandra* (Karrenberg *et al*., 2003). Black poplar usually serves as nucleation site for fluvial island development within this reach (Francis *et al*., 2008).

Soil structure development in fluvial islands

The main goal of this thesis is to understand how soil structure developed within a natural river system under high disturbances as is the case for the Tagliamento river. We would also like to understand what variables support soil structure development. This will help us to understand the system better especially in terms of dealing with plans for river management and rehabilitation.

Soil structure is developed through the arrangement of primary soil particles into secondary units or soil aggregates (Soil Science of America, 2008). Soil structure is important in reducing erosion (Barthes *et al*., 2000; Bryan, 2000; Gyssels *et al*., 2005) and also in maintaining soil porosity (Angers and Caron, 1998), gas exchange (Smith *et al*., 2000) and water infiltration (Bronick and Lal, 2005). Most studies focused on the development of soil structure in agricultural system, but less is known on its dynamics along natural rivers

(Piotrowski *et al*., 2008; Harner *et al*., 2011). These functions are important to maintain vegetative growth which will then further enhance fluvial islands in natural river systems.

Biotic and abiotic factors supporting soil structure development

The development of soil structure is supported by various factors. Soil texture with higher clay content supports better soil structure development (Oades, 1993). Polysaccharides produced by microorganisms and plants, availability of multivalent cations, enmeshment of aggregates by plant roots and hyphae extended from fungi are important variables supporting soil structure development (Oades, 1984; Six *et al*., 2004). Arbuscular mycorrhizal fungi (AMF) has been shown to support the development of soil structure by physical enmeshment of soil particles using its extraradical hyphae (Chaudhary *et al*., 2009; Miller and Jastrow 1990; Rillig *et al*., 2002; Wilson *et al*., 2009; Barto *et al*., 2010). The importance of AMF and other biotic and abiotic variables in supporting soil structure has been studied for example in grassland sites in Germany (Barto *et al*., 2010) but the information on whether these variables play a role under natural setting such as natural river is still lacking. This will be the main topic of chapter 3 in this dissertation.

The role of belowground biomass in withstanding soil erosion

Natural rivers are always being subjected to various disturbances including eroding forces from flow and flood pulses (Bertoldi *et al*., 2009). Study of soil erosion in agricultural system has been mostly conducted for agricultural purposes, which limits the basic knowledge of how such process act in a natural setting (Bryan, 2000). The most thorough knowledge so far is on the role of aboveground biomass in reducing soil erosion (Gyssels *et*

al., 2005), meanwhile some work has been done to understand the relative importance of belowground biomass, focusing on the role of roots (Gyssels and Poesen, 2003; De Baets *et al*., 2006; De Baets *et al*., 2007). Microorganisms, as part of belowground biomass have only been so far assumed to play a role although never tested (Bryan, 2000). We therefore were interested in disentangling the role of belowground biomass, highlighting the role of AMF, microbial community and plant roots in enduring concentrated flow erosion which will be the focus of chapter 4 in this dissertation.

Thesis outline

In chapter 2 we will first focus on the historical development of fluvial islands of different age in Flagogna reach, Tagliamento River. This was done by combining several approaches, including collecting data from river stage records, oblique photographs, aerial images analysis and dendrochronology during field sampling. We will therefore use these data to precisely pinpoint positions of fluvial island nucleation sites after the dispersion of uprooted trees within the reach and to learn about the dynamics of the sites along a certain temporal sequence.

In chapter 3 we will focus on measuring the rate of soil structure development within each age group of fluvial islands within Flagogna reach, Tagliamento River. We will first place soil structure development within a temporal framework to see if there is significant development across different fluvial island ages. We will then ask what, if any, variables support soil structure development, by assessing various biotic and abiotic factors which are

known to support such development in other ecosystems.

In chapter 4, we will go in detail to analyze the level of importance of AMF in withstanding soil erosion which is one of the disturbance factor endured in systems like Flagogna reach, Tagliamento river. We approached this with an extreme simplification of the system, by setting up a greenhouse experiment and then testing the surface soil endurance against concentrated flow erosion and further disentangle the role of various belowground factors, focusing on plant roots, AMF extraradical hyphae and the microbial community.

In chapter 5, we will synthesize the overall results in a summary.

CHAPTER 2

Soil development on fluvial islands: combining information from historical sources, field measurements and laboratory analyses

Ulfah Mardhiah, Matthias C Rillig, Angela Gurnell

The following pre-print version (before peer reviewed) has been modified and accepted as:

Mardhiah, U., Rillig, M.C., Gurnell, A., 2014. Reconstructing the development of sampled sites on fluvial island surfaces of the Tagliamento River, Italy, from historical sources. Earth Surface Processes and Landforms (in press).

http://dx.doi.org/10.1002/esp.3658

Soil development on fluvial islands: combining information from historical sources, field measurements and laboratory analyses

Abstract

In high energy river systems, two opposing hypotheses can be proposed in relation to soil development on islands forming within the active channel. The first is that intense and frequent disturbance by floods and flow pulses may arrest or completely reset soil development on island surfaces as a result of island surface burial or erosion, such that no significant soil development is detectable, at least until island surfaces have aggraded to the level of the floodplain. The second is that as island surfaces aggrade vertically, inundation becomes less frequent and shear stresses experienced by island surfaces decrease, and so soil development proceeds steadily despite continuing disturbance through sediment deposition or removal.

The reported research investigates these two hypotheses on a reach of the Tagliamento River, Italy, using a combination of field sampling and laboratory analysis of island soils (0 - 10 cm depth from the soil surface); dendrochronological dating; and reconstruction of the history of sampled islands using information extracted from aerial and terrestrial images and river flow records.

A chronosequence of island surfaces (0, 2, 8, 12, 40 years from initiation of island development) was investigated. The age and history of island development was

reconstructed with confidence as a result of convergence of evidence from different historical and contemporary sources. Despite the highly disturbed environment of the study reach, three indicators of soil development (total nitrogen, total organic carbon, which are indicators of soil fertility; and mean weight diameter (MWD), which is an indicator of soil aggregation) were found to increase across the sampled chronosequence, with total nitrogen and MWD showing particularly clear and steady increases with island age. This supports the second hypothesis, illustrating that, despite the flashy flow regime of the river, and the historical sequence of bankfull floods, the process of soil development is sufficiently active to show a steady, statistically significant development trajectory across the 40 year period that was investigated.

Keywords:

Soil development, braided river, island development, fluvial processes.

Introduction

Naturally-formed river islands develop as the result of interactions between vegetation and fluvial processes within active river channels. Although wooded islands may be formed predominantly by other mechanisms in wetland systems where flow energy is negligible (Wetzel, 2002, 2005), in most fluvial systems, island formation involves the retention of fine sediment by vegetation and, according to the size, energy and environmental context of the river, this process can be initiated by living aquatic or riparian plants or by dead wood (Gurnell, 2014).

On low-energy systems, stands of emergent macrophytes may trap sediments to build mid-channel and lateral bars that eventually aggrade to the low flow water surface to form islands and benches (Gurnell et al., 2013, Liffen et al., 2013). For example, aquatic plants are fundamental to both bar and island development in the low-energy, anastomosing, Narew River, Poland (Gradzinski et al., 2003), although on other low energy systems, aquatic, riparian and even terrestrial plants appear to play a part (e.g. Gumbricht et al., 2004). However, on most fluvial systems, the process is driven by dead or living riparian vegetation, particularly trees.

Abbe and Montgomery (2003), Montgomery and Abbe (2006) and Collins et al. (2012) describe how large (dead) wood functions to drive landform development within the wandering Queets River, Washington, USA. Accumulations of very large wood pieces, mainly entire uprooted trees, accumulate into wood jams of a variety of morphological

types. These retain sediment and seeds and provide a relatively stable environment within the active river channel, where the seeds can germinate and grow to establish a vegetation cover across the wood jam surface. In this way, a range of morphological features including islands are formed and in many cases they attach and extend the floodplain. Large wood jams that become incorporated into the floodplain as 'hard spots' (Montgomery and Abbe, 2006), form exceedingly stable areas on which trees may develop to provide the oldest patches of trees within the riparian forest. Vegetation regeneration around dead wood to form small, pioneer islands (*sensu* Edwards et al., 1999) has been reported in other river systems, including the Sabie River, South Africa (Pettit and Naiman, 2006) and the ephemeral Kuiseb River, Namibia, Southwest Africa (Jacobson et al., 1999), and as a widespread phenomenon in rivers of the Pacific Northwest, USA (Fetherston et al., 1995).

Patches of tree seedlings and sprouting large wood can also initiate island development. As for example in the linear vegetated ridges observed on point bars in temperate rivers (e.g. McKenney et al., 1995), the multiple parallel linear islands that develop in some dryland anabranching rivers (e.g. Tooth and Nanson, 2000), and the dynamic mosaics of islands found within island-braided systems (e.g. Gurnell et al., 2001). Along island-braided segments of the Tagliamento River, Italy, a cycle of island development has been described, whereby uprooted trees are deposited on gravel bars; trap fine sediment, wood and seeds; and enlarge laterally and vertically to form pioneer islands. Vegetation development, sediment, wood and seed trapping continue so that the pioneer islands enlarge and coalesce to form building islands, which may eventually evolve into large established islands (Gurnell et al., 2001). This sequence of lateral and vertical aggradation, woody vegetation

development and island coalescence leads to the formation of islands of varying age which may eventually merge with the floodplain, or be dissected or removed by fluvial erosion.

As islands develop in all fluvial systems, they are subject to numerous fluvial disturbances but at the same time, interactions between vegetation and sediment may be expected to result in soil development on island surfaces. Here, surface soil development is considered to be the refinement of sediment texture and structure, and an increase in fertility status, which provides a matrix and material for various processes and interactions of different biotic and abiotic variables, and in turn can support vegetation growth (Oades, 1984). In high energy river systems, such as the Tagliamento, two opposing hypotheses can be proposed. The first is that intense and frequent disturbance by floods and flow pulses (Tockner et al., 2000) may arrest or completely reset soil development by burial or erosion of island surfaces, such that no significant soil development is detectable, at least until islands are fully established to the level of the floodplain. The second is that as island surfaces aggrade vertically, inundation becomes less frequent and shear stresses experienced by island surfaces decrease, and so soil development might be expected to proceed steadily despite continuing disturbance through sediment deposition or removal.

The aim of the present research is to test these two hypotheses by investigating island and associated soil development along a 3km island-braided reach of the Tagliamento River. The research combines analysis of historical (secondary) and contemporary (primary) field and laboratory data sets to:

(i) Identify broad areas of a river's active corridor where riparian vegetation colonisation appears to have been initiated by specific large flood events based on river flow records and oblique ground photographs.

(ii) Check the age of the areas using dendrochronology, and sample sediments within vegetated patches (pioneer, building and established islands) to investigate differences in surface sediment properties within and between areas of different age.

(iii) Undertake analysis of historical areal imagery to further establish the age of sampling locations and track historical changes in vegetation cover, within and between sampling areas.

(iv) Explore the degree to which the chronosequence of sampling areas shows evidence of changes in the fertility and structure of sampled surface sediments.

Methods

Study site

The study was conducted on a 3 km long, ca. 600m wide, island-braided reach (Figure II. 1) located at an elevation of 130 metres a.s.l. and between 79 and 81 km from the source of the gravel-bed Tagliamento River, Italy (Tockner et al., 2003), which flows ca. 170km from its source in the Alps to the Adriatic Sea. This Alpine to Mediterranean climatic context results in a flashy, pluvio-nival flow regime, with an average discharge of 90 $m^3.s^{-1}$ and a 5 year return period flood estimated to be 1600 $m^3.s^{-1}$ (Maione and Machne, 1982). The

flashy river flows interact with riparian vegetation and the gravel-sand sediments of the river's active channel and floodplain, to produce a highly dynamic mosaic of braid channels, braid bars and wooded islands, dominated by *Populus nigra* L., although willow species (*Salix alba* L., *S. daphnoides* Vill., *S. eleagnos* Scop., *S. purpurea* L, *S. triandra* .L), particularly *S. eleagnos*, are also abundant (Karrenberg *et al*. 2003). Vegetative regeneration, particularly from uprooted trees, deposited on gravel bars during floods, is an important process in the development of vegetated landforms along the river (Gurnell et al., 2001, 2005; Gurnell and Petts, 2006). Once deposited on gravel bars, the uprooted trees shoot and root into the bar surface, and trap finer sediment, aggrading the bar surface. Published and unpublished measurements show that, although there is high variability, typical relative surface elevations above adjacent bar surfaces for the sequence of island development stages in the study reach are: 0 m (initial deposition of uprooted tree), 0.3-0.8m (pioneer islands), 1.0 – 1.5 m (building islands), ~ 2 m (established islands) (Figure II. 2 illustrates islands at these four stages of island development).

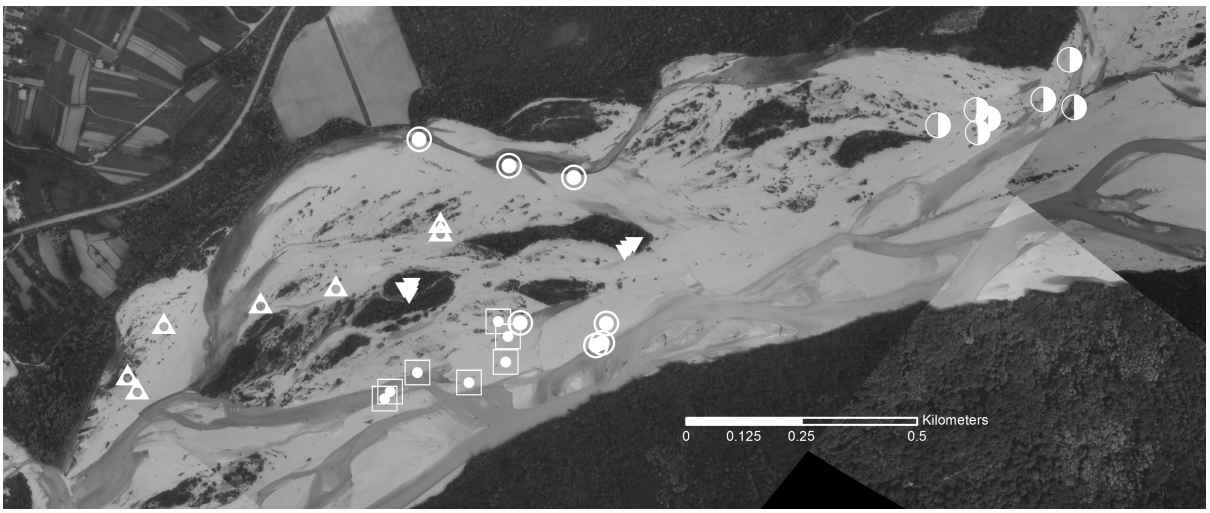

Figure II. 1. The study reach (photographed in 2005) and patches sampled (◉ = age 0; ⊡= age 2; ◑ = age 8; ◬= age 12; ▼= age 40). (air photographs provided by the UK Natural Environment Research Council).

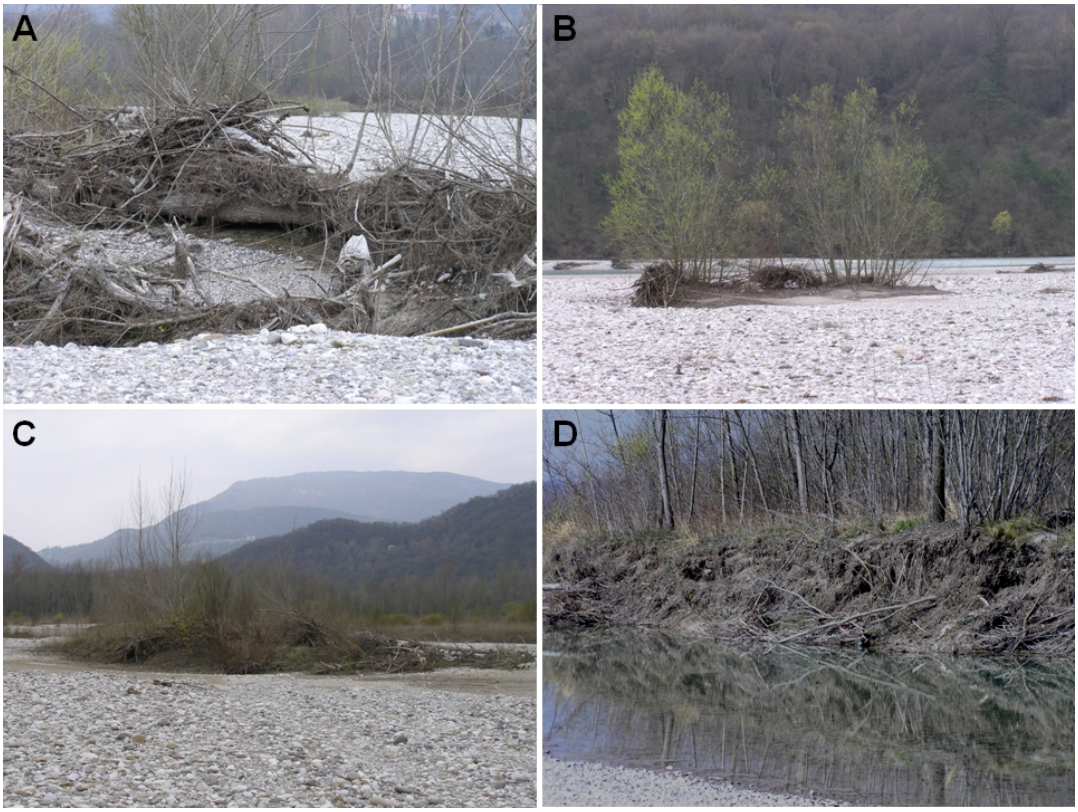

Figure II. 2. Islands at different development stages in the study reach, photographed in April when their morphology is not disguised by foliage. A. An uprooted tree deposited on a gravel bar and retaining large wood. B. A pioneer island showing an early stage of fine sediment retention around a single deposited tree that has sprouted from its trunk to produce a line of new trees. Large wood pieces are accumulating around its root wad (left) and within the line of trees. C. A building island showing major lateral and vertical sediment accretion, retention of significant quantities of wood around its margins and across its surface, and a tree cover that is composed of several tree species. D. The eroded margin of an established island, illustrating major vertical retention of fine sediment that is reinforced by a dense web of tree roots (all photographs by A. Gurnell).

Information from historical data sources.

Three sets of historical data were assembled to support the research: river stage records,

oblique photographs, aerial imagery.

(i) River Stage Records

Extreme flood events, capable of significant disturbance of the vegetated areas within the river's active channel in the study reach, were identified from two complementary sets of river water level records. Average daily river level records, commencing in October 1981, were available from the Villuzza gauge, located at the downstream end of the study reach. In addition, extreme annual river level records were available for most years back to 1886 from the Pioverno-Venzone gauging site, which is located approximately 8 km upstream from the study reach. The latter records were particularly useful for identifying very extreme river levels prior to the commencement of the Viluzza record. The two sets of records were combined to identify the timing of major flood events that may have been followed by vegetation colonisation and subsequent pioneer, building and established islands that could be sampled in the present research.

(ii) Oblique photographs

Oblique photographs taken (by A. Gurnell) from a point overlooking the study reach on 27 occasions between 1999 and 2012, provided information on vegetation dynamics within the study reach (Figure 4 shows some example photographs of one part of the reach). This data set had sufficient spatial resolution to allow identification of individual trees deposited by floods within the study reach, and the high temporal resolution of the data set, allowed broad areas of the active corridor that had been disturbed by floods since 1999 and had subsequently remained relatively undisturbed to the 2012 field sampling campaign, to be delineated. Information from these photographs was combined with the information from river stage records prior to the field campaign to define areas of approximately 2, 8, 12 and

40+ years since major flood disturbance for field sampling.

(iii) Aerial images

An archive of seventeen sets of aerial images dating from 1944 to 2012 and providing decadal or higher temporal resolution, were obtained from various sources (Table II. 1). These were used following the field campaign to track temporal changes in the vegetation cover of field-sampled sites.

Aerial photographs gathered in 1996 had been geocorrected to produce an official Italian orthoimage. Aerial images from 1944, 1954, 1970, 1986, 1991, 1997, 1999 and 2005 were obtained as prints and were scanned to obtain images of approximately 1.2 m resolution. As reported by Zanoni et al. (2008), these scanned images were geocorrected to the Gauss-Boaga projection using the 'image to image' warping tool in Envi 4.3 (ITT Visual Information Solutions), and an error analysis indicated an average ground error of less than 5m. In the present research, information was extracted from these images using ArcGIS 10.1.

Table II. 1. Aerial image dates, types and sources used in the research

Year (date)	Data Type (scale if applicable)	Source
1944 (25.07.1944)*	Aerial photograph (1:20000)	The Aerial Reconnaissance Archives, Keele University
1954 (11.04.1954) *	Aerial photographs (1:27000)	Istituto Geografico Militare Italiano
1970 (no date) *	Aerial photographs (1:15000)	Regione Friuli-Venezia Giulia
1986 (24.12.1986) *	Aerial photographs (1:21000)	Istituto Geografico Militare Italiano
1991 (08.10.1991) *	Aerial photographs (1:5000)	Rossi s.r.l. REVEM Brescia
1996 (no date) *	Orthoimage (1 pixel = 1m)	AIMA del Ministero delle Politiche Agricole Alimentari e Forestali
1997 (16.06.1997)*	Aerial photograph (1:20000)	Autorita di Bacino dei fiumi dell'Alto Adriatico
1999 (11.09.1999) *	Aerial photograph (1:20000)	Autorita di Bacino dei fiumi dell'Alto Adriatico
2002 (21.06.2002) *	Google Earth 7 ™ image (1 pixel < 0.5m)	Digital Globe
2002 (21.07.2002)	Google Earth 7 ™ image (1 pixel < 0.5m)	Digital Globe
2003 (24.06.2003) *	Google Earth 7 ™ image (1 pixel < 0.5m)	Digital Globe
2003 (24.07.2003)	Google Earth 7 ™ image (1 pixel < 0.5m)	Digital Globe
2003 (14.09.2003)	Google Earth 7 ™ image (1 pixel < 0.5m)	European Space Imaging
2003 (27.09.2003)	Google Earth 7 ™ image (1 pixel < 0.5m)	Digital Globe
2005 (23.05.2005)	Aerial photograph (1:10000)	Natural Environment Research Council UK
2005 (21.06.2005) *	Google Earth 7 ™ image (1 pixel < 0.5m)	Digital Globe
2012 (02.03.2012)*	Google Earth 7 ™ image (1 pixel < 0.5m)	Digital Globe

* image used in the analysis of temporal trends

Aerial images for a further eight dates were available from Google Earth 7 ™. These images had already been geocorrected within Google Earth 7 ™, and so it was not possible to fully quantify any errors associated with this process. Information on vegetation cover was extracted from these images using tools available in either Google Earth 7 ™ or Google Earth 7 Pro ™. The spatial resolution of the images was estimated to be less than 0.5 m by counting pixels crossed by a 5 m line drawn parallel to the grid orientation on each image.

In order to investigate the vegetation cover history of each field sampling site, images were selected from those listed in Table 1 to provide a single example for each of the 12 years for which data were available. Where there was more than one image for a year, spring to early autumn images were selected in an attempt to ensure similar leaf cover on the canopies of the predominantly deciduous trees. Geographical co-ordinates for each sampling site were obtained in the field using a hand-held GPS. Circular polygons of radius 10 m were centred on the geographical co-ordinates of every sampling point on all twelve maps. In each circular polygon, smaller polygons were created over each of three cover types: mature (complete cover) vegetation, sparse (mixed pixel) vegetation, and unvegetated (bare sediment or water). The area enclosed by each polygon was estimated using either ArcGIS 10.1 or Google Earth 7 Pro ™ software, from which the percentage cover was estimated.

Images from two different dates were available for 2002, four for 2003, and two for 2005. Of these eight aerial images, one was based on aerial photographs and the others were from Google Earth 7 ™. In all cases no significant floods occurred between the dates at which

images were collected within the same calendar year. Therefore, it was possible to use these multiple images to assess the reliability of the procedure used for extracting information on vegetation cover. Vegetation cover was estimated for all field sampling points from all eight images. The results obtained from images collected in the same year were compared to assess whether there was any statistically significant difference in estimated vegetation cover between same-year images.

The processes of georectification and extracting vegetation cover information from the historical areal images are subject to a range of potential errors. These errors were explored and, where possible, minimised using the following procedures. The size of the circle polygons used for estimating vegetation cover was selected bearing in mind errors in the air photograph image rectification process (average ground error typically < 5m). Such errors vary between images and for every sampling point. The 20 m diameter circle used to estimate vegetation cover was selected to be sufficiently large that the likelihood that the sample site would be located somewhere within the polygon was high. The polygon size was also selected to provide a sufficiently large sample area to support consistent visual vegetation cover identification, although additional information from surrounding pixels also aided this visual assessment. The consistency of the entire data extraction process (georectification, vegetation cover estimation), and also its sensitivity to leaf development on the tree canopies, was assessed by comparing the vegetation cover data extracted from the sets of images obtained within the same year, to identify whether or not the extracted data sets were statistically significant difference between dates. Although there were undoubtedly additional errors relating to the latitude and longitude co-ordinates recorded

for each sampling site by a hand-held GPS, every attempt was made to obtain a stable and reliable reading for each sampling site. Inspection of the sampling positions relative to the most recent image (obtained only four months prior to the field campaign), gave confidence in the accuracy of the co-ordinates. Importantly, any error in the sample site co-ordinates remains the same for all of the images that were analysed.

Field sampling

Field sampling was conducted from 13-16th May 2012 with the aim of investigating whether significant soil structure development had occurred across five sampling areas of different age identified using the historical river stage records and oblique photographs. These sampling areas were recently disturbed open bare sediment (i.e. 0 year), and areas of approximately 2, 8, 12 and at least 40 years since vegetation colonisation was initiated by the deposition of uprooted trees. Hereafter, these areas and samples taken from them are labelled 0, 2, 8, 12 and 40 years.

Within each sampling area, seven patches were chosen for sampling. Within the 2, 8 and 12 year areas, which displayed a mosaic of pioneer and building islands separated by areas of open gravel and sand, seven islands were selected randomly with as wide a geographical spacing as possible, given the constraints of the total area of that age that could be sampled. The 40 year area had a continuous vegetation cover because it was located within the oldest growth areas of the two largest established islands in the study reach, so sampling proceeded around seven of the largest (assumed oldest) trees. In all cases the tree species

was *Populus nigra.* Within the 0 year area sediment was sampled at seven randomly selected sites from the surface of open, recently-disturbed bar surfaces where vegetation cover was absent.

Within all sampled patches apart from those in the 2 year category, the largest (assumed oldest) tree (always *P. nigra*) was cored at 1m above the ground surface and its age was estimated from the number of annual growth rings, which were counted in the field using a hand lens. The annual rings confirmed the age of the 8 and 12 year sampling areas and the minimum 40 year age of the oldest site: the seven cored trees showed 40, 40, 40, 41, 45, 47 and 59 rings. While the few rings in the younger trees were reasonably distinct and easily counted, this was more difficult for the older trees. The 'oldest' tree sampled in the 40 year area appears as an outlier, although its trunk diameter was similar to that of the other sampled trees, suggesting that several of the rings may have been false (i.e. due to other factors than the annual growth cycle). For the 2 year patches, shoots with small side branches sprouting from the trunk of deposited *P. nigra* confirmed deposition at least one full growing season previously (i.e. at least 1.5 years prior to sampling).

Three surface sediment samples were obtained from 0-10 cm depth within all sampled vegetated patches (i.e. 2, 8, 12, 40 year patches). The 2 year patches were centred on a large deposited tree and the three samples were obtained at the root bole, midway along the trunk and within the tree canopy. The 8 and 12 year patches were pioneer or building islands, and the samples were taken at the upstream and downstream ends and centre of each island. For the 40 year patches, the three samples were taken randomly within a 5 x 5 m^2 area centred

on the large tree that had been cored. Only one sample was taken at each patch of age 0 years to sample open bar surface sediments as a baseline for the samples at vegetated sites. In total 91 sediment samples were collected; 7 samples for 0 years and 21 samples each for 2, 8, 12, and 40 years.

Laboratory measurements of sediment fertility and structure

Total nitrogen, organic carbon and soil aggregation were measured for each sediment sample. Nitrogen and organic carbon content are indicators of soil fertility (e.g. Haynes et al., 1991; Mikha and Rice, 2004; Bauer and Black, 1994; Sainju and Good, 1993), whereas soil aggregation is an indicator of soil structure (e.g. Six et al., 2000; Diaz-Zorita et al., 2002; Tisdall and Oades, 1982). These data are presented in more detail elsewhere as part of more comprehensive analysis of physical, chemical and biological properties of soils by Mardhiah et al. (submitted), but these three properties are used in the present research as indicators of soil development, and are subjected to a new statistical analysis to support interpretation of information extracted from the aerial images. The following clarifies how the values of these three indicators were derived.

Total N and organic C were determined using a EuroEA Elemental Analyzer (HEKAtech GmbH, Wegberg, Germany) after the samples had been fumigated with 12 M HCl to remove carbonates (Harris et al., 2001).

To assess soil aggregation, soil samples were sieved through a 4-mm sieve before being

air-dried at room temperature for several days. Aggregate stability was measured as the abundance of water stable aggregates (WSA) by immersing a stack of sieves (from top to bottom: 2-mm, 1-mm, 0.5-mm, 212-µm) in a bucket of water (Kemper and Rosenau, 1986). Fifty grams of air-dried soil was rewetted by capillary action and was then carefully placed on the top sieve of the stack. All sieves were kept immersed while being moved up and down (approximately 3 cm) for 10 min. The material remaining on each sieve was then crushed and passed through the sieve, to separate the material into soil (passing through the sieve) and coarse fractions (remaining on the sieve). Fractions from each sieve size (2-4 mm, 1-2 mm, 0.5-1 mm and 0.2-0.5 mm) were collected, dried at 80°C, and then weighed separately. Total coarse material, primarily sand, was also weighed. These determinations were used to calculate an index of soil aggregation - mean weight diameter (MWD). This is calculated as the sum of the proportion of aggregates in each size class, proportionally weighted by the mean diameter of aggregates in that size class (approached as mean size of the upper and lower limit of sieve sizes used: 3 mm, 1.5 mm, 0.75 mm and 0.356 mm respectively) using the following equation (Barto et al., 2010):

$$MWD = (3\ mm * W_2) + (1.5\ mm * W_1) + (0.75\ mm * W_{0.5}) + (0.365\ mm * W_{0.212})$$

W = coarse material corrected proportion of aggregates in each size class.

The fertility and structure measurements described above were not normally distributed. Therefore, these data were analysed using non-parametric statistical tests (see data analysis section below)

Data analysis

Neither the image-based measures of vegetation cover nor the laboratory determinations of indicators of soil fertility and structure were normally distributed or homoscedastic. In addition, the vegetation cover estimates were percentages. Therefore, all of the data were subjected to hypothesis testing using non-parametric statistical tests. Mann Whitney and Kruskal Wallis tests were used to assess whether there was a significant difference in vegetation cover estimates extracted from aerial images from within the same calendar year. Kruskal Wallis tests were also used to investigate historical changes in vegetation cover and also differences in sediment properties among groups of samples drawn from sampling sites of different age (0, 8, 12, 40 years). Where the Kruskal Wallis test indicated a statistically-significant ($p<0.05$) difference among samples drawn from different groups, it was followed by multiple pairwise comparisons to assess which sample groups were statistically significantly different from one another, using Dunn's procedure with Bonferroni correction. Statistical analyses were conducted using XLSTAT 2011 (Addinsoft) and version 2.14.0 of the R statistics software (R Development Core Team, 2012).

Results

Extreme river stage events that may have initiated significant erosion and deposition of sediment and trees:

Analysis of data sets for the study reach by Bertoldi et al. (2009) related river levels at the Villuzza gauging site to process-form interactions within the study reach. In particular, the

analysis identified that interaction between river flows and sparse vegetated patches commenced at a water level of approximately 200 cm at Villuzza, and severe vegetation disturbance, including the erosion of established island margins and the undermining and uprooting of mature trees, commenced at approximately 300 cm stage. Therefore, the flow records were inspected to identify events that may have initiated island development through significant erosion and deposition of sediment and trees.

Figure II. 3 illustrates all daily flows exceeding 200 cm stage in the 1981-2011 Villuzza river level record. Five flood events in the record greatly exceed 300 cm stage: 1990 (332 cm), 1996 (325 cm and 320 cm), 2000 (358 cm) and 2004 (314 cm). In addition two sizeable flow pulses occurred during the two winters preceding field sampling (262 cm in December 2009 and 260 cm in November 2010).

River levels at the Pioverno gauge are not directly comparable with those at Villuzza. However, the annual maximum water levels observed between 1886 and 1981 at Pioverno show one extreme flood (550 cm stage) in 1966. This is one of only three events that exceed 400 cm stage at this gauging site between 1940 and 1981, the other two being 477 cm in the preceding year (1965) and 438 cm in 1940.

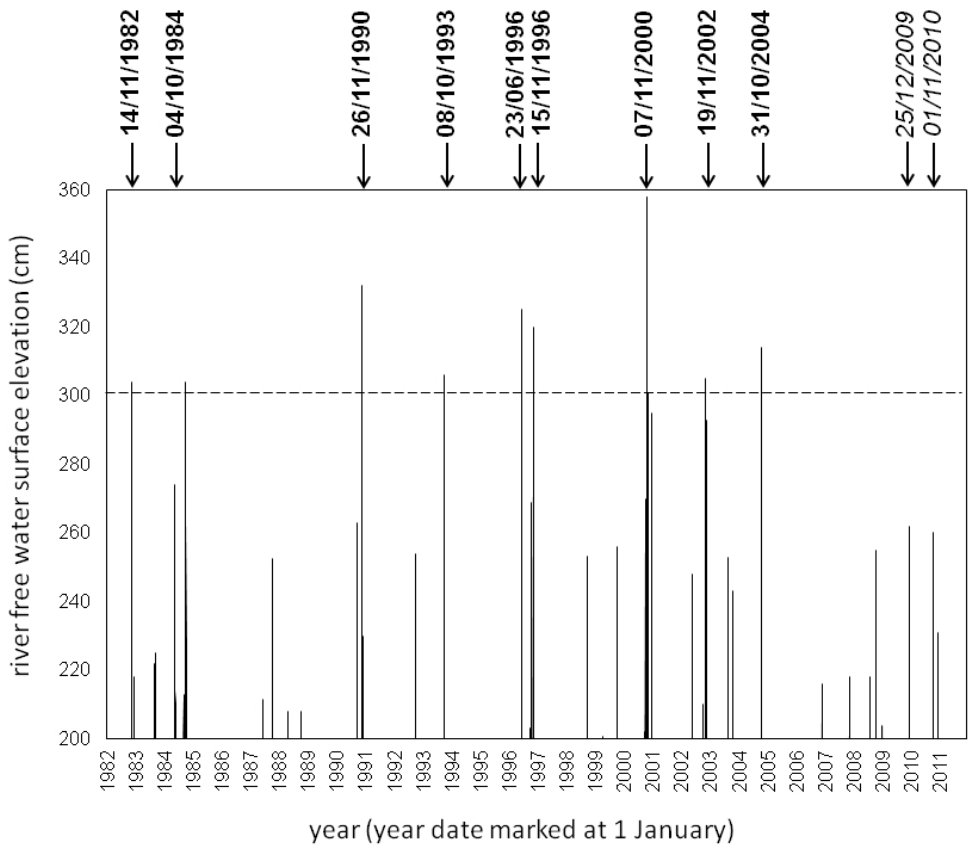

Figure II. 3. River water levels exceeding 200 cm at the Villuzza gauge, 1982-2011. Dates are provided for all river levels exceeding 300 cm (bold font) and for two smaller events exceeding 250 cm in the two winters prior to field sampling (italic font).

Analysis of the oblique photographs taken between 1999 and the present provided supporting evidence of the role of the high stage events identified in the gauge records in initiating the development of islands that had persisted to the present. The earliest photographs (Figure II. 4) showed a few established vegetated islands mainly surrounded by bare gravel bars with only very limited areas of young patchy vegetation, suggesting limited recovery from widespread disturbance by the two 1996 floods. Because of the oblique nature of the photographs, patches of the tallest (oldest) trees present within these islands in 1999 could be identified. These oldest areas were labelled 40+ years, since they

potentially dated back to the largest flood(s) experienced in 1965-1966, although they may have been initiated by later events. Photographs taken in 2001 showed widespread deposition of uprooted trees across the bare gravel bars. Since these trees were not present in photographs taken in summer 2000, they must have been deposited by the flood in November 2000. The area of the braided river bed showing steady pioneer and building island development from these deposited trees to the time of sampling was labelled 12 years. A similar analysis identified a smaller area of the braided channel where intense disturbance had resulted in lateral channel movement, leaving many trees deposited where the channel had been previously located in photographs taken in May 2005. Much of this area had persisted with clear pioneer island development to the sampling date. This area was labelled 8 years. The most recent photographs confirmed areas where trees, eroded by flow pulses in the two winters prior to sampling, had been deposited.

Figure II. 4. Oblique photographs of a part of the study reach taken during summer in 1999, 2001, 2005, 2008, 2010, 2012 (all photographs by A.M. Gurnell).

Historical changes in the vegetation cover of field-sampled sites reconstructed from an analysis of aerial images

In order to check the reliability of the data extraction method, the estimates of vegetation cover from images obtained within the same year were compared. Estimates were only compared for sampling areas where vegetation cover was initiated from floods that occurred before the year of each image. Thus information extracted from the duplicate images for 2002 and 2003 was only compared for the 12 year and 40 year sampling sites, and information from the 2005 images was only compared for the 8 year, 12 year and 40 year sampling sites.

The data for the 40 year sampling sites were not compared statistically across duplicate year images because the percentage covers of mature vegetation, sparse vegetation and unvegetated areas were almost ubiquitously 100%, 0% and 0%, respectively (see dot plots for the data extracted from the four 2003 images in Figure II. 5). However, there was one patch (3 samples) which showed less than 100% mature vegetation cover and a complementary proportion of bare sediment in three of the images (one in each of 2002, 2003 and 2005 image sets). This patch was close to the edge of an established island and so the occasional presence of bare sediment within the sampling polygon can be attributed to slight differences in image georectification among images. In addition two further patches showed a proportion of bare sediment in the May 2005 image. Again these patches were close to an established island edge and the error can be attributed to a slight difference in the georectification of the May 2005 image, which was based on scanned air photographs,

in comparison with the June 2005 image, which was derived from Google Earth.

Mature, sparse and unvegetated proportions from the 12 year area were compared using all of the 2002, 2003 and 2005 duplicate images, and data from the 8 year area was compared using only the 2005 duplicate images, since the other images pre-dated the initiation of vegetation development by the 2004 flood. No mature vegetation was recorded for any of the 8 year or 12 year sampling locations in any of the images. Therefore, comparisons focused on contrasts in sparse vegetation and unvegetated areas among images. The statistical significance of differences in either sparse vegetation or bare sediment cover was assessed using the Kruskal Wallis test (4 images in 2003, Figure II. 5) or Mann Whitney test (2 images in each of 2002 and 2005). No statistically significant differences were found within any of the three years investigated ($p > 0.339$ for all tests). These results provide confidence in the data extraction method, in that any errors between images were too small to generate data sets that were statistically significantly different from one another. Therefore, analysis of the individual images selected to represent each year proceeded, assuming that where statistically-significant differences were identified between images from different years, they indicated true differences in the vegetation cover around the sampling locations.

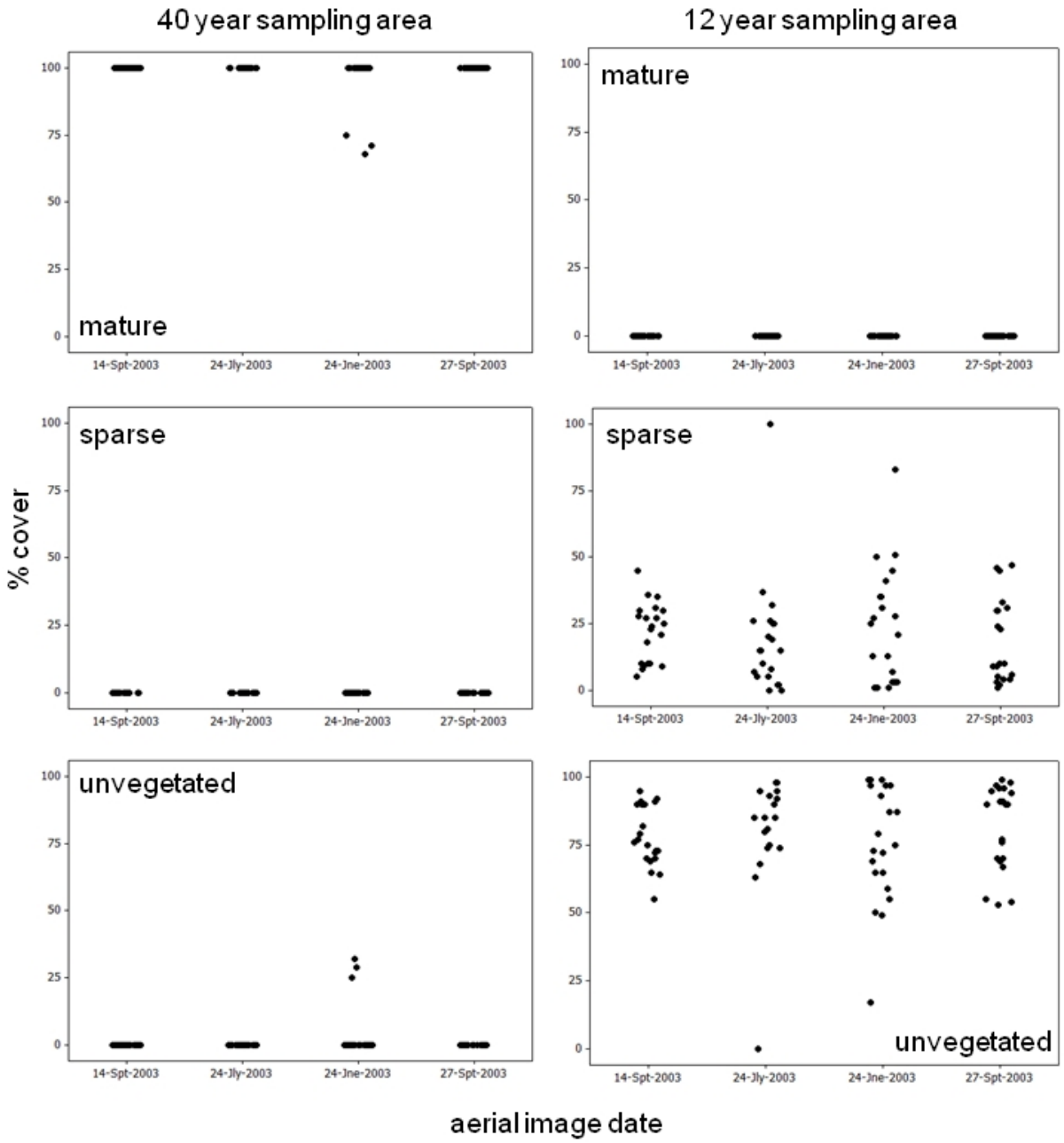

Figure II. 5. Individual dot plots illustrating the percentage cover of mature vegetation (top), sparse vegetation (middle) and unvegetated areas (bottom) estimated from aerial images collected in 2003 within 20m diameter circular polygons centred on the field sampling sites. 40 year sampling sites are shown on the left and 12 year sampling sites are shown on the right.

Dot plots of the values of % mature vegetation cover, % sparse vegetation cover and % unvegetated areas within 20m diameter circular polygons centred on each sampling location

are presented in relation to a time series of image dates for the 40 year, 12 year, 8 year and 2 year areas in Figures 6, 7, 8 and 9, respectively. These Figures provide an indication of whether photographs following the flood event that had disturbed the sampling area showed both a change from the immediately preceding image and a trajectory of vegetation cover development following the flood. They also provided a history of vegetation dynamics from 1944 up to the year of the flood. The latter can indicate whether the younger areas had experienced a history of disturbance and vegetation recovery following previous flood events. Therefore, the occurrence of preceding flood events that had disturbed other sampling areas are marked as vertical dashed lines on each Figure, whereas other events that achieved a river level well in excess of 300 cm are indicated as arrows in the upper graph of each Figure. The results of Kruskal Wallis tests applied separately to the % mature vegetation cover, % sparse vegetation cover and % unvegetated area estimates across the twelve survey dates within each of the 2, 8, 12 and 40 year areas are summarised in Table 2. In all cases, Kruskal Wallis tests were statistically significant ($p<0.0001$, degrees of freedom = 11), and the table lists the aerial image dates that were identified by multiple pairwise comparisons to be statistically significantly different from one another (Bonferroni corrected significance level: $p = 0.0008$).

Table II. 2. Results of Kruskal Wallis tests applied separately to the % mature vegetation cover, % sparse vegetation cover and % unvegetated area estimates at all sample locations across the twelve image dates within each of the 2, 8, 12 and 40 year areas. Kruskal Wallis K values are shown and all are statistically significant ($p<0.0001$, degrees of freedom = 11), followed by lists of the aerial image dates that were identified by multiple pairwise comparisons to be statistically significantly different from one another (Bonferroni corrected significance level: $p=0.0008$). All image years following the initiation of vegetation that has persisted to the present are emboldened..

Sampling area	Cover type	Kruskal Wallis K	Image years showing statistically significant differences in cover type extent
40 year	% mature	218.5	**2012, 2005, 2003, 2002, 1999** > **1991, 1986, 1970**, 1954, 1944 **1996** > **1991, 1970**, 1954, 1944 **1997** > **1970**, 1954, 1944
40 year	% sparse	162.6	**1991, 1986** > **2012, 2005, 2003, 2002, 1999, 1997, 1996, 1970**, 1954, 1944
40 year	% unvegetated	208.8	**1991, 1970**, 1954, 1944 > **2012, 2005, 2003, 2002, 1999, 1997, 1996**
12 year	% mature	109.8	**2012**, 1986 > **2005, 2003, 2002**, 1999, 1997, 1996, 1970, 1954, 1944 1991 > **2005, 2003, 2002**, 1999, 1970, 1954, 1944
12 year	% sparse	120.4	**2005** > **2012**, 1999, 1997, 1996, 1991, 1986, 1970, 1954, 1944 **2003** > 1999, 1997, 1991, 1986, 1970, 1954, 1944 **2002** > 1999, 1991, 1970, 1954, 1944 **2012** > 1954, 1944
12 year	% unvegetated	141.7	**2002**, 1999, 1997, 1996, 1970, 1954, 1944 > **2012** 1999, 1996, 1970, 1954, 1944 > **2005**, 1991, 1986 1970, 1954, 1944 > **2003, 2002**
8 year	% mature	63.6	1991 > **2012, 2005**, 2003, 2002, 1999, 1997, 1996, 1954, 1944 1986, 1970 > **2005**, 1954, 1944
8 year	% sparse	124.4	1999, 1997, 1996, 1991, 1986, 1970 > 2003, 1954, 1944 **2012, 2005** > 1954, 1944 1986 > 2002
8 year	% unvegetated	141.4	1954, 1944 > **2012, 2005**, 2003, 2002, 1997, 1996, 1991, 1986, 1970 2003 > **2012**, 1999, 1996, 1991, 1986, 1970 **2005**, 2002 > 1986
2 year	% mature	62.7	1997, 1996 > **2012**, 2005, 2003, 2002, 1999, 1991, 1986, 1970, 1954, 1944

2 year	% sparse	71.8	1991	>	2005, 2003, 2002, 1999, 1997, 1996, 1970, 1954, 1944
			2012	>	2005, 2003, 1999, 1996, 1970, 1954
2 year	% unvegetated	67.6	1991	>	2005, 2003, 2002, 1999, 1970, 1954, 1944
			2012	>	2005, 2003, 1999, 1970, 1954

For the 40 year area (Figure II. 6, Table II. 2), all images after 1997 show a significantly greater percentage mature vegetation cover around the sampling locations than images before 1996, and the 1996 and 1997 images show a higher percentage cover than the earliest three images (1944, 1954, 1970). The 1991 and 1996 images show a higher percentage sparse vegetation cover than all other images. The earliest four images (1991, 1970, 1954, 1944) show a greater percentage unvegetated area than all other images. These statistically significant differences, illustrate a period when the sampled patches were essentially unvegetated from 1944 to 1991, followed by a period from 1991 to 1996 during which sparse vegetation started to appear and then was replaced from 1997 to present by a complete cover of mature vegetation. Since the 1970 images shows some sparse vegetation cover, this is the latest date at which continuous vegetation development to the present day could have been initiated, suggesting that the 40 year area may actually have been somewhere between 42 (the 1970 image date) and 47 (the timing of the 1965-1966 floods, shown as a solid vertical line on Figure II. 5) years old at the time of sampling in 2012. This range of dates is confirmed by the annual growth rings of all but one of the sampled trees.

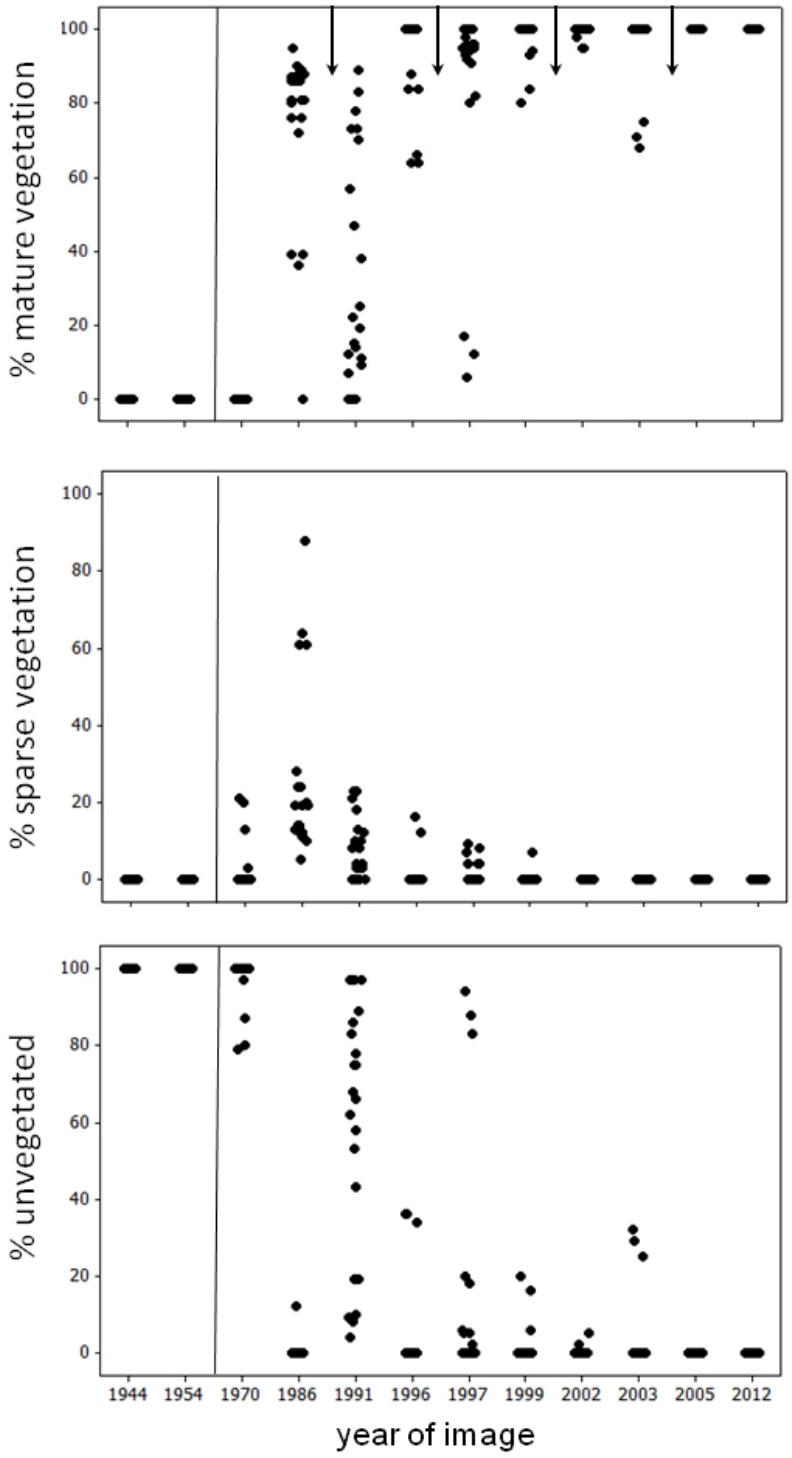

Figure II. 6. Individual dot plots illustrating the percentage cover of mature vegetation (top), sparse vegetation (middle) and unvegetated areas (bottom) around sampling locations in the 40 year area, estimated from 12 aerial images spanning the period 1944 to 2012. The vertical line marks the transition from no vegetation cover to some sparse vegetation development, and also coincides with the gap between images occupied by the 1965-1966

extreme floods. The arrows (top graph) indicate the gaps between images when high river levels were recorded in 1990, 1996, 2000 and 2004. (Note that the 1996 peak stages may have preceded or postdated the 1996 image, since there was no survey date provided for the latter, Table II. 1).

For the 12 year area (Figure II. 7, Table II. 2), there are four images (2002, 2003, 2005, 2012) which cover the period between the 2000 flood (solid vertical line on Figure II. 7) and the sampling date. The 2012 image shows significantly higher percentage mature vegetation cover and significantly lower percentage unvegetated cover than the 2002 image, while the 2005 image shows significantly higher percentage sparse vegetation cover than the 2012 image. These statistically significant results confirm that the vegetation cover has increased and the vegetation has started to mature within the 12 year area following the 2000 flood. It also confirms the age of the sampled patches as indicated by the annual growth rings of the oldest tree in each sampled patch. A previous cycle of vegetation recovery following the 1965-1966 floods (dashed vertical line on Figure II. 7) is also revealed by the Kruskal Wallis tests, through images 1970 to 1991.

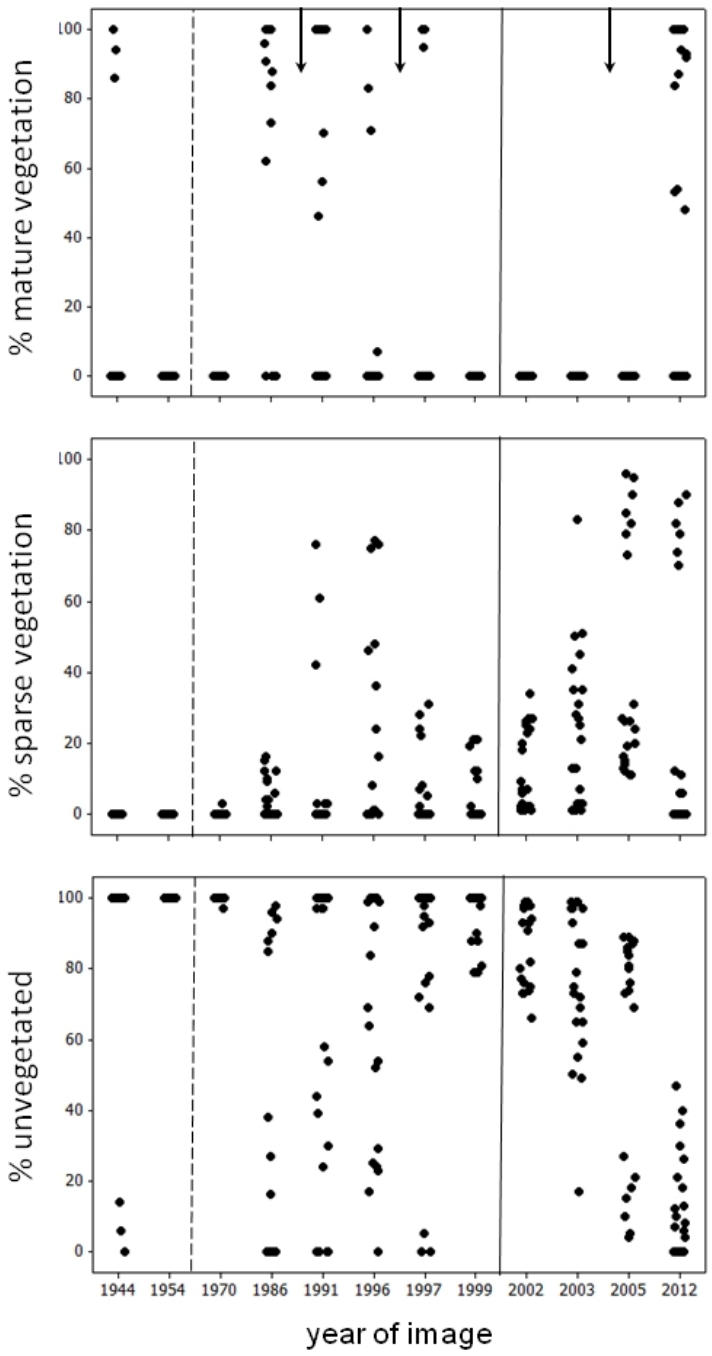

Figure II. 7. Individual dot plots illustrating the percentage cover of mature vegetation (top), sparse vegetation (middle) and unvegetated areas (bottom) around sampling locations in the 12 year area, estimated from 12 aerial images spanning the period 1944 to 2012. The vertical solid line marks the 2000 flood that is believed to have initiated vegetation development within the 12 year area. The dashed line indicates the extreme floods in 1965-1966, and the arrows (top graph) indicate the gaps between images when high river levels were recorded in 1990, 1996, and 2004. (Note that the 1996 peak stages may precede

or postdate the image, since there was no survey date on this orthophoto, Table II. 1).

For the 8 year area (Figure II. 8, Table II. 2), only two images (2005 and 2012) cover the period between the 2004 flood (solid vertical line on Figure II. 8) and the sampling date. Kruskal Wallis tests reveal no significant difference in the proportions of the three cover types in the short period between these dates. However, as with the 40 and 12 year areas, there is a significant increase in the development of vegetation between 1970 and 1999 following the 1965-1966 floods and, although only statistically significant for the percentage unvegetated cover in 2003, there appears to be a response to the 2000 flood (both floods indicated as dashed vertical lines on Figure II. 9).

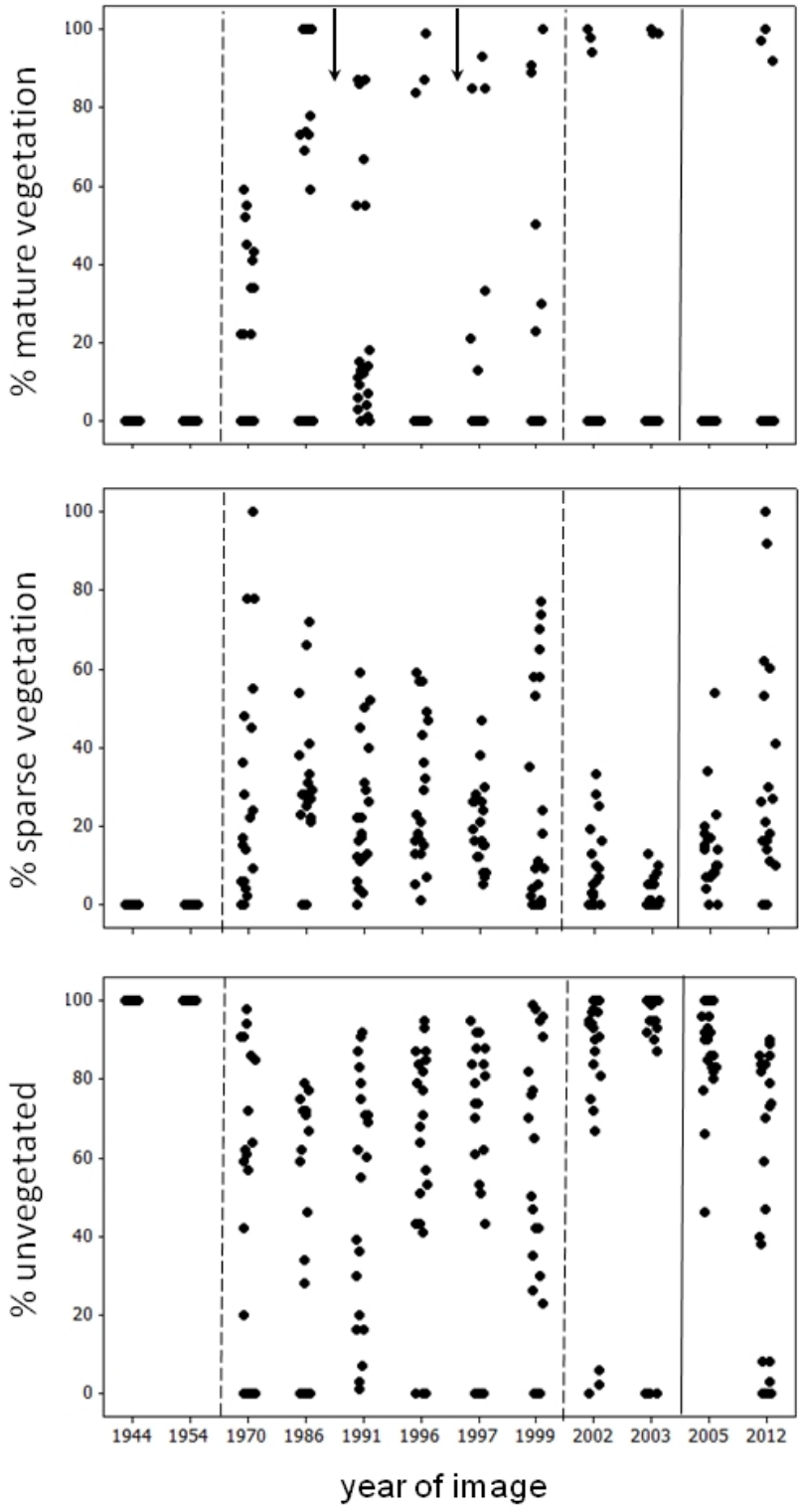

Figure II. 8. Individual dot plots illustrating the percentage cover of mature vegetation (top), sparse vegetation (middle) and unvegetated areas (bottom) around sampling sites in the 8 year area, estimated from 12 aerial images spanning the period 1944 to 2012. The

vertical solid line marks the 2004 flood that is believed to have initiated vegetation development within the 8 year area. The dashed lines indicate floods in 1965-1966 and 2000, and the arrows (top graph) indicate the gaps between images when high river levels were recorded in 1990 and 1996. (Note that the 1996 peak stages may precede or postdate the 1996 image, since there was no survey date on this orthophoto, Table 1).

Finally, only one image (2012) postdates the 2010 flood pulses (solid vertical line on Figure II. 9) that deposited the trees sampled on the 2 year site. However, the 2012 image shows significantly higher percentage unvegetated cover and percentage sparse vegetation cover than the 2005 image (Table II. 2), indicating a response in vegetated area to these flood pulses. There is no clear evidence of vegetation response to previous floods (1965-1966, 2000, 2004 shown as vertical dashed lines on Figure II. 9), probably because this sampling area has had a persistently high percentage unvegetated cover throughout the image record.

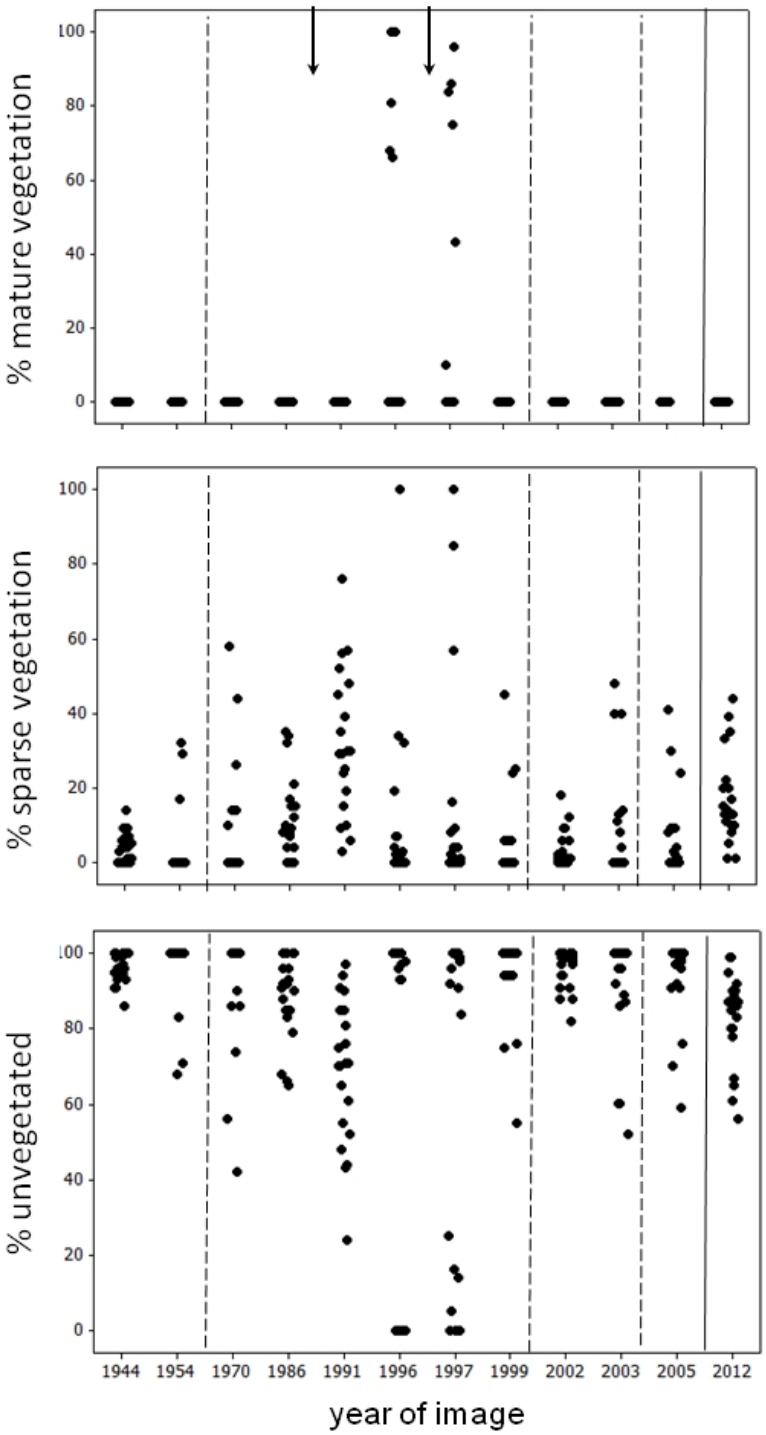

Figure II. 9. Individual dot plots illustrating the percentage cover of mature vegetation (top), sparse vegetation (middle) and unvegetated areas (bottom) around sampling sites located in the 2 year area, estimated from 12 aerial images spanning the period 1944 to 2012. The vertical solid line marks the flood pulses in 2010 that are believed to have initiated recent vegetation development within the 2 year area. The dashed lines indicate the

floods in 1965-66, 2000 and 2004 and the arrows (top graph) indicate the gaps between images when high river levels were recorded in 1990 and 1996. (Note that the 1996 peak stages may precede or postdate the 1996 image, since there was no survey date on this orthophoto, Table 1).

In summary, the annual growth ring, flow stage, oblique photograph and aerial image data sets all confirm site ages of 2, 8, 12 and 40+ years, with only the oldest area showing a slight disagreement in the evidence in relation to the estimated age of one sampled tree.

Fertility and structure of sampled sediments.

Laboratory analysis of the 91 sediment samples collected across the 0, 2, 8, 12 and 40 year sampling areas revealed distinct increases in the three indicators of soil development (percentage total nitrogen, percentage total organic carbon, MWD) with increasing area age (Figure II. 10). For the present study, these data were subjected to Kruskal Wallis tests, which all showed statistically significant differences in these indicators of soil development (K values of 66, 37, 32 for percentage total nitrogen, percentage total organic carbon and MWD, respectively, $p < 0.0001$ in all cases). Percentage total nitrogen values were significantly larger in the 40 year samples than in the 12 year samples, which were larger than in the 8 year samples, and which, in turn, were larger than the 2 and 0 year samples. Percentage organic carbon values were significantly greater in the 40 year samples than in the 12, 8 and 0 year samples, which were larger than in the 2 year samples. MWD values were higher in the 40 year samples than in the 12 and 8 year samples, and the 8 and 2 year samples had higher MWD than the 0 year samples. Although all three properties showed increases with the age of the sampling location, percentage total nitrogen and MWD

showed a more distinct (less variance within sampling areas) and consistent increase with sampling area age than percentage total organic carbon.

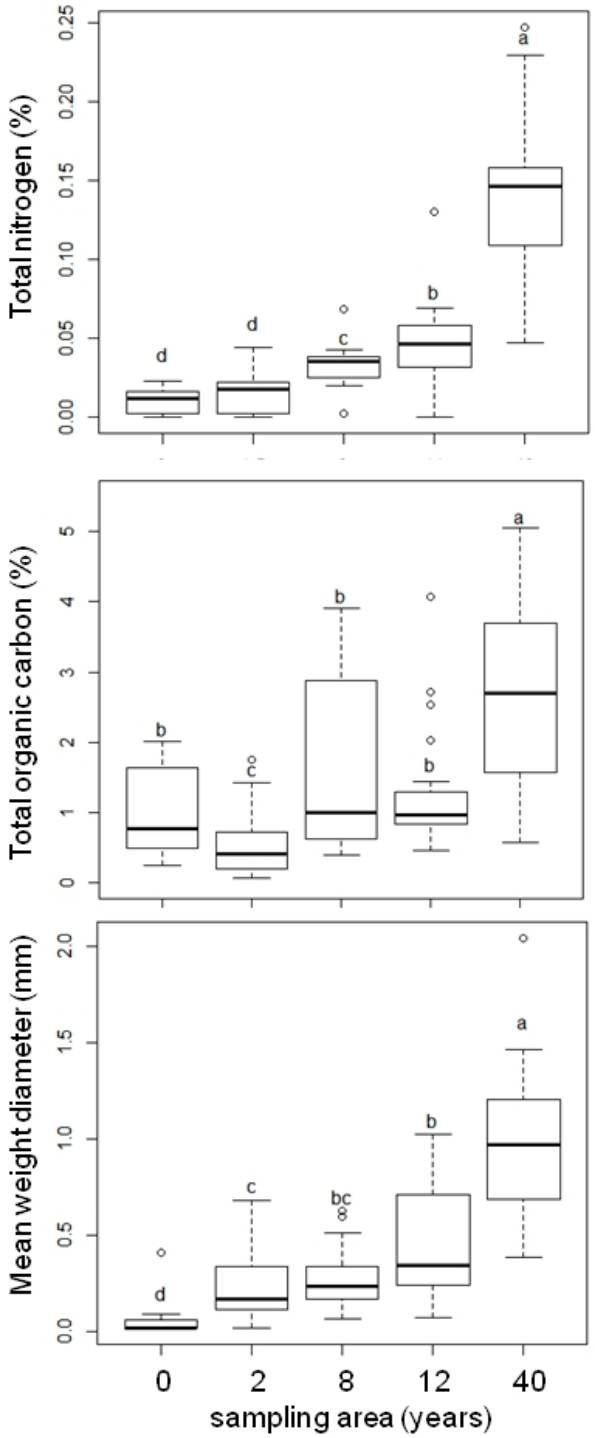

Figure II. 10. Boxplots of the percentage of total nitrogen (top), total organic carbon (centre), and mean weight diameter (bottom) of sediment samples taken from 0-10 cm depth within areas of different age (0, 2, 8, 12, 40 years). Where there is no significant difference between determinations drawn from sampling areas of different age, the box and whiskers for these sampling areas are labelled with the same letter.

Discussion and Conclusions

As stated in the introduction, the present research was designed to investigate island and associated soil development along a 3km island-braided reach of the Tagliamento River. The aim of the research was to establish whether statistically-significant soil development could be observed on islands of different age and could be supported by reconstruction of the history of the sampled islands. The aim of the historical reconstruction was to confirm the age of the sampling areas, patches and locations; and to provide insights into the trajectory of vegetation cover and thus island development (Figure 2) and whether it was consistent across sampling areas. Therefore, this section, first considers evidence for soil development, then considers trajectories of vegetation development and, finally, considers the robustness of these findings and the approaches used to underpin them.

Evidence for soil development

Three indicators of soil development were investigated: total nitrogen, total organic carbon, and mean weight diameter. The first two indicators are representative of the fertility of the sampled sediment (Gupta and Germida, 1988; Haynes et al., 1991; Mikha et al., 2004) and the third indicator represents particle aggregation (Van Bavel, 1950) in which more stable aggregates signify increase of soil stability. Statistically significant increases were found in all of these indicators with increasing island age, and in the cases of total nitrogen and mean weight diameter, increases were consistent and steady across the chronosequence of samples. These observations are similar to a slow increase in soil total organic carbon and

nitrogen content during the first two years of soil development, observed in a field experiment of recovering pasture after topsoil removal (Ross et al., 1982). Furthermore, the observed increase of total nitrogen content as islands evolved from the building stage into the established stage, might reflect its importance in supporting Poplar root growth as shown in an experimental study on Poplar cuttings treated with high soil nitrogen content (Pregitzer et al.,1995).

This evidence supports the second hypothesis stated in the introduction to this paper, that continuous soil development parallels island development in this highly disturbed island-braided study area. Soil development is observed despite the fact that sediment samples were obtained from within 10 cm depth of the soil surface in a system where island surfaces aggrade vertically at a rapid rate as they progress from pioneer, through building to established islands. Building on the three simple indicators of soil development presented here, statistical modelling of a wide range of biological and physical properties of the sampled soils (Mardhiah et al., submitted), has demonstrated that island age is a good linear predictor of soil development within the investigated segment of the Tagliamento River. However, this linear trajectory would be expected to level off if islands achieve greater ages than those observed in this study, since, for example, soils would be unlikely to achieve greater than 80% of particles aggregated.

Vegetation development across sampling areas of different age

Flood events are recognised as crucial to the recruitment of riparian trees through seed

dispersal and germination (e.g. Ahna et al., 2007; Merritt et al., 2010) and to the erosion mobilisation and deposition of large wood and entire trees (Bertoldi et al., 2013). The aerial image analysis presented in this paper indicates that exceptionally large floods are extremely influential events that can reset the islands that have developed on the braid bars. The images prior to 1970 show negligible vegetation cover at the sampled locations (Figs 6 to 9), indicating that the study reach was probably still recovering from the 1940 flood as well as being heavily impacted by the 1965-1966 floods in the early images. Furthermore, the 2000 flood, which is the largest in recent decades, appears to have had some impact on vegetation cover in three of the four sampling areas. The only area that appears to be unaffected is the 40 year area, where the sampling locations had already aggraded ~ 2 m above the adjacent bar surface level by 2001 (Gurnell and Petts, 2006).

High flow events and related erosion and deposition of alluvial sediments disturb vegetated patches and drive a 'shifting habitat mosaic' (Stanford et al., 2005) that is expressed in the temporal and spatial dynamics of islands. This shifting mosaic was illustrated for the Tagliamento River, by the analysis of historical aerial images (Zanoni et al., 2008), and concluded that islands in the study reach rarely persist for more than 24 years. In the present analysis, it is interesting to note that the only sampling area that shows vegetation prior to 1970 is the 2 year area, where some sparse vegetation is recorded at a few of the sampling locations in 1944 and 1954 images, further underlining the highly dynamic history of the study reach. The presence of a strongly shifting mosaic of islands explains why the sampling areas of different age were spatially discrete and, in some cases, quite small in area. The chances of a large area of a particular age persisting for long in such a

dynamic environment are extremely low.

Within the four island sampling areas, the sampling locations show distinct temporal trajectories of vegetation development following widespread tree deposition by a formative flood. The temporal trajectory is clearest in the two oldest sampling areas, simply because there has been sufficient time since their initiation for island development, and there is a sufficient number of historical sources to track the changes. Trees deposited by a formative flood, progress through pioneer and building island stages until they become part of an established island (Figure 2). This process can be tracked by an increasing presence of sparse vegetation through the pioneer island phase. This then gives way to some mature vegetation as the vegetated area expands and the tree canopy closes, with the development of building islands and eventually a complete mature vegetation cover on established islands.

The 40 year sampling area demonstrates all of these phases of island development (Figure 6). A few of the sampling locations show some sparse vegetation cover in the 1970 photograph with the remaining area being unvegetated. This illustrates an early phase of pioneer island development not dissimilar to the condition of the 2 year sampling area in the 2012 image and the 8 year sampling area in the 2005 image. By the time of the 1986 images, no sampling locations are completely unvegetated, and the majority are covered by a mix of sparse and mature vegetation. This pattern is similar to the 12 year area in the 2012 image and indicates that the islands have gone past the pioneer stage and are now mainly building islands. Although there is a decrease in the proportion of mature vegetation cover

and an increase in the unvegetated proportion at many sampling locations in the 1991 image, presumably in response to the 1990 flood; the cover proportions are still indicative of the presence of predominantly building islands. From 1996, the proportions of unvegetated and sparse vegetation cover are very small, and the sampling locations are dominated by mature vegetation indicative of established island development. If the 40 year area was initiated in 1966, these results suggest a pioneer island phase lasting between 4 and 20 years, and a building island phase commencing between 4 and 20 years and lasting up to a maximum of 30 years following island initiation. These estimates are heavily constrained by the low temporal resolution of the images in the 1960 to 1996 period, and the intervention of the 1990 flood, which appears to have delayed the progress of island development to some extent.

The initial development of the 12 year sampling area is represented by a higher temporal frequency of images (Figure 7). These suggest significant development of pioneer islands in the first 5 years following the 2000 flood (2002, 2003, 2005 images show distinct increases in sparse vegetation cover at the expense of unvegetated cover) with the early phases of building island development evident in the 2012 image (mature vegetation cover appears and there is a complementary decrease in the proportions of sparse vegetation cover). The appearance of building islands within 12 years is consistent with the envelope of 4 to 20 years estimated for the 40 year sampling area.

Linking these observations of island development phases to the development of soil structure and fertility across the chronosequence of sampling locations, illustrates that there

is significant soil development even within the pioneer island stage, when the vegetated patches are still relatively small.

Robustness of the research

While laboratory analyses of sediment properties are subject to error, these errors are largely controlled and quantifiable. Furthermore, the design of the field sampling and the use of appropriate statistical analyses, give confidence not only in the data sets that were generated in the laboratory, but also in the conclusions about soil development that were extracted from the data using statistical analysis techniques.

However, reconstructing the historical development of the sampling areas, and particularly the sampling locations from which sediment samples were obtained, was dependent upon the temporal frequency and spatial resolution of the historical sources that were available, as well as the errors that were inevitably introduced during the extraction of information from those sources. Outputs from all historical analyses of river environments are affected by source frequency, resolution and often error (e.g. when historical maps are used), as well as the errors that propagate through the processes used to extract relevant information from the sources (Grabowski et al., in press).

In the present research, these problems were addressed in three main ways. First, a range of different historical sources was used both before and after the field sampling campaign to ensure that the sampling areas of different age were well-defined and that this was checked

using several different sources and approaches. In every case sources were investigated to search for convergence of evidence and likely errors. Second, the methods of information extraction from aerial images were designed with knowledge of as many of the errors as was possible (see methods section). Third, conclusions were drawn through a statistical analysis of data extracted from the images to establish (i) variability within 'control' images (i.e. repeat images within short periods where no change in vegetation cover was expected) as well as (ii) variability among images potentially capturing 'treatment' by floods (i.e. images collected over periods where large floods were known to have occurred with a sufficient intensity to effect changes in vegetation cover).

Of course there is no substitute for direct measurements of soil properties from samples collected during the development of individual islands. However, when long-term temporal analysis is not feasible, this research has demonstrated the value of careful analysis of historical information to provide insights into the history of locations where contemporary sampling is undertaken.

Acknowledgements

Ulfah Mardhiah's research is funded by the SMART Joint Doctoral Programme (Science for MAnagement of Rivers and their Tidal systems), which is financed by the Erasmus Mundus Programme of the European Union. We would like to thank Dr. Walter Bertoldi for support during the field sampling. We also would like to thank Sabine Artelt for help in the laboratory. Finally, we thank Luca Zanoni, who conducted the geocorrection, registration

and mosaicing of the aerial photographs employed in this research.

References

Abbe TB, Montgomery DR. 2003. Patterns and processes of wood debris accumulation in the Queets river basin, Washington. Geomorphology 51: 81–107.

Ahna C, Mosera KF, Sparks RE, White DC. 2007. Developing a dynamic model to predict the recruitment and early survival of black willow (Salix nigra) in response to different hydrologic conditions Ecol Model 204: 315–325.

Barto EK, Alt F, Oelmann Y, Wilcke W, Rillig MC. 2010. Contributions of biotic and abiotic factors to soil aggregation across a land use gradient. Soil Biology and Biochemistry 42 : 2316–2324.

Bauer A, Black AL. 1994. Quantification of the Effect of Soil Organic Matter Content on Soil Productivity. Soil Science Society of America Journal 58 : 185–193.

Bertoldi W, Gurnell AM, Surian N, Tockner K, Zanoni L, Ziliani L, Zolezzi G. 2009. Understanding reference processes: linkages between river flows, sediment dynamics and vegetated landfroms along the Tagliamento River, Italy. River Research and Applications 25: 501-516.

Bertoldi W, Gurnell AM, Welber M. 2013. Wood recruitment and retention: The fate of eroded trees on a braided river explored using a combination of field and remotely-sensed data sources. Geomorphology 180-181(1): 146-155.

Collins BD, Montgomery DR, Fetherston KL, Abbe TB. 2012. The floodplain large-wood cycle hypothesis: A mechanism for the physical and biotic structuring of temperate forested alluvial valleys in the North Pacific coastal ecoregion. Geomorphology 139–140: 460–470.

Díaz-Zorita M, Perfect E, Grove J. 2002. Disruptive methods for assessing soil structure. Soil and Tillage Research 64 : 3–22.

Edwards P., Kollmann J, Gurnell A., Petts G., Tockner K, Ward J. 1999. A conceptual model of vegetation dynamics on gravel bars of a large Alpine river. Wetlands Ecology and Management 7 : 141–153.

Fetherston KL, Naiman RJ, Bilby RE. 1995. Large woody debris, physical process, and riparian forest development in montane river networks of the Pacific Northwest. Geomorphology 13(1-4): 133-144.

Grabowski RC, Gurnell AM. in press. Using historical data in fluvial geomorphology. In: (Kondolf GM, Piégay H, eds), Tools in Geomorphology, John Wiley and Sons Ltd.

Gradzinski R, Baryla J, Doktor M, Gmur D, Gradzinski M, Kedzior A, et al. 2003. Vegetation-controlled modern anastomosing system of the upper Narew River (NE Poland) and its sediments. Sedimentary Geology 157(3-4): 253-276.

Gumbricht T, McCarthy TS, Bauer P. 2005. The micro-topography of the wetlands of the Okavango Delta, Botswana. Earth Surface Processes and Landforms 30(1): 27-39.

Gupta VVSR, Germida JJ. 1988. Distribution of microbial biomass and its activity in different soil aggregate size classes as affected by cultivation. Soil Biology and Biochemistry 20 : 777–786.

Gurnell AM. 2014. Plants as river ecosystem engineers. Earth Surface Processes and Landforms 39: 4-25.

Gurnell AM, O'Hare MT, O'Hare JM, Scarlett P, Liffen TMR. 2013. The geomorphological context and impact of the linear emergent macrophyte, Sparganium erectum L.: a statistical analysis of observations from British rivers. Earth Surface Processes and Landforms 38(15): 1869-1880.

Gurnell AM, Petts GE. 2006. Trees as riparian engineers: the Tagliamento River, Italy. Earth Surface Processes and Landforms 31: 1558-1574.

Gurnell AM, Petts GE, Hannah DM, Smith BPG, Edwards PJ, Kollmann J, et al. 2001.

Riparian vegetation and island formation along the gravel-bed Fiume Tagliamento, Italy. Earth Surface Processes and Landforms 26(1): 31-62.

Gurnell A, Tockner K, Edwards PJ, Petts GE. 2005. Effects of deposited wood on biocomplexity of river corridors. Frontiers in Ecology and Environment 3(7): 377–382.

Harris D, Horwáth WR, Kessel C Van. 2001. Acid fumigation of soils to remove carbonates prior to total organic carbon or carbon-13 isotopic analysis. Soil Science Society of America Journal 65 : 1853–1856.

Haynes RJ, Swift RS, Stephen RC. 1991. Influence of mixed cropping rotations (pasture-arable) on organic matter content, water stable aggregation and clod porosity in a group of soils. Soil and Tillage Research 19 : 77–87.

Jacobson PJ, Jacobson KM, Angermeier PL, Cherry DS. 1999. Transport, retention, and ecological significance of woody debris within a large ephemeral river. Journal of the North American Benthological Society 18(4): 429-444.

Karrenberg S, Kollmann J, Edwards PJ, Gurnell AM, Petts GE. 2003. Basic and Applied Ecology Patterns in woody vegetation along the active zone of a near-natural Alpine river. Basic and Applied Ecology 4 : 157–166.

Kemper W., Rosenau R. 1986. Aggregate Stability and Size Distribution. In Methods of

Soil Analysis, Part 1. Physical and Mineralogical Methods. ,. American Society of Agronomy/Soil Science Society of America; 425–442.

Liffen T, Gurnell AM, O'Hare MT, Pollen-Bankhead N, Simon A. 2013. Associations between the morphology and biomechanical properties of Sparganium erectum: Implications for survival and ecosystem engineering. Aquatic Botany 105: 18-24.

Maione U, Machine G. 1982. Studio sulla formazione delle piene del Fiume Tagliamento. ETACONSULT; Milan.

Mardhiah U, Caruso T, Gurnell AM, Rillig MC. Just a matter of time: fungi and roots significantly and rapidly aggregate soil over four decades along the Tagliamento River, NE Italy, submitted.

McKenney R, Jacobson RB, Wertheimer RC. 1995. Woody vegetation and channel morphogenesis in low-gradient, gravel-bed streams in the Ozark Plateaus, Missouri and Arkansas. Geomorphology 13(1-4): 175-198.

Merritt DM, Scott ML, LeRoy Poff N, Auble GT, Lytle DA. 2010. Theory, methods and tools for determining environmental flows for riparian vegetation: riparian vegetation-flow response guilds. Freshw Biol 55(1): 206-225.

Mikha MM, Rice CW. 2004. Tillage and Manure Effects on Soil and Aggregate-Associated

Carbon and Nitrogen. Soil Science Society of America Journal 68 : 809–816.

Montgomery DR, Abbe TB. 2006. Influence of logjam-formed hard points on the formation of valley-bottom landforms in an old-growth forest valley, Queets River, Washington, USA. Quaternary Research 65(1): 147-155.

Oades JM. 1984. Soil organic matter and structural stability: mechanisms and implications for management. Plant and soil 76 : 319–337.

Pettit NE, Naiman RJ. 2006. Flood-deposited wood creates regeneration niches for riparian vegetation on a semi-arid South African river. Journal of Vegetation Science 17: 615-624.

Pregitzer KS, Zak DR, Curtis PS, Kubiske ME, Teeri JA, Vogel CS. 1995. Atmospheric CO2, soil nitrogen and turnover of fine roots. New Phytologist 129 : 579–585.

R Development Core Team . 2012. R: A Language and Environment for Statistical Computing. R Foundation for Statistical Computing, Vienna, Austria, 2007 [online] Available from: http://www.r-project.org/

Ross DJ, Speir TW, Tate KR, Cairns A, Meyrick KF, Pansier EA. 1982. Restoration of pasture after topsoil removal: Effects on soil carbon and nitrogen mineralization, microbial biomass and enzyme activities. Soil Biology and Biochemistry 14 : 575–581.

Sainju UM, Sciences C, Lisbon N. 1993. Vertical root distribution in relation to soil properties in New Jersey Pinelands forests. Plant and Soil 150 : 87–97.

Six J, Paustian K, Elliott ET, Combrink C. 2000. Soil Structure and Organic Matter I. Distribution of Aggregate-Size Classes and Aggregate-Associated Carbon. Soil Science Society of America Journal 64: 681–689.

Stanford JA, Lorang MS, Hauer FR. 2005. The shifting habitat mosaic of river ecosystems. Verh Internat Verein Limnol 29: 123-136.

Tisdall J., Oades J. 1982. Organic matter and water-stable aggregates in soils. Journal of Soil Science 33 : 141–163.

Tockner K, Malard F, Ward JV. 2000. An extension of the flood pulse concept. Hydrol Process 14(16-17): 2861-2883.

Tockner K, Ward JV, Arscott DB, Edwards PJ, Kollmann J, Gurnell AM, Petts GE, Maiolini B. 2003. The Tagliamento River: a model ecosystem of European importance. Aquatic Sciences 65(3): 239-253.

Tooth S, Nanson GC. 2000. The role of vegetation in the formation of anabranching channels in an ephemeral river, Northern plains, arid central Australia Hydrol Process 14: 3099-3117.

Van Bavel CHM. 1950. Mean Weight-Diameter of Soil Aggregates as a Statistical Index of Aggregation. Soil Science Society of America Journal 14 : 20–23.

Wetzel PR. 2002. Tree Islands of the World. In: Tree islands of the Everglades, (Sklar FH, van der Valk AG, eds). Dordrecht The Netherlands:Kluwer Academic Publishers.

Wetzel PR, van der Valk AG, Newman S, Gawlik DE, Troxler Gann T, Coronado-Molina CA, Childers DL, Sklar FH. 2005. Maintaining tree islands in the Florida Everglades: nutrient redistribution is the key. Frontiers in Ecology and Environment 3(7): 370-376.

Zanoni L, Gurnell AM, Drake N, Surian N. 2008. Island dynamics in a braided river from an analysis of historical maps and air photographs. River Research and Applications 24: 1141-1159.

CHAPTER 3

Just a matter of time: fungi and roots significantly and rapidly aggregate soil over four decades along the Tagliamento River, NE Italy

Ulfah Mardhiah, Tancredi Caruso, Matthias C Rillig, Angela Gurnell

The following version has been published as:

Mardhiah, U., Caruso, T., Gurnell, A., Rillig, M. C., 2014. Just a matter of time: Fungi and roots significantly and rapidly aggregate soil over four decades along the Tagliamento River, NE Italy. Soil Biology and Biochemistry 75, 133-142.

http://dx.doi.org/10.1016/j.soilbio.2014.04.012

Just a matter of time: fungi and roots significantly and rapidly aggregate soil over four decades along the Tagliamento River, NE Italy

Abstract

Fluvial islands are emergent landforms which form at the interface between the permanently inundated areas of the river channel and the more stable areas of the floodplain as a result of interactions between physical river processes, wood and riparian vegetation. These highly dynamical systems are ideal to study soil structure development in the short to medium term, a process in which soil biota and plants play a substantial role. We investigated soil structure development on islands along a 40 year chronosequence within a 3 km island-braided reach of the Tagliamento River, Northeastern Italy. We used several parameters to capture different aspects of the soil structure, and measured biotic (e.g., fungal and plant root parameters) and abiotic (e.g. organic carbon) factors expected to determine the structure. We estimated models relating soil structure to its determinants, and, in order to confer statistical robustness to our results, we explicitly took into account spatial autocorrelation, which is present due to the space for time substitution inherent in the study of chronosequences and may have confounded results of previous studies. We found that, despite the eroding forces from the hydrological and geomorphological dynamics to which the system is subject, all soil structure variables significantly, and in some case greatly increased with site age. We interpret this as a macroscopic proxy for the major direct and indirect binding effects exerted by root variables and extraradical hyphae of arbuscular mycorrhizal fungi (AMF). Key soil structure parameters such as percentage of water stable

aggregates (WSA) can double from the time the island landform is initiated (mean WSA = 30 %) to the full 40 years (mean WSA = 64 %) covered by our chronosequence. The study demonstrates the fundamental role of soil biota and plant roots in aggregating soils even in a system in which intense short to medium term physical disturbances are common.

Keywords: Soil aggregation, fungal hyphae, plant roots, fluvial island, chronoseqeuence, abiotic factors

Introduction

Soil structure emerges from the arrangement of primary soil particles into secondary units or soil aggregates (Soil Science Society of America, 2008). Several properties and functions also emerge from the interaction between the biotic and abiotic components of the soil matrix. Soil structure is of great importance in supporting the growth of plants and soil organisms (Oades, 1984; Passioura, 1991), enhancing the resistance of soil to erosion (Diaz-Zorita *et al.*, 2002), reducing nutrient leaching (Elliot and Coleman, 1988) and assisting carbon sequestration (Wilson *et al.*, 2009). Soil aggregation, the process by which primary soil particles are bound and oriented together to form larger complexes, either through chemical or physical processes in the soil matrix or both (Allison, 1968; Tisdall and Oades, 1982), is a key aspect of soil structure (Six *et al.*, 2000; Diaz-Zorita *et al.*, 2002; Tisdall and Oades, 1982). Tisdall and Oades (1982) suggested a hierarchical hypothesis for soil aggregate formation: aggregation takes place through the binding of clay particles forming microaggregates, which are further bound together to form macroaggregates. Regardless of the specific physico-chemical details of the mechanisms involved in aggregation, several biotic and abiotic factors determine the quality, quantity and speed of soil aggregate formation. These factors include the abundance of primary soil particle sizes (clay, silt or sand) (Allison, 1968; Tisdall and Oades, 1982), biological exudates (Tisdall and Oades, 1982), organo-metallic compounds and cations (Bronick and Lal, 2005), soil carbon and soil nitrogen content (Gupta and Germida, 1988; Haynes *et al.*, 1991; Mikha and Rice, 2004), and the enmeshment of particles by fine roots and fungal hyphae (Tisdall and Oades, 1982; Rillig and Mummey, 2006). Tisdall and Oades (1982) described the

temporal persistence of organic binding from transient (polysaccharides), temporary (root, hyphae and microbial cells) and persistent (humic substances) elements.

Although most studies investigating soil structure have focused on agricultural ecosystems and the agroeconomical aspects of soil structure (Elliot and Coleman, 1988; Jastrow *et al.*, 1998; Diaz-Zorita *et al.*, 2002), there is a growing interest in the study of soil structure dynamics in natural ecosystems, including riparian areas (Piotrowski *et al.*, 2008; Harner *et al.*, 2011). Studying soil structure in such ecosystems provides insights into the natural dynamics of soil structure development and might be used for management purposes in the restoration of natural or semi-natural systems.

River floodplains are areas of low lying land that are constructed by river processes and are subject to frequent fluvial disturbances through inundation, erosion and construction processes (Ward *et al.*, 1999; Naiman *et al.*, 2005). As a result, they are very dynamic, diverse and productive areas (Tockner and Stanford, 2002), which provide an ecotone between the upland terrestrial and river channel aquatic ecosystems (Gregory *et al.*, 1991). Through their ecotonal nature, they display sharp gradients in environmental conditions, ecological processes and plant communities (Gregory *et al.,* 1991). Overall, floodplains offer great opportunities to investigate the process of soil aggregation and its association with issues of applied soil ecology.

Fluvial islands develop at the interface between the permanently inundated areas of the river channel and the more stable areas of the floodplain (the riparian zone), where they

may attach to and extend the floodplain through sediment accretion and island enlargement or they may be excised from the floodplain by fluvial erosion processes (Gurnell *et al.*, 2001). Fluvial islands are particularly interesting with regard to soil aggregation because in most cases they are emergent landforms that develop and grow as a result of interactions between fluvial processes and riparian vegetation including large wood (Osterkamp, 1998; Ward *et al.*, 1999, Gurnell *et al.*, 2005). These 'building' islands (Gurnell *et al.*, 2001) are formed through a successional process that, in highly disturbed, large rivers, commences with the deposition of uprooted trees on gravel bar surfaces during the falling stages of major floods. In the case of riparian Saliceae species (willows and poplars), these stranded trees rapidly produce roots and shoots, which anchor them to the gravel substrate and form a flow-resistant canopy around which finer sediment, more wood pieces and other plant propagules accumulate to form 'pioneer' islands. Pioneer islands aggrade upwards and extend laterally as they accumulate more sediment, wood and seeds, develop an increasingly large and diverse vegetation canopy, and coalesce to form 'building' and eventually large 'established' islands (Edwards *et al.*, 1999; Kollman *et al*., 1999; Gurnell *et al.,* 2001, 2005). Mosaics of islands develop through this process of island growth and coalescence and also as a result of erosion and removal during different flood events, providing island surfaces of different age and elevation that are subject to different levels of disturbance and display different geomorphological characteristics (Gurnell *et al.*, 2001).

Previous research on chronosequences of surfaces within the riparian zone have investigated colonization of roots by arbuscular mychorrizal fungi (AMF) and the growth of AMF extraradical hyphae in the soil matrix, which have been shown to positively

influence the development of soil aggregation (Miller and Jastrow, 1990; Bearden and Petersen, 2000; Rillig *et al.*, 2002; Rillig and Mummey, 2006). A chronosequence study of soil development within the riparian zone of the Nyack River, Montana, USA was conducted by Piotrowski *et al.* (2008), and showed an increase of soil aggregates size class 1-2 mm which coincided with an increase of AMF abundance during the first 13 years of the succession. Harner *et al.* (2011) conducted a study on a reach of the Tagliamento River, Italy, in which they categorized island types into depositional surfaces, pioneer and established islands and showed that soil aggregates size class 1-2 mm increased with site development which correlated positively to root length colonized by AMF and also AMF hyphal length.

The present research takes advantage of the process of island initiation and growth to investigate how soils develop on island surfaces of different age, with a particular emphasis on the process of soil aggregation. Here we aimed at improving our understanding of this process (i) by investigating soil structure development in a spatially explicit way (taking into account autocorrelation); and (ii) by basing inferences on a more comprehensive set of soil structure indices for macroaggregates (diameter 0.212-4 mm) on quantitatively determined island age. The research also investigates the effect of biotic and abiotic parameters on soil structure along a well established and replicated chronosequence of islands on the Tagliamento River, Italy and also assigns importance of the various biotic and abiotic variables for explaining the different soil structure indices.

Methods

Research Site

The research was conducted on fluvial islands of the Tagliamento River, in Northeastern Italy. The Tagliamento is the last morphologically intact Alpine river system in Europe (Müller, 1995; Ward *et al*., 1999), thereby providing a model ecosystem in which riparian processes can be investigated (Tockner et al., 2003). The river traverses a length of 172 km from its headwaters in the Italian Alps to its mouth in the Adriatic Sea. The river has a flashy pluvio-nival regime (mean stream discharge; Q_{mean}): 109 m^3/s, flood flows up to 4000 m^3/s), which, during large floods, supplies the river's active, braided channel and margins with numerous newly uprooted trees that underpin island development (Ward *et al*., 1999).

The research was conducted within a 3 km long, island-braided, gravel bed reach of the Tagliamento River located between 79.5 and 81.5 km from the river's source (46°12'24.03"N, 12°59'40.06"E to 46°12'3.62"N, 12°58'4.82"E). The reach is elevated approximately 140 m.a.s.l., and has an active corridor up to 1 km in width that contains numerous islands at different successional stages (Kollman *et al.*,1999). Geomorphic features within the reach include multiple channels, gravel bars, pools, wooded islands and in the less frequently inundated, relatively stable areas of the floodplain, extensive forest. The dominant tree species is black poplar (*Populus nigra* L.), which sprouts freely following uprooting to drive island development (Gurnell *et al.*, 2001). However, several willow species (*Salix alba* L., *S. daphnoides* Vill., *S. elaeagnos* Scop., *S. purpurea* L., *S.*

triandra L.*)* and alder (*Alnus incana* L.) are also abundant. Particle size distribution between different geomorphological settings (surface of established islands or floodplain, pioneer islands on gravel bar surfaces and open gravel bar surfaces) showed no significant difference (Gurnell *et al.*, 2008).

Sampling sites

The replicated chronosequence of sites that were sampled within the study reach is shown in Figure III. 1. Sites ranged from 0 to 40 years since the initiation of island formation, with site and patch ages established through the analysis of a historical sequence of air photographs, with precise dates confirmed by major flood events in the river flow record (Mardhiah *et al.*, submitted). Field sampling was conducted from 13-16 May 2012.

Areas of the study reach occupied by islands or open gravel bar surfaces of five different ages (0, 2, 8, 12 and 40 years) were identified. Within each of these areas, seven pioneer islands, all centred on *P. nigra,* were randomly selected for soil and root sampling (except for age 0, where no islands were present). However, for the oldest site (40 years), sampled patches were located within established islands where the original pioneer islands were no longer identifiable. Therefore, within this site, sampling was undertaken around seven of the largest trees (all *P. nigra*), which were most likely to date back to the original pioneer islands within the site. To verify the age of each sampled patch, an increment borer was used to extract a core from the central tree at 1 m above the ground surface. The number of annual growth rings was then counted to estimate tree and island age. This approach, combined with the investigation of vegetation cover change from the historical sequence of

air photographs, confirmed our tree and island age (Mardhiah *et al.*, submitted).

Within each sampled patch, one soil sample was taken towards the upstream end of the island (at or approximating the position of the root bole of the original deposited tree), one at the centre of the island (at or approximating the position of the tree trunk), and one towards the downstream end of the island (at or approximating the upper part of the trunk within the canopy) while recording the distance from the root bole. To collect soil samples to a depth of 10 cm, we used a cylindrical corer (core diameter: 5 cm; core volume: 196.25 cm^3). There were two exceptions to this sampling design. At patches of age 0 years (i.e. open bar surface sites where no deposited tree or island was present), only 1 sample was taken in each patch from the open gravel bar surface to provide a baseline for soil structure analysis. For patch age 40, where the original pioneer island forms were no longer identifiable, three samples were taken randomly within a 5 x 5 m^2 area centred on a large black poplar tree. In each case, the sample sites were recorded using a hand held GPS, with additional measurements of distance from the central tree on the age 40 sites, where the tree canopy often made the GPS readings unstable. Overall, 91 soil core samples were obtained, seven for age 0 years and 21 for each of age 2, 8, 12 and 40 years (Figure III. 1).

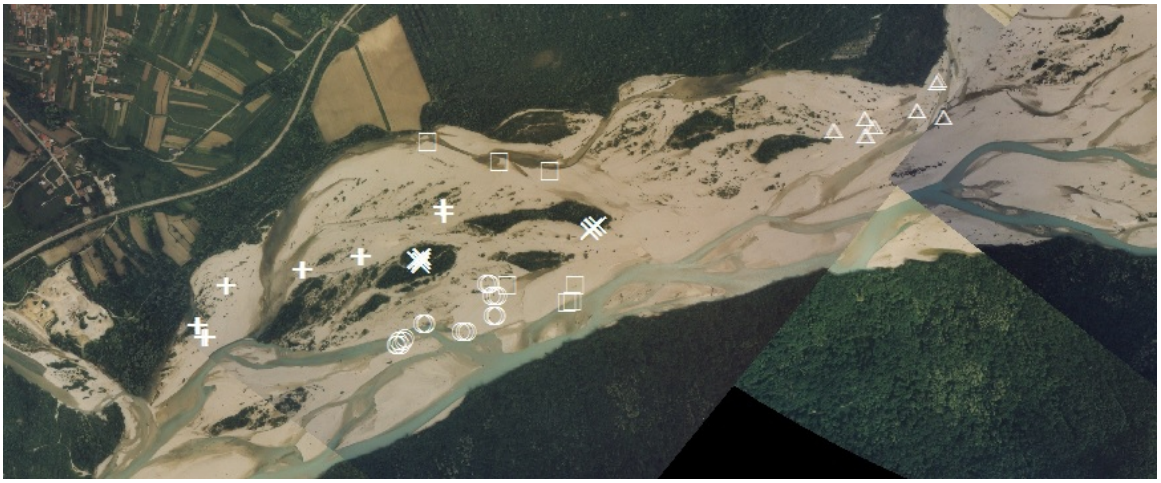

Figure III. 1. The study reach, Tagliamento River, Italy, photographed on 23 May 2005 locating the sampling patches within the sites of different age (□ = age 0; ○ = age 2; Δ = age 8; + = age 12; X = age 40). The figure illustrates the potential for some autocorrelation in the data because of the close proximity of some sampling sites. (photographs provided by the United Kingdom Natural Environment Research Council, and geocorrected and referenced by Luca Zanoni).

Soil aggregation measurements

Soil samples were sieved through a 4-mm sieve before and after being air-dried at room temperature for several days. Aggregate stability was measured as the abundance of water stable aggregates (WSA) by immersing a stack of sieves (from top to bottom: 2-mm, 1-mm, 0.5-mm, 212-μm) in a bucket of water (Kemper and Rosenau, 1986). Well mixed fifty grams of air-dried soil was rewetted by capillary action and was then carefully placed on the top sieve of the stack. All sieves were kept immersed while being moved up and down (approximately 3 cm) for 10 min. The material remaining on each sieve was then crushed and passed through the sieve, to separate the material into soil (passing through the sieve) and coarse (remaining on the sieve) fractions. Soil fractions from each sieve size (2-4 mm, 1-2 mm, 0.5-1 mm and 0.2-0.5 mm) were collected, dried at 80°C, and then weighed separately. Total coarse material, primarily sand, was also weighed.

We approached soil aggregation using indices of aggregates in each size classes (2-4 mm, 1-2 mm, 0.5-1 mm and 0.2-0.5 mm), percent total WSA, mean weight diameter (MWD) and also fractal dimension. To calculate the percentage of WSA in each size class, we calculated the weight of the soil fraction in each size class divided by the total weight of the soil fraction (excluding coarse material fractions). For percent total WSA, we summed all percent WSA from each size class.

Mean weight diameter (MWD) was calculated as the sum of the proportion of aggregates in each size class (2-4 mm, 1-2 mm, 0.5-1 mm and 0.2-0.5 mm), proportionally weighted by the mean diameter of aggregates in that size class (approached as mean size of upper and lower limit of sieve size used: 3 mm, 1.5 mm, 0.75 mm and 0.356 mm respectively) (Barto *et al.*, 2010). Fractal geometry is a way to describe soil architectural complexity using a scaling exponent which relates mass and number of aggregates/particles to aggregate/particle size (Caruso and Rillig, 2011); the scaling exponent is known as the fractal dimension (D). We approached estimation of the fractal dimension using the bounded fractal dimension equation as outlined in Caruso *et al.* (2011) which limits fractal dimension (D) values to the range $0 < D < 3$. Low D values (closer to 0) describe soil samples with a more evenly distributed number of particles of each particle size class. In contrast, high D values (closer to 3) describe soil samples which have a less even distribution of particle numbers of each particle size class.

Bulk density was measured by calculating the proportion of fresh soil mass in the whole

core volume and used to convert mass to volume of soil. Meanwhile, root biomass was measured by extracting well mixed 10.0 grams of air dried soil, applying the root extraction-flotation method (Cook *et al.,* 1988) and then calculating the total root mass per volume of soil. Total root length was measured by scanning and then analyzing the scanned image using WinRhizo Pro 2007d (Regent Instruments Inc., Quebec City, Canada). The root length data was grouped by root diameter, and also by length: very fine root length (0-0.2 mm), fine root length (0.2-1 mm) and coarse root length (> 0.1 mm) (Jastrow *et al.,* 1998; Barto *et al.,* 2010).

Hyphae were extracted from well mixed 4.0 grams of dried soil using a protocol adapted from Jakobsen *et al.* (1992). A 5 ml aliquot was then stained with Trypan Blue for 5 minutes, rinsed with deionized water and transferred to a filter paper. To calculate the AMF extraradical hyphal length (and the length of hyphae stemming from non-AMF), the number of intersects of hyphae with the cross-hair ocular piece within each filter paper was counted for a total of 50 stops at 200X magnification.

Total N and organic C were determined using a EuroEA Elemental Analyzer. The samples were fumigated with 12 M HCl to remove carbonates (Harris *et al.*, 2001). Nitrogen is an indicator of soil fertility and both N and organic C can influence aggregate stability (Haynes *et al.*, 1991; Mikha and Rice, 2004). Soil pH was estimated using a pH electrode by stirring 3 grams of soil with 15 ml of 0.01 M $CaCl_2$ solution.

Statistical analysis

Assessing determinants of soil structure and soil structure variables as a function of age

Soil structure variables (each aggregation size class, total WSA, MWD and fractal dimension) and biotic and abiotic determinants of soil structure (root biomass, AMF extraradical hyphal length, non-AMF hyphal length, total nitrogen, total organic carbon, very fine root length, fine root length, coarse root length and pH) were modelled as a function of soil age (Fig. III. 2; Table III. 1; Suppl. Mat. 2, Fig. III. S1; Suppl. Mat. 2, Fig. III. S2). The models were validated by ensuring that they met the assumptions underlying linear regression analysis. All statistical analyses were conducted using R v.2.14.0 (R Development Core Team, 2011). Different R packages were used to address specific analyses. Violation of homogeneity of variances was corrected using the generalized least squares (GLS) method (package nlme; Pinheiro, *et al.*, 2011). Due to the nature of the sampling design, which is based on multiple locations along a chronosequence, we further checked the assumption of spatial independence through variograms and the analysis of autocorrelation using the package AED (Zuur, 2010; Suppl. Mat. 3, Fig. III. S3) and then corrected the model by adding a spatial correlation structure to the GLS model (package nlme; Pinheiro, *et al.*, 2011). R^2 values for GLS models were generated using the R package MuMIn (Bartoń, 2013).

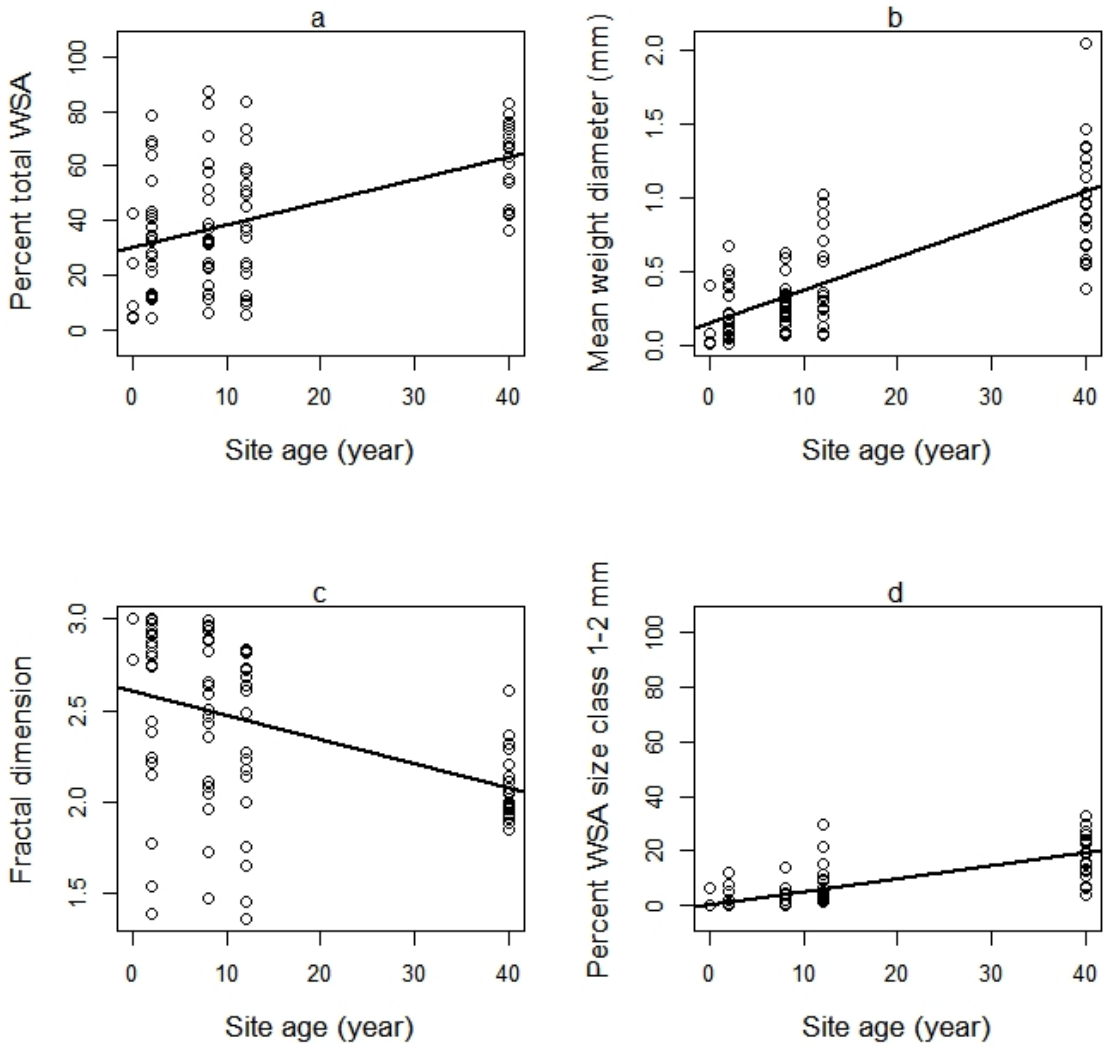
a
Percent total WSA
0
20
40
60
80
100
0
10
20
30
40
Site age (year)
b
Mean weight diameter (mm)
0.0
0.5
1.0
1.5
2.0
0
10
20
30
40
Site age (year)
c
Fractal dimension
1.5
2.0
2.5
3.0
0
10
20
30
40
Site age (year)
d
Percent WSA size class 1-2 mm
0
20
40
60
80
100
0
10
20
30
40
Site age (year)

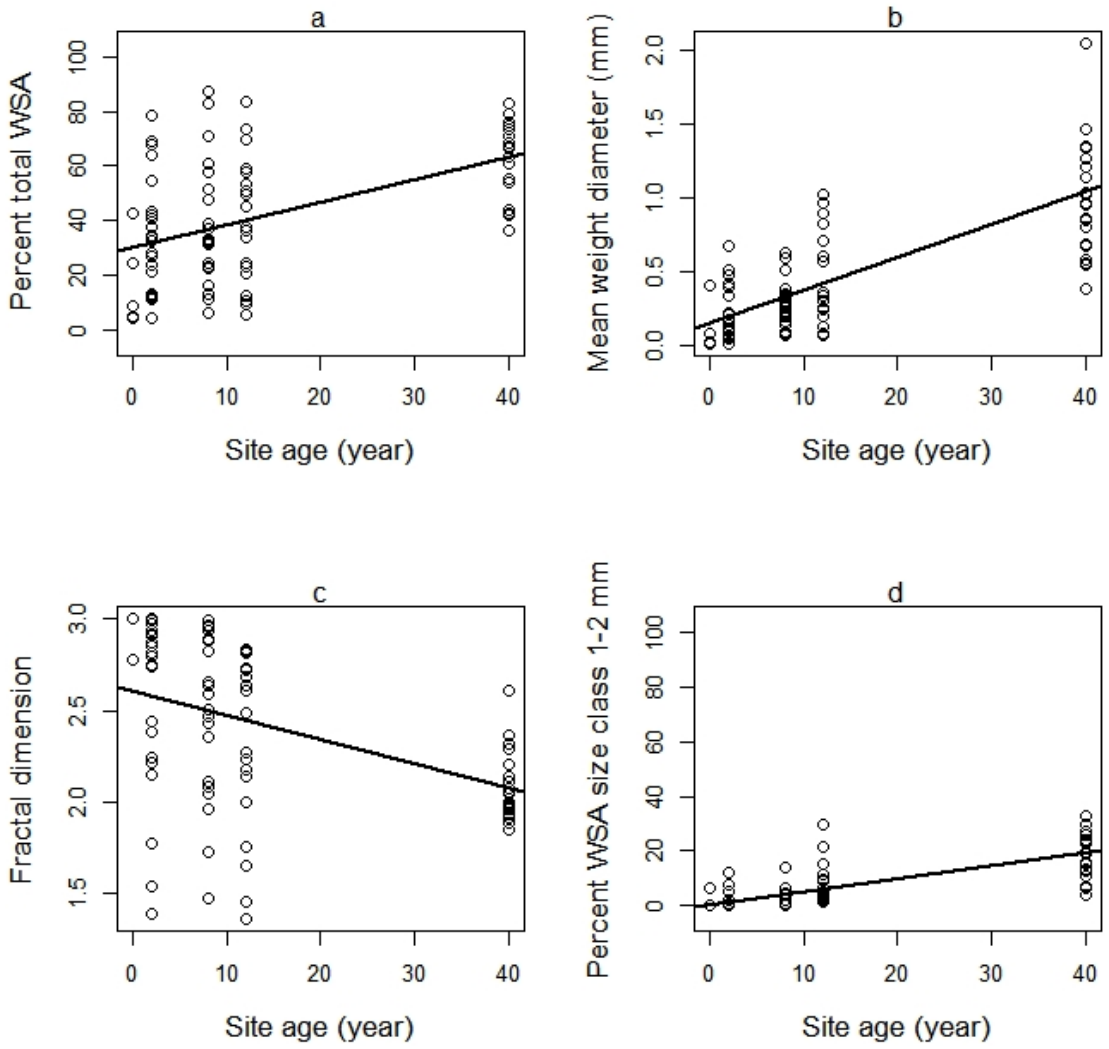

Figure III. 2. The response of soil aggregation (y axis) to soil age (x-axis) is represented using several different indices of soil structure: (a) percent total water stable aggregates (WSA) (a); (b) mean weight diameter (MWD); (c) fractal dimension; and (d) percent WSA for size class 1-2 mm. All linear regression models are fitted following correction for heterogeneity of variances and spatial autocorrelation using the generalized least squares method. Model parameters used to calculate the regression line are given in Table 1.

Correlation within and between soil structure variables: PCA and linear models

All the measured variables were linearly correlated to some extent, as all variables apart

from the fractal dimension and pH increased with soil age. We therefore used ordination multivariate analysis to summarize major patterns of covariation in the data (Suppl. Mat. 2, Table III. S9). We then used the ordination axes as indices of soil structure variables and soil structure determinants to account for different fractions of variation in these two sets of variables. Specifically, we performed three principal components analyses (PCAs) on the correlation matrix of the following datasets: 1) the four soil aggregation size classes (size classes 2-4, 1-2, 0.5-1, and 0.2-0.5 mm); 2) the three soil structure indices (WSA, MWD and fractal dimension); 3) biotic (root biomass, AMF extraradical hyphal length, non-AMF hyphal length, very fine root length, fine root length, and coarse root length) and abiotic (total nitrogen, total organic carbon and pH) determinants of soil structure. PCA axes obtained from the determinants of soil structure were used in GLS regression models as the predictors of the PCA axes obtained from PCA on soil aggregate size classes and soil structure indices, respectively. PCA was calculated using the R vegan package (Oksanen *et al.,* 2010).

Table III.1. Linear models for each of the measured variables, which are here modelled as a function of soil age. The variables are: the four aggregate (Agg.) size classes (see also Suppl. Mat. 3, Fig. III. S1), total water stable aggregates (WSA) (Fig. III. 2a), mean weight diameter (MWD) (Fig. 2b), fractal dimension (Fig. III. 2c), and all the variables that can determine soil structure (root biomass, arbuscular mycorrhizal fungi (AMF) extraradical hyphal length, non-AMF hyphal length, very fine root length, fine root length, coarse root length, total nitrogen content, organic carbon content, and pH; see also Supp. Mat. 3, Fig. III. S2). Models are fitted using the generalized least squares (GLS) method to correct for heterogeneity of variances and spatial autocorrelation. Only in the case of pH were these corrections not necessary. Regression parameters (estimated mean value) in bold were significant at $P < 0.01$. Model intercept is the last parameter in the equation.

Model with estimated parameters (GLS)	**R^2**
Soil structure:	
Agg. size class (2-4 mm) = **0.40** • (year)-0.038	0.83

Agg. Size class (1-2 mm) = **0.47** • (year)+0.556	0.71
Agg. size class (0.5-1 mm) = 0.12 • (year)+14.402	0.16
Agg. size class (0.2-0.5 mm) = **-0.17** • (year)+15.078	0.28
% total WSA = **0.84** • (year)+30.136	0.35
MWD (mm) = **0.02** • (year)+0.153	0.68
Fractal dimension = **-0.01** • (year)+2.603	0.37
Soil structure determinants:	
Root biomass (gr/cm^3) = **0.20** • (year)+0.09	0.81
AMF extraradical hyphal length (m/cm^3) = **0.38** • (year)+1.164	0.69
Non AMF hyphal length (m/cm^3) = **0.15** • (year)+0.14	0.70
Total % nitrogen = **0.003** • (year)+0.008	0.87
% organic carbon = **0.05** • (year)+0.827	0.36
Very fine root length (cm/cm^3) = **0.12** • (year)+0.489	0.44
Fine root length (cm/cm^3) = **0.36** • (year)+1.758	0.48
Coarse root length (cm/cm^3) = **0.02** • (year)-0.005	0.72
pH = **-0.007** • (year)+7.665	0.54

Results

Soil development and determinants of soil structure variables increase along chronosequence

Even after the correction for heterogeneity of variances and spatial autocorrelation, we are able to report that all response variables of soil aggregation (four soil aggregate size classes and three soil aggregation indices) increased significantly (and decreased for fractal dimension) along the chronosequence except for soil aggregate size class 0.5-1 mm, which did not show any significant trend, and soil aggregate size class 0.2-0.5 mm, which showed a significant decrease. For the four aggregate size classes, the strongest increase was observed for soil aggregate size class 1-2 mm (Table III. 1). Meanwhile, for the three soil aggregation indices (percent total WSA, MWD and fractal dimension) the strongest effects

of age (see slope parameter in the linear regression equations of Table 1) was on total WSA, followed by mean weight diameter and fractal dimension, respectively. Given that the slope of the linear regression parameters links variation in soil structure (e.g. WSA) to variation in time (year; see Figure III. 1), the slope is a rate of variation. This rate was as follows for the three key soil structure parameters: WSA (%), 0.84 unit $\cdot$ year^{-1}; MWD, 0.02 mm $\cdot$ year^{-1}; fractal dimension – 0.01 unit $\cdot$ year^{-1}.

For the soil aggregate size class indices, age was only a significant and strong predictor for the 2-4 and 1-2 mm classes (R^2 = 0.83 and 0.71 respectively), while it weakly predicted (R^2 = 0.28) soil aggregate size class 0.2-0.5 mm. There was no significant relationship between soil aggregate size 0.5-1 mm and age. For the soil aggregation indices only 35% of variation of percent total WSA was explained by the linear regression, while 68% and 37%, respectively, of the mean weight diameter and fractal dimension were explained.

All soil structure determinants (biotic and abiotic) increased significantly along the chronosequence except for pH, which decreased significantly. The slopes of the regression equations in Table III. 1 indicated that the increase was relatively high for AMF extraradical hyphal length, fine root length and root biomass, lower for non AMF hyphal and very fine root length, and much lower for percent total organic carbon, coarse root length, percent total nitrogen and pH (Table III. 1). However, even when the effects of age were not very strong, as expected, age remained a good to very good predictor with R^2 values ranging from 0.36 to 0.87.

Linear regressions on PCA-generated indices

The first principal component (aggregate size class PC1), following PCA on the four aggregate size classes, accounted for 47 % of variance in the data set, while the second axis (aggregate size class PC2) accounted for 30 % of variance (Fig. III. 3a). The major pattern of variation was due to the fact that the two largest size classes strongly co-varied (positive correlation) to determine "aggregate size class PC1" and this positive correlation was closely associated with samples drawn from soils of age 12 and 40 years. The two smallest size classes were inversely associated with "aggregate size class PC2" reflecting variations observed in younger soils (particularly ages 2 and 8 years). This suggests that the four size classes behaved differently with time.

Most of the variance in the three soil structure indices (MWD, total WSA, fractal dimension) was accounted for by the first axis of the PCA (soil structure indices PC1, Figure III. 3b), which explained 81 % of the total covariation between the three indices. As expected (Caruso *et al.*, 2011), MWD and WSA were closely correlated and positively loaded on the PC, while fractal dimension was negatively loaded on the PC and thus inversely related to the other two variables (Caruso *et al.*, 2011).

a.

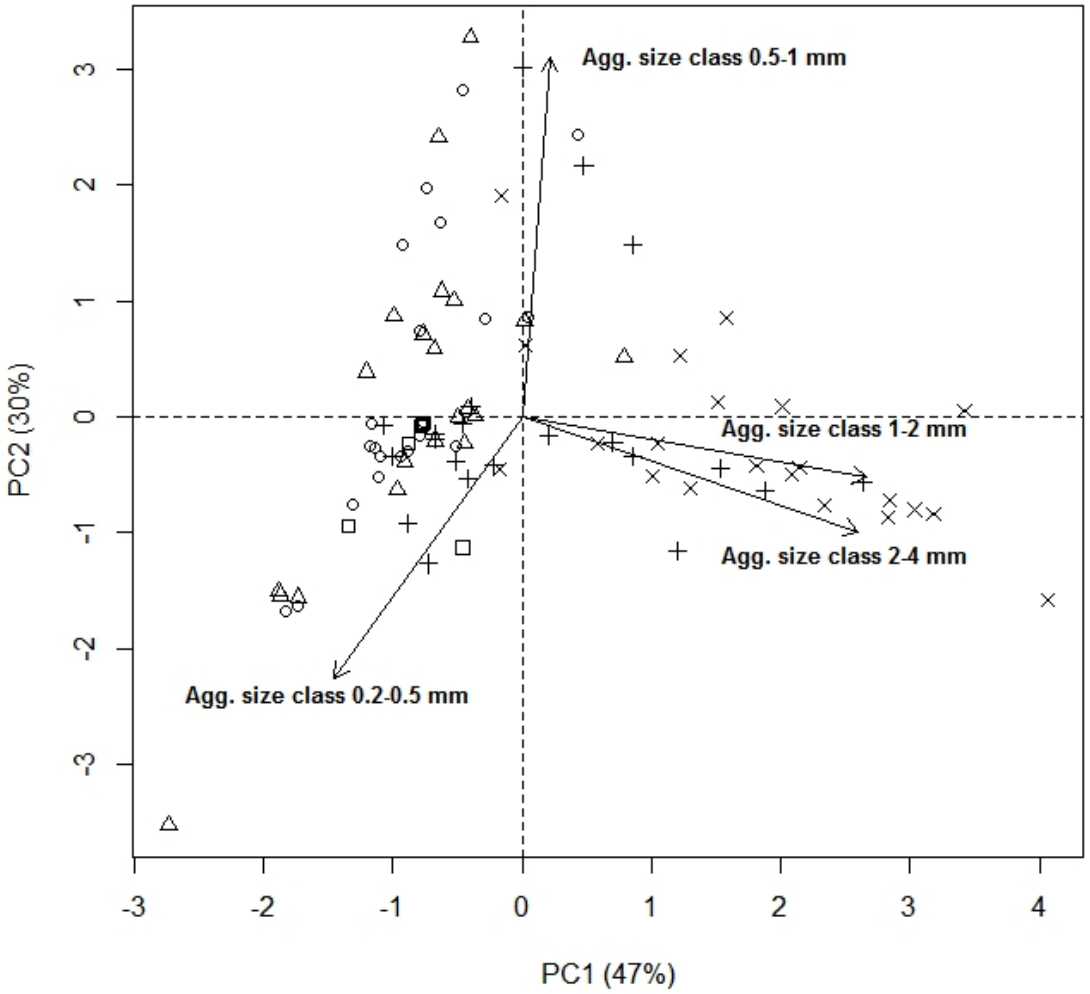

Figure III. 3. For figure legend, see page 77.

b.

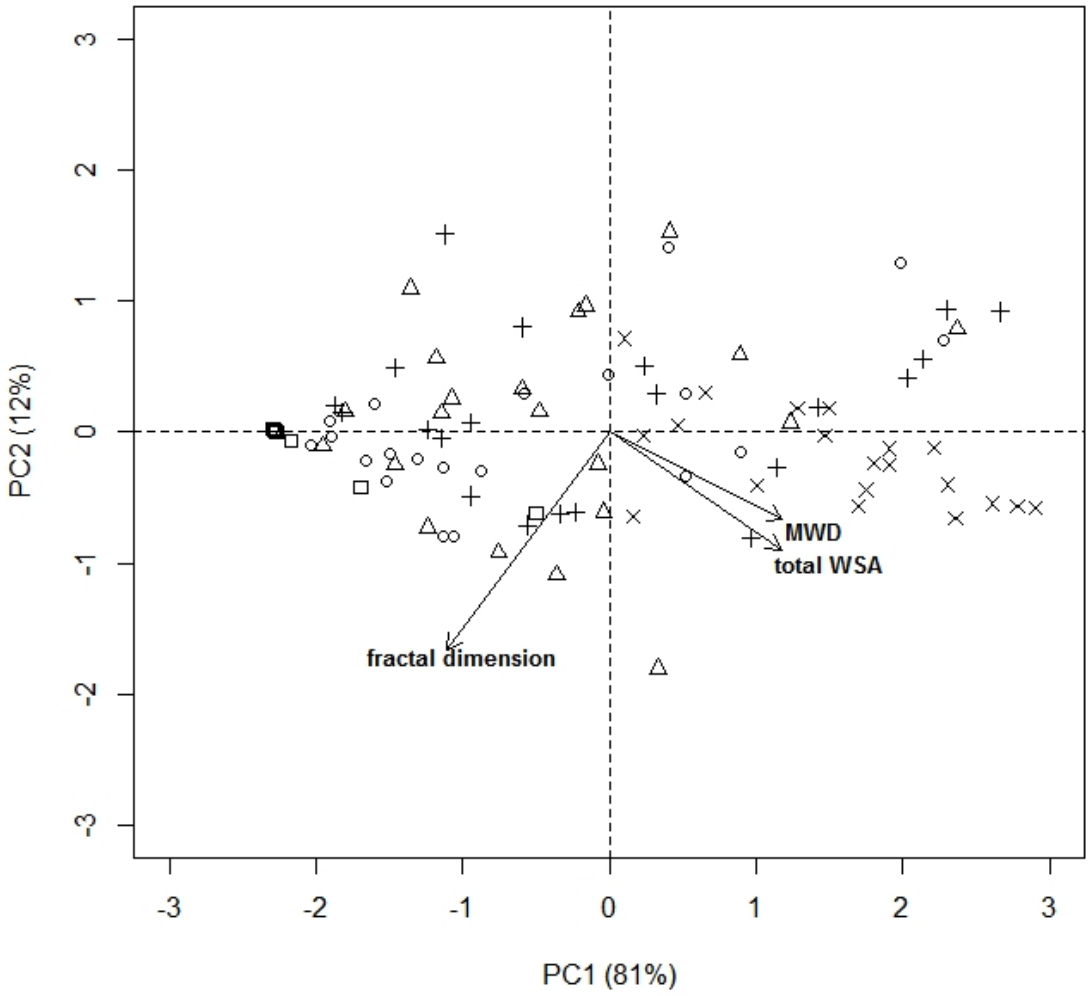

Figure III. 3. For figure legend, see page 77.

c.

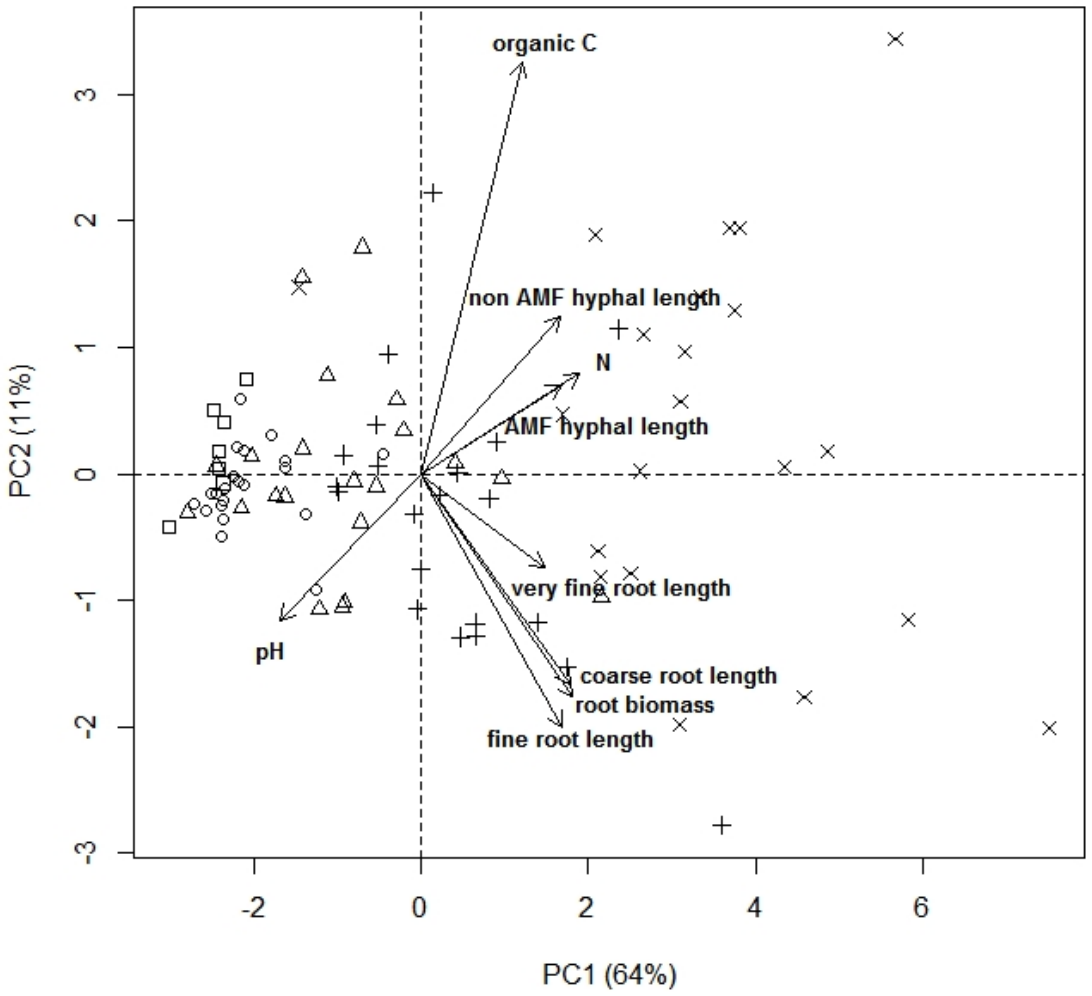

Figure III. 3. Biplots showing variable vectors and samples following Principal Components analysis (PCA) on the following variables: a) aggregate-size classes; b) three soil structure indices, c) soil structure determinants. Sample points are coded according to the age of the site from which they were obtained (□ = age 0; ○ = age 2; Δ = age 8; + = age 12; X= age 40) and clearly show that the distribution of data points along the first two PCA axes is not random relative to age (see Suppl. Mat. 2, Table III. S9). PCA axes were used to model the total effect of soil structure determinants on soil structure (see Fig. III. 4 and Table III. 2).

The first PC (soil structure determinant PC1) revealed by a PCA on the biotic and abiotic factors determining soil structure (Figure III. 3c) accounted for 64% of the variance in the data set and was determined by positive covariation between all variables but pH, which

was negatively loaded on PC1. Considering the scores of the samples on PC1, this pattern clearly reflected soil age, with younger soils having higher pH and lower values for all plant and fungal variables, and C and N. AMF extraradical hyphal length, N, very fine root length, pH and root biomass had the highest loadings on PC1. The second PC (soil structure determinant PC2) accounted for 11 % of the variation with organic C and the fungal variables showing positive loadings and plant root variables and pH showing negative loadings.

Table III. 2. Linear models fitted using the generalized least squares (GLS) method (corrected for heterogeneity of variances and spatial autocorrelation) to test the effect of Soil Structure determinants (Soil str. det., summarized by the first principal component axes (PC1) and the second principal component axes (PC2) illustrated in Fig. 3c) on soil structural parameters (summarized by PC1 illustrated in Fig III. 3b) and on aggregate (Agg.) size class (summarized by PC1 and PC2 illustrated in Fig III. 3a). Models for the same response were compared using the Akaike information criterion (AIC) and the lowest AIC is in bold. Regression parameters (estimated mean value) in bold were significant with $P < 0.01$. The model intercept is the last parameter in the equation.

Model with estimated parameters (GLS)	**AIC**	**R^2**
Agg. size class PC1 = **0.31** • (Soil str. det. PC1) - 0.17	**226.3**	**0.69**
Agg. size class PC1 = 0.0098 • (Soil str. det. PC2) - 2.89	235.9	0.64
Agg. size class PC1 = **0.32** • (Soil str. det. PC1) + 0.05 • (Soil str. det. PC2) - 0.15	230.9	0.69
Agg. size class PC2 = **-0.11** • (Soil str. det. PC1) + 0.05	**278.8**	**0.12**
Agg. size class PC2 = **0.22** • (Soil str. det. PC2) + 0.002 (*)	279.9	0.10
Agg. size class PC2 = **-0.1073** • (Soil str. det. PC1) + 0.15 (Soil str. det. PC2) + 0.03	281.0	0.15
Soil str. PC1 = **0.36** • (Soil str. det. PC1) -0.02	**296.3**	**0.48**
Soil str. PC1 = 0.0007 • (Soil str. det. PC2) + 22.3	305.6	0.37
Soil str. PC1 = **0.37** • (Soil str. det. PC1) + 0.09 (Soil str. det. PC2) - 0.02	300.2	0.48

*P = 0.05

Following the above results, the following GLS models were estimated to model soil structure as a function of major patterns of covariation in biotic and abiotic variables: 1) the size class PC1 (variation in the two largest size classes) was modeled as a function of soil

structure determinants PC1 (essentially AMF extraradical hyphae, N, very fine root length, pH and root biomass) and soil structure determinants PC2 (negative covariation between organic C plus fungal variable, and plant root variables); 2) size class PC2 (negative covariation between the two smaller size classes) as a function of soil structure determinants PC1 and soil structure determinants PC2; 3) soil structure index PC1 (a proxy for progressive increase in WSA and MWD) as a function of soil structure determinants PC1 and soil structure determinants PC2. Based on Akaike information criterion (AIC) model selection, the results showed that the most effective models were: 1) size class PC1 as a function of soil structure determinant PC1; 2) size class PC2 as a function of either PC1 (significant) or PC2 (just on the significance threshold of $P = 0.05$); 3) soil structure PC1 (based on soil structure indices) as a function of soil structure determinant PC1. To further validate our interpretation of multivariate patterns, we conducted a set of linear regression analyses where each aggregate size class and soil structure parameter (MWD, WSA, fractal D) was modelled as a linear combination of all the measured biotic and abiotic variables. These confirmed the results reported above and are provided in Table III. S1-S8 of Suppl. Mat. 1.

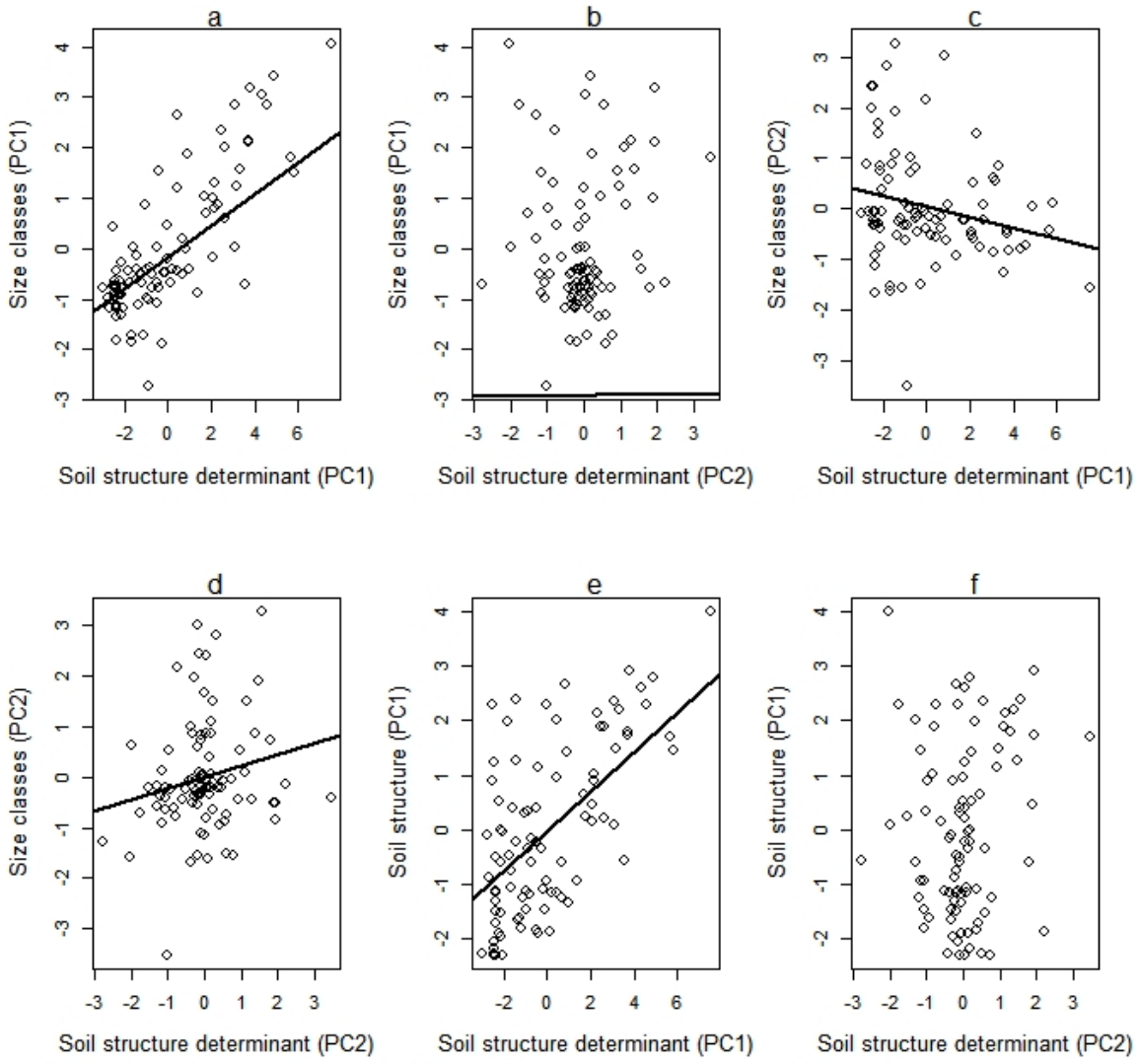

Figure III. 4. The first two principal component analysis (PCA) axes of the PCA of soil structure determinants (Fig. III. 3c) are used as predictor (x axis) of size classes (first principal component axes (PC1) and second principal component axes (PC2), see also Fig. III. 3a) and soil structure (PC1, see also Fig. III. 3b) indices. All linear regression were corrected for heterogeneity of variances and spatial autocorrelation using generalized least squares method (See Table III. 2). Panel a, b and c show linear regression between size classes PC1 to soil structure determinant PC1 and PC2 and between size classes PC2 to soil structure determinant PC1 respectively. Meanwhile, panel e, d, f linear regression between size classes PC2 to soil structure determinant PC2 and between soil structure PC1 to soil structure determinant PC1 and PC2 respectively.

Discussion

In line with other studies (Piotrowski *et al.*, 2008), the results of the present analyses provide robust evidence that soil age is a significant predictor of soil structure and reflects the biotic and abiotic factors that are expected to determine soil structure development. The robustness of these results is ensured by the modelling approach adopted, which for the first time accounts for the confounding effect of spatial autocorrelation, which is inherent in the space for time substitution of chronosequences. It is remarkable that in a system as dynamic as the investigated river islands, soil structure not only builds up consistently in a fairly linear way but also proceeds at apparently high rates. For example, the percentage of water stable aggregates (WSA) increases at 0.84 unit $\cdot$ year^{-1}, which means that when starting from an average of 30 %, WSA could reach an average of about 64 % within 40 years (Fig. III. 2). This means that soil macroaggregates increased 2.11 times within 40 years, a higher formation rate at least when compared to stable macroaggregate formation (also > 0.212 mm aggregate diameter) in a restored tallgrass prairie which increased 1.72 times within 40 years (Jastrow, 1996). We also found that for percent WSA size class 1-2 mm, the rate of formation in our system is higher compare to the chronosequence patches within the floodplain of the unregulated Nyack River (Piotrowski, *et al.* 2008). Within the first to the 40th year, we found that the percent WSA size class 1-2 mm in our system increased 18.87 times compared to 6.55 times in the Nyack River floodplain (Piotrowski, *et al.* 2008). Similarly, the mean weight diameter (mm) increased at 0.02 mm $\cdot$ year^{-1}, meaning that from a starting mean value of 0.15 mm MWD can attain more than 1 mm after 40 years. And as expected, fractal dimension, which is negatively correlated with percent WSA and MWD

(Caruso *et al.*, 2011) decreased at a rate of - 0.01 unit • $year^{-1}$. In fact, the three indices are highly correlated, and the use of fractal D did not really add critical information. The linearity of this development is of course expected to level off in the longer term (for example WSA is unlikely to achieve values above 80 %; even long term restored tallgrass prairie and undisturbed woodland soil can only reach WSA values of ~90% (Jastrow *et al*., 1998; Wright and Upadhyaya, 1998)).

The main mechanisms behind this process of soil structure development are biotic. AMF hyphae facilitate macroaggregate formation and stabilization (Rillig and Mummey, 2006; Six *et al.,* 2004). In combination with roots, they provide a mechanical framework for macroaggregates (Elliot and Coleman, 1988; Gupta and Germida, 1988) and also they release particle binding substances, including proteins (Rillig *et al.*, 2007). Roots influence soil structure in different ways such as through root exudates release, which includes transient polysaccharides that help the binding of clay particles, and also through root penetration, which helps to increase the proportion of stable aggregates through root entanglement (Six *et al.*, 2004).

The data presented here illustrate that as soil structure develops with time, the measured biotic variables also increase, providing good predictors of soil structural variables. Support for the role of biotic variables, particular for AMF, in supporting soil structure has also been found in other ecosystems either through field experiments or observational studies. For example, AMF and soil aggregation correlated positively in a long term experimental field study under diverse management practices (6 and 17 years; prairie of multispecies

communities; Wilson *et al*., 2009); Jastrow *et al*. (1998) also found a positive correlation between biotic factors (roots and external hyphae) with macroaggregate stability on a chronosequence of restored tallgrass prairie; and another positive contribution of AMF and plant roots to soil subsurface stability was found in an observational study in a semiarid shrubland landscape, southern Utah, USA (Chaudhary *et al*., 2009). This relationship is, however, not universal, since biotic contribution might be less prominent when soils are already highly aggregated as found in an observational study on managed grasslands in several areas in Germany (Barto *et al*., 2010). However, this general process is multifaceted and consists of many different minor and major sources of variation in the measured variables. A major process is the progressive accumulation of organic matter and decrease in pH, which is associated with a general increase in fungal hyphal and plant root variables (e.g. Fig. III. 3c). However, organic C is not the major driver of this process and the data suggest that it basically drives the distribution of the smaller aggregates at earlier stages of soil structural development. This was supported by the significant correlation value between soil structure determinants PC2 (mainly being driven by organic C; Fig. III. 3c) with aggregate size class PC2 (mainly driven by smaller aggregate size classes; Fig. III. 3a), although the explained variance is relatively weak ($R^2 = 0.12$; Table 2). Indeed, the calculations also show that although total organic carbon increases along the chronosequence this occurs approximately 17 times more slowly than the rate of total water stable aggregate formation. A similar trend was found in a chronosequence study of a restored tallgrass prairie where organic C accumulation was 35 times slower than the rate of aggregate formation, implying that major improvement in stability can occur without a significant increase of organic C (Jastrow *et al.*, 1998; Jastrow, 1996). Our result further

supports the hypothesis that organic carbon accumulates at a different rate compare to soil aggregates formation, shown by the weak correlation between the two variables. Meanwhile, biotic factors, such as extraradical hyphae and plant roots, remain highly correlated to soil aggregates formation rate throughout the chronosequence, providing the mechanical framework for aggregate formation and its initial stabilization (Tisdall and Oades, 1982; Jastrow *et al*., 1998). Instead, N seems to be a more important promoter of soil structure, especially in the longer term. In fact, nitrogen content is important in increasing plant biomass (Martens *et al.*, 2004) and has been found to be related to soil aggregation and AMF hyphal abundance, at least in an agricultural system (Wilson, *et al.,* 2009). The observed progressive decrease of soil pH can be explained by the total increase of soil organic matter (Russell, 1960) and, although this is a minor source of variation in the data (Fig. III. 3c, PC2), pH shows a negative correlation with organic C and fungal hyphal variables. It is also well known that fungi such as AM-fungi prefer acidic conditions (Clark, 1997; Clark *et al.*, 1999).

The general picture therefore is that in the short to medium term (first 10 years) there is much variation in the smaller aggregate classes and this variation mostly depends on patterns of covariation between organic C and fungal variables, that are positively correlated with each other but negatively associated with pH (Fig. III. 3a and Fig. III. 3c, PC2; patterns in these figures are statistically supported by models in Table III. 2). In the medium to long term (Fig. III. 3a and Fig. III. 3c, PC2) the major process that is apparent is the accumulation of nitrogen and the progressive increase in fungal hyphae and plant roots, which positively correlate with soil structure. From this, it can be inferred that the

progressive increase in fungal hyphae and plant roots promotes soil structure.

Of course, causality cannot be shown from the presented observational data, but the results provide quantitatively robust field support to previous observations on similar floodplain systems. For example, a chronosequence study along the Nyack River, Montana, USA, showed an increase of AMF hyphal length during the succession period up to the 13th year. The AMF abundance increase coincided with a rapid increase of the 1-2 mm aggregate size class (Piotrowski *et al.*, 2008). A previous study on the same reach of the Tagliamento as that investigated in the present research, was based upon a qualitative classification of islands into pioneer, developing and established classes, but it also revealed a positive correlation between soil aggregate size class 1-2 mm and root length colonized by AMF, spore densities, hyphal length and length of fine roots (Harner *et al.*, 2011). We improved these findings by using the exact age of island patches as one explanatory variable, increasing the sample size, extracting the optimum variance of the different soil aggregate variables (either based on the four different soil aggregate size classes or from the three soil structure indices) to calculate the soil structure development, and correcting for the assumptions of linear regression models in our analysis.

The data presented here not only quantitatively describe the rate at which the process of soil structure development progresses in this system but also shed light on the possible underlying mechanisms, thanks to the patterns of covariation that were documented along the chronosequence. Furthermore, the modelling approach adopted in the present analysis is particularly robust as it adequately takes account not only of spatial autocorrelation but also

heterogeneity of variances, which was very pronounced in some cases. Indeed, high levels of variance and heterogeneity of variances might be characteristic of the highly dynamic investigated system, which is subject to frequent (return period approximately 0.5 years) flow pulses that are large enough to interact with the vegetated areas (peak free water surface level exceeding 200 cm measured at the Villuzza gauging station, immediately downstream of the study reach, Bertoldi *et al.*, 2009). Major flow disturbances (floods reaching established island surfaces and exceeding 310 cm at the Villuzza gauge) have occurred on five occasions since records commenced in 1982 (1990, 1996, 1996, 2000, 2004) (Bertoldi *et al.*, 2009). Major floods erode floodplain and island edges, uprooting and dispersing very large numbers of trees. The most recent two large floods were responsible for initiating the sampled pioneer islands aged 8 and 12 years. However, flow pulses (200 to 300 cm) are large enough to erode and deposit sediment inducing morphological changes, and larger pulses are capable of mobilizing trees, as in the case of a pulse in 2010, which initiated the youngest (2 year) pioneer islands that were sampled. Small rainfall events also affect low river levels and, during dry summer months (April-September), help to sustain vegetation growth (Gurnell *et al.*, 2008). Despite the strong influence of these irregular disturbance events, fluvial island soil structure significantly increased through the chronosequence showing improved soil structure through time despite the varying timing and severity of disturbances. While in principle we believe that these results obtained from fluvial islands can be extrapolated to a certain degree to other systems, such as frequently disturbed agricultural systems, there are also aspects rather specific to this study system. For example, a flood pulse might also supply additional propagules (plant and/or fungal propagules) and carry finer soil material for aggregate formation, which would not be the

case in other ecosystems.

The general positive trend in soil development can be attributed to the establishment of plant roots and soil fungi, which contribute to the erosion resistance of the soils. Soil development and consequent resistance to erosion is an important mediator of responses of the river corridor to disturbances. Soil stability helps to maintain and strengthen different geomorphological features, including islands and river banks, and thus to maintain the morphological and habitat complexity of river systems (Corenblit *et al.,* 2007; Gurnell *et al.*, 2012). In addition, soil stability and increase of soil aggregates can also contribute to carbon storage by sequestering carbon inside of stable aggregates (Jastrow *et al.*, 1998). Therefore, the present and future field studies and experiments which unravel the mechanisms contributing to riparian soil development and stability have the potential to contribute to the management and protection of natural rivers, and the design of effective river restoration plans.

Acknowledgments

Ulfah Mardhiah's research is funded by the SMART Joint Doctoral Programme (Science for MAnagement of Rivers and their Tidal systems), which is financed by the Erasmus Mundus Programme of the European Union. We would like to thank Dr. Walter Bertoldi for support during the field sampling. We also would like to thank Sabine Artelt for help in the laboratory. Finally, we thank Luca Zanoni, who conducted the geocorrection, registration and mosaicing of the aerial photographs employed in this research. We would also like to

thank two anonymous reviewers who gave valuable input to improve this paper.

Appendix A. Supplementary Material

References

Allison, F.E., 1968. Soil aggregation-some facts and fallacies as seen by a microbiologist. Soil Science 106, 136–143.

Barto, E.K., Alt, F., Oelmann, Y., Wilcke, W., Rillig, M.C., 2010. Contributions of biotic and abiotic factors to soil aggregation across a land use gradient. Soil Biology and Biochemistry 42, 2316–2324.

Bartoń, K., 2013. MuMIn: multi-model inference. R Package Version 1.9.13.

Bearden, B.N., Petersen, L., 2000. Influence of arbuscular mycorrhizal fungi on soil structure and aggregate stability of a vertisol. Plant Soil 218, 173–183.

Bertoldi, W., Gurnell, A., Surian, N., Tockner, K., Zanoni, L., Ziliani, L., Zolezzi, G., 2009. Understanding reference processes: linkages between river flows, sediment dynamics and vegetated landforms along the Tagliamento River, Italy. River Research and Applications 25, 501–516.

Bronick, C., Lal, R., 2005. Soil structure and management: a review. Geoderma 124, 3–22.

Caruso, T., Barto, E.K., Siddiky, M.R.K., Smigelski, J., Rillig, M.C., 2011. Are power laws that estimate fractal dimension a good descriptor of soil structure and its link to soil biological properties? Soil Biology and Biochemistry 43, 359–366.

Caruso, T., Rillig, M.C., 2011. Direct, positive feedbacks produce instability in models of interrelationships among soil structure, plants and arbuscular mycorrhizal fungi. Soil Biology and Biochemistry 43, 1198–1206.

Chaudhary, V.B., Bowker, M.A., O'Dell, T.E., Grace, J.B., Redman, A.E., Rillig, M.C., Johnson, N.C., 2009. Untangling the Biological Contributions to Soil Stability in Semiarid Shrublands. Ecological Applications 19, 110–122.

Clark, R., 1997. Arbuscular mycorrhizal adaptation, spore germination, root colonization, and host plant growth and mineral acquisition at low pH. Plant Soil 192, 15–22.

Clark, R.B., Zeto, S.K., Zobel, R.W., 1999. Arbuscular mycorrhizal fungal isolate effectiveness on growth and root colonization of Panicum virgatum in acidic soil. Soil Biology and Biochemistry 31, 1757–1763.

Cook, B., Jastrow, J.D., Miller, R., 1988. Root and mycorrhizal endophyte development in a chronosequence of restored taligrass prairie. New Phytologist 110, 355–362.

Corenblit, D., Tabacchi, E., Steiger, J., Gurnell, A.M., 2007. Reciprocal interactions and adjustments between fluvial landforms and vegetation dynamics in river corridors: A review of complementary approaches. Earth-Science Reviews 84, 56–86.

Díaz-Zorita, M., Perfect, E., Grove, J., 2002. Disruptive methods for assessing soil structure. Soil Tillage Research 64, 3–22.

Edwards, P., Kollmann, J., Gurnell, A., Petts, G., Tockner, K., Ward, J., 1999. A conceptual model of vegetation dynamics on gravel bars of a large Alpine river. Wetland Ecology and Management 7, 141–153.

Elliott, E., Coleman, D., 1988. Let the soil work for us. Ecological Bulletins 39, 23–32.

Gregory, S.V, Swanson, F.J., McKee, W.A., Cummins, K.W., 1991. An ecosystem perspective of riparian zones. Bioscience 41, 540–551.

Gupta, V.V.S., Germida, J., 1988. Distribution of microbial biomass and its activity in different soil aggregate size classes as affected by cultivation. Soil Biology and Biochemistry 20, 777–786.

Gurnell, A., Tockner, K., Edwards, P., Petts, G., 2005. Effects of deposited wood on biocomplexity of river corridors. Frontiers in Ecology and the Environment 3, 377–382.

Gurnell, A.M., Bertoldi, W., Corenblit, D., 2012. Changing river channels: the roles of hydrological processes, plants and pioneer fluvial landforms in humid temperate, mixed load, gravel bed rivers. Earth-Science Reviews 111, 129–141.

Gurnell, A.M., Blackall, T.D., Petts, G.E., 2008. Characteristics of freshly deposited sand and finer sediments along an island-braided, gravel-bed river: The roles of water, wind and trees. Geomorphology 99, 254–269.

Gurnell, A.M., Petts, G.E., Hannah, D.M., Smith, B.P.G., Edwards, P.J., Kollmann, J., Ward, J. V., Tockner, K., 2001. Riparian vegetation and island formation along the gravel-bed Fiume Tagliamento, Italy. Earth Surface Processes and Landforms 26, 31–62.

Harner, M.J., Opitz, N., Geluso, K., Tockner, K., Rillig, M.C., 2011. Arbuscular mycorrhizal fungi on developing islands within a dynamic river floodplain: an investigation across successional gradients and soil depth. Aquatic Sciences 73, 35–42.

Harris, D., Horwáth, W.R., Kessel, C.Van., 2001. Acid fumigation of soils to remove carbonates prior to total organic carbon or carbon-13 isotopic analysis. Soil Science Society of America Journal 65, 1853–1856.

Haynes, R.J., Swift, R.S., Stephen, R.C., 1991. Influence of mixed cropping rotations (pasture-arable) on organic matter content, water stable aggregation and clod porosity in a

group of soils. Soil Tillage Research 19, 77–87.

Jakobsen, I., Abbott, L., Robson, A., 1992. External hyphae of vesicular-arbuscular mycorrhizal fungi associated with Trifolium sub terraneum L . New Phytologist 120, 371–380.

Jastrow, J., Miller, R., Lussenhop, J., 1998. Contributions of interacting biological mechanisms to soil aggregate stabilization in restored prairie. Soil Biology and Biochemistry 30, 905–916.

Jastrow, J.D., 1996. Soil aggregate formation and the accrual of particulate and mineral-associated organic matter. Soil Biology and Biochemistry 28, 665–676.

Kemper, W., Rosenau, R., 1986. Aggregate Stability and Size Distribution. In: Methods of Soil Analysis, Part 1. Physical and Mineralogical Methods. Agronomy Monograph No 9. Society of Agronomy/Soil Science Society of America, pp. 425–442.

Kollmann, J., Vieli, M., Edwards, P.J., Tockner, K., Ward, J.V., 1999. Interactions between vegetation development and island formation in the Alpine river Tagliamento. Applied Vegetation Science 2, 25–36.

Martens, D.A., Reedy, T.E., Lewis, D.T., 2004. Soil organic carbon content and composition of 130-year crop, pasture and forest land-use managements. Global Change

Biology 10, 65–78.

Mikha, M.M., Rice, C.W., 2004. Tillage and Manure Effects on Soil and Aggregate-Associated Carbon and Nitrogen. Soil Science Society of America Journal 68, 809–816.

Miller, R.M., Jastrow, J.D., 1990. Hierarchy of root and mycorrhizal fungal interactions with soil aggregation. Soil Biology and Biochemistry 22, 579–584.

Müller, N., 1995. Zum Einfluß des Menschen auf Flora und Vegetation von Flußauen. Schriftenr. Veg. 27, 289–298.

Naiman, R., Decamps, H., McClain, M., 2005. Riparia: ecology, conservation, and management of streamside communities. Academic Press Inc.

Oades, J.M., 1984. Soil organic matter and structural stability: mechanisms and implications for management. Plant Soil 76, 319–337.

Oksanen, J., Blanchet, F., Kindt, R., Legendre, P., O'Hara, R., Simpson, G., Solymos, P., Stevens, M., Wagner, H., 2010. vegan: Community Ecology Package. R package version 1.17-1.

Osterkamp, W.R., 1998. Processes of fluvial island formation, with examples from Plum

Creek, Colorado and Snake River, Idaho. Wetlands 18, 530–545.

Passioura, J., 1991. Soil structure and plant growth. Australian Journal of Soil Research 29, 717–728.

Pinheiro, J., Bates, D., DebRoy, S., Sarkar, D., 2011. nlme: linear and nonlinear mixed effects models.

Piotrowski, J., Lekberg, Y., Harner, M., Ramsey, P., Rillig, M., 2008. Dynamics of mycorrhizae during development of riparian forests along an unregulated river. Ecography 31, 245–253.

R Development Core Team, 2011. R: A Language and Environment for Statistical Computing. R Foundation for Statistical Computing, Vienna, Austria.

Rillig, M.C., Caldwell, B.A., Wösten, H.A.B., Sollins, P., 2007. Role of proteins in soil carbon and nitrogen storage: controls on persistence. Biogeochemistry 85, 25–44.

Rillig, M.C., Mummey, D.L., 2006. Mycorrhizas and soil structure. New Phytologist 171, 41–53.

Rillig, M.C., Wright, S.F., Eviner, V.T., 2002. The role of arbuscular mycorrhizal fungi and glomalin in soil aggregation: comparing effects of five plant species. Plant Soil 238,

325–333.

Russell, J.S., 1960. Soil fertility changes in the long-term experimental plots at Kybybolite, South Australia. I. Changes in pH total nitrogen, organic carbon, and bulk density. Crop and Pasture Science 11, 902–926.

Six, J., Bossuyt, H., Degryze, S., Denef, K., 2004. A history of research on the link between (micro)aggregates, soil biota, and soil organic matter dynamics. Soil and Tillage Research 79, 7–31.

Six, J., Elliott, E.T., Paustian, K., 2000b. Soil Structure and Soil Organic Matter II. A Normalized Stability Index and the Effect of Mineralogy. Soil Science Society of America Journal 64, 1042–1049.

Soil Science Society of America, 2008. Glossary of soil science terms. American Society of Agronomy, SSSA, Madison, WE.

Tisdall, J., Oades, J., 1982. Organic matter and water-stable aggregates in soils. Journal of Soil Science 33, 141–163.

Tockner, K., Stanford, J.A., 2002. Riverine flood plains: present state and future trends. Environmental Conservation 29, 308–330.

Tockner, K., Ward, J. V., Arscott, D.B., Edwards, P.J., Kollmann, J., Gurnell, A.M., Petts, G.E., Maiolini, B., 2003. The Tagliamento River: A model ecosystem of European importance. Aquatic Sciences 65, 239–253.

Ward, J. V, Tockner, K., Edwards, P.J., Kollmann, J., Bretschko, G., Gurnell, A.M., Petts, G.E., Rossaro, B., 1999. A reference river system for the Alps: the "Fiume Tagliamento". Regulated Rivers: Research and Management 15, 63–75.

Wilson, G.W.T., Rice, C.W., Rillig, M.C., Springer, A., Hartnett, D.C., 2009. Soil aggregation and carbon sequestration are tightly correlated with the abundance of arbuscular mycorrhizal fungi: results from long-term field experiments. Ecology Letters 12, 452–461.

Wright, S.F., Upadhyaya, A., 1998. A survey of soils for aggregate stability and glomalin, a glycoprotein produced by hyphae of arbuscular mycorrhizal fungi. Plant Soil 198, 97–107.

Zuur, A., 2010. AED: data files used in mixed effects models and extensions in ecology with R (in Zuur *et al.*, 2009). R package version 1.0.

Zuur, A., Ieno, E. N., Walker, N., Saveliev, A. A., & Smith, G. M., 2009. Mixed effects models and extensions in ecology with R. Springer.

CHAPTER 4

Root and arbuscular mycorrhizal hyphae have contrasting effects on surface soil flow erosion: a greenhouse experiment

Ulfah Mardhiah, Tancredi Caruso, Matthias C Rillig, Angela Gurnell

The following version will be submitted as:

Mardhiah, Ulfah, Caruso, Tancredi, Matthias C. Rillig, and Angela Gurnell. Root and arbuscular mycorrhizal fungal hyphae contrasting effect on surface soil flow erosion: a greenhouse experiment

Root and arbuscular mycorrhizal fungal hyphae contrasting effect on sustaining surface soil flow erosion: a greenhouse experiment

Abstract

Soil erosion problems due to water flow in natural systems have been approached towards understanding the effect of aboveground and belowground biomass, in particular root system, to sustain eroding forces such as concentrated flow. The role of microorganisms, especially arbuscular mycorrhizal fungi (AMF), have been so far implied but never tested directly in a greenhouse experiment. We used two plant species, *Solidago canadensis* and *Achillea millefolium*, grown in the greenhouse with treatments consisting of the addition of AMF, AMF and microbial wash, microbial wash or control. We then subjected each replicate of the surface soil from three layers (0-1 cm, 1-5 cm, > 5 cm) to a constant shear stress in the form of concentrated flow using a hydraulic flume to quantify soil detachment rate through time. We then focused on our *A. millefolium* treatment and tested variables explaining the pattern of the soil detachment rate. The effect of the treatments were only significant for *A. millefolium*, with reduced surface soil detachment rate up to 98% compare to bare soil. Meanwhile, control treatment showed reduced surface soil detachment rate only up to 83%. Contrasting to previous findings, root biomass actually significantly increased soil detachment rate, although the effect might be biased towards coarser roots. Meanwhile, AMF extraradical hyphal length significantly decreased soil detachment rate, implying the probable positive role of AMF in directly alleviating soil erosion.

Keywords: Soil erosion, concentrated flow, soil detachment rate, AMF, hydraulic flume.

Introduction

Of the various problems with which global society is dealing, soil erosion is one of the most important issues due to its damaging effect on the environment and because it causes public health problems (Pimentel, 2006). Pimentel and Kounang (1998) have stated that the loss of soil is 13-40 times faster than the rate of its renewal, and therefore unsustainable. It impacts mainly on agricultural productivity related issues, including loss of crop yield, loss of seedlings, and the necessity to perform more tillage (Lal, 2001; Gyssels and Poesen, 2003; Gyssels *et al*., 2006). Soil erosion also affects soil quality which includes the destruction of soil structure, loss of topsoil, decrease in soil organic matter, and pollution of surface water (Lal, 2001). Compared to agricultural ecosystems, study on how natural soil profiles behave with respect to soil erosion is considerably lacking (Bryan, 2000). For example, geomorphologists are interested in understanding how in fluvial systems soil erosion is related to sediment transported from hillslopes to valleys (Bryan, 2000). This requires a more in depth investigation of properties that would be important for such processes.

Soil erodibility is defined as susceptibility of soil to both detachment and transport of soil particles and it is inversely proportional to the resistance of the soil to erosion (Gyssels *et al*., 2005). Soil is first detached due to breakdown of aggregates by rainsplash, shear or drag force of water and wind and the dissolution of cementing agents, which will be followed by transportation either by wind or flowing water and then deposited after the velocity of the forces decreases (Lal, 2001). It is mainly influenced by aggregate stability, infiltration capacity, soil texture, and organic and chemical content and shear strength (Bryan, 2000;

Gyssels *et al*., 2005). Rill erosion is a process of soil erosion which involves concentrated flow and is mainly related to shear velocity, bed shear stress, streampower, unit stream power and either unit or total discharge (Bryan, 2000; Gyssels and Poesen, 2003).

Vegetation biomass has been identified to play a role in decreasing rill erosion especially when density is high or by densely covering soil surface (De Baets *et al*., 2006; Prosser *et al*., 1995; Gyssels and Poesen, 2003). Gyssels *et al*. (2005) showed how the relationships between vegetation cover and soil detachment due to erosion enacted by splashing water has a linear and exponential decrease when vegetation cover increases. This relationship was also similar when we consider the role of vegetation in relation to soil erodibility with force in the form of interril and rill erosion (Gyssels, *et al*. 2005).

As of late, the focus has been shifted towards understanding the role of belowground biomass in enduring soil erodibility (Gyssels and Poesen, 2003; Gyssels, *et al*., 2005). Root density is highest in topsoils and decreases exponentially with soil depth (De Baets *et al*., 2007). Thus, plant roots will have the largest effect on erosion resistance in the top layer of soils. The rooting effects on soil erosion by concentrated flow of species with a shallow but dense network will be larger than the effects of deep rooted species (Gyssels *et al*., 2006; Zhou and Shangguan, 2007). They also showed how higher root biomass decreases soil erodibility. Meanwhile, the role of soil biota has not been explicitly tested, but it is assumed that soil biota activities increase soil endurance due to its function in developing soil structure (Tisdall and Oades, 1982; Rillig and Mummey, 2006).

Arbuscular mycorrhizal fungi (AMF) are root associated fungi known for their role in increasing soil structure experimentally (Bearden and Petersen 1999; van der Heijden *et al*., 2006) or based on findings in the field (Mummey and Rillig, 2008; Barto *et al*., 2010; Mardhiah *et al*., 2014). These fungi increase soil structure directly by extended extraradical hyphae in the rhizosphere by physically enmeshing and gluing soil particles to form aggregates (Tisdall & Oades, 1982; Oades, 1984; Auge *et al*., 2001; Rillig and Mummey, 2006) and indirectly by stimulating root growth (Bearden and Petersen, 1999) which will then together enmesh the soil particle into aggregates (Rillig and Mummey, 2006). Furthermore, the availability of AMF extraradical hyphae and their products can help the stabilization of aggregates (Rillig *et al*., 2010) further highlighting their important role in soil structure development.

The role of rhizosphere microbes in enhancing soil structure is less clear due to the difficulties in disentangling effects of the various microbes in the rhizoshpere (Bronick and Lal, 2005). They are thought to have a more pronounced influence to the formation of microaggregates (Tisdall and Oades, 1982; Lupwayi *et al*., 2001). In some cases, the addition of a microbial community (total bacteria, actinomycetes, anaerobes, P solubilizers and non-AMF fungi) can increase soil aggregation (Andrade *et al*., 1998) and this ability is assumed to be due to excretion of extracellular compounds which help to bind soil particles into aggregates (Bronick and Lal, 2005).

Our study focuses on disentangling the role of soil microorganisms (AMF and soil microbes) from plant roots in resisting soil erosion. We wished to test if the role of AMF

and or other soil microbes in enduring soil erodibility is related to their indirect ability of increasing soil aggregation by stimulating fine root growth, or directly through hyphal enmeshment, or all these processes simultaneously. This will be the first experimental study to investigate the relative importance of these soil biota in enduring surface soil erosion due to concentrated flow. Although this is an extremely simplified system compared to the dynamics of a natural river and its associated landforms (eg. river islands), our study started off from previous findings on how AMF hyphae and plant roots are related to soil structure development along natural rivers (Piotrowski *et al*., 2008; Harner *et al*., 2011; Mardhiah *et al*., 2014) and in association related to sustainability against soil erosion due to flow and flood pulses.

Materials and Methods

Experimental design

A full factorial design with two plant species and four treatments was used. The treatments are addition of (1) AMF inoculum and non-microbial wash (AMF treatment), (2) non-AMF inoculum and microbial wash (MW, microbial wash treatment), (3) AMF inoculum and microbial wash (AMF + MW, AMF with microbial wash treatment), (4) and non-AMF inoculum and non-microbial wash (control). We also prepared bare soils as a baseline for measuring maximum soil detachment rate under bare soil condition. 10 replicates were set up for each of the treatments, totalling 90 pots placed in the greenhouse.

Experimental setup

We used two flowering plant species *Solidago canadensis* (goldenrod) and *Achillea millefolium* (yarrow). Both species develop fibrous root system and are mycorrhizal. Seedlings were taken from Berlin (*S. canadensis*) and from a local grassland near Berlin (*A. millefolium)*. Seeds were surfaced sterilized by dipping the seeds into 70% ethanol for 1 minute and into 5% commercial bleach for 30 minutes, and then rinsing the seeds by washing several times with distilled water. To ensure germination, seeds were stratified by keeping in moist conditions at 4°C for one month before germination at room temperature.

We used sandy loam alluvial soil excavated from a local grassland. Soil was autoclaved twice (121°C, 20 minutes) and was re-mixed with a 4-mm sieve before carefully placed into each pot (diameter = 13 cm). We added approximately 1.3 kg of soil per pot and then arranged the pots randomly in the greenhouse. Distances between pots were noted for possible correction of spatial autocorrelation. For the AMF treatment, we used commercial *Glomus intraradices* (*Rhizophagus irregularis*) which is a cosmopolitan species and has been found to be beneficial for host nutrient uptake and in improving soil aggregation. We added 150 *G. intraradices* spores per pot by pipetting the inoculum suspension on top of the soil surface and the same concentration of blank carrier material as the non-AMF treatment. We extracted the microbial wash from the same sandy loam alluvial soil. Microbial wash was extracted by sieving a mixture of 200 g soil with 1 L sterile deionized water and the slurry was used after sieving through a 20 μm size sieve. The non-microbial wash treatment was prepared by autoclaving the slurry. For the microbial wash treatment, we added 2 ml of microbial wash per pot (100 g soil/l) and the same amount of

non-microbial wash for the non-microbial wash treatment. The greenhouse temperature was 22°C during the day and 16°C during the night. The plants were treated with daylight from 7.00-21.00. Plants were automatically watered as much as 30 ml per day during the first week and then changed to 15 ml per day for the rest of the experiment. The experiment lasted from 25th of April until 6th of October 2014 (~23 weeks).

Hydraulic Flume Experiments

To measure the surface soil erosion after being subjected to concentrated flow, we conducted a soil erosion experiment set up in an hydraulic flume. The flume was constructed using a transparent Plexi glass wall, 2 m length, 10 cm width, and 11 cm height (Trento University, Italy). At the start of the flume, two chambers (length = 9.5 and 7.5 cm respectively, height = 20 cm) were separated by 7.5 cm height x 1 cm thick wall. The first was used to capture the flow from the tap water, and the second to receive the overflow. The flow was then passed through a set of three layers of transparent plastic pipes (14.5 cm length) whose function was to reduce turbulence and to create a laminar flow. At 20 cm before the end of the flume, a hole with 9 cm external diameter was set up to hold the soil core. At the start of every experiment, carefully cored samples (9 cm diameter) were pushed towards the surface of the flume bottom using a piston and supported by flanges at its sides (Figure IV. 1).

a. b.

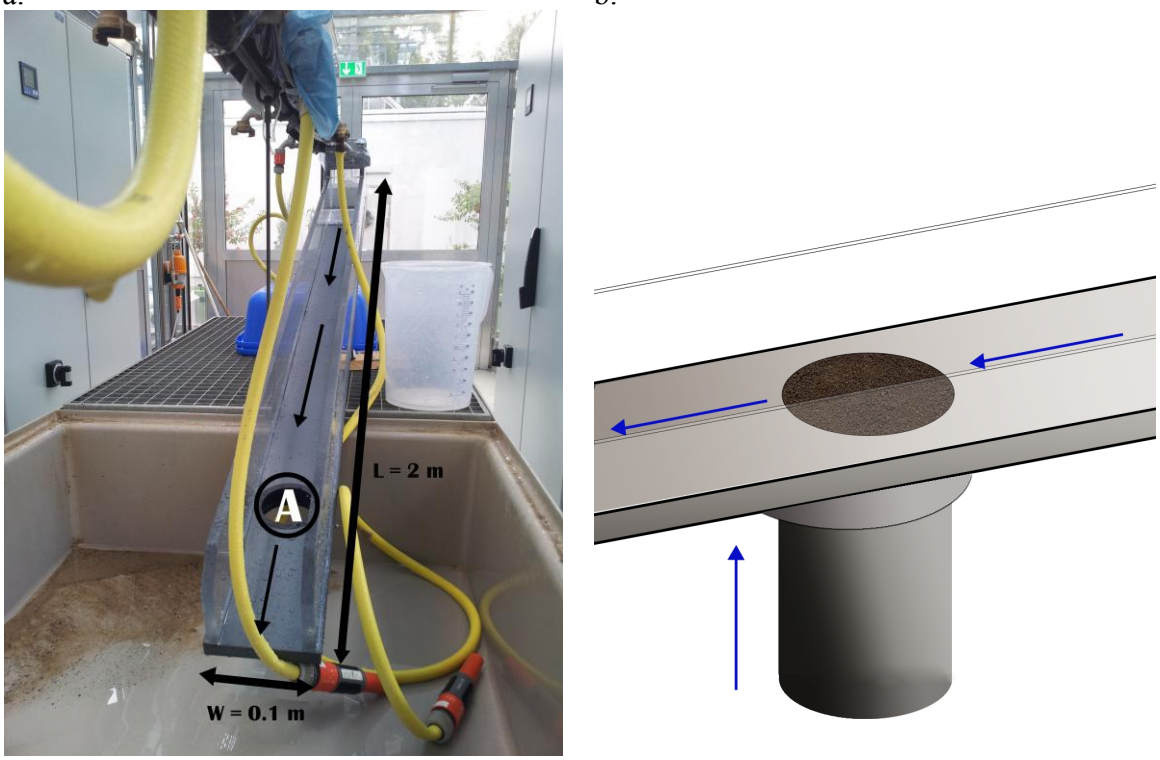

Figure IV. 1. Hydraulic flume (left) used to measure soil detachment rates of surface soil samples. Samples were attached at 'A'. Black arrows indicate concentrated flow direction. The hole (right) is where the soil core was attached to. Surface soil samples were pushed upwards from the core up to the same level as the flume surface.

The flume was set at a 18° slope, and the tap water discharge was kept constant at maximum (0.0003 m^3/s) and the value was recorded. Mean flow velocity (mean = 1.17 ± 0.01 m/s) was measured every day at the beginning of experiment. Using the equation in Suppl. Mat. Equation IV. S1, we calculated that the mean bottom flow shear stress was 7.75 Pa.

We adjusted methods applied by De Baets *et al*. (2006). We first clipped the aboveground

biomass at the soil surface and took a soil core of a known volume (~6.7 cm^3) to measure soil dry bulk density and moisture content. We placed the samples in a constant water level of 4.5 cm below the soil surface to allow slow capillary rise for 8 hours to obtain the field capacity for all samples. We then took the samples out for draining, 12 hours before the experiment. We applied a constant discharge for 150 s of clear tap flow and collected runoff samples and detached soil using a 5 L bucket. We first let the flow run for 20 seconds to establish the laminar flow and to avoid large variance of detached soil within that time range. We then took runoff samples every 15s for 10 seconds, totalling 5 runoff samples. We assigned the time range of 0.20: 0.30, 0.45: 0.55, 1.10: 1.20, 1.35: 1.45 and 2:00-2:10 as time points 1, 2, 3, 4 and 5 (R1, R2, R3, R4 and R5) respectively. To study the difference of soil detachment rate through depth, we applied the runoff on the 0-1 cm, 1-5 cm, and > 5cm layers (TS1, TS2 and TS3 samples respectively). The deeper layers were retained by carefully cutting the soil surface at the 1^{st} and 5^{th} cm layers. Soil which was left in the corer was retained after each runoff application by carefully taking out the soil from the core still in its cored form, to ensure that the samples will be kept intact even after dried. Soil samples were kept in paper bags and then oven dried at 30°C for several days. Meanwhile, the detached sediment and water runoff were let to settle for 1 hour and the water was decanted. Sediments were oven dried at 65°C and weighed. We retained 15 detached soil samples for each replicate (TS1.R1-5, TS2.R1-5, TS3.R1-5), totalling ~1350 dried detached soil samples.

Water stable aggregates, hyphal length and root variables measurements

To ensure that the root, hyphal length, and water stable aggregates measurements did not

include soil and roots which were affected by the soil erosion experiment, we carefully scraped a thin layer of the surface layer off each cored soil subjected to the runoff, trimming all protruding roots. We then carefully sieved the remaining soil through a 4-mm sieve. Aggregate stability was measured by re-wetting 4 g of soil with distilled water for several minutes using capillary action on a 250 μm sieve. Wet soil was then sieved in a wet-sieving machine for 5 min (Eijkelkamp, the Netherlands), leaving stable aggregates and coarse material which were then dried at 65°C. The dried material remaining on the sieve was then crushed and passed through the sieve, to separate the stable aggregates (passed through the sieve; < 250 μm) from the coarse (remaining on the sieve; > 250 μm) fractions.

Root biomass was measured by retaining the roots using an extraction-flotation method (Cook *et al.,* 1988) and then calculating the total root mass per volume of soil. Total root length was measured by scanning and then analyzing the scanned image using WinRhizo Pro 2007d (Regent Instruments Inc., Quebec City, Canada). The root length data was grouped by root diameter, and also by length: very fine root length (0-0.2 mm), fine root length (0.2-1 mm) and coarse root length (> 0.1 mm) (Jastrow *et al*., 1998; Barto *et al*., 2010).

Hyphae were extracted from 4.0 grams of dried soil using a protocol adapted from Jakobsen *et al*. (1992). A 2 ml aliquot was then stained with Trypan Blue for 5 minutes, rinsed with deionized water and transferred to a filter paper. To calculate the AMF extraradical hyphal length (and the length of hyphae stemming from non-AMF), the number of intersects of hyphae with the cross-hair ocular piece within each filter paper was counted for a total of

50 stops at 200X magnification.

Statistical analyses

Assessment of soil detachment rate change through time

To assess the different soil detachment rates both at each time point and cumulatively through time between all treatments, we applied linear regression models to data per time point and to cumulative soil detachment rate through time (time range of 0.20: 0.30, 0.45: 0.55, 1.10: 1.20, 1.35: 1.45 and 2:00-2:10 as time points 1, 2, 3, 4 and 5 respectively). If necessary, the linear models were corrected for violation of homogeneity (chosen based on lower Akaike information criterion (AIC) value, with p value <0.05). R^2 values were generated using R package MuMIn (Barton, 2013).

Assessment of soil detachment rate differences between treatments

We first tested the difference of soil detachment rate (gram soil/10 seconds runoff time) from each surface both at each time point and cumulatively (TS1.R1-5, TS2.R1-5 and TS3.R1-5) comparing different treatments (*A. millefolium* as control (A), *A. millefolium* with AMF treatment (AA), *A. millefolium* with AMF + MW treatment (AAM), *A. millefolium* with MW treatment (AM), *S. canadensis* as control (S), *S. canadensis* with AMF treatment (SA), *S. canadensis* with AMF + MW treatment (SAM), *S. canadensis* with MW treatment (SM), and bare soil (B)). We tested the normality of data distribution using Shapiro-Wilk Normality Test ($p < 0.05$, alpha value = 0.05) and applied accordingly Kruskal Wallis test ($p <0.05$, alpha value = 0.05, correction = Bonferroni) for non-normally distributed data set and ANOVA followed by Tukey's test ($p < 0.05$, alpha value = 0.05) for

normally distributed data set. Significant differences are identified by different letters assigned to each treatment.

Assessment of water stable aggregates, hyphal length and root variables differences between treatments

We focused our measurements of water stable aggregates, hyphal length, and root variables on the 0-1 cm layer samples of *Achillea millefolium* treatments (TS1; A, AA, AAM and AM treatments). Explanatory variables which might explain the soil detachment rate include total percent WSA, root biomass, very fine root length, fine root length, coarse root length, AMF extraradical hyphal length and non-AMF extraradical hyphal length. We applied similar statistical tests as before by testing normality of data using Shapiro-Wilk Normality Test and applied either Kruskal Wallis or ANOVA followed by Tukey's test to see the differences between all four treatments.

Correlation of soil detachment rate with explanatory variables: linear models and PCA

We first ran a linear model correlating each soil detachment rate (TS1.R1, TS1.R2, TS1.R3, TS1.R4 and TS1.R5) with each explanatory variable (total percent WSA, root biomass, very fine root length, fine root length, coarse root length, AMF extraradical hyphal length and non-AMF extraradical hyphal length) as main effect. We also ran linear models by gradually adding all the explanatory variables and tested the main effect of all variables within the model. To validate our use of linear regressions, we corrected our assumption of homogeneity of variances. We also checked our assumptions of spatial independence through variograms and analysis of spatial autocorrelation (package AED, Zuur, 2010). Before adding an interaction effect test within the linear models, we tested for

multicollinearity between the explanatory variables by applying Pearson's product moment correlation test (95% confidence interval, p value <0.05). Since some explanatory variables were correlated to some extent, in addition to linear models, we also used ordination multivariate analysis to summarize major covariation patterns within the dataset. We performed two principal component analysis on the (1) soil detachment rate from time point 1-5 and on the (2) explanatory variables (total percent WSA, root biomass, very fine root length, fine root length, coarse root length, AMF extraradical hyphal length and non-AMF extraradical hyphal length). We then extracted (1) the first ordination axis as indices of soil detachment rate (PC1) and first and second ordination axis as (2) indices of soil detachment rate determinants (PC1) and (3) soil detachment rate determinants (PC2) (R vegan package, Oksanen *et al*., 2010).

We then applied linear regression models correlating each point soil detachment rate and indices of soil detachment rate (TS1.R1, TS1.R2, TS1.R3, TS1.R4, TS1.R5 and Soil detachment rate PC1) with soil detachment rate determinants PC1 and PC2. We also validated our use of linear regression model by checking and correcting our assumption of homogeneity of variances (R package nlme, Pinheiro *et al*., 2011). R^2 values of all GLS models were generated using R package MuMIn (Barton, 2013).

All statistical analyses within this study were conducted using version 2.14.0 of the R statistics software (R Development Core Team, 2012).

Results

At the end of the experiment, we lost several replicates which left us with 10 replicates of *A. millefolium* with AMF treatment and *A. millefolium* with AMF and microbial wash treatment, 9 replicates of *A. millefolium* as control, *A. millefolium* with microbial wash treatment and Bare soil; 6 replicates of *S. canadensis* as control, 8 replicates of *S. canadensis* with AMF treatment, 5 replicates of *S. canadensis* with AMF and microbial wash treatment, and 7 replicates of *S. canadensis* with microbial wash treatment.

Assessment of soil detachment rate change through time

For all treatments at all three layers, the amount of soil detached was the highest at the beginning of the runoff experiment and the lowest at the end, except for the case of *S. canadensis* with AMF + microbial wash treatment and *A. millefolium* with microbial wash treatment, both at the 0-1 cm layer (Table IV. 1).

As an overview, when comparing the different slopes of soil detachment rate between all four treatments between soil planted with *S. canadensis* and *A. millefolium,* we found that in all cases, *S. canadensis* treatments had lower slopes compared to both *A. millefolium* and bare soil treatments. The slope pattern of each treatment for of *S. canadensis* within each soil layer (TS1, TS2 and TS2) differed. In TS1, the highest slope was found for the microbial wash treatment, AMF with microbial wash treatment, control, and AMF treatment respectively (Table IV. 1). In TS2, the highest slope was for the microbial wash treatment, followed by AMF with microbial wash treatment, AMF treatment, and control.

While in TS3, the highest slope was in the AMF and microbial wash treatment, followed by microbial wash treatment, AMF treatment, and control, respectively (Table IV. 1). In almost all treatments, soil detachment rate also increased with soil layer depth, except for the case of *S. canadensis* control between the TS2 and TS3 layer, for which the slope of TS2 is higher than for TS3.

Table IV. 1. Linear model fitted using the generalized least square (GLS) method corrected for heterogeneity of variances (var = varExp(form=~time)) to test the response of soil detachment rate (TS1, TS2 and TS3) through time (R1, R2, R3, R4 and R5) for each treatment (A = *A. millefolium* control, AA = *A. millefolium* with AMF treatment, AAM = *A. millefolium* with AMF and microbial wash treatment, AM = *A. millefolium* with microbial wash treatment, B = Bare soil, S = *S. canadensis* control, SA = *S. canadensis* with AMF treatment, SAM = *S. canadensis* with AMF and microbial wash treatment, SM = *S. canadensis* with microbial wash treatment). Significant regression parameters (estimated mean value) are shown in bold (p-values <0.05). Models were compared using the Akaike information criterion (AIC) and the lowest AIC is shown in this table. The model intercept is the last parameter in the equation. The value of the best fitted line (R^2) is provided.

Model with estimated parameters (GLS)	**AIC**	**R^2**
B.TS1 detach. soil (gr/10s) = **(7.69)** time + 8.11	317.9365	0.79
B.TS2 detach. soil (gr/10s) = **(6.14)** time + 16.37	363.3954	0.48
B.TS3 detach. soil (gr/10s) = **(4.60)** time + 8.50	260.0141	0.7
S.TS1 detach. soil (gr/10s) = **(0.25)** time + 0.2	53.59928	0.46
S.TS2 detach. soil (gr/10s) = (0.90) time + 2.22	171.1732	0.096
S.TS3 detach. soil (gr/10s) = **(1.67)** time + 0.62	123.1841	0.67
SA.TS1 detach. soil (gr/10s) = **(0.24)** time + 0.15	44.57807	0.61
SA.TS2 detach. soil (gr/10s) = **(0.76)** time + 1.36	88.235	0.75
SA.TS3 detach. soil (gr/10s) = **(1.51)** time + 1.55	237.6694	0.16
SM.TS1 detach. soil (gr/10s) = **(0.33)** time + 0.32	87.85732	0.38
SM.TS2 detach. soil (gr/10s) = **(1.32)** time + 2.17	188.3384	0.33
SM.TS3 detach. soil (gr/10s) = **(2.11)** time + 1.89	204.6274	0.33
SAM.TS1 detach. soil (gr/10s) = (0.46) time + 0.29	106.3643	0.39
SAM.TS2 detach. soil (gr/10s) = **(1.18)** time + 1.66	122.6936	0.39
SAM.TS3 detach. soil (gr/10s) = **(2.06)** time + 2.26	160.0411	0.21
A.TS1 detach. soil (gr/10s) = **(1.23)** time + 1.80	258.7143	0.22
A.TS2 detach. soil (gr/10s) = **(1.51)** time + 3.26	243.533	0.28
A.TS3 detach. soil (gr/10s) = **(1.9)** time + 4.37	277.6574	0.22
AA.TS1 detach. soil (gr/10s) = **(0.17)** time + 0.18	58.09909	0.38
AA.TS2 detach. soil (gr/10s) = **(1.33)** time + 1.01	217.7717	0.53
AA.TS3 detach. soil (gr/10s) = **(1.61)** time + 2.65	225.0245	0.52
AM.TS1 detach. soil (gr/10s) = (1.17)time + 1.84	303.9369	0.17

AM.TS2 detach. soil (gr/10s) = **(1.59)** time + 4.65	258.0904	0.24
AM.TS3 detach. soil (gr/10s) = **(2.54)** time + 4.44	297.0948	0.32
AAM.TS1 detach. soil (gr/10s) = **(0.5)** time + 1.14	222.6298	0.1
AAM.TS2 detach. soil (gr/10s) = **(1.09)** time + 2.47	223.7167	0.36
AAM.TS3 detach. soil (gr/10s) = **(1.34)** time + 2.50	241.9477	0.38

For the *A. millefolium* treatment, a more regular pattern can be found. Within the TS1 and TS2 layer, the highest soil detachment rate was found in *A. millefolium* with microbial wash treatment, followed by control, AMF with microbial wash treatment, and AMF treatment. Meanwhile, in the TS3 layer, the highest slope was found for the microbial wash treatment, followed by AMF, control, and AMF with microbial wash treatment, respectively. As in the case for *S. canadensis,* the deeper the layer, the higher the soil detachment rate (See Fig. IV. 2, Table IV. 1).

a.

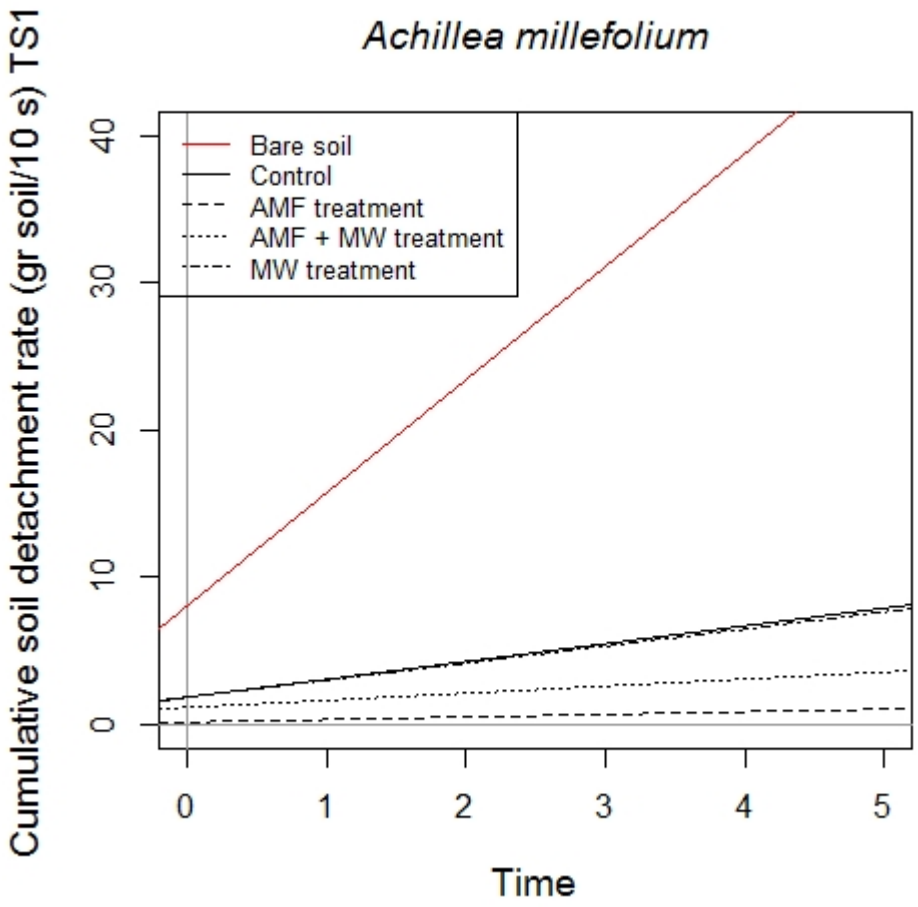

Figure IV. 2. For figure legend, see next page.

b.

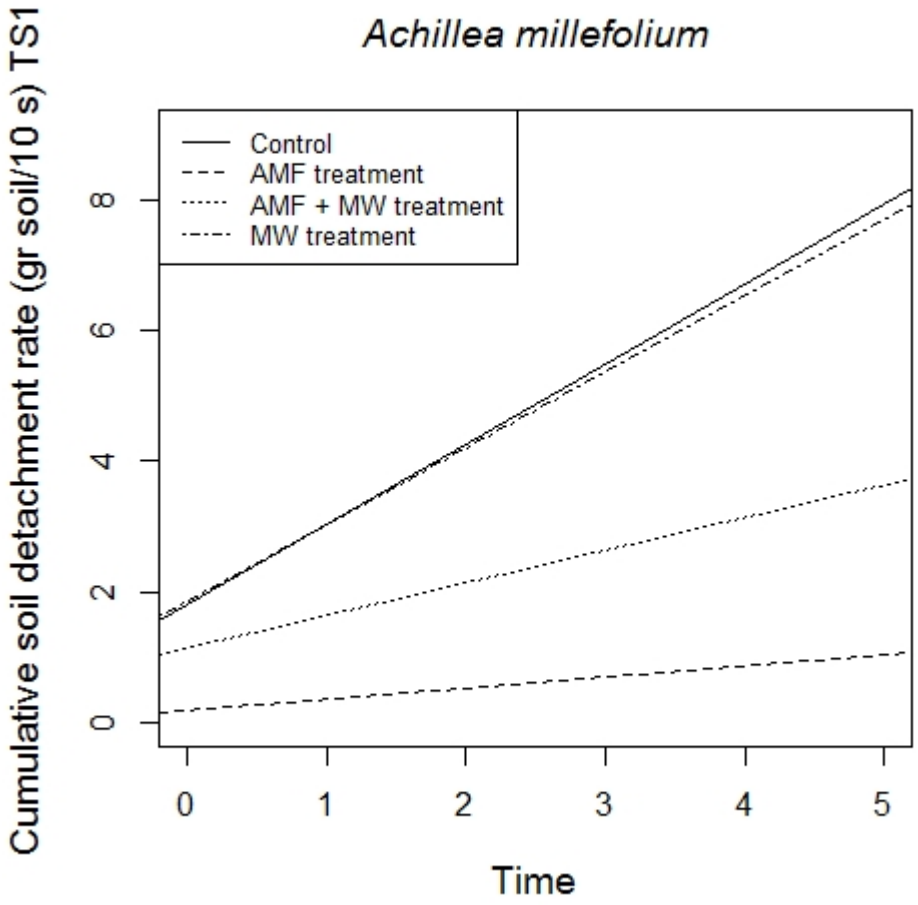

Figure IV. 2. Linear model fitted using the generalized least square (GLS) method corrected for heterogeneity of variances were used to plot cumulative soil detachment rate (0-1 cm layer) through time (R1, R2, R3, R4, R5) for different treatments (A = *A. millefolium* control, AA = *A. millefolium* with AMF treatment, AAM = *A. millefolium* with AMF and microbial wash treatment, AM = *A. millefolium* with microbial wash treatment, B = Bare soil). Figures are fitted lines of *A. millefolium* treatments and bare soil (a) and of *A. millefolium* treatments only (b). The figures show only the fitted lines, omitting data points.

Assessment of soil detachment rate differences between treatments

In general, we found that the application of AMF treatments significantly decreased soil detachment rate for the 0-1 cm layer compared to control. AMF and microbial wash treatment also decreased soil detachment rate, although not as strong as the AMF only

effect. The microbial wash treatment effect generally was not significantly different from the control (Suppl. Mat. Table IV. S1, Fig. IV. 3). This pattern is consistent as the flow runoff experiment ran through the length of the experiment, although analyzing the detachment rate by time point, showed that the mean difference of AMF treatment against control were the highest at time point 1 and 2 (0:20- 0:30 and 0:45- 0:55), followed by time point 3 and 4 (1:10- 1:20 and 1:35- 1:45) and the least different at time point 5 (2:00- 2:10) (Suppl. Mat. Table IV. S1). We only found this significant difference when soil was grown with *Achillea millefolium*. Soil grown with *Solidago canadensis* did not show differences between treatments and generally, the four treatments of *S. canadensis* have the least soil detached from their surface compared to *A. millefolium* treatments. Bare soil naturally had the highest amount of soil detached at all time points and for all three layers (Suppl. Mat. Table IV. S1).

a.

b.

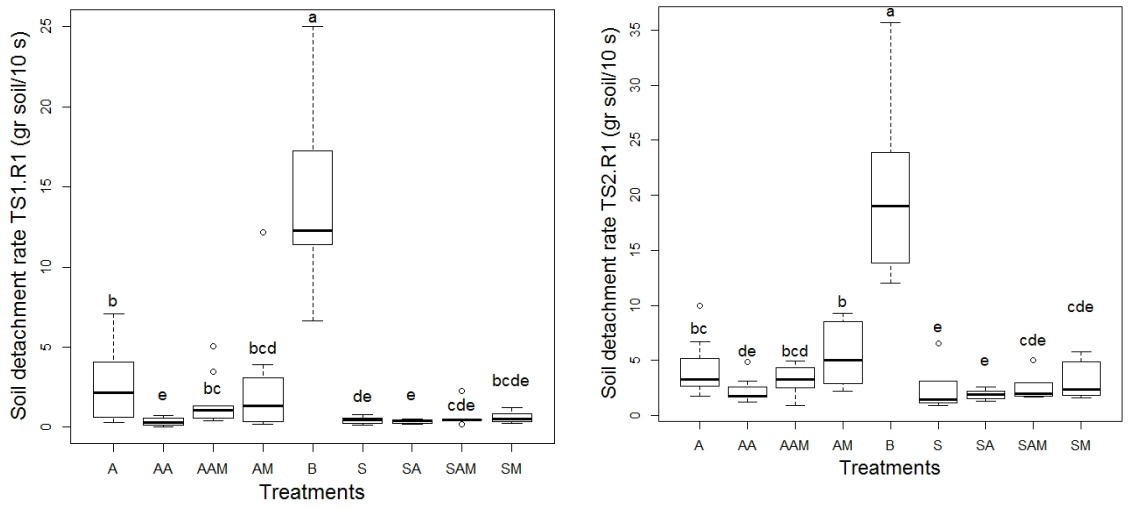

c.

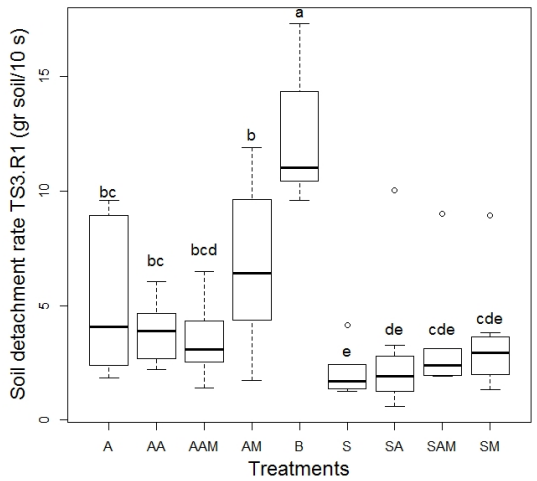

Figure IV. 3. The boxplots show the differences among treatments (x axis) (A = *A. millefolium* control, AA = *A. millefolium* with AMF treatment, AAM = *A. millefolium* with AMF and microbial wash treatment, AM = *A. millefolium* with microbial wash treatment, B = Bare soil, S = *S. canadensis* control, SA = *S. canadensis* with AMF treatment, SAM = *S. canadensis* with AMF and microbial wash treatment, SM = *S. canadensis* with microbial wash treatment) on the amount of soil detached (y axis; gram soil per 10 seconds) during surface soil erosion within the first layer (0-1 cm) (a), second layer (1-5 cm) (b) and third layer (>5 cm) (c) at time point 0:20 - 0: 30 (time point R1). The test used was Kruskal Wallis test ($p < 0.05$, alpha value = 0.05, correction = Bonferroni). Different letters points at significant differences between the treatment groups.

A similar pattern can be found when comparing the surface soil detachment rate from the 1-5 cm layer soil, although with less pronounced differences between treatments when soil was planted with *A. millefolium* (Suppl. Mat. Table IV. S1, Fig. IV. 3) compared to the pattern visible in the 0-1 cm layer. Meanwhile, the surface soil detachment rate from the > 5 cm layer soil showed no differences between treatments both in soil grown with *A. millefolium* and *S. canadensis* (Suppl. Mat. Table IV. S1, Fig. IV. 3).

Table IV. 2. Kruskal Wallis test ($p < 0.05$, alpha value = 0.05, correction = Bonferroni) were used to test the differences of treatment groups (A = *A. millefolium* control, AA = *A. millefolium* with AMF treatment, AAM = *A. millefolium* with AMF and microbial wash treatment, AM = *A. millefolium* with microbial wash treatment) of several variables assumed to explain the variances of the soil detachment rates. Values are mean ± SE. Different letters indicate significant difference between treatment groups (p value < 0.05). *used ANOVA followed by Tukey's Test ($p < 0.05$, alpha = 0.05).

Variables	**A**	**AA**	**AAM**	**AM**
Total dry aboveground biomass (gr)	6.02 ± 0.28a	4.74 ± 0.59ab	4.43 ± 0.30b	4.98 ± 0.59a
Total root biomass (>212 µm) (gr/cm^3)	0.01 ± 0.00a	0.01 ± 0.00a	0.02 ± 0.00a	0.012 ± 0.00a
Total percentage of WSA	34.96 ± 1.31a	38.20 ± 3.72a	35.34 ± 3.03a	36.64 ± 2.44a
Very fine root length (>212 µm) (cm/cm^3)*	47.57 ± 5.49a	49.41 ± 4.51a	47.19 ± 4.12a	47.26 ± 7.82a
Fine root length (>212 µm) (cm/cm^3)	13.15 ± 1.23ab	12.21 ± 0.78b	15.22 ± 1.34ab	14.32 ± 1.98ab
Coarse root length (>212 µm) (cm/cm^3)*	0.58 ± 0.11a	0.55 ± 0.11a	0.75 ± 0.11a	0.54 ± 0.13a
AMF extraradical hyphal length (m/cm^3)	0.85 ± 0.15c	2.91 ± 0.24a	1.83 ± 0.16b	1.13 ± 0.12c
non-AMF extraradical hyphal length (m/cm^3)	0.16 ± 0.03bc	0.25 ± 0.04ab	0.35 ± 0.05a	0.15 ± 0.03bc

Assessment of water stable aggregates, hyphal length and root variables differences between treatments

We assessed various variables which might explain the soil detachment rate pattern, focusing on the first centimeter layer of soil planted with *A. millefolium* which showed the most pronounced effect of treatments compared to other layers and the *S. canadensis* treatments. Of all variables (total root biomass, very fine root length, fine root length, coarse root length, total WSA, AMF extraradical hyphal length and non-AMF extraradical

hyphal length), we only found significant differences in AMF extraradical hyphal length between treatments (see Fig. IV. 4, Table IV. 2). Treatments with AMF had the greatest length of AMF extraradical hyphae, followed with AMF + microbial wash treatment, and the lowest values were found in the microbial wash treatment and control (see Fig. IV. 4, Table IV. 2).

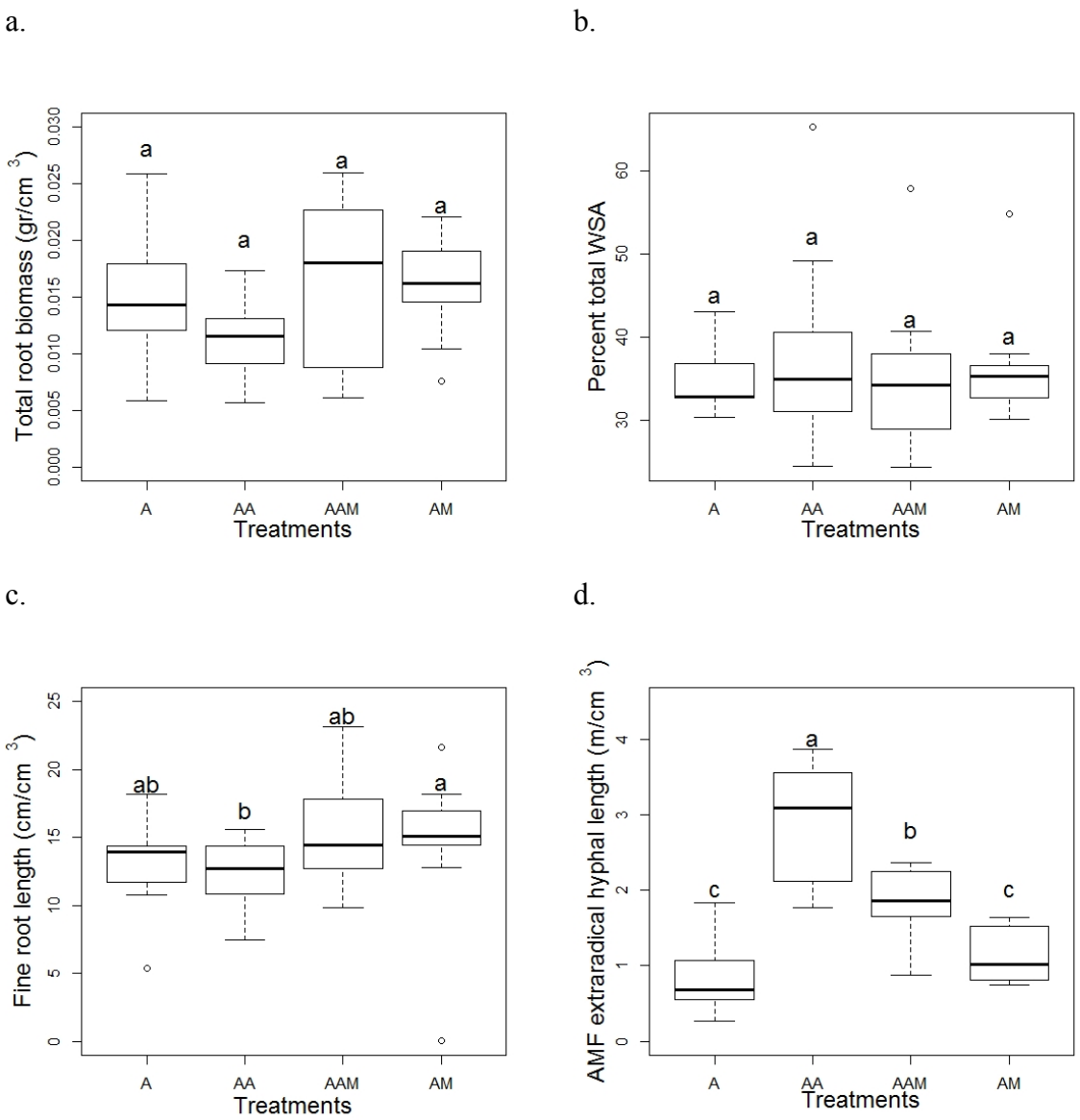

Figure IV. 4. The boxplots show several variables comparing the different effect of the

treatments (x axis) (A = A. millefolium control, AA = A. millefolium with AMF treatment, AAM = A. millefolium with AMF and microbial wash treatment, AM = A. millefolium with microbial wash treatment) on total root biomass (a), percent total WSA (b), fine root length (c) and AMF extraradical hyphal length (d). The test used was Kruskal Wallis test ($p < 0.05$, alpha value = 0.05, correction = Bonferroni). Different letters show a significant difference between the treatment groups.

Correlation of soil detachment rate with explanatory variables: linear models and PCA

After correction of heterogeneity, we found two explanatory variables which almost always correlated significantly with soil detachment rate at all five time points (TS1.R1-TS1.R5). When tested the variables individually as a main effect. Total root biomass was significantly positively correlated with increase in soil detachment rate at TS1.R2 and TS1.R5 (p value <0.05), and almost significantly at TS1.R3 (p value = 0.05) ($R^2 = 0.78$, 0.63 and 0.66, respectively; See Suppl. Mat. Table IV. S2.a, Fig. IV. S1, Fig. IV. 5.a). Meanwhile, AMF extraradical hyphal length was significantly negatively correlated with increase of soil detachment rate at TS1.R1, TS1.R3, TS1.R4 and TS1.R5 (p value <0.05, R^2 = 0.68, 0.67, 0.62 and 0.61 respectively; See Suppl. Mat. Table IV. S2.a, Fig. IV. S1, Fig. IV. 5.b). Other significant correlations were found in (1) TS1.R1, in which non-AMF extraradical hyphae significantly decreased as soil detachment rate increased (p value <0.01, $R^2 = 0.7$) and (2) TS1.R5, in which coarse root length significantly increased as soil detachment rate increased (p value <0.05, R2 = 0.59) (Suppl. Mat. Table IV. S2.a, Fig. IV. S1).

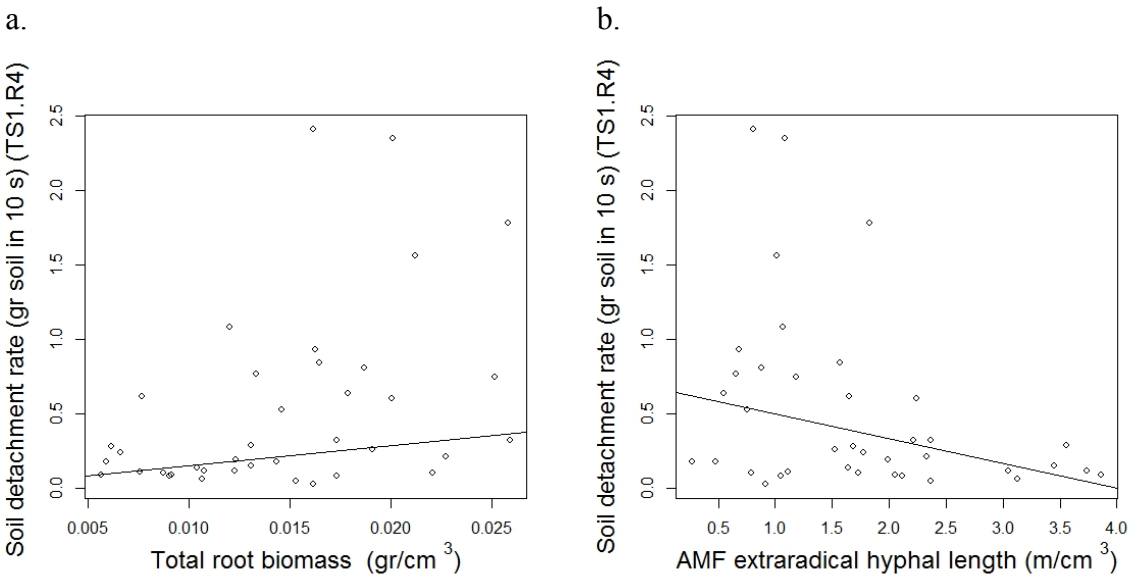

Figure IV. 5. Linear model fitted using the generalized least square (GLS) method corrected for heterogeneity of variances (var = varIdent(form=~1|fcategorical)) and spatial autocorrelation) were used to correlate soil detachment rate (0-1 cm soil layer; time point R4; y axis) to total root biomass (a) and AMF extraradical hyphal length (b).

When all seven explanatory variables were used altogether as main effect, for TS1.R1, and TS1.R2, total root biomass, fine root length, and AMF extraradical hyphal length showed significant correlation with the soil detachment rate (R^2 = 0.69 and 0.86, respectively; Suppl. Mat. Table IV. S2.b). For TS1.R3 and TS1.R5, both total root biomass and AMF extraradical hyphal length were significantly correlated with the soil detachment rate (R^2 = 0.74 and 0.73, respectively, Suppl. Mat. Table IV. S2.b). AMF extraradical hyphal length was the only variable which significantly correlated with TS1.R4 (R^2 = 0.69). For all significant correlations, total root biomass and coarse root length were always positively correlated with soil detachment rate. Meanwhile, fine root length, AMF extraradical hyphal length and non-AMF extraradical hyphal length were always negatively correlated with soil detachment rate.

Due to issues of multicollinearity (Suppl. Mat, Table IV. S3), we were not able to discern the relative importance of interaction effects of the various explanatory variables. We therefore sought to disentangle this issue by referring to our ordination multivariate analysis which showed that after running PCA on the seven explanatory variables, the first principal component axis explained 37% of the variance (soil detachment rate determinant PC1), followed by 24% explained variance in the second principal component axis (soil detachment rate determinant PC2) (Suppl. Mat. Table IV. S4, Fig. IV. 6.a). The first principal component axis was mainly driven by the root variables, especially the finer fractions (very fine and fine root length) (Suppl. Mat. Table IV. S4, Fig. IV. 6.a). By contrast, the second principal component axis was mainly driven positively by AMF and non AMF extraradical hyphal length and negatively by coarse root length and root biomass (Suppl. Mat. Table IV. S4, Fig. IV. 6.a).

a.

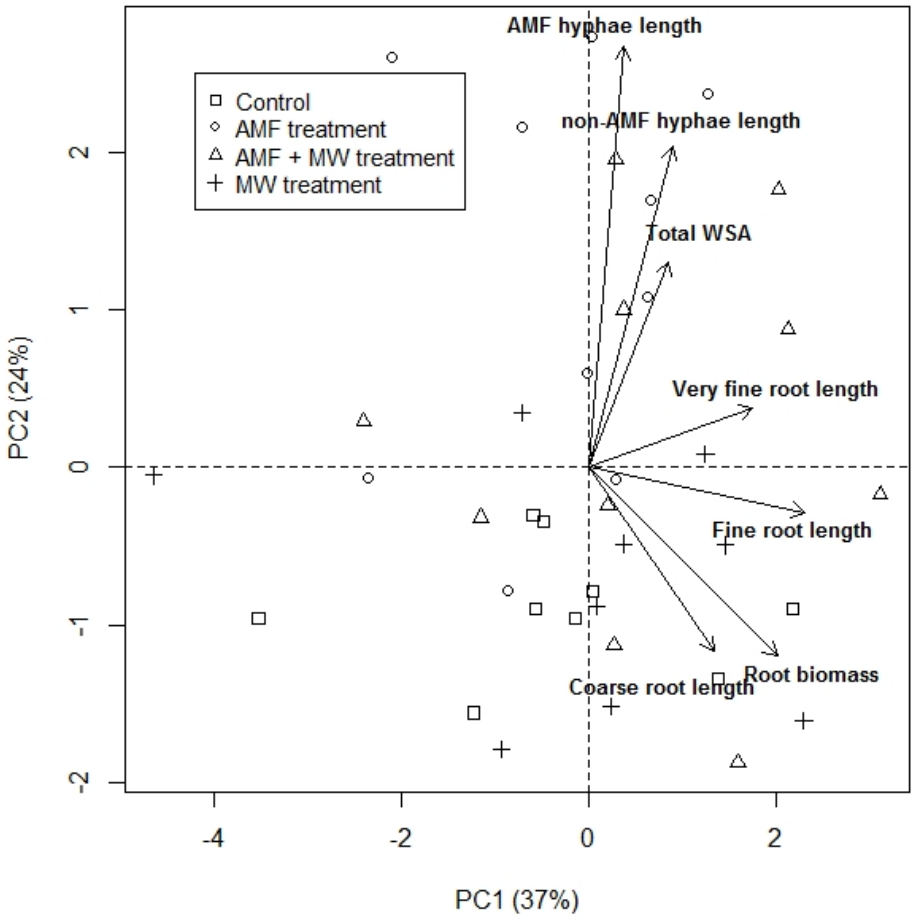

Figure IV. 6. For figure legend, see next page.

b.

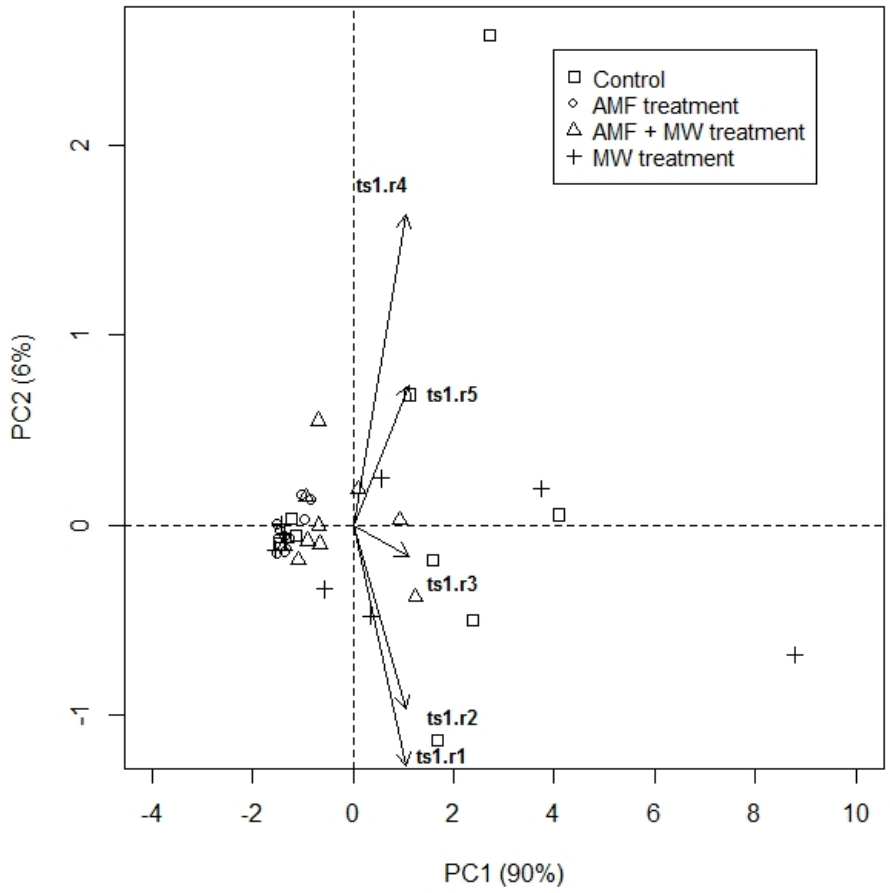

Figure IV. 6. The biplots show variable vectors and samples following Principal Components analysis (PCA) on the following variables: a) soil detachment rate determinants and b) soil detachment rate at five time points. Data points are coded according to the treatment groups (□ = control, ○ = AMF treatment, △ = AMF + MW treatment, + = MW treatment) which show that the distribution of data points along the first two PCA axis is not random. PCA axes were used to model the effect of soil detachment rate determinants on soil detachment rate.

The distribution of data points based on different treatments cannot be easily discerned visually within the first PC axis, but the data points were more clearly grouped in the second PC axis, in which AMF treatment and AMF + microbial wash treatments seemed to

be driven by the AMF and non-AMF extraradical hypal length and total WSA variables. Control and microbial wash treatments seemed to be driven by the coarse root length and root biomass variables (See Fig. IV. 6.a).

To describe the pattern of soil detachment rate, we extracted total variance from PCA run on the five time points of soil detachment rate. The first PCA axis explained 90% of total variance with all variables positively driving the pattern. The strongest driving variables were from the third and fifth time points of soil detachment rate (TS1.R3 and TS1.R5) (Suppl. Mat. Table IV. S4, Fig. IV. 6.b).

Table IV. 3. Linear model fitted using the generalized least square (GLS) method corrected for heterogeneity of variances (var = varIdent(form=~1|fcategorical)) and spatial autocorrelation) to test the response of soil detachment rate (PC.1, TS1.R1, TS.R2, TS1.R3, TS1.R4 and TS1.R5) to soil detachment rate determinants PC1 and PC2 used as main effect. Regression parameters (estimated mean value) with significant p-values are shown in bold. Models were compared using the Akaike information criterion (AIC) and the lowest AIC is in bold. The model intercept is the last parameter in the equation. The value of the best fitted line (R^2) is provided.

Model with estimated parameters (GLS)	**AIC**	**R^2**
Soil detach. rate (PC1) = (0.082) Soil detach. rate det (PC1) -1.183	143.4574	0.64
Soil detach. rate (PC1) = (**-0.466**) Soil detach. rate det (PC2) - 0.41	**139.3601**	**0.66**
Soil detach. rate (TS1.R1) = (0.03) Soil detach. rate det (PC1) + 0.389	156.3755	0.63
Soil detach. rate (TS1.R1) = (**-0.13**) Soil detach. rate det. (PC2) + 0.535	**152.2156**	**0.67**
Soil detach. rate (TS1.R2) = (0.034) Soil detach. rate det. (PC1) + 0.25	114.3379	0.78
Soil detach. rate (TS1.R2) = (**-0.191**) Soil detach. rate det. (PC2) + 0.6	**114.6869**	**0.77**
Soil detach. rate (TS1.R3) = (**0.02**) Soil detach. rate det. (PC1) + 0.19	70.55417	0.66
Soil detach. rate (TS1.R3) = (**-0.178**) Soil detach. rate det. (PC2) + 0.507	**66.94217**	**0.67**
Soil detach. rate (TS1.R4) = (0.022) Soil detach. rate det. (PC1) + 0.162	58.01224	0.59
Soil detach. rate (TS1.R4) = (**-0.105**) Soil detach. rate det (PC2) + 0.355	**56.55729**	**0.59**
Soil detach. rate (TS1.R5) = (0.058) Soil detach. rate det. (PC1) + 0.271	68.5598	0.58
Soil detach. rate (TS1.R5) = (**-0.135**) Soil detach. rate det. (PC2) + 0.409	**62.68108**	**0.64**

Based on our findings from correlating each soil detachment rate to all explanatory variables as main effect, we found that correlating the six soil detachment rate variables

(Soil detachment rate PC1, TS1.R1, TS1.R2, TS1.R3, TS1.R4 and TS1.R5) with the first soil detachment rate determinants PC1 resulted in a non-significant correlation (Table IV. 3, Fig. IV. 7.a). Meanwhile, correlating the soil detachment rate variables with soil detachment rate determinants PC2 resulted in significant correlations (p value <0.05) with R^2 values of 0.66, 0.67, 0.77, 0.67, 0.59 and 0.64 respectively (Table IV. 3, Fig. IV. 7.b).

a. b.

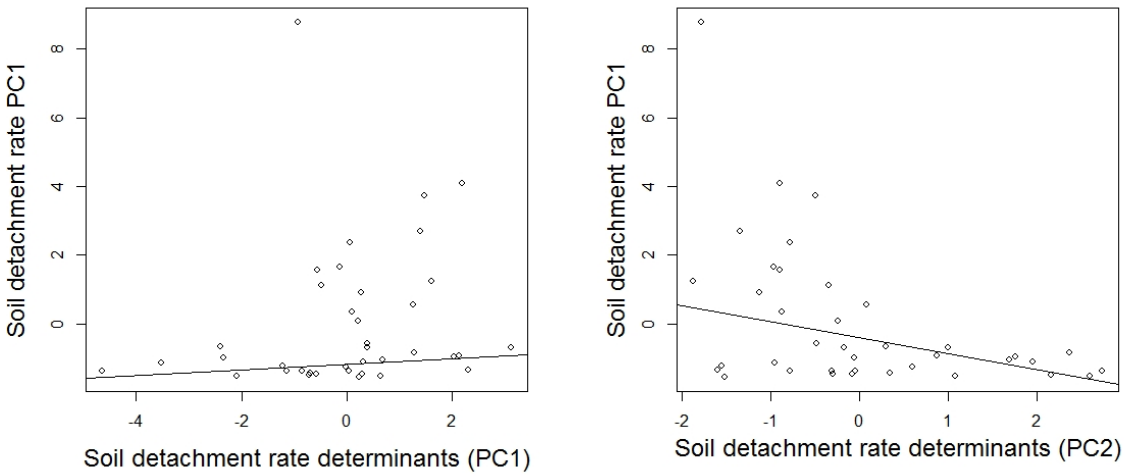

Figure IV. 7. The first two principal component analysis (PCA) axis of the soil detachment rate determinants (PC1 and PC2) (panels a and b respectively) were also used as predictor (x axis) of the first principal component analysis of soil detachment rate (PC1) (y axis). Linear model were fitted using generalized least square (GLS) method corrected for heterogeneity of variances and spatial autocorrelation.

Comparing the slopes of correlation between the five time points soil detachment rate to the soil detachment rate determinants PC2, we found that the highest slope was found in TS1.R2, followed by TS1.R3, TS1.R5, TS1.R1, and TS1.R4 respectively (Table IV. 3, Fig. IV. 8). As a reminder, the detachment rate of TS2 and TS1 corresponds to significant correlation with total root biomass, fine root length and AMF extraradical hyphae.

Meanwhile, the detachment rate of TS1.R3 and TS1.R5 corresponds to significant correlation with total root biomass and AMF extraradical hyphae, while the soil detachment rate of TS4 corresponds significantly only to AMF extraradical hyphal length. This implies that at the first two time points, soil detachment rate corresponds largely to total root biomass, fine root length, and AMF extraradical hyphal length. Meanwhile during later time points, the soil detachment rate of TS1.R3, TS1.R5, and TS1.R4, showed that the significance of fine root length was diminished, and the pattern of soil detachment was solely correlated to total root biomass and AMF extraradical hyphal length (for TS1.R3 and TS1.R5) or AMF extraradical hyphal length only (for TS1.R4).

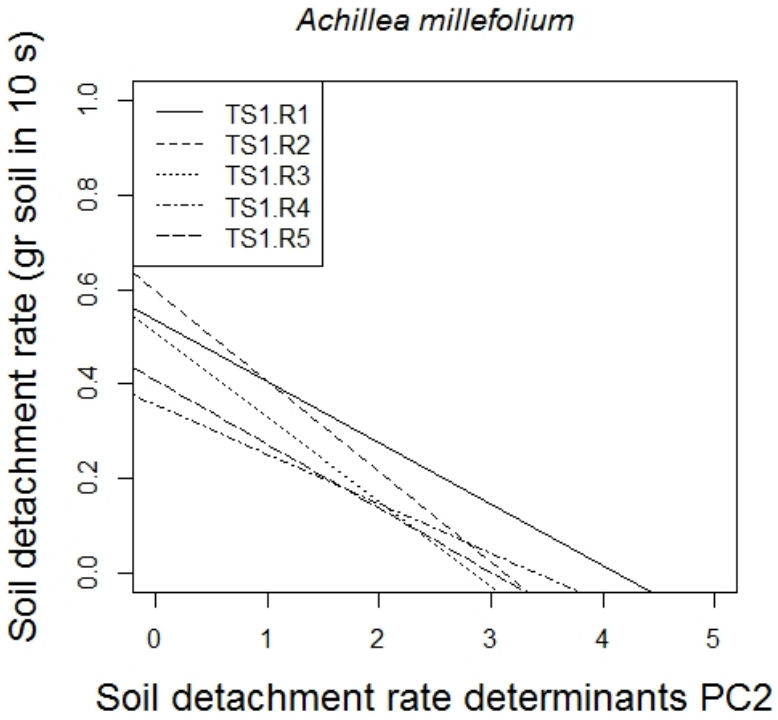

Figure IV. 8. Linear model fitted using generalized least square (GLS) method corrected for heterogeneity of variances an spatial autocorrelation were used to correlate soil detachment rate (0-1 cm soil layer, time point R1, R2, R3, R4 and R5) (y axis) with soil detachment rate determinants (PC2) (x axis). The diagram shows only the fitted lines, omitting data points.

Discussion

As predicted, we found that soils which were planted were able to sustain concentrated flow erosion despite having all aboveground biomass clipped. The general trend was that the soil detachment rate was highest at the beginning of the flume experiment and lowest by the end of the experiment. Despite not showing any differences between treatments, soils planted with *S. canadensis* were able to reduce surface soil erosion up to 94-97% compared to bare soil. Meanwhile, within the *A. millefolium* treatment, surface soil erosion was reduced up to ~98% by AMF treatment, followed by ~93, ~85 and ~83% for AMF with microbial wash, microbial wash and control treatments respectively, compared to surface soil erosion in bare soil. This reduced surface soil erosion due to AMF treatments when using *A. millefolium* was even higher compared to the study by Prosser *et al*., (1995) whereas complete aboveground clipping reduced 11-38% of surface flow erosion compare to 90% reduced value when soil was densely covered with grass, although in this case, the experiment used tall bunch grass planted on a field plot.

Soil erosion resistance for each treatment was reduced as the tests were conducted at deeper soil layers (1-5 cm and >5 cm layers). This trend might be due to differences of moisture content through deeper layers. One of the justifications for adjusting water content for all samples towards field capacity was to ensure that the moisture content of the samples were not different due to differences at the time of conducting the flume experiment. Govers *et al*., (1990) has shown that dry soil has higher potential to be eroded by concentrated flow erosion compare to wet soil. Thus soil moisture does not seem to explain the higher surface

soil erosion as deeper layers were tested. The trend might also be explained simply by the reduced root density through depth as was the findings of De Baets, *et al*. (2007) which showed that root density decreased exponentially with soil depth. Unfortunately we are as of yet not able to determine exactly which variables might be responsible for this trend.

Our study clearly showed that the main drivers of soil detachment rate were root biomass and AMF extraradical hyphal length. This is to our knowledge, the first time that AMF extraradical hyphal length was shown to have direct effect in reducing surface soil erosion due to concentrated flow in a flume experiment. Interestingly, our analysis showed that root biomass can increase soil detachment rate which is in contrast to various studies testing the role of root biomass. Kort *et al*. (1998), Gyssels *et al*. (2005) and a flume experiment by De Baets *et al*. (2006) showed that the increase of root biomass has a negative exponential relation with soil detachment rate. This might actually be due to the type of root which contributes to total root biomass. Our analysis showed that coarse root length together with root biomass were highly correlated and driving our ordination analysis negatively. This means that at least when root biomass is mainly contributed by coarse root length, at least in our case, it has a positive correlation with soil detachment rate. In a flume experiment testing the role of different root architectures, using finely branched grass roots and a tap root system, De Baets *et al.* (2007) found that root system with larger diameter has less efficiency in sustaining surface soil erosion compared to finer root system. Nevertheless, in contrast to our findings, the correlation between the larger diameter roots (5-15 mm) in De Baets *et al.* (2007) study was still negative towards soil detachment rate. Thus, further studies are required for us to understand the mechanism behind these findings.

Our results showed that the inoculation of AMF and AMF with microbial wash in soil planted with *A. millefolium* was able to significantly reduce surface soil erosion. This effect is shown despite the fact that AMF inoculation did not increase root biomass significantly and even caused reduced aboveground biomass compared to control. The role of AMF in sustaining surface soil erosion, at least in this case, seems to be due to the ability of AMF to produce more extraradical hyphae. A study of AMF role against wind erodibility of soil in a wind tunnel experiment showed that AMF treatments significantly had smaller aboveground biomass and smaller root systems than non-mycorrhizal plants, but were able to significantly decrease soil loss (Burri *et al*., 2011). Burri *et al*. (2011) did not address directly the role of extraradical hyphae but showed increased root colonization with decreased soil loss.

The addition of microbial wash which might introduce natural saprobic fungi and bacteria, seems to be affecting the efficiency of the AMF treatment negatively. This was shown by the reduced mean length of AMF extraradical hyphae when both inocula were applied together. Nevertheless, the addition of microbial wash did not seem to reduce soil detachment rate significantly compared to the control treatment.

Although soil stability can be implied through the development of soil structure measured as the amount of stable aggregates (Bearden and Petersen 2000; Chaudary *et al*., 2009), we did not find significant difference between total WSA of the four treatments for *A. millefolium.* We also did not find significant correlations of soil detachment rate with total WSA in our linear model nor significant correlation between total WSA with AMF

extraradical hyphal length (data not shown). Nevertheless, in our ordination multivariate analysis, although to a lesser extent, total WSA, together with hyphal length variables drove the significant axis positively which correlated negatively with increase of soil detachment rate. The stability of soil aggregates has been shown to play a role in sustaining simulated rainfall erosion (Bajracharya and Lal, 1998; Fox and Le Bissonnais, 1998). The apparent lack of its role in our experiment might implied that soil aggregate stability might not be an important factor in sustaining soil erosion due to concentrated flow.

Studies shown that microbial crusts, which are assemblages of microbiota (mosses, liverworts, cyanobacteria, lichen, fungi and bacteria) that form associations with surface soil (Eldridge and Greene, 1994), can play a role in changing the microtopography of soil surfaces (Belnap *et al*., 2003), increasing soil surface roughness and to an extent, reducing surface soil erosion (Campbell *et.al*., 1989; Hu *et al*., 2002). This is in contrast to physical soil crusts whose increased formation can lead to the degradation of surface structure, hence, increasing soil erosion (Auzet *et al*., 1995). Further studies are required for us to understand if this variable might play a role in sustaining soil erosion under similar settings as our experiment.

The effects of AMF treatments were not found in the soil planted with *S. canadensis*, which in fact, are better in reducing surface soil erosion compare to *A. millefolium* (except for *A. millefolium* with AMF treatment). In fact, both plants are known to have fibrous roots with rhizome system. It is probable that the effect of AMF extraradical hyphae was diminished because of the length of experiment which led to a more extensive growth of fibrous root

system in *S. canadensis* compared to *A. millefolium* which in the end played a dominant role in reducing soil erosion in this plant.

Previous studies on an island braided reach of the Tagliamento River, Italy, implied that soil structure increased through time (Harner *et al*., 2011; Mardhiah *et al*., 2014). The development of soil structure on these islands might help this river landform to sustain eroding forces from hydrological and geomorphological forces and dynamics. Mardhiah *et al*. (2014) were able to show that the role of root variables and extraradical hyphae significantly influence the development of soil structure, although direct causality cannot be concluded just through this findings. Although our experiment is an extreme simplification of such natural system, we were able to show that AMF extraradical hyphae have a substantial role in decreasing soil detachment rate after being subjected to a constant water flow. Further work is necessary to improve the ability to detect such roles, probably by reducing the period of the greenhouse experiment (Leifheit *et al.*, 2014), adjusting pot size for plants with larger size as in the case of *S. canadensis*, and or subjecting the soil to different mean bottom flow shear stress.

Soil degradation due to erosion is a serious problem by not just causing the degradation of crop production (Pimentel, 2006) or decreasing natural landforms stability (Gurnell *et al*., 2012) but also by virtue of its effect on soil carbon dynamics (Lal, 2001). This underscores the importance of studying the role of AMF in such processes for better soil erosion management.

Acknowledgments

Ulfah Mardhiah's research is funded by the SMART Joint Doctoral Programme (Science for MAnagement of Rivers and their Tidal systems), which is financed by the Erasmus Mundus Programme of the European Union. We would like to thank Dr. Walter Bertoldi from the Faculty of Engineering, University of Trento, for providing the hydraulic flume. We would also like to thank Dr. Marco Redolfi for the invaluable discussion on the flume experimental setup and design.

Appendix B. Supplementary Materials

References

Andrade, G., Mihara, K.L., Linderman, R.G., Bethlenfalvay, G.J., 1998. Soil aggregation status and rhizobacteria in the mycorrhizosphere. Plant Soil 202, 89–96.

Auge, R.M., Stodola, A.J.W., Tims, J.E., Saxton, A.M., 2001. Moisture retention properties of a mycorrhizal soil. Plant Soil 230, 87–97.

Auzet, A.V., Boiffin, J., Ludwig,B., 1995. Concentrated flow erosion in cultivated catchments: influence of soil surface state. Earth Surface Processes and Landforms 20, 759-767.

Bajracharya, R.M., Lal, R., 1998. Crusting effects on erosion processes under simulated rainfall on a tropical Alfisol. Hydrological processes 12, 1927-1938.

Barto, E.K., Alt, F., Oelmann, Y., Wilcke, W., Rillig, M.C., 2010. Contributions of biotic and abiotic factors to soil aggregation across a land use gradient. Soil Biology and Biochemistry. 42, 2316–2324.

Bearden, B.N., Petersen, L., 2000. Influence of arbuscular mycorrhizal fungi on soil structure and aggregate stability of a vertisol. Plant Soil 173–183.

Belnap, J., Prasse, R., Harper, K.T., 2003. Influence of biological soil crusts on soil environments and vascular plants. In Biological soil crusts: structure, function, and management, 281-300. Springer Berlin Heidelberg.

Bronick, C., Lal, R., 2005. Soil structure and management: a review. Geoderma 124, 3–22.

Bryan, R.B., 2000. Soil erodibility and processes of water erosion on hillslope. Geomorphology 32, 385–415.

Burri, K., Gromke, C., Lehning, M., Graf, F., 2011. Aeolian sediment transport over vegetation canopies: A wind tunnel study with live plants. Aeolian Research 3, 205–213.

Campbell, S.E., Seeler, J.S., Golubic, S., 1989. Desert crust formation and soil stabilization.

Arid Land Research and Management 3, 217-228.

Chaudhary, V.B., Bowker, M.A., O'Dell, T.E., Grace, J.B., Redman, A.E., Rillig, M.C., Johnson, N.C., 2009. Untangling the Biological Contributions to Soil Stability in Semiarid Shrublands. Ecological Applications 19, 110–122.

Cook, B., Jastrow, J.D., Miller, R., 1988. Root and mycorrhizal endophyte development in a chronosequence of restored taligrass prairie. New Phytologist 110, 355–362.

De Baets, S., Poesen, J., Gyssels, G., Knapen, A., 2006. Effects of grass roots on the erodibility of topsoils during concentrated flow. Geomorphology 76, 54–67.

De Baets, S., Poesen, J., Knapen, A., Galindo, P., 2007. Impact of root architecture on the erosion-reducing potential of roots during concentrated flow. Earth Surface Processes and Landforms 32, 1323–1345.

Eldridge, D.J., Greene, R.S.B., 1994. Microbiotic soil crusts-a review of their roles in soil and ecological processes in the rangelands of Australia.Soil Research 32, 389-415.

Fox, D.M., Le Bissonnais, Y., 1998. Process-based analysis of aggregate stability effects on sealing, infiltration, and interrill erosion. Soil Science Society of America Journal 62, 717-724.

Govers, G., Everaert, W., Poesen, J., Rauws, G., De Ploey, J., & Lautridou, J. P., 1990. A long flume study of the dynamic factors affecting the resistance of a loamy soil to concentrated flow erosion. Earth Surface Processes and Landforms 15, 313-328.

Gurnell, A.M., Bertoldi, W., Corenblit, D., 2012. Changing river channels: the roles of hydrological processes, plants and pioneer fluvial landforms in humid temperate, mixed load, gravel bed rivers. Earth-Science Reviews 111, 129-141.

Gyssels, G., Poesen, J., 2003. The importance of plant root characteristics in controlling concentrated flow erosion rates. Earth Surface Processes and Landforms 28, 371–384.

Gyssels, G., Poesen, J., Bochet, E., Li, Y., 2005. Impact of plant roots on the resistance of soils to erosion by water: a review. Progress in Physical Geography 29, 189–217.

Gyssels, G., Poesen, J., Liu, G., Van Dessel, W., Knapen, A., De Baets, S., 2006. Effects of cereal roots on detachment rates of single- and double-drilled topsoils during concentrated flow. European Journal of Soil Science 57, 381–391.

Harner, M.J., Opitz, N., Geluso, K., Tockner, K., Rillig, M.C., 2011. Arbuscular mycorrhizal fungi on developing islands within a dynamic river floodplain: an investigation across successional gradients and soil depth. Aquatic Sciences 73, 35–42.

Hu, C., Liu, Y., Song, L., Zhang, D., 2002. Effect of desert soil algae on the stabilization of

fine sands. Journal of Applied Phycology 14, 281-292.

Jakobsen, I., Abbott, L., Robson, A., 1992. External hyphae of vesicular-arbuscular mycorrhizal fungi associated with Trifolium sub terraneum L . New Phytologist 120, 371–380.

Jastrow, J., Miller, R., Lussenhop, J., 1998. Contributions of interacting biological mechanisms to soil aggregate stabilization in restored prairie. Soil Biology and Biochemistry 30, 905–916.

Kort, J., Collins, M., Ditsch, D., 1998. A review of soil erosion potential associated with biomass crops. Biomass and Bioenergy 14, 351–359.

Lal, R., 2001. Soil degradation by erosion. Land Degradation and Development 12, 519–539.

Leifheit, E.F., Veresoglou, S.D., Lehmann, A., Morris, E.K., Rillig, M.C., 2014. Multiple factors influence the role of arbuscular mycorrhizal fungi in soil aggregation—a meta-analysis. Plant and Soil 374, 523-537.

Lupwayi, N., Arshad, M., Rice, W., Clayton, G., 2001. Bacterial diversity in water-stable aggregates of soils under conventional and zero tillage management. Applied Soil Ecology 16, 251–261.

Mardhiah, U., Caruso, T., Gurnell, A., Rillig, M.C., 2014. Just a matter of time: Fungi and roots significantly and rapidly aggregate soil over four decades along the Tagliamento River, NE Italy. Soil Biology and Biochemistry 75, 133–142.

Mummey, D. L., Rillig, M. C., 2008. Spatial characterization of arbuscular mycorrhizal fungal molecular diversity at the submetre scale in a temperate grassland. FEMS microbiology ecology 64, 260-270.

Oades, J.M., 1984. Soil organic matter and structural stability: mechanisms and implications for management. Plant Soil 76, 319–337.

Pimentel, D., 2006. Soil erosion: a food and environmental threat. Environment, development and sustainability 8, 119-137.

Pimentel, D., Kounang, N., 1998. Ecology of soil erosion in ecosystems. Ecosystems 1, 416-426.

Piotrowski, J., Lekberg, Y., Harner, M., Ramsey, P., Rillig, M., 2008. Dynamics of mycorrhizae during development of riparian forests along an unregulated river. Ecography 31, 245-253.

Prosser, I.P., Dietrich, W.E., Stevenson, J., 1995. Flow resistance and sediment transport by

concentrated overland flow in a grassland valley. Geomorphology 13, 71–86.

R Development Core Team, 2012. R: A Language and Environment for Statistical Computing. R Foundation for Statistical Computing, Vienna, Austria.

Rillig, M.C., Mummey, D.L., 2006. Mycorrhizas and soil structure. New Phytologist 171, 41–53.

Rillig, M.C., Mardatin, N.F., Leifheit, E.F., Antunes, P.M., 2010. Mycelium of arbuscular mycorrhizal fungi increases soil water repellency and is sufficient to maintain water-stable soil aggregates. Soil Biology and Biochemistry 42, 1189–1191.

Tisdall, J., Oades, J., 1982. Organic matter and water-stable aggregates in soils. Journal of Soil Science 33, 141–163.

Van der Heijden, M.G., Streitwolf-Engel, R., Riedl, R., Siegrist, S., Neudecker, A., Ineichen, K., Boller, T., Wiemken, A., Sanders, I.R., 2006. The mycorrhizal contribution to plant productivity, plant nutrition and soil structure in experimental grassland. New Phytologist 172, 739–752.

Zhou, Z., Shangguan, Z., 2007. The effects of ryegrass roots and shoots on loess erosion under simulated rainfall. Catena 70, 350–355.

CHAPTER 5

Summary

Flagogna reach endures various disturbances, mainly due to the natural dynamics of the river system. As described in Bertoldi *et al*., (2009), river flow with water levels of approximately 200 cm (as measured in the local Villuzza gauge), will cause an interaction between the river flow and the various vegetated patches within the reach. Further increase of water level (above 300 cm) will cause severe vegetation disturbance, most importantly erosion on fluvial island margins and the uprooting of mature trees which will later disperse within the reach serving as fluvial island nucleation points. We used both field measurements (dendrochronology) and historical sources (river stage records, oblique photographs, and aerial image analysis) to construct the historical changes of different age patches within the reach. We found that both approaches sufficiently support each other and help us to specifically identify the time of uprooted trees establishment and how they developed or eroded through certain temporal sequence. We also found that the aerial image analysis is a valuable tool and statistically correct in supporting our current analysis.

We managed to use the various tools to understand the phases of island development within the reach. Our oldest sampling area, for example, showed the evolution of fluvial islands before the dispersal of uprooted trees, right after the establishment of uprooted trees, and then followed the evolution from pioneer, building and finally established island as its current state. We also found that historically, the dispersal of uprooted trees does not guarantee that these pioneer islands develop into established islands. Our data showed

(Chapter 2) that various island age groups can take different rates of development constrained by the particular dynamics experienced within each of the different age groups. The permanence of fluvial islands in such dynamic system has been known to be relatively unstable, with islands usually incapable of sustaining more than a decadal temporal range (Wyrick and Klingeman, 2011). This study showed how at least in our period of study (~40 years) uprooted trees can be deposited and developed into established island and how the development of younger islands (building and pioneer islands) will mainly be constrained by the coming flood pulses and their magnitude.

We understood from our system that the aggrading process and relative distance of vegetated island patches to the water table is an important factor which ensures a gradual evolution of fluvial islands. We also understood that disturbances like flood and flow pulses will be able to reset the development of fluvial islands. We found that as fluvial islands develop through time, so does the surface soil structure (Chapter 3). In fact our system reaches ~80% macroaggregate content within 40 years. We found that the rate of growth was constrained differently; such that in the short to medium term it was highly varied and mostly depended on the organic carbon content, fungal variables and also pH. With islands developing in the medium to long term, soil structure was mainly correlated with the accumulation of nitrogen and increases of fungal hyphae and plant roots displaying a two phase development of fluvial islands. Our findings emphasize the possible role of fungal variables, especially AMF, for contributing towards soil structure development. This implied the role of AMF in maintaining soil stability and to an extent, functioning as one of the protective components against soil erosion. Nevertheless, the analysis could not derive

causality between these two components.

Our greenhouse experiment was conducted to partially answer our question about the role of AMF in sustaining flow stress which would cause soil erosion. A simplified system of a hydraulic flume was used to identify the role of AMF in alleviating the effect of soil erosion due to flow shear stress. We found that at least in one of the test plants we used, did the addition of AMF inoculum decrease soil erosion. We found this result, despite the fact that AMF inoculum addition did not increase aboveground or belowground biomass of the plants. Interestingly, in contrast to previous findings, our results shown that root biomass can actually increase soil erosion. This finding is most likely related to the high correlation between the coarse root length with root biomass rather than the effect of finer root length. AMF extraradical hyphal length was able to decrease soil erosion (Chapter 4). This showed for the first time a direct role of AMF towards the alleviation of soil erosion due to concentrated flow.

Synthesis

In conducting field work, especially work that covers a huge variance due to the underlying decadal time scale, it is important to be able to compile information from various sources, confirmed through statistical approaches (Chapter 2). This would enable us to pin point the exact time when high impact processes change the system. In our case, the use of both historical and field data to study the vegetation change and island deposition time along our studied reach, helped us to understand the dynamics within the region with greater precision. This was later used to justify our sampling approaches (Chapter 3). We were able

to strongly conclude, that in a dynamic system such as the Tagliamento River, soil structure can develop significantly through time. Various variables which contributed to the development showed a shift through time. In the short term, soil structure development was mainly driven by organic carbon and fungal variables. In the longer term, the role of organic carbon was decreased and total nitrogen and plant roots played a more significant role for soil structure development. Nevertheless, fungal variables contributed to the development throughout the whole period. This motivated us to conduct a greenhouse experiment accompanied with a direct soil erosion test, which showed that the role of fungal variables, especially through AMF extraradical hypae, is significant and important to aid soil sustainability. In fact, root variables can increase soil erosion when focusing on the role of coarse proportion of the biomass (Chapter 4).

Future perspective

The result of this dissertation requires further extensive study especially to properly disentangle the relative contributions of AMF and plant roots in sustaining against the effect of soil erosion due to flow shear stress. This can be done by conducting a relatively shorter greenhouse experiment to enable us to see the contribution of soil aggregation towards soil stability. This would enable us to see a clear correlation between soil erosion, soil structure, AMF hyphal length, and plant roots variables. Further measurements of root colonization would also be required for better understanding of AMF role within the process.

CHAPTER 6

Zusammenfassung

Der Einflussbereich des Flagogna (ein Teilabschnitt des Tagliamento-Flusses) muss vielen Störungen standhalten, die hauptsächlich auf die natürliche Dynamik des Flusssystems zurückzuführen sind. Flüsse, die mit einer Fließhöhe von 200 cm (gemessen in der lokalen Messstation von Villuzza) verlaufen, verursachen eine Interaktion zwischen der geführten Wassermenge und bewachsener Abschnitte innerhalb des Einflussbereiches (Bertoldi *et al*., 2009). Ein zusätzlicher Anstieg des Wasserlevels über 300 cm würde indes zu schweren Vegetationsstörungen führen. Zu den bedeutsamsten Folgen solcher Störereignisse gehören die Erosion an Rändern von fluvialen Inseln sowie das Entwurzeln ausgewachsener Bäume, die nach anfänglicher Dispersion im Einflussbereich zu Initiationskernen zukünftiger fluvialer Inseln werden können.

Im Rahmen unserer Studien wurden sowohl Feldmessungen (Dendrochronologie) als auch historische Quellen (Flussabschnitt-spezifische Datensätze, Schrägbilder und Analysen von Luftaufnahmen) genutzt, um die Entstehung und die sukzessive Veränderungen der fluvialen Inseln im Einflussbereich des Flagogna zu rekonstruieren. Wir fanden heraus, dass die Ergebnisse, die durch beide Ansätze gewonnen wurden, zu gleichen Schlussfolgerungen führen und uns somit die zeitliche Einordnung der Etablierung von entwurzelten Bäumen als fluviale Inselinitiationskerne und deren Erosion oder Weiterentwicklung zu fluvialen Inseln ermöglichen. Zudem zeigte sich, dass die Analyse der historischen Luftaufnahmen ein wertvolles, statistisch auswertbares Werkzeug für unsere Analysen war.

Die verschiedenen Methoden halfen uns die Phasen der Inselentwicklung innerhalb des Flagogna Einflussbereiches zu verstehen. Unser ältestes Beprobungsgebiet zeigte z.B. die Evolution der fluvialen Inseln vor und nach der Inkorporation von entwurzelten Bäumen sowie deren darauffolgende Entwicklung, Aufbau und finale Etablierung (im Zustand, wie wir sie heute vorfinden können). Wir konnten ebenfalls belegen, dass die Verbreitung von entwurzelten Bäumen kein Garant dafür ist, dass Pioniereinseln sich auch entwickeln und etablieren können. Wie unsere Daten zeigen, können verschiedene Altersklassen von Inseln unterschiedliche Entwicklungsraten aufweisen, die entsprechend der Kräfteeinwirkungen innerhalb der jeweiligen Altersklassen vorgegeben werden (Kapitel 2). Die Beständigkeit der fluvialen Inseln in solchen dynamischen Systemen ist relative kurz, da solche Inseln selten länger als eine Dekade überdauern (Wyrick and Klingeman, 2011). In unserer Studie konnten wir zeigen, dass im Zeitrahmen unserer Untersuchungen (ca. 40 Jahre) entwurzelte Bäume sich in Einflussbereichen ablagern und zu etablierten Inseln entwickeln können und das die Entwicklung junger, fluvialer Inseln (sich aufbauende und Pionierinseln) hauptsächlich durch eintretende Flutungspulse und deren Stärke begrenzt wird.

Eine wichtige Erkenntnis unserer Studien war, dass der Prozess des Aggradierens sowie die relative Entfernung von bewachsenen Inselabschnitten zum Wasserspiegel entscheidende Faktoren sind, die die graduelle Evolution von fluvialen Inseln gewährleistet. Des Weiteren unterstrichen unsere Ergebnisse die Bedeutsamkeit von Störungen wie Überflutungen und Flutungspulsen für die Zurücksetzung des Entwicklungsstadiums von fluvialen Inseln. Hier zeigte sich, dass sich fluviale Inseln und im Speziellen ihre Bodenoberflächenstruktur über die Zeit hinweg entwickeln (Kapitel 3), wobei Bodenproben unseres Testsystem bis zu 80%

Makroaggregatanteile innerhalb einer Zeitspanne von 40 Jahren erreichen konnten. Die Wachstumsrate von Inseln in unserem Testsystem wurde durch verschiedenste Faktoren beeinflusst. Für kurz- bis mittelfristige Zeiträume waren die Wachstumsraten höchst variabel und hauptsächlich durch den Anteil an organischem Kohlenstoff, Pilzhyphenlänge sowie Boden-pH beeinflusst. Für mittel- bis langfristige Zeiträume verbesserte sich die Bodenstruktur mit steigenden Gehalten von Bodenstickstoff, Pilzhyphen und Pflanzenwurzeln; dies spiegelt den zwei Phasen-Charakter der Entstehung von fluvialen Inseln wider. Unsere Ergebnisse unterstreichen zudem die potenziell bedeutsame Rolle von Pilzen, hier im Speziellen von arbuskulären Mykorrhizapilzen (AMF), für die Entwicklung von Bodenstruktur auf fluvialen Inseln. Somit sind AMF potenziell bedeutsam für den Erhalt von Bodenstabilität sowie dem Schutz vor Bodenerosion in unserem Testsystem; hierbei konnte jedoch keine Kausalität nachgewiesen werden.

Die Durchführung unseres Gewächshausexperiments diente der Beantwortung der Frage, inwieweit AMF und Pflanzenwurzeln die Widerstandsfähigkeit von Boden gegenüber dem Stressfaktor Wasserfluss und damit einhergehender Bodenerosion verbessern können. Ein simplifiziertes Model eines Schwemmkanals wurde hierfür genutzt. Im Gegensatz zu früheren Untersuchungsergebnissen zeigen unsere Daten, dass eine höhere Wurzelbiomasse zu verstärkter Bodenerosion führen kann. Dies liegt wahrscheinlich am hohen Anteil der groben Wurzeln an der Gesamtwurzelbiomasse der Testpflanzen, die eine eher geringe Menge an Feinwurzeln aufwiesen. Für eine unserer getesteten Pflanzenarten senkte die Inokulation mit AMF die Bodenerosion, obwohl AMF weder über- noch unterirdischen Biomassenzuwachs bewirken konnte. Diese Ergebnisse stellen den ersten Nachweis für

einen positiven Einflusses von AMF auf die Minimierung von Bodenerosion dar (Kapitel 4).

Synthese

Bei der Durchführung von Feldstudien, besonders bei Arbeiten die eine große Zeitspanne umfassen, ist es entscheidend Informationen aus verschiedensten Quellen zusammenzutragen und diese durch statistische Analysen zu untermauern (Kapitel 2). Dies ermöglicht die zeitliche Eingrenzung von Ereignissen mit hohem Einfluss auf Systemänderungen. In unserem Testsystem erwies sich der Einsatz von historischen und Felddaten als besonders wertvoll für die Studie von Vegetationsänderungen und Inselablagerungen entlang des Einflussbereiches des Flagogna und verbesserte unser Verständnis der dynamischen Prozesse in dieser Region. Diese Erkenntnisse bildeten später die Grundlage für unsere Probennahmen (Kapitel 3). Mit den gesmmelten Proben konnten wir nachweisen, dass sich in einem dynamischen System wie dem Fluss Tagliamento Bodenstruktur signifikant über die Zeit hinweg entwickeln kann. Für kurzfristige Zeiträume wird die Bodenstrukturentwicklung hauptsächlich durch organischen Kohlenstoff und Pilzhyphenlänge bestimmt. Für längerfristige Zeiträume wird die Rolle von organischem Kohlenstoff zunehmend bedeutungslos, während Bodenstickstoff, Pilzhyphenlänge sowie Pflanzenwurzeln an Einfluss gewinnen. Jedoch schien der Pilzfaktor eine beständige Rolle für die Bodenstrukturentwicklung für junge als auch alte Inseln zu spielen. Diese Erkenntnis führte zur Durchführung unseres Gewächshausexperimentes, bei dem Bodenerosion direkt gemessen wurde. Hier zeigte sich, dass der Pilzfaktor (hier im Speziellen die extraradikale Hyphenlänge von AMF) signifikant bedeutsam ist für die

Bodenstabilität. Im Gegensatz dazu kann der Pflanzenfaktoren (hier im Speziellen die groben Wurzelanteile des gesamten Wurzelsystems) Bodenerosion verstärken (Kapitel 4).

Zukunftsperspektiven

Die Ergebnisse dieser Dissertation müssen durch zusätzliche intensive Studien erweitert werden, um den relativen Beitrag von AMF und Pflanzenwurzeln für die Widerstandskraft des Bodens gegen die Flussscherkräfte der Bodenerosion zu ermitteln. Dies könnte in einem relativ kurzen Gewächshausexperiment erreicht werden, bei dem die Bedeutung von Bodenaggregation für die Bodenstabilität bewertet werden sollte. Somit könnte eine Korrelation zwischen Bodenstruktur, Bodenerosion, AMF Hyphenlänge und Pflanzenfaktoren ermittelt werden. Die Erhebungen von Wurzelkolonisationsdaten würde zusätzlich das Verständnis für die Rolle von AMF innerhalb dieses Prozesses verbessern.

BIBLIOGRAPHIC REFERENCES

Angers, D. A., Caron, J., 1998. Plant-induced changes in soil structure: processes and feedbacks. In Plant-induced soil changes: Processes and feedbacks, 55-72. Springer Netherlands.

Arscott, D.B., Tockner, K., Ward, J.V., 2000. Aquatic habitat diversity along the corridor of an Alpine floodplain river (Fiume Tagliamento, Italy). Archiv für Hydrobiologie 149, 679-704.

Barthes, B., Azontonde, A., Boli, B., Prat, C., Roose, E., 2000. Field-scale run-off and erosion in relation to topsoil aggregate stability in three tropical regions (Benin, Cameroon, Mexico). European Journal of Soil Science 51, 485–495.

Barto, E.K., Alt, F., Oelmann, Y., Wilcke, W., Rillig, M.C., 2010. Contributions of biotic and abiotic factors to soil aggregation across a land use gradient. Soil Biology and Biochemistry 42, 2316–2324.

Bertoldi, W., Gurnell, A., Surian, N., Tockner, K., Zanoni, L., Ziliani, L., Zolezzi, G., 2009. Understanding reference processes: linkages between river flows, sediment dynamics and vegetated landforms along the Tagliamento River, Italy. River Research and Appication 25, 501–516.

Bronick, C., Lal, R., 2005. Soil structure and management: a review. Geoderma 124, 3–22.

Bryan, R.B., 2000. Soil erodibility and processes of water erosion on hillslope. Geomorphology 32, 385–415.

Chaudhary, V.B., Bowker, M.A., O'Dell, T.E., Grace, J.B., Redman, A.E., Rillig, M.C., Johnson, N.C., 2009. Untangling the Biological Contributions to Soil Stability in Semiarid Shrublands. Ecological Application 19, 110–122.

De Baets, S., Poesen, J., Gyssels, G., Knapen, A., 2006. Effects of grass roots on the erodibility of topsoils during concentrated flow. Geomorphology 76, 54–67.

De Baets, S., Poesen, J., Knapen, A., Galindo, P., 2007. Impact of root architecture on the erosion-reducing potential of roots during concentrated flow. Earth Surface Processes and Landforms 32, 1323–1345.

Edwards, P., Kollmann, J., Gurnell, A., Petts, G., Tockner, K., Ward, J., 1999. A conceptual model of vegetation dynamics on gravel bars of a large Alpine river. Wetlands Ecology and Management 7, 141–153.

Francis, R.A., Tibaldeschi, P., McDougall, L., 2008. Fluvially-deposited large wood and riparian plant diversity. Wetlands Ecology and Management 16, 371–382.

Gurnell, A. M., Petts, G. E., Hannah, D. M., Smith, B. P., Edwards, P. J., Kollmann, J., Tockner, K., 2001. Riparian vegetation and island formation along the gravel-bed Fiume Tagliamento, Italy. Earth Surface Processes and Landforms 26, 31-62.

Gurnell, A. M., Petts, G. E., 2002. Island-dominated landscapes of large floodplain rivers, a European perspective. Freshwater Biology 47, 581-600.

Gyssels, G., Poesen, J., 2003. The importance of plant root characteristics in controlling concentrated flow erosion rates. Earth Surface Processes and Landforms 28, 371–384.

Gyssels, G., Poesen, J., Bochet, E., Li, Y., 2005. Impact of plant roots on the resistance of soils to erosion by water: a review. Progress in Physical Geography 29, 189–217.

Harner, M.J., Opitz, N., Geluso, K., Tockner, K., Rillig, M.C., 2011. Arbuscular mycorrhizal fungi on developing islands within a dynamic river floodplain: an investigation across successional gradients and soil depth. Aquatic Sciences 73, 35–42.

Junk, W. J., Bayley, P. B., Sparks, R.E., 1989. The flood pulse concept in river-floodplain systems. Canadian special publication of fisheries and aquatic sciences 106, 110-127.

Karrenberg, S., Kollmann, J., Edwards, P.J., Gurnell, A.M., Petts, G.E., 2003. Basic and Applied Ecology Patterns in woody vegetation along the active zone of a near-natural Alpine river. Basic and Applied Ecology 4, 157–166.

Kollmann, J., Vieli, M., Edwards, P.J., Tockner, K., Ward, J. V., 1999. Interactions between vegetation development and island formation in the Alpine river Tagliamento. Applied Vegetation Science 2, 25–36.

Miller, R.M., Jastrow, J.D., 1990. Hierarchy of root and mycorrhizal fungal interactions with soil aggregation. Soil Biology and Biochemistry 22, 579–584.

Naiman, R.J., Decamps, H., Pollock, M., 1993. The role of riparian corridors in maintaining regional biodiversity. Ecological Application 3, 209–212.

Naiman, J., Decamps, H., 1997. The ecology of interfaces : Riparian Zones. Annual Review of Ecology, Evolution, and Systematics 28, 621–658.

Oades, J.M., 1984. Soil organic matter and structural stability: mechanisms and implications for management. Plant Soil 76, 319–337.

Oades, J.M., 1993. The role of biology in the formation, stabilization and degradation of soil structure. Geoderma 56, 377-400.

Osterkamp, W.R., 1998. Processes of fluvial island formation, with examples from Plum Creek, Colorado and Snake River, Idaho. Wetlands 18, 530–545.

Piotrowski, J., Lekberg, Y., Harner, M., Ramsey, P., Rillig, M., 2008. Dynamics of mycorrhizae during development of riparian forests along an unregulated river. Ecography (Cop.) 31, 245–253.

Rillig, M.C., Wright, S.F., Eviner, V.T., 2002. The role of arbuscular mycorrhizal fungi and glomalin in soil aggregation: comparing effects of five plant species. Plant Soil 238, 325–333.

Six, J., Bossuyt, H., Degryze, S., Denef, K., 2004. A history of research on the link between (micro)aggregates, soil biota, and soil organic matter dynamics. Soil and Tillage Research 79, 7–31.

Smith, K. A., Dobbie, K. E., Ball, B. C., Bakken, L. R., Sitaula, B. K., Hansen, S., Brumme, R., Borken, W., Christensen, S., Priemé, A., Fowler, D., Macdonald, J. A., Skiba, U., Klemedtsson, L., Kasimir-Klemedtsson, A., Degórska, A., Orlanski, P., 2000. Oxidation of atmospheric methane in Northern European soils, comparison with other ecosystems, and uncertainties in the global terrestrial sink. Global Change Biology 6, 791-803.

Soil Science Society of America, 2008. Glossary of soil science terms. American Society of Agronomy, SSSA, Madison, WE.

Stromberg, J.C., 2001. Restoration of rivarian vegetation in the south-western United States: importance of flow regimes and fluvial dynamism. Journal of Arid Environments 49,

17–34.

Tabacchi, E., Correll, D.L., Hauer, R., Pinay, G., Planty-Tabacchi, A.-M., Wissmar, R.C., 1998. Development, maintenance and role of riparian vegetation in the river landscape. Freshwater Biology 40, 497–516.

Tockner, K., Stanford, J.A., 2002. Riverine flood plains: present state and future trends. Environmental Conservation 29, 308–330.

Tockner, K., Ward, J. V., Arscott, D.B., Edwards, P.J., Kollmann, J., Gurnell, A.M., Petts, G.E., Maiolini, B., 2003. The Tagliamento River: A model ecosystem of European importance. Aquatic Sciences 65, 239–253.

Toner, M., Keddy, P., 1997. River Hydrology and Riparian Wetlands : A Predictive Model for Ecological Assembly. Ecological Application 7, 236–246.

Ward, J. V, Tockner, K., Edwards, P.J., Kollmann, J., Bretschko, G., Gurnell, A.M., Petts, G.E., Rossaro, B., 1999. A reference river system for the Alps: the “Fiume Tagliamento”. Regulated Rivers: Research and Management 15, 63–75.

Ward, J. V., Tockner, K., Arscott, D.B., Claret, C., 2002. Riverine landscape diversity. Freshwater Biology 47, 517–539.

Wilson, G.W.T., Rice, C.W., Rillig, M.C., Springer, A., Hartnett, D.C., 2009. Soil aggregation and carbon sequestration are tightly correlated with the abundance of arbuscular mycorrhizal fungi: results from long-term field experiments. Ecology Letters 12, 452–461.

Wyrick, J.R., Klingeman, P.C., 2011. Proposed fluvial island classification scheme and its use for river restoration. River Research and Application 825, 814–825.

CONTRIBUTION TO PUBLICATIONS

I. Mardhiah, U., Rillig, M.C., Gurnell, A., 2014. Soil development on fluvial islands: combining information from historical sources, field measurements and laboratory analyses. Earth Surface Processes and Landforms (in press)

Own contribution:

UM performed the analysis on the river stage records, aerial images, field sampling data, the laboratory measurements and wrote the manuscript. AG assisted the field sampling, performed analysis for the oblique photographs, and mentored the analysis and manuscript writing. All authors reviewed the manuscript.

II. Mardhiah, U., Caruso, T., Gurnell, A., Rillig, M.C., 2014. Just a matter of time: fungi and roots significantly and rapidly aggregate soil over four decades along the Tagliamento River, NE Italy. Soil Biology & Biochemistry 75, 133-142.

Own contribution:

UM performed the field sampling, all the analysis and wrote the manuscript. AG assisted the field sampling. CT mentored the analysis and wrote several R script. All authors reviewed the manuscript.

III. Mardhiah, U., Caruso, T., Gurnell, A., Rillig, M.C., Root and arbuscular mycorrhizal hyphae contrasting effect on surface soil flow erosion: a greenhouse experiment.

Own contribution

UM designed the experiment, performed all the analyses and wrote the manuscript. All authors reviewed the manuscript.

APPENDIX A

Supplementary Material for Chapter 3

Supplementary material 1

Table III. S1. Linear model fitted using the generalized least square method (gls) to test the response of soil aggregate size class 2-4 mm to soil structure determinants (extraradical AMF hyphal length, non-AMF hyphal length, root biomass, very fine root length, fine root length, coarse root length, total nitrogen, total organic carbon and pH) used as the main effect. Regression parameters (estimated mean value) with significant p-values are shown in bold.

size class 2-4 mm

Coefficients:

	Value	Std.Error	t-value	p-value
(Intercept)	54.02	33.68	1.60	0.11
root biomass (gr/cm^3)	1.21	0.46	2.65	**<0.01**
AMF extraradical hyphae (m/cm^3)	0.15	0.15	0.98	0.33
non AMF hyphae (m/cm^3)	-0.32	0.38	-0.86	0.39
total % Nitrogen	108.01	20.67	5.22	**<0.0001**
% organic Carbon	-0.50	0.38	-1.32	0.19
very fine root length (cm/cm^3)	0.30	0.48	0.63	0.53
fine root length (cm/cm^3)	-0.13	0.17	-0.76	0.45
coarse root length (cm/cm^3)	-6.68	2.88	-2.32	**<0.05**
pH	-7.20	4.39	-1.64	0.10

Correlation:

	(Intercept)	root biomass	AMF hyphae	non AMF hyphae	total % N	% organic C	very fine root length	fine root length	coarse root length	pH
root biomass (gr/cm^3)	0.093									
AMF extraradical hyphae (m/cm^3)	0.081	-0.176								
non AMF hyphae (m/cm^3)	-0.143	-0.012	-0.480							
total % Nitrogen	-0.424	-0.300	-0.132	-0.175						
% organic Carbon	-0.033	0.060	-0.181	0.029	-0.128					
very fine root length (cm/cm^3)	-0.031	-0.057	0.009	-0.018	-0.021	0.001				
fine root length (cm/cm^3)	0.041	-0.278	-0.099	-0.058	0.043	-0.102	-0.569			
coarse root length (cm/cm^3)	-0.073	-0.564	0.170	-0.021	-0.052	0.007	-0.124	-0.124		
pH	-1.000	-0.091	-0.083	0.144	0.420	0.026	0.029	-0.042	0.074	

Table III. S2. Linear model fitted using the generalized least square method (gls) to test the response of soil aggregate size class 1-2 mm to soil structure determinants (extraradical AMF hyphal length, non-AMF hyphal length, root biomass, very fine root length, fine root length, coarse root length, total nitrogen, total organic carbon and pH) as the main effect. Significant p-value is in bold.

size class 1-2 mm

Coefficients:

	Value	Std.Error	t-value	p-value
(Intercept)	56.92	41.61	1.37	0.18
root biomass (gr/cm^3)	-0.02	0.53	-0.05	0.96
AMF extraradical hyphae (m/cm^3)	0.02	0.18	0.10	0.92
non AMF hyphae (m/cm^3)	0.12	0.39	0.31	0.76
total % Nitrogen	62.29	28.60	2.18	**<0.05**
% organic Carbon	-0.23	0.48	-0.48	0.63
very fine root length (cm/cm^3)	0.41	0.51	0.80	0.42
fine root length (cm/cm^3)	0.31	0.21	1.50	0.14
coarse root length (cm/cm^3)	-3.60	3.36	-1.07	0.29
pH	-7.40	5.42	-1.36	0.18

Correlation:

	(Intercept)	root biomass	AMF hyphae	non AMF hyphae	total % N	% organic C	very fine root length	fine root length	coarse root length	pH
root biomass (gr/cm^3)	0.084									
AMF extraradical hyphae (m/cm^3)	0.099	-0.160								
non AMF hyphae (m/cm^3)	-0.062	-0.009	-0.268							
total % Nitrogen	-0.412	-0.254	-0.227	-0.254						
% organic Carbon	-0.075	0.047	-0.202	-0.052	-0.010					
very fine root length (cm/cm^3)	0.057	-0.136	-0.043	0.165	-0.047	-0.104				
fine root length (cm/cm^3)	-0.027	-0.272	-0.048	-0.162	-0.037	-0.045	-0.444			
coarse root length (cm/cm^3)	-0.093	-0.525	0.189	0.024	-0.046	0.045	-0.079	-0.197		
pH	-1.000	-0.082	0.101	-0.064	0.408	0.067	-0.059	0.025	0.094	

Table III. S3. Linear model fitted using the generalized least square method (gls) to test the response of soil aggregate size class 0.5-1 mm to soil structure determinants (extraradical AMF hyphal length, non-AMF hyphal length, root biomass, very fine root length, fine root length, coarse root length, total nitrogen, total organic carbon and pH) as the main effect.

Size class 0.5-1 mm

Coefficients:

	Value	Std.Error	t-value	p-value
(Intercept)	336.15	177.96	1.89	0.06
root biomass (gr/cm^3)	0.80	1.07	0.75	0.46
AMF extraradical hyphae (m/cm^3)	-0.24	0.45	-0.52	0.60
non AMF hyphae (m/cm^3)	0.11	1.04	0.11	0.91
total % Nitrogen	-140.55	76.75	-1.83	0.07
% organic Carbon	2.37	1.69	1.40	0.16
very fine root length (cm/cm^3)	-0.02	1.06	-0.01	0.99
fine root length (cm/cm^3)	-0.73	0.61	-1.20	0.24
coarse root length (cm/cm^3)	-2.90	8.12	-0.36	0.72
pH	-41.12	23.09	-1.79	0.08

Correlation:

	(Intercept)	root biomass	AMF hyphae	non AMF hyphae	total % N	% organic C	very fine root length	fine root length	coarse root length	pH
root biomass (gr/cm^3)	0.201									
AMF extraradical hyphae (m/cm^3)	0.058	-0.091								
non AMF hyphae (m/cm^3)	0.067	0.274	-0.099							
total % Nitrogen	-0.594	-0.399	-0.148	-0.471						
% organic Carbon	-0.201	0.085	-0.151	-0.084	-0.040					
very fine root length (cm/cm^3)	0.042	-0.085	-0.024	0.069	-0.135	-0.293				
fine root length (cm/cm^3)	-0.200	-0.422	-0.020	-0.068	0.122	0.021	-0.242			
coarse root length (cm/cm^3)	-0.197	-0.583	-0.031	-0.173	0.116	0.161	0.132	-0.136		
pH	-1.000	-0.196	-0.064	-0.068	0.593	0.194	-0.042	0.192	0.195	

Table III. S4. Linear model fitted using the generalized least square method (gls) to test the response of soil aggregate size class 0.2-0.5 mm to soil structure determinants (extraradical AMF hyphal length, non-AMF hyphal length, root biomass, very fine root length, fine root length, coarse root length, total nitrogen, total organic carbon and pH) as the main effect.

size class 0.2-0.5 mm

Coefficients:

	Value	Std.Error	t-value	p-value
(Intercept)	-137.09	94.77	-1.45	0.15
root biomass (gr/cm^3)	-0.83	0.46	-1.82	0.07
AMF extraradical hyphae (m/cm^3)	-0.14	0.19	-0.74	0.46
non AMF hyphae (m/cm^3)	0.19	0.44	0.42	0.68
total % Nitrogen	41.01	34.54	1.19	0.24
% organic Carbon	-1.55	0.79	-1.97	0.05
very fine root length (cm/cm^3)	0.34	0.45	0.76	0.45
fine root length (cm/cm^3)	0.07	0.28	0.23	0.81
coarse root length (cm/cm^3)	3.91	3.53	1.11	0.27
pH	19.71	12.25	1.61	0.11

Correlation:

	(Intercept)	root biomass	AMF hyphae	non AMF hyphae	total % N	% organic C	very fine root length	fine root length	coarse root length	pH
root biomass (gr/cm^3)	0.327									
AMF extraradical hyphae (m/cm^3)	-0.014	0.022								
non AMF hyphae (m/cm^3)	0.150	0.368	-0.106							
total % Nitrogen	-0.727	-0.481	-0.073	-0.481						
% organic Carbon	-0.243	0.052	-0.087	-0.046	-0.086					
very fine root length (cm/cm^3)	0.017	-0.132	-0.137	-0.044	-0.045	-0.303				
fine root length (cm/cm^3)	-0.353	-0.515	-0.033	-0.077	0.266	0.104	-0.209			
coarse root length (cm/cm^3)	-0.219	-0.647	-0.208	-0.298	0.170	0.172	0.240	0.010		
pH	-1.000	-0.323	0.008	-0.150	0.727	0.234	-0.015	0.345	0.216	

Table III. S5. Linear model fitted using the generalized least square method (gls) to test the response of soil structure index, percent total WSA, to soil structure determinants (extraradical AMF hyphal length, non-AMF hyphal length, root biomass, very fine root length, fine root length, coarse root length, total nitrogen, total organic carbon and pH) as the main effect.

percent total WSA

Coefficients:

	Value	Std.Error	t-value	p-value
(Intercept)	355.56	199.39	1.78	0.08
root biomass (gr/cm^3)	1.47	1.14	1.29	0.20
AMF extraradical hyphae (m/cm^3)	0.30	0.48	0.63	0.53
non AMF hyphae (m/cm^3)	-0.88	1.14	-0.77	0.44
total % Nitrogen	113.19	80.14	1.41	0.16
% organic Carbon	0.92	1.83	0.50	0.62
very fine root length (cm/cm^3)	0.66	1.18	0.56	0.58
fine root length (cm/cm^3)	-0.83	0.63	-1.32	0.19
coarse root length (cm/cm^3)	-6.90	8.78	-0.79	0.43
pH	-42.05	25.88	-1.62	0.11

Correlation:

	(Intercept)	root biomass	AMF hyphae	non AMF hyphae	total % N	% organic C	very fine root length	fine root length	coarse root length	pH
root biomass (gr/cm^3)	0.208									
AMF extraradical hyphae (m/cm^3)	0.005	-0.050								
non AMF hyphae (m/cm^{3}3)	0.074	0.317	-0.204							
total % Nitrogen	-0.669	-0.417	-0.077	-0.438						
% organic Carbon	-0.144	0.104	-0.149	-0.023	-0.188					
very fine root length (cm/cm^3)	0.016	-0.056	-0.077	-0.034	-0.067	-0.254				
fine root length (cm/cm^3)	-0.183	-0.423	-0.041	-0.065	0.189	0.042	-0.353			
coarse root length (cm/cm^3)	-0.146	-0.616	-0.139	-0.236	0.063	0.125	0.186	-0.103		
pH	-1.000	-0.205	-0.009	-0.074	0.669	0.137	-0.015	0.176	0.145	

Table III. S6. General linear model to test the response of soil structure index, MWD, to soil structure determinants (extraradical AMF hyphal length, non-AMF hyphal length, root biomass, very fine root length, fine root length, coarse root length, total nitrogen, total organic carbon and pH) as the main effect. Regression parameters (estimated mean value) with significant p-values are in bold.

MWD

Coefficients:

	Value	Std.Error	t-value	p-value
(Intercept)	5.50	2.25	2.44	0.02
root biomass (gr/cm^3)	0.05	0.02	3.00	**<0.005**
AMF extraradical hyphae (m/cm^3)	0.01	0.01	1.28	0.21
non AMF hyphae (m/cm^3)	-0.02	0.02	-1.45	0.15
total % Nitrogen	3.93	1.03	3.81	**<0.0005**
% organic Carbon	-0.01	0.02	-0.24	0.81
very fine root length (cm/cm^3)	0.02	0.02	1.31	0.20
fine root length (cm/cm^3)	-0.01	0.01	-1.58	0.12
coarse root length (cm/cm^3)	-0.25	0.13	-2.03	**<0.05**
pH	-0.70	0.29	-2.38	**<0.05**

Correlation:

	(Intercept)	root biomass	AMF hyphae	non AMF hyphae	total % N	% organic C	very fine root length	fine root length	coarse root length	pH
root biomass (gr/cm^3)	0.119									
AMF extraradical hyphae (m/cm^3)	0.032	-0.138								
non AMF hyphae (m/cm^3)	-0.022	0.223	-0.335							
total % Nitrogen	-0.585	-0.368	-0.080	-0.366						
% organic Carbon	-0.069	0.113	-0.186	-0.002	-0.226					
very fine root length (cm/cm^3)	-0.002	0.013	-0.018	-0.032	-0.080	-0.169				
fine root length (cm/cm^3)	-0.039	-0.350	-0.065	-0.067	0.155	-0.011	-0.496			
coarse root length (cm/cm^3)	-0.103	-0.601	-0.006	-0.154	-0.021	0.084	0.086	-0.162		
pH	-1.000	-0.117	-0.035	0.023	0.584	0.062	0.002	0.033	0.104	

Table III. S7. Linear model fitted using the generalized least square method (gls) to test the response of soil structure index, fractal dimension, to soil structure determinants (extraradical AMF hyphal length, non-AMF hyphal length, root biomass, very fine root length, fine root length, coarse root length, total nitrogen, total organic carbon and pH) as the main effect. Regression parameters (estimated mean value) with significant p-values are in bold.

Fractal dimension

Coefficients:

	Value	Std.Error	t-value	p-value
(Intercept)	-8.57	3.04	-2.82	**<0.01**
root biomass (gr/cm^3)	-0.04	0.01	-2.94	**<0.005**
AMF extraradical hyphae (m/cm^3)	0.001	0.01	0.11	0.91
non AMF hyphae (m/cm^3)	0.02	0.01	1.42	0.16
total % Nitrogen	2.05	1.13	1.82	0.07
% organic Carbon	-0.02	0.03	-0.60	0.55
very fine root length (cm/cm^3)	0.004	0.01	-0.29	0.77
fine root length (cm/cm^3)	0.01	0.01	0.83	0.41
coarse root length (cm/cm^3)	0.30	0.12	2.62	**<0.01**
pH	1.36	0.39	3.50	**<0.001**

Correlation:

	(Intercept)	root biomass	AMF hyphae	non AMF hyphae	total % N	% organic C	very fine root length	fine root length	coarse root length	pH
root biomass (gr/cm^3)	0.353									
AMF extraradical hyphae (m/cm^3)	-0.023	-0.049								
non AMF hyphae (m/cm^3)	0.163	0.370	-0.089							
total % Nitrogen	-0.737	-0.500	-0.006	-0.472						
% organic Carbon	-0.335	-0.014	-0.032	-0.075	0.083					
very fine root length (cm/cm^3)	0.049	-0.132	-0.118	-0.030	-0.087	-0.330				
fine root length (cm/cm^3)	-0.372	-0.537	-0.003	-0.084	0.260	0.108	-0.169			
coarse root length (cm/cm^3)	-0.290	-0.655	-0.080	-0.298	0.293	0.283	0.184	0.038		
pH	-0.999	-0.343	0.005	-0.162	0.726	0.315	-0.045	0.366	0.271	

Table III. S8. The table shows correlation test results, based on the Pearson's product moment correlation test, with 95% confidence intervals between all explanatory variables of soil structure determinants (extraradical AMF hyphal length, non-AMF hyphal length, root biomass, very fine root length, fine root length, coarse root length, total nitrogen, total organic carbon and pH) as main effect to each of the response variables of four aggregate-size classes (aggregate size class 2-4, 1-2, 0,.5-1, and 0.2-0.5 mm) and three soil structure indices (percent total WSA, MWD and fractal dimension). The table shows t-values, p-values and correlation values, respectively. Correlations exceeding 0.60 are in bold.

t-value

response variables	size class 2-4	size class 1-2	size class 0.5-1	size class 0.2-0.5	percent total WSA	MWD	fractal dimension			
size class 2-4 mm										
size class 1-2 mm	10.80									
size class 0.5-1 mm	-0.82	0.12								
size class 0.2-0.5 mm	-1.93	-2.57	-2.60							
percent total WSA	5.69	6.28	7.74	NS						
MWD (mm)	20.96	14.79	2.59	-2.06	12.14					
fractal dimension	-4.70	-6.19	-9.19	6.07	-8.39	-8.88				
explanatory variables	site age	root biomass	AMF hyphae	non AMF hyphae	total % N	% organic C	very fine root length	fine root length	coarse root length	pH
site age (year)										
root biomass (gr/cm^3)	9.61									
AMF extraradical hyphae (m/cm^3)	10.25	7.85								
non AMF hyphae (m/cm^3)	10.00	6.53	9.02							
total % Nitrogen	16.91	11.22	9.14	11.17						
% organic Carbon	6.23	3.24	5.15	4.91	6.06					
very fine root length (cm/cm^3)	4.70	6.36	5.35	5.10	6.18	4.34				
fine root length (cm/cm^3)	6.00	11.88	6.66	5.81	7.31	3.32	9.23			
coarse root length (cm/cm^3)	10.66	17.97	7.40	7.18	10.35	3.05	5.64	10.39		
pH	-10.07	-7.46	-6.68	-8.24	-14.67	-5.24	-5	-5.72	-7.66	

p-value

response variables	size class 2-4	size class 1-2	size class 0.5-1	size class 0.2-0.5	percent total WSA	MWD	fractal dimension			
size class 2-4 mm										
size class 1-2 mm	<.0001									
size class 0.5-1 mm	NS	NS								
size class 0.2-0.5 mm	0.05689	<.05	<.05							
percent total WSA	<.0001	<.0001	<.0001	NS						
MWD (mm)	<.0001	<.0001	0.01132	<.05	<.0001					
fractal dimension	<.0001	<.0001	<.0001	<.0001	<.0001	<.0001				
explanatory variables	site age	root biomass	AMF hyphae	non AMF hyphae	total % N	% organic C	very fine root length	fine root length	coarse root length	pH
site age (year)										
root biomass (gr/cm^3)	<.0001									
AMF extraradical hyphae (m/cm^3)	<.0001	<.0001								
non AMF hyphae (m/cm^3)	<.0001	<.0001	<.0001							
total % Nitrogen	<.0001	<.0001	<.0001	<.0001						
% organic Carbon	<.0001	<.005	<.0001	<.0001	<.0001					
very fine root length (cm/cm^3)	<.0001	<.0001	<.0001	<.0001	<.0001	<.0001				
fine root length (cm/cm^3)	<.0001	<.0001	<.0001	<.0001	<.0001	<.0001	<.0001			
coarse root length (cm/cm^3)	<.0001	<.0001	<.0001	<.0001	<.0001	<.005	<.0001	<.0001		
pH	<.0001	<.0001	<.0001	<.0001	<.0001	<.0001	<.0001	<.0001	<.0001	

correlation value

response variables	size class 2-4	size class 1-2	size class 0.5-1	size class 0.2-0.5	percent total WSA	MWD	fractal dimension			
size class 2-4 mm										
size class 1-2 mm	**0.75**									
size class 0.5-1 mm	-0.09	0.01								
size class 0.2-0.5 mm	-0.20	-0.26	-0.27							
percent total WSA	0.52	0.55	**0.63**	NS						
MWD (mm)	**0.91**	**0.84**	0.26	-0.21	**0.79**					
fractal dimension	-0.45	-0.55	**-0.70**	0.54	**-0.66**	**-0.69**				
explanatory variables	site age	root biomass	AMF hyphae	non AMF hyphae	total % N	% organic C	very fine root length	fine root length	coarse root length	pH
site age (year)										
root biomass (gr/cm^3)	**0.71**									
AMF extraradical hyphae (m/cm^3)	**0.74**	**0.64**								
non AMF hyphae (m/cm^3)	**0.73**	0.57	**0.69**							
total % Nitrogen	**0.87**	**0.77**	**0.70**	**0.76**						
% organic Carbon	0.55	0.32	0.48	0.46	0.54					
very fine root length (cm/cm^3)	0.45	0.56	0.49	0.48	0.55	0.42				
fine root length (cm/cm^3)	0.54	**0.78**	0.58	0.52	**0.61**	0.35	**0.70**			
coarse root length (cm/cm^3)	**0.75**	**0.89**	**0.62**	**0.61**	**0.74**	0.31	0.51	**0.74**		
pH	**-0.73**	**-0.62**	-0.58	**-0.66**	**-0.84**	-0.49	-0.47	-0.52	**-0.63**	

Supplementary material 2

Table III. S9. Results of a Principal Components Analysis (PCA) of soil aggregate-size classes (aggregate size class 2-4, 1-2, 0,.5-1, and 0.2-0.5 mm), soil structure indices (percent total WSA, MWD and fractal dimension), and soil structure determinants (extraradical AMF hyphal length, non-AMF hyphal length, root biomass, very fine root length, fine root length, coarse root length, total nitrogen, total organic carbon and pH). We include the results of varimax rotation of the PCs, and also the standard deviation, eigenvalue, proportion and cumulative proportion of the variance explained by the PCs (see also Fig. III. 3).

PCA of proportion of soil-aggregate size classes	rotation			
	PC1	PC2	PC3	PC4
WSA size class 2-4 mm	0.65	-0.25	-0.16	-0.70
WSA size class 1-2 mm	0.67	-0.13	-0.20	0.71
WSA size class 0.5-1 mm	0.06	0.78	-0.62	-0.08
WSA size class 0.2-0.5 mm	-0.36	-0.56	-0.74	0.03
standard deviation	1.37	1.10	0.82	0.49
eigenvalue	1.88	1.22	0.66	0.24
proportion of variance	0.47	0.30	0.17	0.06
cumulative proportion	0.47	0.77	0.94	1.00

PCA of soil structure	rotation		
	PC1	PC2	PC3
total percent WSA	0.59	-0.45	0.68
MWD	0.59	-0.33	-0.73
fractal dimension	-0.56	-0.83	-0.07
standard deviation	1.56	0.60	0.46
eigenvalue	2.43	0.36	0.21
proportion of variance	0.81	0.12	0.07
cumulative proportion	0.81	0.93	1.00

PCA of soil structure determinants	rotation								
	PC1	PC2	PC3	PC4	PC5	PC6	PC7	PC8	PC9
root biomass (gr/cm3)	0.36	-0.35	0.13	-0.14	0.31	-0.01	0.24	0.38	-0.64
AMF extraradical hyphae (m/cm3)	0.33	0.14	0.08	0.68	0.23	0.58	-0.03	-0.08	0.03
non AMF hyphae (m/cm3)	0.33	0.25	0.23	0.43	-0.38	-0.63	-0.04	-0.04	-0.20
total % Nitrogen	0.38	0.16	0.22	-0.20	-0.13	0.06	0.19	0.60	0.57
% organic Carbon	0.24	0.65	-0.42	-0.21	0.50	-0.19	-0.01	-0.06	-0.05
very fine root length (cm/cm3)	0.30	-0.15	-0.69	0.02	-0.48	0.14	0.39	-0.09	-0.03

fine root length (cm/cm3)	0.34	-0.40	-0.30	0.02	0.08	-0.14	-0.75	0.11	0.17
coarse root length (cm/cm3)	0.36	-0.33	0.22	-0.13	0.28	-0.21	0.30	-0.61	0.34
pH	-0.34	-0.23	-0.28	0.48	0.36	-0.38	0.31	0.31	0.26
standard deviation	2.40	0.98	0.84	0.68	0.65	0.52	0.45	0.36	0.29
eigenvalue	5.77	0.95	0.71	0.46	0.42	0.27	0.20	0.13	0.08
proportion of variance	0.64	0.11	0.08	0.05	0.05	0.03	0.02	0.01	0.01
cumulative proportion	0.64	0.75	0.83	0.88	0.92	0.95	0.98	0.99	1.00

Supplementary material 3

Figure III. S1. The response of soil aggregation (y axis) to soil age (x-axis) is represented using several different indices of soil structure: percent WSA for size class 2-4mm (a), percent WSA for size class 0.5-1 mm (b) and percent WSA for size class 0.2-0.5mm (c). All linear regression models are fitted following correction for heterogeneity of variances and spatial autocorrelation. Model parameters used to calculate the regression line are in Table III. 1.

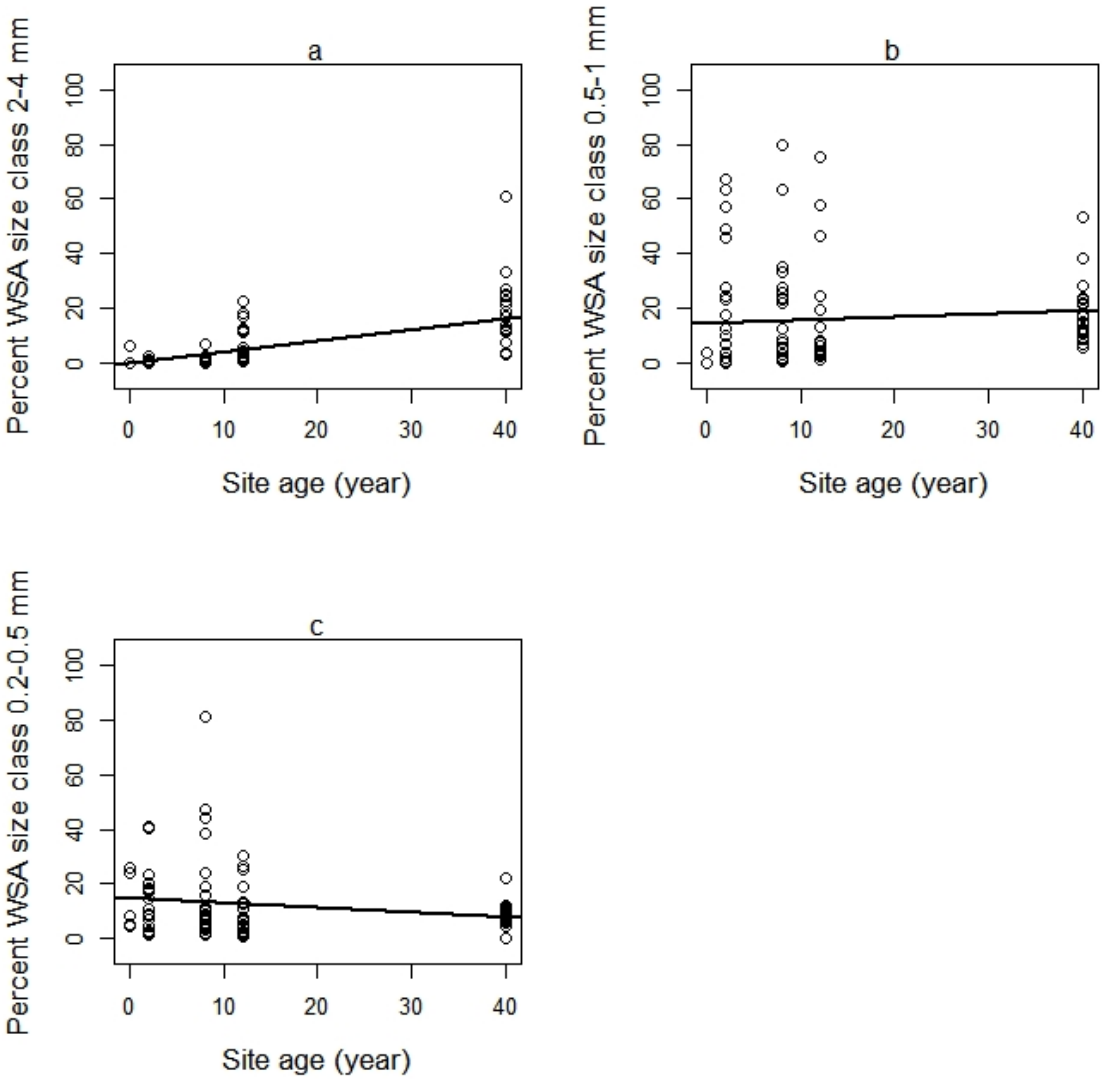

Figure III. S2. The response of soil structure determinants (y axis) to soil age (x-axis) is represented using several different parameters which might contributed to soil structure development including: root biomass (a), AMF extraradical hyphal length (b), non-AMF hyphal length (c), very fine root length (dia. 0-0.2 mm) (d) fine root length (dia. 0.2-1 mm) (e), coarse root length (dia. >1 mm) (f), % total Nitrogen (g), % total organic Carbon (h), and pH (i). Model parameters used to calculate the regression line are in Table III. 1.

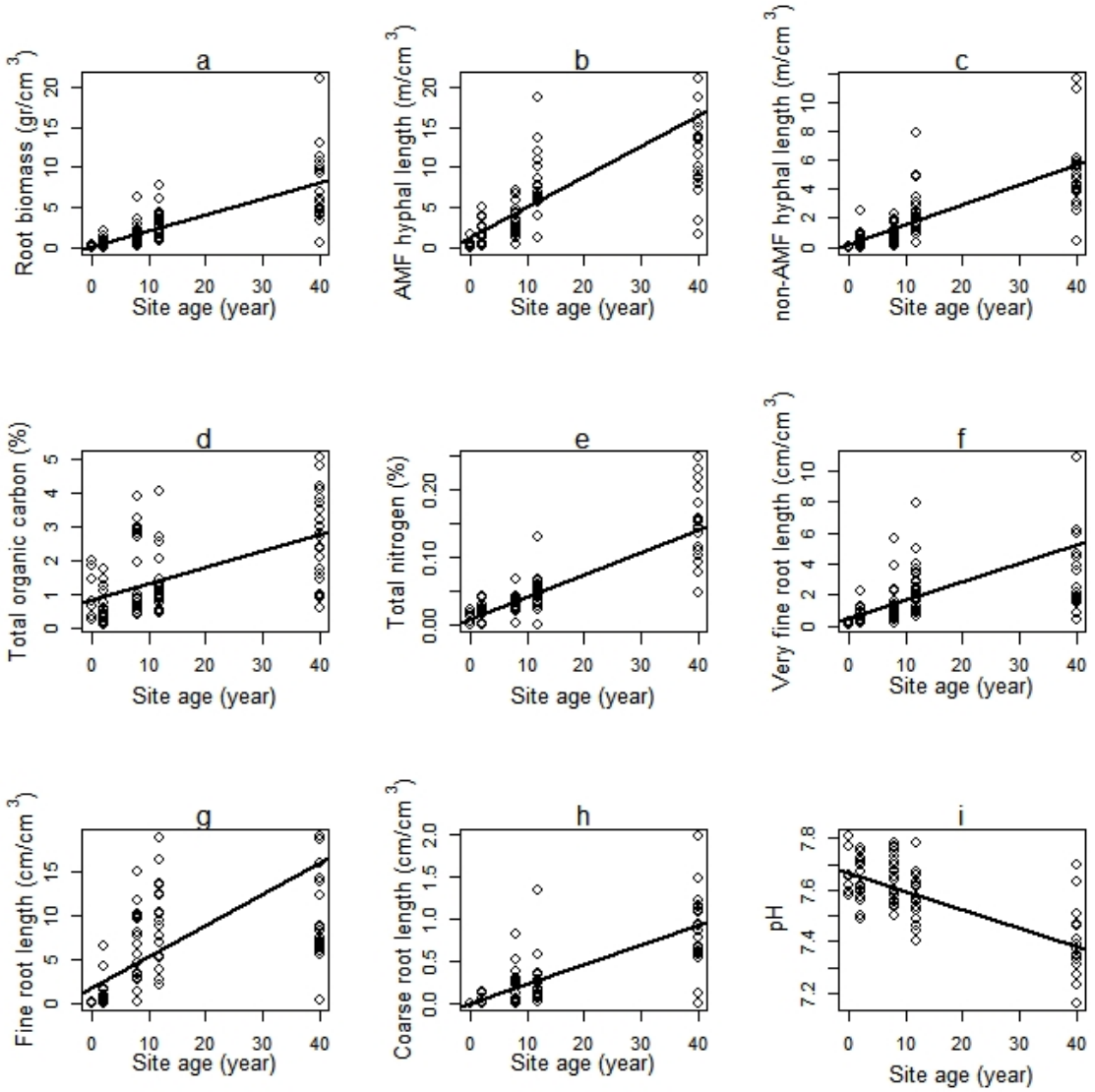

Figure III. S3. Spatial autocorrelation is visually displayed using a variogram as response values (y axis) to all possible distances between sampling-points (x axis) with an exponential fitted line for soil aggregate size class 1-2 mm (a). Notice that for soil aggregate size class 1-2 mm where spatial autocorrelation correction was significantly necessary, the fitted line has yet to level off within 800 m of the UTM distance, implying that all the data points within the linearly increasing slope are still spatially correlated. Another way to display the spatial autocorrelation is by plotting standardized residuals obtained from a linear regression model of soil aggregate size class 1-2 mm (b) against x-y coordinates with black dots representing negative residuals and grey dots representing positive residuals, whereas clustering of the positive and negative residuals shows spatial autocorrelation.

a.

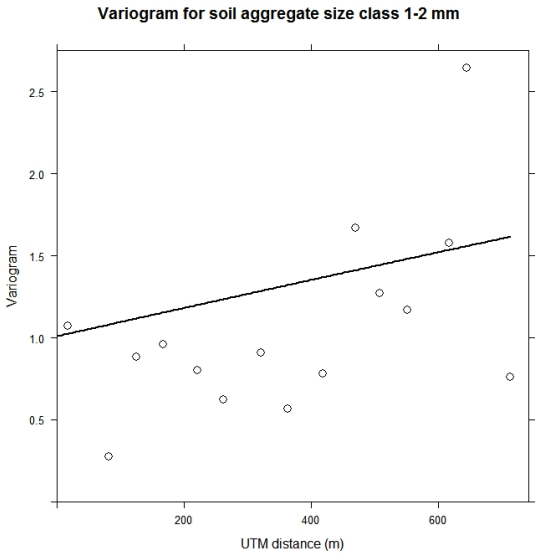

b.

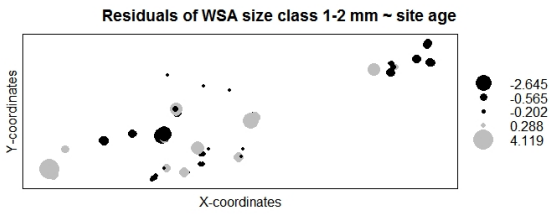

APPENDIX B

Supplementary Material for Chapter 4

Figure IV. S1. L inear model fitted using the generalized least square (GLS) method corrected for heterogeneity of variances (var = varIdent(form=~1|fcategorical)) and spatial autocorrelation) were used to correlate soil detachment rate (0-1 cm soil layer; time point R5; y axis) to total root biomass (a), AMF extraradical hyphal length (b), fine root length (c) and coarse root length (d).

a.

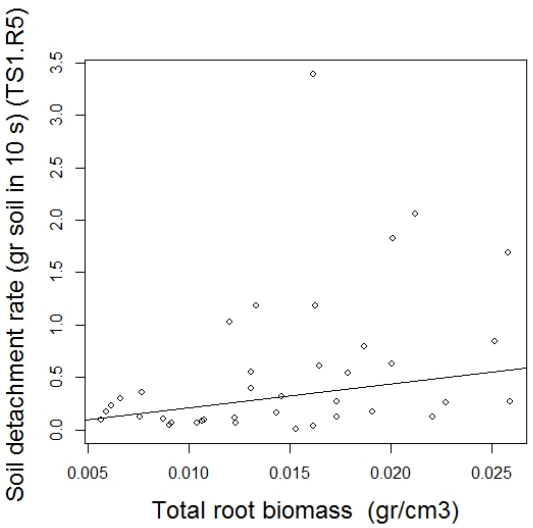

b.

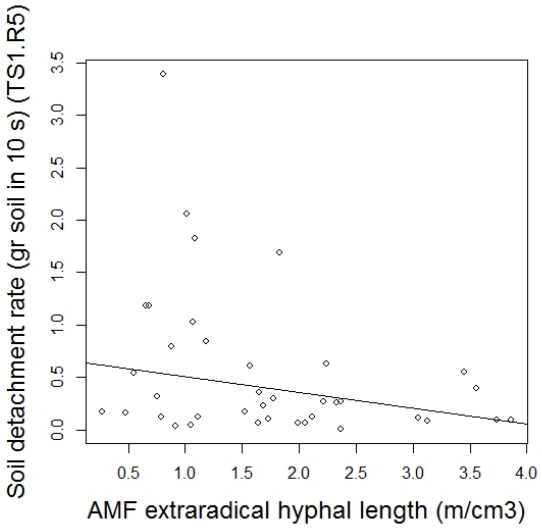

c.

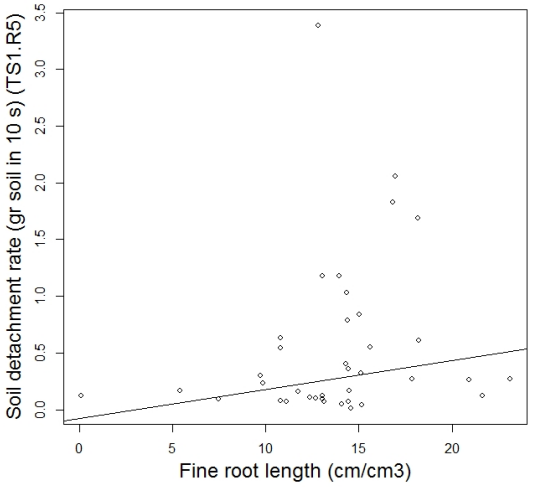
Soil detachment rate (gr soil in 10 s) (TS1.R5)
0.0
0.5
1.0
1.5
2.0
2.5
3.0
3.5
0
5
10
15
20
Fine root length (cm/cm3)

d.

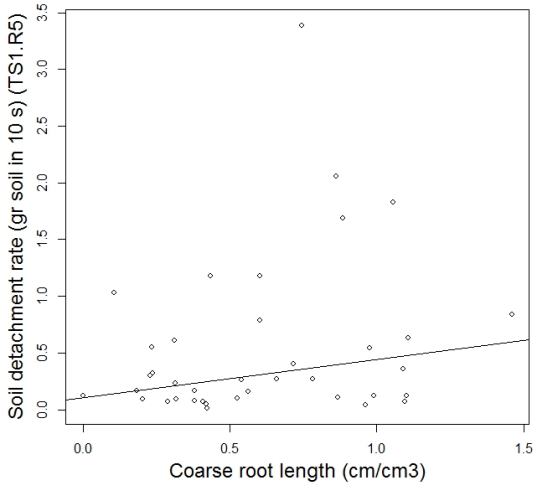
Soil detachment rate (gr soil in 10 s) (TS1.R5)
0.0
0.5
1.0
1.5
2.0
2.5
3.0
3.5
0.0
0.5
1.0
1.5
Coarse root length (cm/cm3)

Table IV. S1. Kruskal Wallis test ($p < 0.05$, alpha value = 0.05, correction = bonferroni) were used to test the differences of soil detachment rates for each treatments (A = *A. millefolium* control, AA = *A. millefolium* with AMF treatment, AAM = *A. millefolium* with AMF and microbial wash treatment, AM = *A. millefolium* with microbial wash treatment, B = Bare soil, S = *S. canadensis* control, SA = *S. canadensis* with AMF treatment, SAM = *S. canadensis* with AMF and microbial wash treatment, SM = *S. canadensis* with microbial wash treatment) at each time point (R1, R2, R3, R4 and R5). Values are mean ± SE. Different alphabet indicates significant difference between treatment of similar time point (p value < 0.05). Each treatment data are not normally distributed.

variables	A	AA	AAM	AM	B	S	SA	SAM	SM
TS1.R1	2.75 ± 0.83b	0.34 ± 0.07e	1.52 ± 0.49bc	2.67 ± 1.27bcd	14.2 ± 1.89a	0.44 ± 0.10de	0.38 ± 0.05e	0.75 ± 0.38cde	0.63 ± 0.14bcde
TS1.R2	1.93 ± 0.57b	0.21 ± 0.04e	0.69 ± 0.14bc	2.08 ± 0.98bcd	10.39 ± 0.91a	0.28 ± 0.07de	0.24 ± 0.04de	0.45 ± 0.24cde	0.41 ± 0.12cde
TS1.R3	1.05 ± 0.24b	0.17 ± 0.02d	0.52 ± 0.10bc	0.91 ± 0.43bcd	7.85 ± 0.66a	0.23 ± 0.06cd	0.24 ± 0.08d	0.40 ± 0.22cd	0.37 ± 0.11cd
TS1.R4	0.89 ± 0.26b	0.13 ± 0.02d	0.42 ± 0.08bc	0.66 ± 0.27bc	6.97 ± 0.88a	0.28 ± 0.09bcd	0.24 ± 0.07cd	0.69 ± 0.55cd	0.27 ± 0.06bcd
TS1.R5	0.87 ± 0.22b	0.18 ± 0.06c	0.38 ± 0.09bc	0.77 ± 0.39bc	5.81 ± 0.59a	0.18 ± 0.05c	0.16 ± 0.04c	0.18 ± 0.06c	0.18 ± 0.04c
TS2.R1	4.34 ± 0.86bc	2.23 ± 0.35de	3.28 ± 0.42bcd	5.50 ± 0.95b	20.76 ± 2.55a	2.46 ± 0.88e	1.89 ± 0.16e	2.68 ± 0.63cde	0.70 ± 0.70cde
TS2.R2	2.23 ± 0.23bc	1.68 ± 0.24cd	1.73 ± 0.23cd	2.84 ± 0.39b	9.25 ± 1.12a	2.12 ± 1.05d	1.15 ± 0.06d	1.62 ± 0.40d	1.82 ± 0.47cd
TS2.R3	1.54 ± 0.17b	1.12 ± 0.09bc	1.10 ± 0.15cd	1.70 ± 0.21b	6.12 ± 0.59a	0.77 ± 0.10d	0.84 ± 0.08cd	1.12 ± 0.30cd	1.29 ± 0.36cd
TS2.R4	1.36 ± 0.31ab	1.45 ± 0.48bc	0.68 ± 0.07cd	1.12 ± 0.15ab	5.02 ± 0.71a	0.54 ± 0.06d	0.62 ± 0.05d	0.91 ± 0.27bcd	1.00 ± 0.32bcd
TS2.R5	0.97 ± 0.11ab	0.70 ± 0.10bcd	0.59 ± 0.07de	0.86 ± 0.08abc	4.73 ± 0.74a	0.43 ± 0.05e	0.48 ± 0.05de	0.72 ± 0.23cde	0.74 ± 0.19bcde
TS3.R1	5.30 ± 1.07bc	3.87 ± 0.39bc	3.55 ± 0.52bcd	6.59 ± 1.23b	12.22 ± 0.88a	2.09 ± 0.45e	2.82 ± 1.07de	3.67 ± 1.35cde	3.49 ± 0.98cde
TS3.R2	3.64 ± 0.68b	2.50 ± 0.31bc	2.02 ± 0.28bc	3.55 ± 0.78b	6.80 ± 0.40a	1.98 ± 0.29bc	1.91 ± 0.41c	3.15 ± 1.07bc	2.87 ± 0.58bc
TS3.R3	1.86 ± 0.18bcd	1.61 ± 0.22cd	1.30 ± 0.20de	2.38 ± 0.62bc	4.43 ± 0.50a	1.75 ± 0.12bcd	1.56 ± 0.26cd	2.18 ± 0.49bc	2.44 ± 0.31ab
TS3.R4	1.36 ± 0.16bcd	1.08 ± 0.17cd	0.96 ± 0.16d	2.09 ± 0.81bcd	3.26 ± 0.37a	1.55 ± 0.19bc	1.39 ± 0.28bcd	1.69 ± 0.47bc	1.72 ± 0.26b
TS3.R5	1.06 ± 0.12bc	0.74 ± 0.10c	0.77 ± 0.12c	1.46 ± 0.43bc	2.72 ± 0.32a	1.43 ± 0.12ab	1.21 ± 0.29bc	1.34 ± 0.23b	1.44 ± 0.20b

Table IV. S2.a. Linear model fitted using the generalized least square (GLS) method corrected for heterogeneity of variances (var = varIdent(form=~1|fcategorical)) and spatial autocorrelation) to test the response of soil detachment rate (TS1.R1, TS.R2, TS1.R3, TS1.R4 and TS1.R5) to seach of the oil detachment rate determinants (total root biomass, total percent WSA, very fine root length, fine root length, coarse root length, extraradical AMF hyphal length and non-AMF hyphal length) used as the main effect. Regression parameters (estimated mean value) with significant p-values are shown in bold (in addition *p-value = 0.09, **p-value=0.08, and ***p-value= 0.059). Models were compared using the Akaike information criterion (AIC) and the lowest AIC is in bold. The model intercept is the last parameter in the equation.

Correlation	**AIC**	**R^2**
Soil detachment rate (TS1.R1)		
Soil detach. rate (TS1.R1) = (21.53) Total root biomass + 0.14	144.40	0.63
Soil detach. rate (TS1.R1) = (**-0.24**) AMF extraradical hyphal length + 1.07	150.21	0.68
Soil detach. rate (TS1.R1)= (-0.0007) Total percent WSA + 0.40	161.10	0.63
Soil detach. rate (TS1.R1) = (0.004) very fine root length + 0.171	160.95	0.64
Soil detach. rate (TS1.R1) = (0.07) fine root length + 0.76	156.95	0.64
Soil detach. rate (TS1.R1) = (0.20) coarse root length + 0.27	153.30	0.64
Soil detach. rate (TS1.R1)= (**-1.33**) non AMF extraradical hyphal length + 0.7	145.94	0.7
Soil detachment rate (TS1.R2)		
Soil detach. rate (TS1.R2) = (**25.47**) Total root biomass -0.023	101.83	0.78
Soil detach. rate (TS1.R2) = (-0.71) AMF extraradical hyphal length + 2.41	112.63	0.78
Soil detachment rate (TS1.R3)		
Soil detach. rate (TS1.R3) = (15.35) Total root biomass + 0.02***	57.81	0.66
Soil detach. rate (TS1.R3) = (**-0.19**) AMF extraradical hyphal length + 0.79	66.67	0.67
Soil detachment rate (TS1.R4)		
Soil detach. rate (TS1.R4) = (13.45) Total root biomass + 0.015**	45.58	0.6
Soil detach. rate (TS1.R4) = (**-0.16**) AMF extraradical hyphal length + 0.66	52.92	0.62
Soil detachment rate (TS1.R5)		
Soil detach. rate (TS1.R5) = (**22.95**) Total root biomass -0.02	53.40	0.63
Soil detach. rate (TS1.R5) = (**-0.15**) AMF extraradical hyphal length + 0.65	64.89	0.61
Soil detach. rate (TS1.R5) = (0.03) fine root length -0.07*	70.30	0.58
Soil detach. rate (TS1.R5) = (**0.34**) coarse root length + 0.10	65.20	0.59

Table IV. S2.b. Linear model fitted using the generalized least square (GLS) method corrected for heterogeneity of variances (var = varIdent(form=~1|fcategorical)) and spatial autocorrelation) to test the response of soil detachment rate (TS1.R1, TS.R2, TS1.R3, TS1.R4 and TS1.R5) to all soil detachment rate determinants (total root biomass, total percent WSA, very fine root length, fine root length, coarse root length, extraradical AMF hyphal length and non-AMF hyphal length) used as the main effect. Regression parameters (estimated mean value) with significant p-values are shown in bold. Models were compared using the Akaike information criterion (AIC) and the lowest AIC is in bold. The model intercept is the last parameter in the equation. The value of best fitted line (R^2) value is provided.

Est = Estimated mean value

SE = Standard error

t -val = t - value

p - val = p value, significant at <0.05

	AIC	R^2	coefficients	Est	SE	t-val	p-val
Soil detach.rate (TS1.R1)	160.66	0.69	(Intercepts)	2.32	1.06	2.19	0.04
			Total root biomass	**187.66**	**58.96**	**3.18**	**0.00**
			Total WSA	0.00	0.02	-0.03	0.98
			Very fine root length	0.03	0.02	1.38	0.18
			Fine root length	**-0.27**	**0.13**	**-2.08**	**0.05**
			Coarse root length	-0.14	0.65	-0.22	0.83
			AMF extraradical hyphae	**-0.82**	**0.27**	**-2.98**	**0.01**
			non-AMF extraradical hyphae	0.43	1.57	0.27	0.79
Soil detach. rate (TS1.R2)	126.65	0.86	(Intercepts)	1.22	0.33	3.65	0.00
			Total root biomass	**65.40**	**15.32**	**4.27**	**0.00**
			Total WSA	0.01	0.01	0.76	0.45
			Very fine root length	0.00	0.01	-0.43	0.67
			Fine root length	**-0.08**	**0.03**	**-2.31**	**0.03**

			Coarse root length	0.00	0.20	0.02	0.99
			AMF extraradical hyphae	**-0.27**	**0.10**	**-2.77**	**0.01**
			non-AMF extraradical hyphae	-0.09	0.45	-0.20	0.85
Soil detach. rate (TS1.R3)	88.10	0.74	(Intercepts)	0.79	0.28	2.80	0.01
			Total root biomass	**40.73**	**14.35**	**2.84**	**0.01**
			Total WSA	0.00	0.01	-0.01	0.99
			Very fine root length	0.00	0.01	0.67	0.51
			Fine root length	-0.05	0.03	-1.50	0.15
			Coarse root length	-0.04	0.17	-0.22	0.83
			AMF extraradical hyphae	**-0.22**	**0.07**	**-2.99**	**0.01**
			non-AMF extraradical hyphae	-0.02	0.40	-0.05	0.96
Soil detach. rate (TS1.R4)	79.04	0.69	(Intercepts)	0.41	0.24	1.68	0.10
			Total root biomass	16.45	12.15	1.35	0.19
			Total WSA	0.01	0.00	1.10	0.28
			Very fine root length	0.00	0.01	0.69	0.50
			Fine root length	-0.03	0.03	-1.08	0.29
			Coarse root length	0.17	0.15	1.13	0.27
			AMF extraradical hyphae	**-0.20**	**0.07**	**-3.06**	**0.00**
			non-AMF extraradical hyphae	0.09	0.34	0.27	0.79
Soil detach. rate (TS1.R5)	85.56	0.73	(Intercepts)	0.42	0.24	1.74	0.09
			Total root biomass	**25.81**	**11.53**	**2.24**	**0.03**
			Total WSA	0.01	0.01	0.97	0.34
			Very fine root length	0.00	0.01	0.66	0.51
			Fine root length	-0.04	0.02	-1.46	0.16
			Coarse root length	0.17	0.15	1.13	0.27
			AMF extraradical hyphae	**-0.15**	**0.07**	**-2.27**	**0.03**
			non-AMF extraradical hyphae	-0.32	0.34	-0.95	0.35

Table IV. S3. The table shows correlation test results, based on the Pearson's product moment correlation test, with 95% confidence intervals between all explanatory variables of soil detachment rate determinants (total root biomass, total percent WSA, very fine root length, fine root length, coarse root length, extraradical AMF hyphal length and non-AMF hyphal length) as main effect. The table shows t-values, p-values and correlation values, respectively. Significant correlations are in bold with correlation value ranging from 36-76%.

t-value

explanatory variables	1	2	3	4	5	6	7
Total root biomass (1)							
Total WSA (2)		1.13					
Very fine root length (3)		**2.34**	0.69				
Fine root length (4)		**6.11**	1.25	**7.04**			
Coarse root length (5)		**4.10**	0.13	0.10	**2.40**		
AMF extraradical hyphal length (6)		-1.02	1.55	1.31	0.16	-0.69	
non-AMF extraradical hypha length (7)		0.44	1.36	0.60	1.43	0.87	**3.44**

p-value

explanatory variables	1	2	3	4	5	6	7
Total root biomass (1)							
Total WSA (2)	0.27						
Very fine root length (3)	**0.02**	0.50					
Fine root length (4)	**0.00**	0.22	**0.00**				
Coarse root length (5)	**0.00**	0.90	0.92	**0.02**			
AMF extraradical hyphal length (6)	0.31	0.13	0.20	0.87	0.49		
non-AMF extraradical hypha length (7)	0.66	0.18	0.55	0.16	0.39	**0.00**	

correlation value

explanatory variables	1	2	3	4	5	6	7
Total root biomass (1)							
Total WSA (2)	0.18						
Very fine root length (3)	**0.36**	0.11					
Fine root length (4)	**0.71**	0.20	**0.76**				
Coarse root length (5)	**0.56**	0.02	0.02	**0.37**			
AMF extraradical hyphal length (6)	-0.17	0.25	0.21	0.03	-0.11		
non-AMF extraradical hypha length (7)	0.07	0.22	0.10	0.23	0.14	**0.50**	

Table IV. S4. Results of a Principal Components Analysis (PCA) of soil detachment rate (a (TS1.R1, TS.R2, TS1.R3, TS1.R4 and TS1.R5) and soil detachment rate determinants (total root biomass, total percent WSA, very fine root length, fine root length, coarse root length, extraradical AMF hyphal length and non-AMF hyphal length). We include the results of varimax rotation of the PCs, and also the standard deviation, eigenvalue, proportion and cumulative proportion of the variance explained by the PCs (see also Fig. IV. 4).

Table IV. 4a
PCA for explanatory variables

	Rotation						
variables	PC1	PC2	PC3	PC4	PC5	PC6	PC7
Total root biomass	0.50	-0.30	0.15	-0.10	-0.03	-0.73	-0.29
Total WSA	0.22	0.33	0.17	-0.88	0.00	0.19	-0.04
Very fine root length	0.44	0.09	-0.62	0.12	0.10	0.33	-0.53
Fine root length	0.58	-0.07	-0.23	0.05	-0.16	0.08	0.76
Coarse root length	0.34	-0.29	0.60	0.19	0.43	0.46	-0.07
AMF extraradical hyphae	0.10	0.67	0.02	0.20	0.62	-0.31	0.15
non-AMF extraradical hyphae	0.23	0.51	0.38	0.34	-0.63	0.07	-0.17
importance of components:							
Standard deviation	1.61	1.29	1.04	0.92	0.67	0.53	0.31
Proportion of Variance	0.37	0.24	0.15	0.12	0.06	0.04	0.01
Cumulative Proportion	0.37	0.61	0.76	0.88	0.95	0.99	1.00

Table IV. 4b
PCA for each time point for TS1

variables	PC1	PC2	PC3	PC4	PC5
TS1.R1	0.44	-0.53	0.51	-0.04	0.51
TS1.R2	0.44	-0.40	-0.79	0.15	0.01
TS1.R3	0.46	-0.07	0.33	0.28	-0.77
TS1.R4	0.44	0.68	-0.01	0.46	0.37
TS1.R5	0.46	0.31	-0.06	-0.83	-0.08
importance of components:					
Standard deviation	2.12	0.53	0.40	0.20	0.14
Proportion of Variance	0.90	0.06	0.03	0.01	0.00
Cumulative Proportion	0.90	0.96	0.99	1.00	1.00

Equation IV. S1

Q = flow discharge (0.0003 m^3/s)
u = mean surface flow velocity (1.17 m/s)
a = flume width (0.1 m)
d = depth of water in the flume (m)
q = unit flow discharge (m^2/s)
R = hydraulic radius (m)

$q = Q/a$
$= 0.003\ m^2/s$

$d = q/u$
$= 0.0026$ m

$$R = \frac{a.d}{a+2d}$$
$= 0.0025$ m

$\tau = \rho_w gRS$

τ = mean bottom flow shear stress (Pa)
ρ_w = water density (1000 kg/m^3)
g = acceleration due to gravity (10 m^2/s)
S = sin ($\alpha°$); α is slope angle of soil surface (°)
$\alpha = 18$, sin (18°) = 0.31

$\tau = 7.75$ Pa.

Equation and calculation were adjusted from De Baets, et al. (2006).

APPENDIX C

Preliminary data set for a meta-analysis study

To investigate the potential of riparian system to store carbon, we conducted data collection step for a meta-analysis. We are investigating whether:

1. Riparian system can store more carbon compares to its adjacent upland
2. Riparian system carbon storage capacity depends on stand age, vegetation type, disturbance level, soil water content, soil depth, soil texture and soil pH.

To do so, we collected data from published papers using several online search engines. The results are as follows:

Table S1. Overview of search engine results from data collection step for a meta-analysis investigating the potential of riparian system to store carbon.

Search engine	Date of inquiry	Search term	Generated results	Data collection state
Google scholar	24/07/2014	Riparian upland "soil carbon"	3000	58 papers were used to extract data in Table S2
Web of science	29/09/2014	riparia* upland soil carbon	90	List of papers generated in this inquiry was cross checked with list of papers from Table S2
Web of science	29/09/2014	riparia* soil carbon	665	Cross checking with list of papers from Table S2 has not yet been conducted

Table S2, Extracted values and data from 58 papers generated from Google scholar search to investigate the potential of riparian system in storing carbon.

No	Citation	carbon type	soil carbon unit	landform	depth (cm)	vegetation	disturbance level/treatment	soil type/texture	age (year)	mean	n	SE	SD	CV (%)	bulk density	pH	water content	Site location/latitude, longitude	average annual temperature (° C)	average annual rainfall (mm)
	term: RIPARIAN VS UPLAND																			
1	Neal, Andrew W. Soil Carbon and Nitrogen Dynamics across the Hillslope-Riparian Interface in Adjacent Watersheds with Contrasting Cellulosic Biofuel Systems. Diss. Virginia Polytechnic Institute and State University, 2014.	total soil C/soil organic matter	g/kg	riparian	0-15	young-pine with understory: Pinus taeda	biofuel plantation	Entisol, Ultisol, Entisol, Ultisol/fine sandy loam	5	16.2	9	2.7	8.1	50	1.52	5.18	5.34 + 0.02	Weyerhaeuser Alabama Cellulosic Biofuel Research site, Upper Coastal Plain, Alabama.		
2				riparian	15-30	idem	biofuel plantation		5	3.6	9	0.3	0.9	25						
3				riparian	0-15	Thinned-intercropped: loblolly pine & switchgrass	biofuel plantation		5	27	9	4	12	44.44444444						
4				riparian	15-30	idem	biofuel plantation		5	6.4	9	0.5	1.5	23.4375						
5				riparian	0-15	Age-zero-Intercropped: loblolly pine & switchgrass	biofuel plantation		0	15.5	9	1.3	3.9	25.16129032						
6				riparian	15-30	idem	biofuel plantation		0	12.7	9	1.1	3.3	25.98425197						
7				riparian	0-15	Switchgrass-only	biofuel plantation		1	13.1	9	2.4	7.2	54.96183206						
8				riparian	15-30	idem	biofuel plantation		1	9.6	9	1.5	4.5	46.875						
9				riparian	0-15	Mid-rotation reference	reference		19	17.1	9	1.3	3.9	22.80701754						
10				riparian	15-30	idem	reference		19	6.1	9	0.7	2.1	34.42622951						
11			Mg/ha	riparian	0-15	young-pine with understory: Pinus taeda	biofuel plantation		5	33.9	9	4.2	12.6	37.16814159						
12				riparian	15-30	idem	biofuel plantation		5	8.3	9	0.7	2.1	25.30120482						
13				riparian	0-15	Thinned-intercropped: loblolly pine & switchgrass	biofuel plantation		5	41.1	9	5.5	16.5	40.14598540						
14				riparian	15-30	idem	biofuel plantation		5	13.6	9	1.2	3.6	26.47058824						
15				riparian	0-15	Age-zero-Intercropped: loblolly pine & switchgrass	biofuel plantation		0	33.2	9	3.1	9.3	28.01204819						
16				riparian	15-30	idem	biofuel plantation		0	28.4	9	2.3	6.9	24.29577465						
17				riparian	0-15	Switchgrass-only	biofuel plantation		1	27.8	9	5	15	53.95683453						
18				riparian	15-30	idem	biofuel plantation		1	22.7	9	2.9	8.7	38.32599119						
19				riparian	0-15	Mid-rotation reference	reference		19	36.4	9	2.8	8.4	23.07692308						

No	Citation	carbon type	soil carbon unit	landform	depth (cm)	vegetation	disturbance level/treatment	soil type/texture	age (year)	mean	n	SE	SD	CV (%)	bulk density	pH	water content	Site location/latitude, longitude	average annual temperature (° C)	average annual rainfall (mm)
20				riparian	15-30	idem	reference		19	14.7	9	1.4	4.2	28.57142857						
21				upland	0-15	young-pine with understory	biofuel plantation		5	13.1	9	1.8	5.4	41.22137405	1.65	5.34				
22				upland	15-30	idem	biofuel plantation		5	3.7	9	0.4	1.2	32.43243243						
23				upland	0-15	Thinned-intercropped: loblolly pine & switchgrass	biofuel plantation		5	7.1	9	1.3	3.9	54.92957746						
24				upland	15-30	idem	biofuel plantation		5	3.9	9	0.6	1.8	46.15384615						
25				upland	0-15	Age-zero-Intercropped: loblolly pine & switchgrass	biofuel plantation		0	19.4	9	1.7	5.1	26.28865979						
26				upland	15-30	idem	biofuel plantation		0	15.9	9	1.2	3.6	22.64150943						
27				upland	0-15	Switchgrass-only	biofuel plantation		1	10	9	1.9	5.7	57						
28				upland	15-30	idem	biofuel plantation		1	9.1	9	1.2	3.6	39.56043956						
29				upland	0-15	Mid-rotation reference	reference		19	18.4	9	1.8	5.4	29.34782609						
30				upland	15-30	idem	reference		19	7.4	9	0.6	1.8	24.32432432						
31				upland	0-15	young-pine with understory	biofuel plantation		5	29.2	9	4.1	12.3	42.12328767						
32				upland	15-30	idem	biofuel plantation		5	9.5	9	0.9	2.7	28.42105263						
33				upland	0-15	Thinned-intercropped: loblolly pine & switchgrass	biofuel plantation		5	17.3	9	3.3	9.9	57.22543353						
34				upland	15-30	idem	biofuel plantation		5	9.5	9	1	3	31.57894737						
35				upland	0-15	Age-zero-Intercropped: loblolly pine & switchgrass	biofuel plantation		0	40.8	9	4.2	12.6	30.88235294						
36				upland	15-30	idem	biofuel plantation		0	36.4	9	3.5	10.5	28.84615385						
37				upland	0-15	Switchgrass-only	biofuel plantation		1	21.8	9	3.6	10.8	49.5412844						
38				upland	15-30	idem	biofuel plantation		1	23.6	9	2.8	8.4	35.59322034						
39				upland	0-15	Mid-rotation reference	reference		19	42.8	9	4.4	13.2	30.8411215						
40				upland	15-30	idem	reference		19	19.3	9	1.5	4.5	23.31606218						

No	Citation	carbon type	soil carbon unit	landform	depth (cm)	vegetation	disturbance level/treatment	soil type/texture	age (year)	mean	n	SE	SD	CV (%)	bulk density	pH	water content	Site location/latitude, longitude	average annual temperature (° C)	average annual rainfall (mm)
41	Giese, Laura AB, et al. "Biomass and carbon pools of disturbed riparian forests." Forest Ecology and Management 180.1 (2003): 493-508.	soil carbon	%	riparian	0-10	herbaceous vegetation and blackbery	high; artificial regeneration		2	4.2	18	1.9	8.061017306	191.9289835						
42				riparian	0-10	early successional species: willow, alder	high; natural regeneration		8	4.7	9	1.3	3.9	82.9787234						
43				riparian	0-10	willow, maple, alder	high; none		12	4	28	1.3	6.878953409	171.9738352						
44				riparian	0-10	mature hardwood forest	low; none		60	11.4	29	4.2	22.61769219	198.4008087						
45		soil carbon	kg/ha	upland	0-10	herbaceous vegetation and blackbery	high; artificial regeneration		2	4	3	2	3.464101615	86.60254038						
46				upland	0-10	early successional species: willow, alder	high; natural regeneration		8	1.7	3	1	1.732050808	101.8853416						
47				upland	0-10	willow, maple, alder	high; none		12	2.4	6	2	4.898979486	204.1241452						
48				upland	0-10	mature hardwood forest	low; none		60	3.3	5	2	4.472135955	135.5192714						
49	Giese, Laura AB, et al. "Biomass and carbon pools of disturbed riparian forests." Forest Ecology and Management 180.1 (2003): 493-508.	organic matter	%	riparian	0-10	herbaceous vegetation	high; artificial regeneration		2	12.3	18	6	25.45584412	206.9580823						
50				riparian	0-10	early successional species: willow, alder	high; natural regeneration		8	12.9	9	3	9	69.76744186						
51				riparian	0-10	willow, maple, alder	high; none		12	10.7	28	3	15.87450787	148.3598866						
52		organic matter	kg/ha	upland	0-10	herbaceous vegetation	high; artificial regeneration		2	8.2	3	4	6.928203 23	84.4902833						
53				upland	0-10	early successional species: willow, alder	high; natural regeneration		8	4.6	3	3	5.196152423	112.9598353						
54				upland	0-10	willow, maple, alder	high; none		12	7.4	6	6	14.69693846	198.6072764						
55				upland	0-10	mature hardwood riparian forest	low; none		60	8.6	5	6	13.41640786	156.0047426						

No	Citation	carbon type	soil carbon unit	landform	depth (cm)	vegetation	disturbance level/treatment	soil type/texture	age (year)	mean	n	SE	SD	CV (%)	bulk density	pH	water content	Site location/latitude, longitude	average annual temperature (° C)	average annual rainfall (mm)
56	Ritchie, Jerry C., and Gregory W. McCarty. "137Cesium and soil carbon in a small agricultural watershed." Soil and Tillage Research 69.1 (2003): 45-51.	soil carbon	%	riparian	0-20	bottomland forest				11.7	24	17.1	83.77254 92	716.004 694				Northern Coastal Plain, USDA-ARS, Beltsville Agricultural Research Center, near Beltsville, MD, USA	13	1035
57				riparian	20-40	bottomland forest				18.3	24	17.5	85.73214 1	468.481 6448						
58		soil carbon	kg/m2	upland	0-20	bottomland forest				1.2	12	0.4	1.38 5640 646	115.470 0538						
59				upland	20-30	bottomland forest				0.5	12	0.3	1.03 9230 485	207.846 0969						
60	Pacific, Vincent J., et al. "Landscape structure, groundwater dynamics, and soil water content influence soil respiration across riparian–hillslope transitions in the Tenderfoot Creek Experimental Forest, Montana."Hydrological Processes 25.5 (2011): 811-827.	soil carbon	%	riparian	20	understory dominance: bluejoint reedgrass				2.34	8	0.470 2260 09	1.33	56.8376 0684	0.96 2			US Forest Servise Tenderfoot Creek Experimental Forest: Little Belt Mountains within the Lewis and Clark National Forest of central Montana; 46° 55'N, 110° 52'W	0	880
61			%	riparian	50	understory: grass				1.77	8	0.314 6625 18	0.89	50.2824 8588						
62				upalnd	20	Tree: pine, fir				2.74	8	0.636 3961 03	1.8	65.6934 3066						
63				upland	50	Tree: pine, fir				1.34	8	0.243 9518 4	0.69	51.4925 3731						
64	Clinton, Barton D., et al. "Can structural and functional characteristics be used to identify riparian zone width in southern Appalachian headwater catchments?." Canadian journal of forest research 40.2 (2010): 235-253.	soil carbon	Mt/ha	riparian	0-20	overstory: mixed hardwoods		Haplumbrepts; loamy-skeletal		91.923 08651	16	7.307 6238 99	29.23049 56	31.7988 6219				Nantahala Ranger District, Nantahala National Forest, Blue Ridge Physiographic Province of western North Carolina; 35° 6' N, 83° 6'W	12.6	
65				riparian	0-20	overstory: mixed hardwoods				89.807 56218	16	7.307 6238 99	29.23049 56	32.5479 2234						

No	Citation	carbon type	soil carbon unit	landform	depth (cm)	vegetation	disturbance level/treatment	soil type/texture	age (year)	mean	n	SE	SD	CV (%)	bulk density	pH	water content	Site location/latitude, longitude	average annual temperature (° C)	average annual rainfall (mm)
66				riparian	0-20	overstory: mixed hardwoods				93.46164966	16	5.19209956	20.76839827	22.22130505						
67				riparian	0-20	overstory: mixed hardwoods				89.61524179	16	5.00033036	20.00132094	22.31910615						
68				riparian	>20	overstory: mixed hardwoods				71.53877797	16	8.46154662	33.84618505	47.3116623						
69				riparian	>20	overstory: mixed hardwoods				66.154358	16	3.84640787	15.38563 15	23.25716999						
70				riparian	>20	overstory: mixed hardwoods				60.76993804	16	6.15370153 7	24.61480615	40.50490578						
71				riparian	>20	overstory: mixed hardwoods				55.38551808	16	2.88425484 4	11.53701938	20.83038992						
72				upland	0-20			Hapludults; loamy to coarse loamy		79.99977317	16	3.07712629 9	12.30850 52	15.38567512						
73				upland	0-20					80.57673435	16	3.46176708 7	13.84706835	17.18494607						
74				upland	0-20					81.15369553	16	5.00033036	20.00132094	24.64622321						
75				upland	0-20					74.99999399	16	3.46176708 7	13.84706835	18.46275927						
76				upland	0-20					82.30761789	16	4.23104866 1	16.92419465	20.56212424						
77				upland	0-20					76.92319793	16	3.26889563 2	13.07558253	16.99823054						
78				upland	>20					50.00109812	16	3.46176708 7	13.84706835	27.69352848						
79				upland	>20					44.61667815	16	-2.884805906	-11.53922362	-25.86302723						
80				upland	>20					39.23225819	16	2.88480590 6	11.53922362	29.41259095						
81				upland	>20					33.84783823	16	6.34602193 1	25.38408772	74.99470882						
82				upland	>20					28.46341827	16	3.46121602 5	13.84486 41	48.64090451						
83				upland	>20					23.07899831	16	4.80745878 1	19.22983512	83.3217927						

No	Citation	carbon type	soil carbon unit	landform	depth (cm)	vegetation	disturbance level/treatment	soil type/texture	age (year)	mean	n	SE	SD	CV (%)	bulk density	pH	water content	Site location/latitude, longitude	average annual temperature (° C)	average annual rainfall (mm)
84	Ullah, Sami, and Tim R. Moore. "Biogeochemical controls on methane, nitrous oxide, and carbon dioxide fluxes from deciduous forest soils in eastern Canada." Journal of Geophysical Research: Biogeosciences (2005–2012) 116.G3 (2011).	C:N and total soil N (g/m2)	g/m2	riparian	0-10	American beech	low (old growth forest); never logged	Humic Gleysols; silt loam	140 - >400	17520	3	2678.8	4639.817703	26.48297776	0.42	5		Montreal, Monteregial Hill.	5.8	1046
85				riparian	0-10	eastern hemlock			140 - >400	8475	3	2008.5	3478.824047	41.04807135	0.48	4.8				
86				riparian	0-10	sugar maple			60-120	7616	3	574.8	995.5828042	13.07225321	0.61	5.6			6.2	979
87				riparian	0-10	sugar maple			60-120	10336	3	1339	2319.216031	22.4382356	0.52	5.8				
88				upland	0-10	American beech		Orthic Dystric Brunisols; sandy loam	140 - >400	6448	3	1206.4	2089.546094	32.40611188	0.67	4.7				
89				upland	0-10	eastern hemlock		Orthic Dystric Brunisols; loamy sand	140 - >400	8850	3	2014	3488.350326	39.41638787	0.78	4.6				
90				upland	0-10	sugar maple	low (old growth forest); semi managed	Melanic Brunisols; loamy sand	60-120	4528	3	678.1	1174.503653	25.93868491	1.19	5.1				
91				upland	0-10	sugar maple		Melanic Brunisols; silt foam	60-120	4890	3	753.2	1304.580668	26.67854127	1.14	5.9				
92	Demers, Jason D., et al. "Legacy mercury and stoichiometry with C, N, and S in soil, pore water, and stream water across the upland‐wetland interface: The influence of hydrogeologic setting." Journal of Geophysical Research: Biogeosciences 118.2 (2013): 825-841.	soil carbon	mg2/m	riparian	50	alder, occassional red spruce and American larch.	shallow peat mean M vs upland M			0.022704471	2	0.013277672	0.018777464	82.70294 96		5.5		Sunday Lake watershed, southwestern boundary of Adirondack region, NY, USA; 43° 51'40" N; 74° 06'07"W		1300
93				riparian	50	alder, occassional red spruce and American larch.	shallow peat mean O vs upland O			0.035559234	2	0.054499085	0.077073345	216.7463626		5.5				
94				riparian	50	sedges, broadleaved deciduous shurbs	deep peat mean O vs upland O			0.147041485	2	0.685113177	0.968896347	658.9272029		4.8				

No	Citation	carbon type	soil carbon unit	landform	depth (cm)	vegetation	disturbance level/treatment	soil type/texture	age (year)	mean	n	SE	SD	CV (%)	bulk density	pH	water content	Site location/latitude, longitude	average annual temperature (° C)	average annual rainfall (mm)
95				riparian	50	sphagnum moss, scrub-forest fringe dominated by spruce & larch	headwater mean O vs upland O			0.126091475	2	0.89593253	1.267039938	1004.857729						
96				upland	50		shallow peat mean M vs upland M			0.072132512	6	0.03406808	0.083449 43	116.998654						
97				upland	50		shallow peat mean O vs upland O			0.073991444	6	0.12428261 4	0.304428988	411.4380953						
98				upland	50		deep peat mean O vs upland O			0.073991444	6	0.12428261 4	0.304428988	411.4380953						
99				upland	50		headwater mean O vs upland O			0.073991444	6	0.12428261 4	0.304428988	411.4380953						
100	Hoogmoed, M., et al. "Is there more soil carbon under nitrogen-fixing trees than under non-nitrogen-fixing trees in mixed-species restoration plantings?." Agriculture, Ecosystems & Environment 188 (2014): 80-84.	total C	t/ha	riparian	0-10	N-fixers: Acacia	restoration plantings; never harvested; former pastures	Chromosol; loam	18	60.1189	20	4.937	22.07893521	36.725 44775	0.97			four young tree plantings near Benalla, Northern Victoria, Australia; 36.5538° S, 145.9815° E		
101				riparian	0-10	N-fixers: Acacia	restoration plantings; never harvested; former pastures	Sodosol; sandy loam	15	31.0026	20	2.0564	9.196500378	29.6636 4233	0.91					
102				riparian	0-10	Non-N-fixers : Eucalyptus	restoration plantings; never harvested; former pastures	Chromosol; loam	18	43.2743	20	2.8807	12.88288205	29.7702 8408	0.86					
103				riparian	0-10	Non-N-fixers : Eucalyptus	restoration plantings; never harvested; former pastures	Sodosol; sandy loam	15	26.9167	20	2.882	12.88869582	47.8836 4035	1.11					
104				riparian	10-20	N-fixers: Acacia	restoration plantings; never harvested; former pastures	Chromosol; loam	18	27.7872	20	2.4193	10.81943852	38.9367 713	1.19					
105				riparian	10-20	N-fixers: Acacia	restoration plantings; never harvested; former pastures	Sodosol; sandy loam	15	26.4773	20	1.6117	7.207741519	27.2223 4336	1.1					
106				riparian	10-20	Non-N-fixers : Eucalyptus	restoration plantings; never harvested; former pastures	Chromosol; loam	18	25.8991	20	1.4548	6.506063387	25.1208 0878	1.05					
107				riparian	10-20	Non-N-fixers : Eucalyptus	restoration plantings; never harvested; former pastures	Sodosol; sandy loam	15	23.6235	20	0.8064	3.606330434	15.2658 5999	1.16					

No	Citation	carbon type	soil carbon unit	landform	depth (cm)	vegetation	disturbance level/treatment	soil type/texture	age (year)	mean	n	SE	SD	CV (%)	bulk density	pH	water content	Site location/latitude, longitude	average annual temperature (° C)	average annual rainfall (mm)
108				upland	0-10	N-fixers: Acacia	restoration plantings; never harvested; former pastures	Sodosol; Sandy loam	18	71.4359	20	2.4679	11.03678432	15.44991289	1.08					
109				upland	0-10	N-fixers: Acacia	restoration plantings; never harvested; former pastures	Sodosol; Sandy loam	15	68.6574	20	4.5268	20.24446504	29.48620985	1.83					
110				upland	0-10	Non-N-fixers : Eucalyptus	restoration plantings; never harvested; former pastures	Sodosol; Sandy loam	18	56.2387	20	4.5268	20.24446504	35.99739155	0.94					
111				upland	0-10	Non-N-fixers : Eucalyptus	restoration plantings; never harvested; former pastures	Sodosol; Sandy loam	15	88.4389	20	4.9396	22.09056276	24.97833328	1.89					
112				upland	10-20	N-fixers: Acacia	restoration plantings; never harvested; former pastures	Sodosol; Sandy loam	18	35.2455	20	0.8225	3.678331823	10.43631619	1.18					
113				upland	10-20	N-fixers: Acacia	restoration plantings; never harvested; former pastures	Sodosol; Sandy loam	15	21.4358	20	2.8213	12.61723717	58.86058449	1.1					
114				upland	10-20	Non-N-fixers : Eucalyptus	restoration plantings; never harvested; former pastures	Sodosol; Sandy loam	18	31.5865	20	3.6302	16.23474794	51.39774253	0.97					
115				upland	10-20	Non-N-fixers : Eucalyptus	restoration plantings; never harvested; former pastures	Sodosol; Sandy loam	15	18.9852	20	1.6129	7.213108082	37.99332154	1.08					
116	Weitzman, Julie N., et al. "Potential nitrogen and carbon processing in a landscape rich in milldam legacy sediments." Biogeochemistry: 1-21.	total soil C	g/m2	riparian	0-20		agricultural site, milldam site, legacy riparian	Fluventic Endoaquepts, silty loam		3269	11	130	431.1612227	13.189391959	0.78			Northward-flowing tributary of Mill Creek, Lancaster County, Pennsylvania.		
117				riparian	20					1542	11	174	577.0927135	37.424949	1.06					
118				riparian	21					2326	11	377	1250.367546	53.756128 37	0.76					
119		Organic matter	%	riparian	0-20					7.59	11	1.06	3.515622278	46.31913409	0.78					
120				riparian	20					4.37	11	0.27	0.895488693	20.49173211	1.06					
121				riparian	20					4.61	11	0.63	2.089473618	45.32480733	0.76					
122				upland	0-20		agricultural site, milldam site, non-legacy	Eutrudepts, silty loam		3313	18	144	610.9402589	18.440669601	0.78					

No	Citation	carbon type	soil carbon unit	landform	depth (cm)	vegetation	disturbance level/treatment	soil type/texture	age (year)	mean	n	SE	SD	CV (%)	bulk density	pH	water content	Site location/latitude, longitude	average annual temperature (° C)	average annual rainfall (mm)
123				upland	20					1264	18	130	551.5432893	43.6347539	1.11					
124				upland	20					1107	18	175	742.4621202	67.06974889	1.08					
125				upland	0-20					6.84	18	0.16	0.678822 51	9.924305701	0.78					
126				upland	20					3.87	18	0.13	0.55 1543 289	14.25176458	1.11					
127				upland	20					3.33	18	0.2	0.84 8528 137	25.48132545	1.08					
128	Ricker, Matthew C., et al. "Soil Organic Carbon Pools in Riparian Landscapes of Southern New England." Soil Science Society of America Journal 77.3 (2013): 1070-1079. (and Davis et al. 2004)	total soil organic carbon	Mg/ha	riparian	100	Forested, dominated by maple, gum and oak				246	29		95.94	39				Narragansett Bay (n = 10), Pawcatuck River (n = 13), and Thames River (n = 6), Rhode Island, eastern Connecticut, Southern Massachusetts.		
129				riparian	100					270	29		108	40						
130				riparian	102					246	29		95.94	39						
131				riparian	103					270	29		108	40						
132				upland	100					110	20		16.5	15						
133				upland	100					136	29		39.44	29						
134				upland	70					100	20		17	17						
135				upland	74					127	29		43.18	34						
136				riparian			forested riparian			210	6		71.4	34						
137				riparian			mixed riparian			236	8		122.72	52						
138				riparian			urban riparian			244	8		73.2	30						
139				riparian			agriculture riparian			292	7		105.12	36						
140				riparian						230	19		87.4	38			poorly drained			
141				riparian						282	10		109.98	39			very poorly drained			
142				riparian						211	10		84.4	40						

No	Citation	carbon type	soil carbon unit	landform	depth (cm)	vegetation	disturbance level/treatment	soil type/texture	age (year)	mean	n	SE	SD	CV (%)	bulk density	pH	water content	Site location/latitude, longitude	average annual temperature (° C)	average annual rainfall (mm)
143				riparian						234	8		39.78	17						
144				riparian						287	11		123.41	43						
145				riparian						188	10		50.76	27						
146				riparian						277	19		99.72	36						
147				riparian				Endoaquents		201	2		18.09	9						
148				riparian				Fluvaquents		222	6		51.06	23						
149				riparian				Humaquepts		253	11		108.79	43						
150				riparian				Humaquepts		301	7		108.36	36						
151	Neuman, Amber D., and Ken W. Belcher. "The contribution of carbon-based payments to wetland conservation compensation on agricultural landscapes." Agricultural Systems 104.1 (2011): 75-81.	soil organic carbon density	t/ha	riparian	0-30	wetlands: grasses, sedges, rushe, poplar, willow	uncultivated; were cultivated in the past till 1968.	calcicryolls, haplocyrolls, aquic argicryolls),argicryoll, calcareous argic cryaquolls; sandy loam - gravely sandy loam.		135	39	14.987995 2	93.6	69.33333333				north St Denis, Saskatchewan, 40 km east of Saskatoon. (St. Denis National Wildlife Area).		
152				riparian	0-30	trees	uncultivated; cultivated in the past			195	12	24.7105915 2	85.6							
153				riparian	0-30		cultivated wetlands			98.9	44	5.80409338 3	38.5							
154				upland	0-30		cultivated wetlands			67.4	28.66666667	5.59070380 1	29.93333333							
155	Silva, Lucas CR, et al. "Expansion of gallery forests into central Brazilian savannas." Global Change Biology 14.9 (2008): 2108-2118.	soil organic carbon	T/ha	riparian	0-10	trees and shrubs	conservation area; protected against fire	calcium rich patches		106.289	5	6.29	14.06486758				seasonal flooding	Ecological Reserve of the Brazilian Institute of Geography and Statistics near city of Brasilia, Federal District, Brazil. ; 15° 56'41" S and 47° 56'07" W		1426
156				riparian	10-20	trees and shrubs				94.9686	5	3.7735	8.437802513							
157				riparian	20-30	trees and shrubs				95.5975	5	11.3205	25.31340754							
158				riparian	30-40	trees and shrubs				119.497	5	10.063	22.50155206							

No	Citation	carbon type	soil carbon unit	landform	depth (cm)	vegetation	disturbance level/treatment	soil type/texture	age (year)	mean	n	SE	SD	CV (%)	bulk density	pH	water content	Site location/latitude, longitude	average annual temperature (° C)	average annual rainfall (mm)
159				riparian	40-50	trees and shrubs				110.063	5	4.402	9.843171237							
160				riparian	50-60	trees and shrubs				95.5975	5	10.0625	22.500434 02							
161				riparian	60-70	trees and shrubs				85.5346	5	2.5157	5.625276211							
162				riparian	70-80	trees and shrubs				69.8113	5	5.0315	11.25077603							
163				riparian	80-90	trees and shrubs				61.0063	5	3.7736	8.438026 12							
164				riparian	90-100	trees and shrubs				120.126	5	17.61	39.37715708							
165				riparian	0-10	trees and shrubs	conservation area; protected against fire	nutrient poor Cambisols		49.056 6	5	1.8868	4.219013 06							
166				riparian	10-20	trees and shrubs				42.767 3	5	1.8868	4.219013 06							
167				riparian	20-30	trees and shrubs				45.283	5	1.8868	4.219013 06							
168				riparian	30-40	trees and shrubs				36.188 7	5	1.5471	3.459420 768							
169				riparian	40-50	trees and shrubs				30.188 7	5	3.1413	7.024160 338							
170				riparian	50-60	trees and shrubs				38.993 7	5	1.2579	2.812749 909							
171				riparian	60-70	trees and shrubs				32.704 4	5	2.5157	5.625276211							
172				riparian	70-80	trees and shrubs				35.349 1	5	3.0157	6.743310 2							
173				riparian	80-90	trees and shrubs				32.704 4	5	0	0							
174				riparian	90-100	trees and shrubs				35.220 1	5	0	0							
175				upland	0-10	grasses	conservation area; protected against fire			28.301 9	5	3.7736	8.438026 12							
176				upland	10-20	grasses				27.673	5	4.4025	9.844289271							
177				upland	20-30	grasses				25.157 2	5	4.4025	9.844289271							

No	Citation	carbon type	soil carbon unit	landform	depth (cm)	vegetation	disturbance level/treatment	soil type/texture	age (year)	mean	n	SE	SD	CV (%)	bulk density	pH	water content	Site location/latitude, longitude	average annual temperature (° C)	average annual rainfall (mm)
178				upland	30-40	grasses				27.044	5	6.9183	15.46978909							
179				upland	40-50	grasses				25.1572	5	10.6919	23.90781521							
180				upland	50-60	grasses				24.5283	5	9.434	21.095 0653							
181				upland	60-70	grasses				19.4969	5	6.2893	14.06330233							
182				upland	70-80	grasses				16.3522	5	2.5157	5.625276211							
183				upland	80-90	grasses				14.4654	5	3.7736	8.438026 12							
184				upland	90-100	grasses				11.9497	5	1.8868	4.219013 06							
185				upland	0-10	grasses				31.4465	5	3.1447	7.031762969							
186				upland	10-20	grasses				30.8176	5	3.1447	7.031762969							
187				upland	20-30	grasses				26.4151	5	3.1446	7.031539362							
188				upland	30-40	grasses				20.1258	5	2.5157	5.625276211							
189				upland	40-50	grasses				20.1258	5	0.6289	1.406263151							
190				upland	50-60	grasses				18.8679	5	1.8868	4.219013 06							
191				upland	60-70	grasses				13.2075	5	1.8868	4.219013 06							
192				upland	70-80	grasses				12.5786	5	1.2579	2.812749909							
193				upland	80-90	grasses				11.3208	5	2.5157	5.625276211							
194				upland	90-100	grasses				13.8365	5	1.2578	2.812526302							

No	Citation	carbon type	soil carbon unit	landform	depth (cm)	vegetation	disturbance level/treatment	soil type/texture	age (year)	mean	n	SE	SD	CV (%)	bulk density	pH	water content	Site location/latitude, longitude	average annual temperature (° C)	average annual rainfall (mm)
195	Hazlett, P. W., et al. "Stand carbon stocks and soil carbon and nitrogen storage for riparian and upland forests of boreal lakes in northeastern Ontario."Forest Ecology and Management 219.1 (2005): 56-68.		%	riparian	0-6	black spruce feathermoss, mixedwood herb rich, conifer mixed herb	undisturbed fire-origin boreal forest	podzolic; silt loam	~95	0.75	8	0.25	0.707106781		1.11	4.2		Esker Lakes Research Area, 75 km north Cochrane, northeastern Ontario; 49° 38' N; 81° 00'W	1.6	884
196				riparian	6-15	idem	idem	podzolic; loam		2.04	8	0.68	1.923330445		1.01	5.3				
197				riparian	15-27	idem	idem	podzolic; silt loam		0.71	8	0.18	0.509116882		1.12	5.9				
198				riparian	27-41	idem	idem	podzolic; clay loam		0.55	8	0.14	0.395979797		1.43	7.6				
199				riparian	41-+75	idem	idem	podzolic; loam		0.17	8	0.05	0.141421356		1.48	7.7				
200				upland	0-4	black spruce feathermoss, mixedwood herb rich, conifer mixed herb	undisturbed fire-origin boreal forest	podzolic; silt loam	~95	0.57	8	0.15	0.424264069		1.37	4.2				
201				upland	4-9	idem	idem	podzolic; loam		2.44	8	0.23	0.650538239		1.03	5.1				
202				upland	9-23	idem	idem	podzolic; silt loam		1.79	8	0.3	0.848528137		1.17	5.2				
203				upland	23-37	idem	idem	podzolic; clay loam		0.71	8	0.1	0.282842712		1.29	6.3				
204				upland	37-+75	idem	idem	podzolic; loam		0.2	8	0.04	0.113137085		1.34	7				
205	Billett, Michael F., et al. "Connecting organic carbon in stream water and soils in a peatland catchment." Journal of Geophysical Research: Biogeosciences (2005–2012) 111.G2 (2006).	soil organic carbon	mg/cm3	riparian		dominant: Sphagnum, Eriphorum, heather	managed for deer and grouse; periodic burning	fluvisol		53	8	3.500178567	9.9			4.38		Brocky Burn catchment, River Dee, NE, Scotland.		1131
206				upland	50	idem	idem	histosol		41	10	2.340085469	7.4			3.94				
207				upland	150	idem	idem	histosol		42.5	8	3.358757211	9.5							

No	Citation	carbon type	soil carbon unit	landform	depth (cm)	vegetation	disturbance level/treatment	soil type/texture	age (year)	mean	n	SE	SD	CV (%)	bulk density	pH	water content	Site location/latitude, longitude	average annual temperature (° C)	average annual rainfall (mm)
208				upland	250	idem	idem	histosol		44	6	3.592584956	8.8							
209				upland	350	idem	idem	histosol		44.7	4	3.45	6.9							
210				upland	450	idem	idem	histosol		49.8	2	5.444722215	7.7							
211				upland		idem	idem	Podzol		87.5	8	8.591347391	24.3							
212				upland		idem	idem	Podzol		15.2	8	4.949747468	14							
213				upland		idem	idem	Ranker		83.3	8	7.071067812	20							
214				upland		idem	idem	Ranker		22.9	8	3.500178567	9.9							
215	Scott Bechtold, J., and Robert J. Naiman. "Soil texture and nitrogen mineralization potential across a riparian toposequence in a semi-arid savanna."Soil Biology and Biochemistry 38.6 (2006): 1325-1333.	total organic carbon	g/m2	riparian	0-10	annual grasses, forbs, reeds, leadwood	floodplain	Inceptisols or Entisols; sand		262	40	54	341.5259873		1.4	7.4		Phugwane River, Kruger National Park, South Africa.		400-600
216				riparian	0-50	annual grasses, forbs, reeds, leadwood	floodplain	Inceptisols or Entisols; sand		643	40	193	1220.639177							
217				riparian	0-10	perennial grass	riverbank	Inceptisols or Entisols; loamy sand	~20	821	12	151	523.0793439		1.3	7.4				
218				riparian	0-50	perennial grass	riverbank	Inceptisols or Entisols; loamy sand	> 100	5731	12	607	2102.70968							
219				riparian	0-10	woodland	terrace	Inceptisols or Entisols; loam	> 100	1872	12	251	869.4895054		1.1	6.9				
220				riparian	0-50	woodland	terrace	Inceptisols or Entisols; loam	> 100	7783	12	555	1922.576396							
221				riparian	0-10	woodland	hillslope	Inceptisols or Entisols; sandy loam	> 100	1301	10	92	290.9295447		1.2	6.7				
222				riparian	0-50	woodland	hillslope	Inceptisols or Entisols; sandy loam	> 100	6838	10	508	1606.437051							
223				upland	0-10	savanna	terrestrial	Inceptisols or Entisols; sandy loam	> 100	1036	9	75	225		1.4	6.3				

No	Citation	carbon type	soil carbon unit	landform	depth (cm)	vegetation	disturbance level/treatment	soil type/texture	age (year)	mean	n	SE	SD	CV (%)	bulk density	pH	water content	Site location/latitude, longitude	average annual temperature (° C)	average annual rainfall (mm)
224				upland	0-50	savanna	terrestrial	Inceptisols or Entisols; sandy loam		3108	9	224	672							
225				upland	0-10	savanna	terrestrial	Inceptisols or Entisols; sandy loam		1036	9	75	225		1.4	6.3				
226				upland	0-50	savanna	terrestrial	Inceptisols or Entisols; sandy loam		3108	9	224	672							
227				upland	0-10	savanna	terrestrial	Inceptisols or Entisols; sandy loam		1036	9	75	225		1.4	6.3				
228				upland	0-50	savanna	terrestrial	Inceptisols or Entisols; sandy loam		3108	9	224	672							
229				upland	0-10	savanna	terrestrial	Inceptisols or Entisols; sandy loam		1036	9	75	225		1.4	6.3				
230				upland	0-50	savanna	terrestrial	Inceptisols or Entisols; sandy loam		3108	9	224	672							
231	Sponseller, Ryan A., and Stuart G. Fisher. "The influence of drainage networks on patterns of soil respiration in a desert catchment." Ecology89.4 (2008): 1089-1100.	Soil organic matter	kg/m2	riparian	0-12	52.6% Velvet mesquite	ephemeral flow	sandy loam		7.2	5	0.6	1.34 1640 786					Sycamore Creek arises in the Mazatzal Mountains, 52 km northern Phoenix, Arizona, USA.		300-600 mm
232				riparian	0-12	52.7% Velvet mesquite	ephemeral flow	sandy loam		3.4	5	0.4	0.89 4427 191							
233				riparian	0-12	63.3% Velvet mesquite	intermittent flow	sandy loam		10.9	5	1.2	2.68 3281 573							
234				riparian	0-12	63.4% Velvet mesquite	intermittent flow	sandy loam		5.7	5	1.2	2.68 3281 573							
235				riparian	0-12	77.8% Velvet mesquite	perennial flow	sandy loam		6.4	5	1.2	2.68 3281 573							
236				riparian	0-12	77.9% Velvet mesquite	perennial flow	sandy loam		5.5	5	0.6	1.34 1640 786							
237				upland	0-12	35.7% Velvet mesquite	episodic flow	sandy loam		5.9	5	0.6	1.34 1640 786							
238				upland	0-12	35.8% Velvet mesquite	episodic flow	sandy loam		4	5	0.3	0.67 0820 393							
239				upland	0-12	35.9% Velvet mesquite	episodic flow	sandy loam		5.9	5	0.6	1.34 1640 786							
240				upland	0-12	35.10% Velvet mesquite	episodic flow	sandy loam		4	5	0.3	0.67 0820 393							

No	Citation	carbon type	soil carbon unit	landform	depth (cm)	vegetation	disturbance level/treatment	soil type/texture	age (year)	mean	n	SE	SD	CV (%)	bulk density	pH	water content	Site location/latitude, longitude	average annual temperature (° C)	average annual rainfall (mm)
241				upland	0-12	35.11% Velvet mesquite	episodic flow	sandy loam		5.9	5	0.6	1.341640786							
242				upland	0-12	35.12% Velvet mesquite	episodic flow	sandy loam		4	5	0.3	0.670820393							
	term: WETLAND VS UPLAND																			
246	Silveira, M. L., et al. "Soil properties as indicators of disturbance in forest ecosystems of Georgia, USA." ecological indicators 9.4 (2009): 740-747.	total carbon		riparian (wetland)	0-20			wetland and hydric soils/Sandy loam		47.3	186	4.113451576	56.1			4.9		Fort Benning, Phoenix City, AL, USA. Along Chattahoochee River.		>1300
247				upland	0-20	Forest of pine		well-excessive drained Ultisols & Entisols, sandy clay loam		12.9	186	6.55	89.33009012			5.2				
248	Young-Mathews, Anna, et al. "Plant-soil biodiversity relationships and nutrient retention in agricultural riparian zones of the Sacramento Valley, California." Agroforestry Systems 80.1 (2010): 41-60.	total carbon	%	riparian (wetland)	0-100	woody perennials 16.4 %, invasive/noxious weeds 69.2 %		silt loam		1.1	20	0.1	0.447213595			6.9		western Yolo County, Sacramento Valley, California, USA; 38° N, 122° W		470
249				riparian (wetland)	0-100	woody perennials 19.1 %, invasive/noxious weeds 39.8 %		silt loam		0.8	20	0.1	0.447213595			7.8				
250				riparian (wetland)	0-100	woody perennials 16.4 %, invasive/noxious weeds 29.7 %		silt loam		1.1	20	0.1	0.447213595			7				
251				riparian (wetland)	0-100	woody perennials 19.1 %, invasive/noxious weeds 39.8 %		silt loam		0.8	20	0.1	0.447213595			7.3				
252				upland		woody perennials 1.9 %, invasive/noxious weeds 59 %		silt loam		0.13	20	0.01	0.04472136			6.5				
253				upland		woody perennials 1.9 %, invasive/noxious weeds 5.8 %		silt loam		0.13	20	0.01	0.04472136			6.5				
254				upland		woody perennials 1.9%, invasive/noxious weeds 59%		silt loam		0.11	20	0.01	0.04472136			6.5				

No	Citation	carbon type	soil carbon unit	landform	depth (cm)	vegetation	disturbance level/treatment	soil type/texture	age (year)	mean	n	SE	SD	CV (%)	bulk density	pH	water content	Site location/latitude, longitude	average annual temperature (° C)	average annual rainfall (mm)
255				upland		woody perennials 1.9 %, invasive weeds 5.8 %		silt loam		0.11	20	0.01	0.044721 36			6.5				
	term: RIPARIAN																			
256	Gillham, Marla L. Physical and Chemical Characteristics of Riparian Soils: Two Third-Order Streams in the Western Cascades of Oregon. Diss. Oregon State University, 1990.	total soil carbon	%	riparian	0-15	dominant: fir	ephemeral debris dam ~100 years ago.	Hapludolls (floodplain), Fluventic dystrochrepts (stream terrace) and fluventic eutrochrepts (alluvial-collovial fans)		7.87	28	0.52	2.751581364			5.61		Blue River, Oregon, Oregon	0.4-20.3	2276
257				riparian	0-15	dominant: red alder	log jam causing channel constriction and erosion.			7.76	30	0.65	3.560196624			5.51		Blue River District, Willamette National Forest	-21.8	
258				riparian	15-30	Tsuga heterophylla transition zone				4.74	28	0.47	2.487006232			5.92				
259				riparian	15-30	Tsuga heterophylla zone				1.21	30	0.02	0.109544512			5.76				
260	Bush, J. K. "Soil nitrogen and carbon after twenty years of riparian forest development." Soil Science Society of America Journal 72.3 (2008): 815-822.	organic carbon	g/kg	riparian		no vegetation	(1718) ditches construction, (1938) cultivated farmland, channelization began. (1979) historical par	thermic Cumulic Haplustolls; silt loam	5	18.0716	3	1.65410852 1	2.865					San Antonio Missions National Historical Park.	15.5	710
261				riparian		total 0.33 %, acacia 0.29 %, celtis 0.0035 %			25	32.8375	3	5.21682156 2	9.0358							
262				riparian		total 0.28 %, acacia 0.19 %, celtis 0.05%			29	27.5482	3	0.63618226 2	1.1019							
263				riparian		total 0.28 %, acacia 0.19 %, celtis 0.06%			33	32.6171	3	3.18096904 3	5.5096							
264				riparian					25	40.7713	3	2.92653077 9	5.0689							
265				riparian		total 0.32 %, acacia 0.08 %, celtis 0.13%			45	55.978	3	1.65410852 1	2.865							
266				riparian		total 0.33 %, acacia 0.004 %, celtis 0.18%			49	65.2342	3	3.94439930 4	6.8319							
267				riparian		total 0.22 %, acacia 0 %, celtis 0.19%			53	43.416	3	2.41753878 2	4.1873							

No	Citation	carbon type	soil carbon unit	landform	depth (cm)	vegetation	disturbance level/treatment	soil type/texture	age (year)	mean	n	SE	SD	CV (%)	bulk density	pH	water content	Site location/latitude, longitude	average annual temperature (° C)	average annual rainfall (mm)
268				riparian		canopy			15	12.8407	3	2.533874861	4.3888							
269				riparian		intercanopy			15	22.0381	3	2.253917716	3.9039							
270				riparian		canopy			25	30.1571	3	3.520393266	6.0975							
271				riparian		intercanopy			25	34.2339	3	7.182583759	12.4406							
272	McLaughlin, James. "Boreal mixed-wood watershed riparian zone cation cycling during two contrasting climatic years." Soil Science Society of America Journal 73.4 (2009): 1408-1418.	total carbon	kmol/ha	riparian	Forest floor	Forested riparian: birch, fir, aspen, pine	60 year old forest regenerated after fire	Haplorthids; coarse loamy sand	60	1083	24	8.573 2141	42			4.3		Ontario; 43° 21' N; 85° 21'"W	-14.2 - 14.7.	1090
273				riparian	Mineral soil				60	5250	24	255.1551815	1250			5.1				
274				riparian	Total				60	6333	24	0.2041241 45	1							
275				riparian	Forest floor	Alder watershed			60	3167	24	221.0664493	1083			4.9				
276				riparian	Mineral soil				60	23750	24	5494.409617	26917			6.3				
277				riparian	Total				60	26917	24	0.4082482 9	2							
278	Clément, Jean-Christophe, Gilles Pinay, and Pierre Marmonier. "Seasonal dynamics of denitrification along topohydrosequences in three different riparian wetlands." Journal of Environmental Quality 31.3 (2002): 1025-1037.		g/kg	riparian	0-25	Herbaceous species, grass, marsh	was still grazed during summer period; understory and forest has been abandoned earlier after pasture; has upland of agricultural landscape, with maize and wheat as dominant crops.	Typic Haplaquoll/silty clay loam		53.2	3	4.8	8.313843876			4.8		riparian wetland, southwest Mont Saint-Michel Bay (Brittany, France), Hermitage River. ; 48.3° N, 1.3° W	12.5	850-900
279				riparian	25-50	idem	idem	idem		7.7	3	0.4	0.692820323			4.8				
280				riparian	50-75	idem	idem	idem		4.6	3	0.3	0.519615242			5.2				
281				riparian	0-25	Herbaceous species, meadow grass, marsh foxtail	idem	idem		61.4	3	7.3	12.643970 9			4.8				

No	Citation	carbon type	soil carbon unit	landform	depth (cm)	vegetation	disturbance level/treatment	soil type/texture	age (year)	mean	n	SE	SD	CV (%)	bulk density	pH	water content	Site location/latitude, longitude	average annual temperature (° C)	average annual rainfall (mm)
282				riparian	25-50	idem	idem	idem		8.2	3	8.2	14.20281662			4.8				
283				riparian	50-75	idem	idem	idem		5.6	3	5.6	9.699484522			5.2				
284				riparian	0-25	Herbaceous species, meadow grass, marsh	idem	idem		25.6	3	0.6	1.039230485			4.8				
285				riparian	25-50	idem	idem	idem		12.5	3	1.3	2.251666605			4.8				
286				riparian	50-75	idem	idem	idem		7.4	3	1.4	2.424871131			5.2				
287				riparian	0-25	Understory plants, no mature trees.	idem	idem		34.6	3	1.7	2.944486373			4.8				
288				riparian	25-50	idem	idem	idem		11.4	3	0.9	1.558845727			4.8				
289				riparian	50-75	idem	idem	idem		4.6	3	0.3	0.519615242			5.2				
290				riparian	0-25	Abundant understory plants, no mature trees.	idem	idem		46.8	3	6.3	10.91192009			4.8				
291				riparian	25-50	idem	idem	idem		11.1	3	0.3	0.519615242			4.8				
292				riparian	50-75	idem	idem	idem		6	3	0.1	0.173205081			5.2				
293				riparian	0-25	Abundant understory plants, no mature trees.	idem	idem		27.7	3	1.6	2.771281292			4.8				
294				riparian	25-50	idem	idem	idem		20.2	3	0.4	0.692820323			4.8				
295				riparian	50-75	idem	idem	idem		6.5	3	0.1	0.173205081			5.2				
296				riparian	0-25	Wetland trees: oak, willow	idem	idem	20	94.2	3	7.2	12.47076581			4.8				
297				riparian	25-50	idem	idem	idem		11.4	3	1.3	2.251666605			4.8				
298				riparian	50-75	idem	idem	idem		4.6	3	0.7	1.212435565			5.2				
299				riparian	0-25	Wetland trees: oak, willow	idem	idem		57.9	3	8.5	14.72243186			4.8				

No	Citation	carbon type	soil carbon unit	landform	depth (cm)	vegetation	disturbance level/treatment	soil type/texture	age (year)	mean	n	SE	SD	CV (%)	bulk density	pH	water content	Site location/latitude, longitude	average annual temperature (° C)	average annual rainfall (mm)
300				riparian	25-50	idem	idem	idem		13.5	3	1.6	2.771281292			4.8				
301				riparian	50-75	idem	idem	idem		6.1	3	1.1	1.905255888			5.2				
302				riparian	0-25	Wetland trees: oak, willow	idem	idem		38.4	3	3	5.196152423			4.8				
303				riparian	25-50	idem	idem	idem		15.1	3	0.8	1.385640646			4.8				
304				riparian	50-75	idem	idem	idem		7.1	3	0.1	0.173205081			5.2				
305	Giese, Laura A., et al. "Spatial and temporal patterns of carbon storage and species richness in three South Carolina coastal plain riparian forests."Ecological Engineering 15 (2000): S157-S170.		%	riparian		mature riparian hardwood forest	minimal; selective logging occured in 1940s.	histosols	60	13.19	66	0.30034332438	2.44							
306				riparian		mid-successional riparian forest	high disturbance (nuclear production; sediment erosion)	thapto-histic fluvaquents	11	4.06	75	0.26211702222	2.27							
307				riparian		early successional riparian forest	high disturbance (nuclear production; sediment erosion)	endoaquepts, fluvaquents	7	4.32	48	0.28290163232	1.96							
308				riparian		early successional riparian forest		endoaquepts, fluvaquents	7	4.68	27	0.24248711313	1.26							
309	Schilling, Keith E., et al. "Vertical distribution of total carbon, nitrogen and phosphorus in riparian soils of Walnut Creek, southern Iowa." Catena 77.3 (2009): 266-273.	total carbon	%	riparian		cool season grass		Silty Clay Loam		1.26	26	0.16277639292	0.83					Southern Iowa Drift Plain region of Iowa, Walnut Creek watershed.		
310				riparian		big bluestern and grass		Silt Loam		1.12	37	0.13645115959	0.83							
311				riparian		cool season grasses, continuous grazing		Silt Loam		1.31	37	0.11343530101	0.69							
312				riparian		dense stands of riparian forest		Silt Loam		1.5	22	0.38802530304	1.82							

No	Citation	carbon type	soil carbon unit	landform	depth (cm)	vegetation	disturbance level/treatment	soil type/texture	age (year)	mean	n	SE	SD	CV (%)	bulk density	pH	water content	Site location/latitude, longitude	average annual temperature (° C)	average annual rainfall (mm)
313	Oberbauer, S. F., et al. "Environmental effects on CO2 efflux from riparian tundra in the northern foothills of the Brooks Range, Alaska, USA." Oecologia92.4 (1992): 568-577.	soil carbon	%	riparian	0-5	Carex dominated		organic horizon		29.8	6	2.8	6.858571 28		0.078	5.208	aerated to anaerobic	Imnavait Creek, arctic Alaska, 68° 38' N, 149° 25' W		
314				riparian		Eriophorum dominated		Loose organic horizons.		20	6	1.5	3.674234 614		0.153	5.84	frequently flooded			
315	Rotkin-Ellman, Miriam, et al. "Tree species, root decomposition and subsurface denitrification potential in riparian wetlands." Plant and soil263.1 (2004): 335-344.	soil carbon	%	riparian		red maple (100%)	RM-1	haplaquepts; sandy loam		0.28	3	0.03	0.051961 524					41° 30' N, 71° 30' W		
316				riparian		red maple 82%; other deciduous 18%	RM-2			0.13	2	0.02	0.028284 271					41° 27' N, 71° 42' W		
317				riparian		red maple 12%, white pine 77%, other decidous 11%	WP-1	udipsamments; loamy sand		0.39	3	0.06	0.103923 048					41° 22' N, 71° 42' W		
318				riparian		Red maple 7%, white pine 71%, other decidous 21%	WP-2	humaquepts; sandy loam		0.37	2	0.03	0.042426 407					41° 30' N, 71° 37' W		
319	Petrone, R. M., et al. "Spatial variability of CO< sub> 2</sub> exchange for riparian and open grasslands within a first-order agricultural basin in Southern Ontario." Agriculture, ecosystems & environment 125.1 (2008): 137-147.	total soil carbon	%	riparian	0-30	dominant: warm season tall grasses (79% areal cover)	adjacent to agricultural land (corn) upland; residential	Luvisols, Brunisols and humic gleysols/clay loam		6.22	4	0.65	1.3		1.14	6		Strawberry Creek Watershed, South Western Ontario; 80° 23'15" W, 43° 33'10"N	6.7	909
320				riparian	0-30	dominant: warm season tall grasses (79% areal cover)	adjacent to sloped grassland extends to upland; residential, agricultural	idem		4.89	4	0.9	1.8		1.13	7.3				
321				grassland	0-30	grass	open grassland field with similar vegetation to riparian areas	idem		5.22	4	0.75	1.5		1.33	6.5				

No	Citation	carbon type	soil carbon unit	landform	depth (cm)	vegetation	disturbance level/treatment	soil type/texture	age (year)	mean	n	SE	SD	CV (%)	bulk density	pH	water content	Site location/latitude, longitude	average annual temperature (° C)	average annual rainfall (mm)
322	Edmonds, Robert L., and Kerri Mikkelsen Tuttle. "Red alder leaf decomposition and nutrient release in alder and conifer riparian patches in western Washington, USA." Forest ecology and management 259.12 (2010): 2375-2381.	total soil carbon	%	riparian	0-5	red Alder dominated	original riparian forest	Entisols; gravelly cobbly loamy sand	41-53	6.31	3	3.643080199	6.31			5.54		Skokomish River basin, Olympic National Forest, Washington, Brown creek; 123° 18'36" N, 47° 25'12" W	10.5	280
323				riparian	0-5	conifer dominated	original riparian forest	Entisols; gravelly cobbly loamy sand	27-53	4.12	3	1.339452625	2.32			5.33				
324	Fortier Truax Gagnon Lambert. 2013. Root biomass and soil carbon.	soil C stock	t/ha	riparian	0-20	Natural riparian woodlot			27-200	73.33	16	4.62	18.48					southern region of the province of Quebec, Canada.		
325				riparian		Herbaceous buffer; unmanaged, free growing buffer			-	46.7	16	4.58	18.32							
326				riparian		Hybrid poplar buffer			9	41.03	48	4.1	28.40563324							
327				riparian	20-40	Natural riparian woodlot			27-200	29.23	16	3.59	14.36							
328				riparian		Herbaceous buffer; unmanaged, free growing buffer			-	36.41	16	3.59	14.36							
329				riparian		Hybrid poplar buffer			9	42.83	48	0.21	1.454922678							
330				riparian	40-60	Natural riparian woodlot			27-200	20.51	16	2.57	10.28							
331				riparian		Herbaceous buffer; unmanaged, free growing buffer			-	21.54	16	2.56	10.24							
332				riparian		Hybrid poplar buffer			9	21.54	48	3.08	21.33886595							
333				riparian	0-60	Natural riparian woodlot			27-200	123.59	16	6.15	24.6							
334				riparian		Herbaceous buffer; unmanaged, free growing buffer			-	105.13	16	6.67	26.68							
335				riparian		Hybrid poplar buffer			9	92.31	48	6.66	46.14183351							
336			t/ha	riparian	0-20	Woodlot - Hemlock	Primary forest; 71% natural and managed forest, 28% agriculture, 1% urban	loam	200	118.39	4	8.78	17.56		0.76	5.35				

No	Citation	carbon type	soil carbon unit	landform	depth (cm)	vegetation	disturbance level/treatment	soil type/texture	age (year)	mean	n	SE	SD	CV (%)	bulk density	pH	water content	Site location/latitude, longitude	average annual temperature (° C)	average annual rainfall (mm)
337				riparian		Woodlot - White cedar	Secondary forest - livestock access; 71% natural and managed forest, 28% agriculture, 1% urban	Loam	72	64.86	4	8.32	16.64		0.85	4.53				
338				riparian		Woodlot - Grey birch	Secondary forest ; 71% natural and managed forest, 28% agriculture, 1% urban	Loam	27	32.82	4	8.31	16.62		1.16	4.93				
339				riparian		Woodlot - Sugar maple	Secondary forest ; 9% land use	Loam	54	74.54	4	7.85	15.7		0.66	4.25				
340				riparian		Hybrid poplar buffer	Riparian buffer in pasture; 71% natural and managed forest, 28% agriculture, 1% urban	Loam	9	35.07	12	8.77	30.38017116		1.14	6.37				
341				riparian		Hybrid poplar buffer	Riparian buffer in pasture; 71% natural and managed forest, 28% agriculture, 1% urban	Loam	9	40.97	12	8.32	28.82132544		0.9	5.63				
342				riparian		Hybrid poplar buffer	Riparian buffer in hayfield71% natural and managed forest, 28% agriculture, 1% urban	Loam	9	38.26	12	7.4	25.63435195		1.23	6.18				
343				riparian		Hybrid poplar buffer	Riparian buffer in pasture; 9% land use	Loam	9	45.09	12	8.322	28.82825364		1.07	5.44				
344				riparian		Herbaceous buffer	Riparian buffer in pasture; 71% natural and managed forest, 28% agriculture, 1% urban	Loam	-	46.45	4	8.32	16.64		0.9	6.15				
345				riparian		Herbaceous buffer	Riparian buffer in pasture; 71% natural and managed forest, 28% agriculture, 1% urban	sandy loam	-	39.16	4	8.77	17.54		1.12	5.73				
346				riparian		Herbaceous buffer	Riparian buffer in annual crop; 71% natural and managed forest, 28% agriculture, 1% urban	sandy loam	-	34.63	4	9.24	18.48		1.22	7.23				
347				riparian		Herbaceous buffer	Riparian buffer in pasture; 9% land use	silt loam	-	63.51	4	8.32	16.64		0.92	5.48				

No	Citation	carbon type	soil carbon unit	landform	depth (cm)	vegetation	disturbance level/treatment	soil type/texture	age (year)	mean	n	SE	SD	CV (%)	bulk density	pH	water content	Site location/latitude, longitude	average annual temperature (° C)	average annual rainfall (mm)
348				riparian	20-40	Woodlot - Hemlock	Primary forest; 71% natural and managed forest, 28% agriculture, 1% urban	Sandy Clay Loam	200	5.54	4	6.47	12.94		1.21	6.5				
349				riparian		Woodlot - White cedar	Secondary forest - livestock access; 71% natural and managed forest, 28% agriculture, 1% urban	Sandy Loam	72	22.11	4	7.39	14.78		0.86	4.95				
350				riparian		Woodlot - Grey birch	Secondary forest ; 71% natural and managed forest, 28% agriculture, 1% urban	Loam	27	27.59	4	6.47	12.94		1.33	5.15				
351				riparian		Woodlot - Sugar maple	Secondary forest ; 9% land use	Silt Loam	54	60.16	4	6.93	13.86		0.81	4.8				
352				riparian		Hybrid poplar buffer	Riparian buffer in pasture; 71% natural and managed forest, 28% agriculture, 1% urban	Loam	9	18.44	12	7.4	25.63435195		1.33	6.18				
353				riparian		Hybrid poplar buffer	Riparian buffer in pasture; 71% natural and managed forest, 28% agriculture, 1% urban	Loam	9	23.92	12	6.93	24.00622419		1	5.75				
354				riparian		Hybrid poplar buffer	Riparian buffer in hayfield71% natural and managed forest, 28% agriculture, 1% urban	Loam	9	34.88	12	7.86	27.22783869		1.35	6.09				
355				riparian		Hybrid poplar buffer	Riparian buffer in pasture; 9% land use	Loam	9	37.62	12	6.93	24.00622419		1.03	5.78				
356				riparian		Herbaceous buffer	Riparian buffer in pasture; 71% natural and managed forest, 28% agriculture, 1% urban	Silt Loam	-	38.05	4	7.4	14.8		1.21	5.73				
357				riparian		Herbaceous buffer	Riparian buffer in pasture; 71% natural and managed forest, 28% agriculture, 1% urban	Sandy Loam	-	33.53	4	6	12		1.08	6.1				
358				riparian		Herbaceous buffer	Riparian buffer in annual crop; 71% natural and managed forest, 28% agriculture, 1% urban	Sandy Loam	-	38.94	4	6.93	13.86		1.35	6.3				

No	Citation	carbon type	soil carbon unit	landform	depth (cm)	vegetation	disturbance level/treatment	soil type/texture	age (year)	mean	n	SE	SD	CV (%)	bulk density	pH	water content	Site location/latitude, longitude	average annual temperature (° C)	average annual rainfall (mm)
359				riparian		Herbaceous buffer	Riparian buffer in pasture; 9% land use	Silt Loam	-	31.71	4	6.93	13.86		0.98	5.78				
360				riparian	40-60	Woodlot - Hemlock	Primary forest; 71% natural and managed forest, 28% agriculture, 1% urban	Sandy Clay Loam	200	3.21	4	6.01	12.02		1.54	6.8				
361				riparian		Woodlot - White cedar	Secondary forest - livestock access; 71% natural and managed forest, 28% agriculture, 1% urban	Sandy Loam	72	12.86	4	5.08	10.16		0.92	5.45				
362				riparian		Woodlot - Grey birch	Secondary forest ; 71% natural and managed forest, 28% agriculture, 1% urban	Loam	27	29.3	4	5.54	11.08		1.32	5.18				
363				riparian		Woodlot - Sugar maple	Secondary forest ; 9% land use	Silt Loam	54	34.74	4	5.08	10.16		0.99	4.9				
364				riparian		Hybrid poplar buffer	Riparian buffer in pasture; 71% natural and managed forest, 28% agriculture, 1% urban	Sandy Loam	9	21.96	12	5.55	19.22576396		1.22	6.22				
365				riparian		Hybrid poplar buffer	Riparian buffer in pasture; 71% natural and managed forest, 28% agriculture, 1% urban	Sandy Loam	9	11.5	12	5.08	17.597662		0.87	5.85				
366				riparian		Hybrid poplar buffer	Riparian buffer in hayfield71% natural and managed forest, 28% agriculture, 1% urban	Sandy Clay Loam	9	35.23	12	4.16	14.41066272		1.38	6.2				
367				riparian		Hybrid poplar buffer	Riparian buffer in pasture; 9% land use	Loam	9	19.23	12	5.08	17.597662		0.92	5.95				
368				riparian		Herbaceous buffer	Riparian buffer in pasture; 71% natural and managed forest, 28% agriculture, 1% urban	Silt Loam	-	29.72	4	6.01	12.02		1.32	5.95				
369				riparian		Herbaceous buffer	Riparian buffer in pasture; 71% natural and managed forest, 28% agriculture, 1% urban	Sandy Loam	-	13.74	4	5.55	11.1		1.1	6.18				

No	Citation	carbon type	soil carbon unit	landform	depth (cm)	vegetation	disturbance level/treatment	soil type/texture	age (year)	mean	n	SE	SD	CV (%)	bulk density	pH	water content	Site location/latitude, longitude	average annual temperature (° C)	average annual rainfall (mm)
370				riparian		Herbaceous buffer	Riparian buffer in annual crop; 71% natural and managed forest, 28% agriculture, 1% urban	Sandy Loam	-	27.48	4	6	12		1.4	6.35				
371				riparian		Herbaceous buffer	Riparian buffer in pasture; 9% land use	Sandy Loam	-	14.63	4	5.55	11.1		0.94	6.03				
372	Bedison, James E., Frederick N. Scatena, and Jerry V. Mead. "Influences on the spatial pattern of soil carbon and nitrogen in forested and non-forested riparian zones in the Atlantic Coastal Plain of the Delaware River Basin."Forest Ecology and Management 302 (2013): 200-209.	total soil C	%	riparian	0-30	Forested: typically closed canopy, mesic mixed hardwoods	agriculture	Entisols, Histosols, Inceptisols, or Ultisols.		4.8	20	1.1	4.919349 55	101	0.3		well/excessively drained or moderately well drained.	Atlantic Coastal Plain physiographic province, southern New Jersey, southeastern Pennsylvania, primarily in the DRB.		
373			%	riparian	0-30	Non-forested				2.3	9	0.3	0.9	41	0.4					
374			Mg/ha	riparian	0-30	Forested				100.3	20	15	67.08203 932	67	0.3					
375			Mg/ha	riparian	0-30	Non-forested				90.6	9	12.1	36.3	40	0.4					
376	Hodson, Amanda K., et al. "Nematode food webs associated with native perennial plant species and soil nutrient pools in California riparian oak woodlands." Geoderma 228 (2014): 182-191.	total soil C	mg/g	riparian	0-7.5	dominant: manzanita, oak. Cover of grasses and herbaceous plants <20%	isome signs of animal disturbance	Loam		3.8	22	0.533001791	2.5	65.78947368		7.7	0.40%	the Audubon Bobcat ranch reserve, western Yolo County, California, USA. ; 38° 31'57"N, 122° 02'18"W	9.5-24.4	579
377				riparian		dominant: manzanita, oak. Cover of grasses and herbaceous plants <20%	heavily eroded in patches.	Sandy loam		3.2	28	0.340168026	1.8	56.25		7.6	0.40%			
378	Kachenchart, Boonlue, et al. "Seasonal nitrous oxide emissions from different land uses and their controlling factors in a tropical riparian ecosystem." Agriculture, Ecosystems & Environment 158 (2012): 15-30.	total soil C	%	riparian	0-5	Reforestation, N-fixing trees	trees harvested for lac	loam	15	1.78	15	0.02	0.077459667	4.351666681	1.35	6.15	gravimetric soil water content (%) = 18.4	18° 37'13.04" N, 100° 45'44.20"E; 18° 35'04.89"N, 100° 45'46.79"E, 18° 33'27.91" N, 100° 45'46.29"E.	21.8-34.6 (wet season) and 13.4-36.5 (dry season)	1090 (wet season); 177 (dry season)

No	Citation	carbon type	soil carbon unit	landform	depth (cm)	vegetation	disturbance level/treatment	soil type/texture	age (year)	mean	n	SE	SD	CV (%)	bulk density	pH	water content	Site location/latitude, longitude	average annual temperature (° C)	average annual rainfall (mm)
379				riparian	0-5	Maize (Zea mays)	double crop for 20 years; fertilizer application	silt loam		1.49	15	0.01	0.038729833	2.599317682	1.33	6.19	13.8			
380				riparian	0-5	Wet		nd		1.63	45	0.02	0.134164079	8.230925071	1.34	6.13	22.5			
381				riparian	0-5	Dry		nd		1.64	45	0.02	0.134164079	8.180736503	1.34	6.21	9.8			
382	Cooper, D. J., and D. C. Andersen. "Novel plant communities limit the effects of a managed flood to restore riparian forests along a large regulated river." River Research and Applications 28.2 (2012): 204-215.	total soil C	%	riparian	0-10	point bar	artificial disturbance: pre-flood vegetation manipulation. C,H,P,P+H = C control, H herbicide, P ploughing, P + H = herbicide then ploughing.			1.13	10	0.26	0.822192192	72.760377094				Green River, Browns Park National Wildlife Refuge, Colodaro.		210
383				riparian	0-10	point bar	C,H,P,P+H			1.52	10	0.65	2.055480479	135.2289789						
384				riparian	0-10	abandoned channels	C,H,P,P+H			1.68	10	0.38	1.201665511	71.527700898						
385				riparian	0-10	abandoned channels	C,H,P,P+H			1.35	10	0.28	0.885437745	65.5879811						
386				riparian	0-10	abandoned channels	C,H,P,P+H			1.38	10	0.27	0.853814968	61.870649987						
387				riparian	0-10		C			1.5	10	0.48	1.517893277	101.1928851						
388	Cierjacks, A., et al. "Organic matter distribution in floodplains can be predicted using spatial and vegetation structure data." River Research and Applications27.8 (2011): 1048-1057.	soil carbon concentration	%	riparian	17	Tree layer 50.4%, shrub layer 19%, herb layer 58.1 %.	Poplar restoration covers 40% of study area	calcaric fluvisols		3	67	0.2	1.637070554	54.569001848				Donau-Auen National Park, 48° 8' N, 16° 36' E and 48° 7' N, 16° 48' E	9.8	533
389				riparian	17	Tree layer 50.4%, shrub layer 19%, herb layer 58.1 %.		calcaric fluvisols		1.7	67	0.1	0.818535277	48.149133395						
390		C stocks	t/ha	riparian	0-100	Tree layer 50.4%, shrub layer 19%, herb layer 58.1 %.		calcaric fluvisols		177	67	7	57.29746 94	32.371405164						

No	Citation	carbon type	soil carbon unit	landform	depth (cm)	vegetation	disturbance level/treatment	soil type/texture	age (year)	mean	n	SE	SD	CV (%)	bulk density	pH	water content	Site location/latitude, longitude	average annual temperature (° C)	average annual rainfall (mm)
391	McClain, Michael E., et al. "Dissolved organic matter and terrestrial - lotic linkages in the Central Amazon Basin of Brazil." Global Biogeochemical Cycles 11.3 (1997): 295-311.	soil organic carbon	%	riparian	0-20	closed canopy of Campina forest	protected forest reserves	Spodosols		3.27	4	0.18	0.36	11.00917431				2° 30' S, 60° 00'W		
392				riparian	21-40	idem	idem	Spodosols		0.73	4	0.29	0.58	79.45205479						
393				riparian	41-60	idem	idem	Spodosols		1.68	4	0.645	1.29	76.78571429						
394				riparian	61-80	idem	idem	Spodosols		1.64	4	0.19	0.38	23.17073171						
395				riparian	81-100	idem	idem	Spodosols		2.1	4	0.29	0.58	27.61904762						
396				riparian	0-20	idem	idem	Spodosols; coarse sand		1.46	3	0.762102355	1.32	90.4109589						
397				riparian	21-40	idem	idem	Spodosols; coarse sand		0.29	3	0.138564065	0.24	82.75862069						
398				riparian	41-60	idem	idem	Spodosols; coarse sand		0.06	3	0.040414519	0.07	116.6666667						
399				riparian	61-80	idem	idem	Spodosols; coarse sand		0.05	3	0.028867513	0.05	100						
400				riparian	81-100	idem	idem	Spodosols; coarse sand		0.05	3	0.017320508	0.03	60						
401				riparian	101-150	idem	idem	Spodosols; coarse sand		0.04	3	0.005773503	0.01	25						
402				riparian	151-200	idem	idem	Spodosols; coarse sand		0.04	3	0.017320508	0.03	75						
403				riparian	0-20	largely undisturbed catchment.	Great abundance of palms	Hydromorphic Oxisols; coarse sand		1.15	4	0.305	0.61	53.04347826				2° 60' S, 59° 60'W		
404				riparian	21-40	idem	idem	Hydromorphic Oxisols; coarse sand		0.63	4	0.1	0.2	31.74603175						
405				riparian	41-60	idem	idem	Hydromorphic Oxisols; coarse sand		0.75	4	0.165	0.33	44						
406				riparian	61-80	idem	idem	Hydromorphic Oxisols; coarse sand		1.14	4	0.365	0.73	64.03508772						
407				riparian	81-100	idem	idem	Hydromorphic Oxisols; coarse sand		0.97	4	0.395	0.79	81.44329897						
408				riparian	101-150	idem	idem	Hydromorphic Oxisols; coarse sand		0.36	4	0.145	0.29	80.55555556						

No	Citation	carbon type	soil carbon unit	landform	depth (cm)	vegetation	disturbance level/treatment	soil type/texture	age (year)	mean	n	SE	SD	CV (%)	bulk density	pH	water content	Site location/latitude, longitude	average annual temperature (° C)	average annual rainfall (mm)
409				riparian	151-200	idem	idem	Hydromorphic Oxisols; coarse sand		0.13	4	0.02	0.04	30.76923077						
410				riparian	0-20	idem	idem	Oxisols; coarse sand		0.99	3	0.27712829	0.48	48.484844848						
411				riparian	21-40	idem	idem	Oxisols; coarse sand		0.84	3	0.0866025 4	0.15	17.857142 86						
412				riparian	41-60	idem	idem	Oxisols; coarse sand		0.52	3	0.0635085 3	0.11	21.153844 615						
413				riparian	61-80	idem	idem	Oxisols; coarse sand		0.35	3	0.0750555 35	0.13	37.142857 14						
414				riparian	81-100	idem	idem	Oxisols; coarse sand		0.25	3	0.0288675 13	0.05	20						
415				riparian	101-150	idem	idem	Oxisols; coarse sand		0.18	3	0.0288675 13	0.05	27.777777 78						
416				riparian	151-200	idem	idem	Oxisols; coarse sand		0.12	3	0.0519615 24	0.09	75						
417				riparian	201-250	idem	idem	Oxisols; coarse sand		0.11	3	0.0346410 16	0.06	54.545454 55						
418				riparian	251-300	idem	idem	Oxisols; coarse sand		0.06	3	0.0057735 03	0.01	16.666666 67						
419				riparian	301-350	idem	idem	Oxisols; coarse sand		0.05	3	0.0115470 05	0.02	40						
420				riparian	351-400	idem	idem	Oxisols; coarse sand		0.05	3	0.0230940 11	0.04	80						
421				riparian	401-450	idem	idem	Oxisols; coarse sand		0.06	3	0.0057735 03	0.01	16.666666 67						
422	Shah, Jennifer Jo Follstad. Effects of Flood Regime and Riparian Plant Species on Soil Nitrogen Cycling Along the Middle Rio Grande: Implications for Restoration. Diss. The University of New Mexico, 2006.	soil organic matter	%	riparian	0-30	P. deltoides, flooded; native plant species; 1-3 floods	three diversion dams; less frequent flooding after dam installation	Typic Ustifluvents; clay	35-61	4.54	64	0.12	0.96	21.145377445	1.1	7.55		middle Rio Grande of New Mexico, from Otowi gauge in the north to the Elephant Butte gauge in the south.		
423				riparian	0-30	idem		Typic Ustifluvents; clay loam	35-61	4.22	64	0.15	1.2	28.436018 96	1.1	7.41				
424				riparian	0-30	T. chinensis, flooded; invasive species; never flooded during 2001-2004		Typic Ustifluvents; clay	16-26	4.64	64	0.12	0.96	20.689655 17	1.03	7.52				

No	Citation	carbon type	soil carbon unit	landform	depth (cm)	vegetation	disturbance level/treatment	soil type/texture	age (year)	mean	n	SE	SD	CV (%)	bulk density	pH	water content	Site location/latitude, longitude	average annual temperature (° C)	average annual rainfall (mm)
425				riparian	0-30	idem		Typic Ustifluvents; loam	16-26	2.4	64	0.18	1.44	60	1.19	7.59				
426		Soil carbon	%	riparian	0-30	P. deltoides, flooded; native plant species; 1-3 floods		Typic Ustifluvents; clay	35-61	2.14	32	0.06	0.339411255	15.86033902						
427				riparian	0-30	idem		Typic Ustifluvents; clay loam	35-61	2.21	32	0.05	0.282842712	12.79831278						
428				riparian	0-30	T. chinensis, flooded; invasive species; never flooded		Typic Ustifluvents; clay	16-26	1.76	32	0.05	0.282842712	16.07060866						
429				riparian	0-30	idem		Typic Ustifluvents; loam	16-26	1.34	32	0.12	0.678822 51	50.65839626						
430				riparian	0-30	P. deltoides, flooded; native plant species; 1-3 floods		Typic Ustifluvents; clay	35-61	2.15	32	0.08	0.452548 34	21.04876						
431				riparian	0-30	idem		Typic Ustifluvents; clay loam	35-61	2.24	32	0.08	0.452548 34	20.20305089						
432				riparian	0-30	T. chinensis, flooded; invasive species; never flooded		Typic Ustifluvents; clay	16-26	1.88	32	0.05	0.282842712	15.04482513						
433				riparian	0-30	idem		Typic Ustifluvents; loam	16-26	1.27	32	0.12	0.678822 51	53.45059133						
434	Raimbault, Beverly Anne. "Litter input, soil quality and soil carbon dioxide production rates in varying riparian land uses along a first order stream in Southern Ontario, Canada." (2011).	soil organic carbon	g/kg	riparian	0-10	rehabilitated buffer, silver maple, poplar, alder and shrubs	rehabilitated riparian zone	Podzolic, loamy sand.	25	55	8	4.2	11.87939392	21.59889804		7.84		Washington Creek, Oxford County, Ontario, Canada. ; 43° 18' N; 80° 33'"W	7.2	912
435				riparian		upstream from the rehabilitated area, a grass-forb buffer, cattle grazing	grass riparian zone	Podzolic, loamy sand.		89.1	8	8.3	23.47594514	26.3478621		7.67				
436				riparian		a natural forest	forest riparian zone	Podzolic, loamy sand.		89.4	8	7.3	20.64751801	23.09565773		7.74				
437				riparian	10-20	rehabilitated buffer, silver maple, poplar, alder and shrubs	rehabilitated riparian zone	Podzolic, loamy sand.		51	8	5.1	14.42497834	28.28427125		8.01				
438				riparian		upstream from the rehabilitated area, a grass-forb buffer, cattle grazing	grass riparian zone	Podzolic, loamy sand.		78	8	12	33.94112 55	43.51426346		7.56				
439				riparian		a natural forest	forest riparian zone	Podzolic, loamy sand.		80.8	8	9.9	28.00142853	34.65523334		7.56				

No	Citation	carbon type	soil carbon unit	landform	depth (cm)	vegetation	disturbance level/treatment	soil type/texture	age (year)	mean	n	SE	SD	CV (%)	bulk density	pH	water content	Site location/latitude, longitude	average annual temperature (° C)	average annual rainfall (mm)
440				riparian	20-30	rehabilitated buffer, silver maple, poplar, alder and shrubs	rehabilitated riparian zone	Podzolic, loamy sand.		37.2	8	3.4	9.616652224	25.85121566		8.03				
441				riparian		upstream from the rehabilitated area, a grass-forb buffer, cattle grazing	grass riparian zone	Podzolic, loamy sand.		85	8	19.3	54.58864351	64.22193354		7.8				
442				riparian		a natural forest	forest riparian zone	Podzolic, loamy sand.		79.4	8	8.1	22.91025971	28.85423137		6.99				
443				riparian	30-40	rehabilitated buffer, silver maple, poplar, alder and shrubs	rehabilitated riparian zone	Podzolic, loamy sand.		27.4	8	3	8.485281374	30.96681802		8.15				
444				riparian		upstream from the rehabilitated area, a grass-forb buffer, cattle grazing	grass riparian zone	Podzolic, loamy sand.		70.7	8	14	39.59797975	56.00845792		7.38				
445				riparian		a natural forest	forest riparian zone	Podzolic, loamy sand.		76.6	8	16	45.254834	59.07941775		6.83				
446				riparian	0-40	rehabilitated buffer, silver maple, poplar, alder and shrubs	rehabilitated riparian zone	Podzolic, loamy sand.		42.6	8	3	8.485281374	19.91850088		8.01				
447				riparian		upstream from the rehabilitated area, a grass-forb buffer, cattle grazing	grass riparian zone	Podzolic, loamy sand.		80.7	8	12.4	35.07249635	43.46034244		7.6				
448				riparian		a natural forest	forest riparian zone	Podzolic, loamy sand.		81.5	8	9.2	26.02152955	31.92825711		7.28				
449		soil organic stock	g/m2	riparian	0-10	rehabilitated buffer, silver maple, poplar, alder and shrubs	rehabilitated riparian zone	Podzolic, loamy sand.		5035	8	373	1055.003318	20.9533926		7.84				
450				riparian		upstream from the rehabilitated area, a grass-forb buffer, cattle grazing	grass riparian zone	Podzolic, loamy sand.		6268	8	412	1165.311975	18.59144824		7.67				
451				riparian		a natural forest	forest riparian zone	Podzolic, loamy sand.		6495	8	400	1131.37085	17.41910469		7.74				
452				riparian	10-20	rehabilitated buffer, silver maple, poplar, alder and shrubs	rehabilitated riparian zone	Podzolic, loamy sand.		4833	8	516	1459.468396	30.19798048		8.01				
453				riparian		upstream from the rehabilitated area, a grass-forb buffer, cattle grazing	grass riparian zone	Podzolic, loamy sand.		5772	8	491	1388.757718	24.06025153		7.56				

No	Citation	carbon type	soil carbon unit	landform	depth (cm)	vegetation	disturbance level/treatment	soil type/texture	age (year)	mean	n	SE	SD	CV (%)	bulk density	pH	water content	Site location/latitude, longitude	average annual temperature (° C)	average annual rainfall (mm)
454				riparian		a natural forest	forest riparian zone	Podzolic, loamy sand.		5874	8	692	1957.27157	33.32093242		7.56				
455				riparian	20-30	rehabilitated buffer, silver maple, poplar, alder and shrubs	rehabilitated riparian zone	Podzolic, loamy sand.		3860	8	273	772.1606051	20.00416075		8.03				
456				riparian		upstream from the rehabilitated area, a grass-forb buffer, cattle grazing	grass riparian zone	Podzolic, loamy sand.		6430	8	911	2576.697111	40.07304993		7.8				
457				riparian		a natural forest	forest riparian zone	Podzolic, loamy sand.		5561	8	448	1267.135352	22.78610595		6.99				
458				riparian	30-40	rehabilitated buffer, silver maple, poplar, alder and shrubs	rehabilitated riparian zone	Podzolic, loamy sand.		2788	8	243	687.3077913	24.6523598		8.15				
459				riparian		upstream from the rehabilitated area, a grass-forb buffer, cattle grazing	grass riparian zone	Podzolic, loamy sand.		5932	8	1050	2969.848481	50.06487662		7.38				
460				riparian		a natural forest	forest riparian zone	Podzolic, loamy sand.		5840	8	1076	3043.387586	52.11280113		6.83				
461				riparian	0-40	rehabilitated buffer, silver maple, poplar, alder and shrubs	rehabilitated riparian zone	Podzolic, loamy sand.		4129	8	243	687.3077913	16.64586562		8.01				
462				riparian		upstream from the rehabilitated area, a grass-forb buffer, cattle grazing	grass riparian zone	Podzolic, loamy sand.		6100	8	614	1736.654255	28.46974188		7.6				
463				riparian		a natural forest	forest riparian zone	Podzolic, loamy sand.		5942	8	531	1501.894803	25.27591389		7.28				
464	Tanzosh, Joyce K. Soil carbon dynamics and gaseous emissions in riparian zones in Coshocton, Ohio. Diss. The Ohio State University, 2005.	soil organic carbon	g/kg	riparian	0-5	grass	native forest converted to agricultural landuse ~1930s	silt loam, Typic Hapludults.		22.06	3	1.179	2.042087902	9.256971451	0.977		very well drained; moderate permeability, medium soil moisture capability.	North Appalachian Experimental Watershed, Allegheny Plateau in Coshocton County, Ohio, USA. ; 40° 22' N, 81° 48' W	9	965
465				riparian		forest	trees species dominated	idem	70	29.384	3	2.276	3.942147638	13.41596664	0.965					
466				riparian		upland	upland cropland	idem		18.77	3	1.77	3.065729929	16.33313761	1.162					
467				riparian	5-10	grass	agricultural landuse	idem		12.36	3	1.35	2.338268 59	18.91803067	1.44					

No	Citation	carbon type	soil carbon unit	landform	depth (cm)	vegetation	disturbance level/treatment	soil type/texture	age (year)	mean	n	SE	SD	CV (%)	bulk density	pH	water content	Site location/latitude, longitude	average annual temperature (° C)	average annual rainfall (mm)
468				riparian		forest	trees species dominated	idem		22.89	3	2.27	3.931755333	17.17673802	1.055					
469				riparian		upland	upland cropland	idem		11.43	3	1.77	3.065729929	26.82178416	1.321					
470				riparian	10-20	grass	agricultural landuse	idem		17.32	3	1.35	2.338268 59	13.50039602	1.39					
471				riparian		forest	trees species dominated	idem		20.18	3	2.36	4.087639906	20.25589646	1.086					
472				riparian		upland	upland cropland	idem		9.99	3	1.85	3.204293994	32.07501495	1.331					
473				riparian	20-30	grass	agricultural landuse	idem		22.53	3	1.18	2.043819953	9.071548837	1.368					
474				riparian		forest	trees species dominated	idem		17.64	3	2.28	3.949075841	22.38705125	1.128					
475				riparian		upland	upland cropland	idem		9.13	3	1.86	3.221614502	35.28602 96	1.32					
476				riparian	30-50	grass	agricultural landuse	idem		18.31	3	1.09	1.887935 38	10.31095238	1.42					
477				riparian		forest	trees species dominated	idem		12.16	3	2.35	4.070319398	33.47302136	1.287					
478				riparian		upland	upland cropland	idem		8.28	3	1.68	2.909845357	35.14305986	1.298					
479				riparian	50-70	grass	agricultural landuse	idem		20.15	3	1.34	2.320948082	11.51835276	1.409					
480				riparian		forest	trees species dominated	idem		12.4	3	2.19	3.793191269	30.59025217	1.393					
481				riparian		upland	upland cropland	idem		4.39	3	1.86	3.221614502	73.38529617	1.45					
482				riparian	70-100	grass	agricultural landuse	idem		17.78	3	1.18	2.043819953	11.49505035	1.398					
483				riparian		forest	trees species dominated	idem		15.75	3	2.19	3.793191269	24.08375409	1.302					
484				riparian		upland	upland cropland	idem		5.06	3	1.76	3.048409421	60.24524548	1.456					
485				riparian	0-5	grass	agricultural landuse	idem		25.33	3	2.52	4.364768035	17.23161482	0.885		moderate permeability, medium moisture capacity.			

No	Citation	carbon type	soil carbon unit	landform	depth (cm)	vegetation	disturbance level/treatment	soil type/texture	age (year)	mean	n	SE	SD	CV (%)	bulk density	pH	water content	Site location/latitude, longitude	average annual temperature (° C)	average annual rainfall (mm)
486				riparian		forest	trees species dominated	idem		44.1	3	4.92	8.521689973	19.32356003	0.655					
487				riparian		upland	upland cropland	idem		24.55	3	3.03	5.248113947	21.37724622	1.065					
488				riparian	5-10	grass	agricultural landuse	idem		17.6	3	2.52	4.364768035	24.79981838	1.059					
489				riparian		forest	trees species dominated	idem		16.46	3	4.66	8.071356763	49.03618933	0.963					
490				riparian		upland	upland cropland	idem		12.16	3	2.9	5.022947342	41.30713275	1.176					
491				riparian	10-20	grass	agricultural landuse	idem		14.03	3	2.15	3.723909236	26.54247496	1.133					
492				riparian		forest	trees species dominated	idem		13.15	3	4.91	8.504369465	64.67201114	1.121					
493				riparian		upland	upland cropland	idem		8.47	3	2.78	4.815101245	56.84889309	1.436					
494				riparian	20-30	grass	agricultural landuse	idem		13.62	3	2.52	4.364768035	32.04675503	1.2					
495				riparian		forest	trees species dominated	idem		10.84	3	5.79	10.02857418	92.51452192	1.147					
496				riparian		upland	upland cropland	idem		5.03	3	2.78	4.815101245	95.72765895	1.53					
497				riparian	30-50	grass	agricultural landuse	idem		10.94	3	2.39	4.139601 43	37.83913556	1.241					
498				riparian		forest	trees species dominated	idem		9.42	3	4.54	7.863510666	83.47675867	1.321					
499				riparian		upland	upland cropland	idem		4.37	3	3.15	5.455960044	124.8503443	1.566					
500				riparian	50-70	grass	agricultural landuse	idem		7.37	3	2.65	4.589934 64	62.2786247	1.36					
501				riparian		forest	trees species dominated	idem		8.25	3	4.79	8.296523368	100.5639196	1.426					
502				riparian		upland	upland cropland	idem		2.94	3	2.77	4.797780737	163.189821	1.597					
503				riparian	70-100	grass	agricultural landuse	idem		6.2	3	2.4	4.156921938	67.04712803	1.494					

No	Citation	carbon type	soil carbon unit	landform	depth (cm)	vegetation	disturbance level/treatment	soil type/texture	age (year)	mean	n	SE	SD	CV (%)	bulk density	pH	water content	Site location/latitude, longitude	average annual temperature (° C)	average annual rainfall (mm)
504				riparian		forest	trees species dominated	idem		8.84	3	4.92	8.521689973	96.399207 84	1.457					
505				riparian		upland	upland cropland	idem		5.81	3	3.02	5.230793439	90.030868 14	1.659					
506	Waters, Emily R., et al. "Differential Carbon and Nitrogen Controls of Denitrification in Riparian Zones and Streams along an Urban to Exurban Gradient." Journal of Environmental Quality 43.3 (2014): 955-963.	organic matter	%	riparian		Forested riparian	exurban; forested 14%, residential 23%, agricultural 57%	cobble, gravel, clay, sand		8	6	0.37	0.906311205	11.328890 06			0.29%	39° 35'36" N, 76° 58'03"W		
507				riparian		Forested riparian	suburban: forested 10%, residential 37%, agricultural 0%	fine silt, cobble, gravel, sand		6.7	6	0.17	0.416413256	6.215123228			0.26%	39° 28'18" N, 76° 49'02"W		
508				riparian	0-10	Forested riparian	urban: forested 9%, residential 42%, agricultural 3%	bedrock, pebble, cobble		7.5	6	0.82	2.008581589	26.781087 85			0.25%	39° 17'45" N, 76° 44'38"W		
509				riparian		Forested riparian	forested: 100%	fine silt, cobble, gravel, sand		14	6	2.3	5.633826408	40.241617 2			0.50%	39° 28'49" N, 76° 41'16"W		
510				riparian		Herbaceous riparian	exurban; forested 14%, residential 23%, agricultural 57%; restored, exposed matting	cobble, gravel, pebble, bouder		8.3	6	0.58	1.420704051	17.116916 27			0.29%	Cranberry Branch; drains into Patapsco River; 39° 35'36" N, 76° 58'03"W		
511				riparian		Herbaceous riparian	suburban: forested 10%, residential 37%, agricultural 0%; trash and bricks in stream	pebble, cobble, gravel, sand		7.4	6	0.38	0.930806102	12.578460 84			0.30%	39° 28'18" N, 76° 49'02"W		
512				riparian		Herbaceous riparian	urban: forested 9%, residential 42%, agricultural 3%; concrete and trash in stream	fine silt, gravel		8.6	6	0.59	1.445198948	16.804638 93			0.28%	39° 17'45" N, 76° 44'38"W		
513				riparian		Herbaceous riparian	forested: 100%			11	6	0.13	0.318433667	2.8948515 14			0.59%	39° 28'49" N, 76° 41'16"W		
514	Groffman, Peter M., and Marshall Kamau Crawford. "Denitrification potential in urban riparian zones." Journal of Environmental Quality 32.3 (2003): 1144-1149.	soil organic matter	g/kg	riparian	0-10	reed	Urban riparian	disturbed and variable		90	11	10	33.166624 79	36.851386 56			270 g/kg	76° 30' W, 39° 15' N		1090

No	Citation	carbon type	soil carbon unit	landform	depth (cm)	vegetation	disturbance level/treatment	soil type/texture	age (year)	mean	n	SE	SD	CV (%)	bulk density	pH	water content	Site location/latitude, longitude	average annual temperature (° C)	average annual rainfall (mm)
515				riparian		Festuca, Poa, Lolium	Rural riparian	disturbed and variable		110	11	10	33.16624 79	30.15113446			450 g/kg			
516				riparian		dominated: Acer rubrum	Forested riparian	fine-loamy, Fragiudults		100	12	10	34.64101 615	34.64101615			340 g/kg			
517				riparian		mixture of sedges	Herbaceous riparian	disturbed and variable		100	10	10	31.62277 66	31.6227766			390 g/kg			
518	Hill, Alan R., and Mia Cardaci. "Denitrification and organic carbon availability in riparian wetland soils and subsurface sediments." Soil Science Society of America Journal 68.1 (2004): 320-325.	organic carbon	%	riparian	0-10	dominant: northern white cedar	peat deposit, fine gravel layers			18.6	10	0.95	3.004163777	16.15141816				floodplain on north side of Boyne River, 70 km north of Toronto, ON.		
519				riparian		patches of cedar interspersed with deciduous trees	mixed forest			10.9	10	0.66	2.087103256	19.14773629						
520				riparian		green bulrush, cattails, grasses.	marsh			4.8	10	0.66	2.087103256	43.48131783						
521				riparian		dominant: cedar, tamarack	peat deposit, fine gravel layers			38.9	10	1.04	3.288768767	8.454418423						
522				riparian			layers of sand and muds; interbedded sediment			2.19	10	0.73	2.308462692	105.4092553						
523		organic matter	%	riparian	0-10	dominant: northern white cedar	peat deposit, fine gravel layers			36.6	10	1.77	5.597231458	15.292928213						
524				riparian		patches of cedar interspersed with deciduous trees	mixed forest			19.6	10	1.04	3.288768767	16.77943248						
525				riparian		green bulrush, cattails, grasses.	marsh			9.4	10	0.95	3.004163777	31.95918912						
526				riparian		dominant: cedar, tamarack	peat deposit, fine gravel layers			58.9	10	1.93	6.103195884	10.36196245						
527				riparian			layers of sand and muds; interbedded sediment			3.57	10	0.88	2.782804341	77.949700143						
528	Orr, Cailin H., et al. "Effects of restoration and reflooding on soil denitrification in a leveed Midwestern floodplain." Ecological Applications 17.8 (2007): 2365-2376.	Organic matter	%	riparian			Forest; undisturbed reference zone	silt loam over sand subsurface		11.138	10	0.771	2.438116076	21.890007071			~50 %	Baraboo River floodplain, Waterfowl Production Area, Wisconsin, USA.		

No	Citation	carbon type	soil carbon unit	landform	depth (cm)	vegetation	disturbance level/treatment	soil type/texture	age (year)	mean	n	SE	SD	CV (%)	bulk density	pH	water content	Site location/latitude, longitude	average annual temperature (° C)	average annual rainfall (mm)
529				riparian			Dry field; crop agriculture	silt loam over sand subsurface		6.447	10	0.428	1.353454839	20.99356039			~30 %			
530				riparian			Wet field; row crop agriculture	silt loam over sand subsurface		9.546	10	0.429	1.356617116	14.21136723			~60 %			
531				riparian			Marsh; row crop agriculture	silt loam over sand subsurface		10.591	10	0.599	1.894204318	17.88503747			~60 %			
532				riparian			Open water; row crop agriculture	silt loam over sand subsurface		19.94	10	2.398	7.583141829	38.02979854			~65 %			
533	Cabezas, A., Francisco A. Com!n, and D. E. Walling. "Changing patterns of organic carbon and nitrogen accretion on the middle Ebro floodplain (NE Spain)." Ecological Engineering 35.10 (2009): 1547-1558.	total organic carbon	%	riparian	0-91	oxbow lake	permanently flooded condition, riparian succession	Calcareous fluvisol		2.41	46	0.1680838 3	1.14	47.30290456				Middle Ebro River, NE Spain.		
534				riparian	0-69	oxbow lake	permanently flooded condition, riparian succession	Calcareous fluvisol		1.91	35	0.1436762 23	0.85	44.5026178						
535				riparian	1-25	mature forest	mature forest; used to be agricultural fields	Calcareous fluvisol		2.42	13	0.1830510 65	0.66	27.272727 27						
536				riparian	1-80	young forest	young forest; used to be agricultural fields	Calcareous fluvisol		1.05	40	0.0569209 98	0.36	34.285714 29						
537			g/m2	riparian	0-91	oxbow lake	permanently flooded condition, riparian succession	Calcareous fluvisol		128.36	46	6.6452089 64	45.07	35.11218448						
538				riparian	0-69	oxbow lake	permanently flooded condition, riparian succession	Calcareous fluvisol		100.06	35	4.9171074 54	29.09	29.07255647						
539				riparian	1-25	mature forest	mature forest; used to be agricultural fields	Calcareous fluvisol		243.69	13	12.727596	45.89	18.831302 06						
540				riparian	1-80	young forest	young forest; used to be agricultural fields	Calcareous fluvisol		95.38	40	2.4808068 24	15.69	16.44998952						
541			%	riparian	91-241	oxbow lake	permanently flooded condition; used to be agricultural fields	Calcareous fluvisol		0.83	74	0.0197620 99	0.17	20.48192771						
542				riparian	69-241	oxbow lake	permanently flooded condition; used to be agricultural fields	Calcareous fluvisol		0.92	85	0.0303702 64	0.28	30.43478261						
543				riparian	25-280	mature forest	mature forest; used to be agricultural fields	Calcareous fluvisol		0.53	127	0.0301701 21	0.34	64.15094 34						

No	Citation	carbon type	soil carbon unit	landform	depth (cm)	vegetation	disturbance level/treatment	soil type/texture	age (year)	mean	n	SE	SD	CV (%)	bulk density	pH	water content	Site location/latitude, longitude	average annual temperature (° C)	average annual rainfall (mm)
544			g/m2	riparian	91-241	oxbow lake	permanently flooded condition; used to be agricultural fields	Calcareous fluvisol		72.18	74	1.399621557	12.04	16.68052092						
545				riparian	69-241	oxbow lake	permanently flooded condition; used to be agricultural fields	Calcareous fluvisol		80.29	85	2.9806244 9	27.48	34.225931						
546				riparian	25-280	mature forest	mature forest; used to be agricultural fields	Calcareous fluvisol		65.12	127	3.577821446	40.32	61.916461 92						
547	Wang, L. L., C. C. Song, and G. S. Yang. "Dissolved organic carbon characteristics in surface ponds from contrasting wetland ecosystems: a case study in the Sanjiang Plain, Northeast China." Hydrology and Earth System Sciences 17.1 (2013): 371-378.	soil organic matter	%	riparian	0-20	Perennial grass	Wetland; seasonally inundated			9.47	3	0.43	0.744781847	7.864644638			12.49 cm	Sanjiang plain, Heilong river, Wusuli river, and Songhua river.		
548				riparian		Sedges	Permanently inundated			20.77	3	0.71	1.229756073	5.920828471			23.79 cm		19	414
549				riparian			Riparian wetland; highly fluctuative flooding			7.3	3	0.23	0.398371686	5.457146 38			23.99 cm			
550				riparian			Riparian wetland; highly fluctuative flooding			7.43	3	0.44	0.762102355	10.25709765			24.61 cm			
551				riparian			Riparian wetland; highly fluctuative flooding			7.73	3	0.22	0.381051178	4.929510707			25.52 cm			
552				riparian		rice paddy land	artificial wetland			5.57	3	0.38	0.658179307	11.81650461			8.83 cm			
553				riparian			degraded wetland			4.07	3	0.23	0.398371686	9.788002107			8.75 cm			
554	McIntyre, Rebecca ES, Mark A. Adams, and Pauline F. Grierson. "Nitrogen mineralization potential in rewetted soils from a semi-arid stream landscape, north-west Australia." Journal of arid environments 73.1 (2009): 48-54.	soil organic carbon	%	riparian	0-5	mid dense low woodland		loam		1.1	8	0.13	0.367695526	33.426866602	1.33	7.66		Barnett Creek, Pilbara region, north-west Australia.	winter: 11-24; hot: 26-40.	350
555				riparian		n/a		sand		0.73	8	0.15	0.424264069	58.11836558	1.7	7.88				

No	Citation	carbon type	soil carbon unit	landform	depth (cm)	vegetation	disturbance level/treatment	soil type/texture	age (year)	mean	n	SE	SD	CV (%)	bulk density	pH	water content	Site location/latitude, longitude	average annual temperature (° C)	average annual rainfall (mm)
556				riparian		sparse low scrub		loamy-sand		0.4	8	0.08	0.226274 17	56.56854249	1.83	7.76				
557				riparian		sparse open Eucalyptus woodland		loam		0.98	8	0.09	0.254558 441	25.97535115	0.67	8				
558				riparian		mid-dense Eucalyptus closed woodland		loam		0.83	8	0.09	0.254558 441	30.66969171	1.04	7.97				
559				riparian		Mid-dense thicket forest		loam		0.93	8	0.11	0.311126984	33.45451438	0.8	7.48				
560	Ma, W. K., R. E. Farrell, and S. D. Siciliano. "Soil formate regulates the fungal nitrous oxide emission pathway." Applied and environmental microbiology 74.21 (2008): 6690-6696.	soil organic carbon	%	riparian	0-15	convex, topographically high positions with a positive profile curvature that sheds water.	cultivated; CX; land use: agricultured; cultivated	Calciborolls, Haploborolls, Argiborolls, Cryaquolls.		2.3	3	0.1	0.173205081	7.530655685				St. Denis National Wildlife Area, central Saskatchewan, Canada; 52° 12' N, 106° 5' W		
561				riparian		cultivated depression centre, temporarily collect water	cultivated; agricultured	Calciborolls, Haploborolls, Argiborolls, Cryaquolls.		3.2	3	0.2	0.346410162	10.82531755						
562				riparian		riparian grass; non level fringe, driest areas	non cultivated; non-agricultured	Calciborolls, Haploborolls, Argiborolls, Cryaquolls.		2.4	3	0.1	0.173205081	7.216878365						
563				riparian		basin center, covered by nongrass plant species	non cultivated; non-agricultured	Calciborolls, Haploborolls, Argiborolls, Cryaquolls.		3.5	3	0.1	0.173205081	4.948716593						
564	Meier, Claudio I., Brian L. Reid, and Orlyn Sandoval. "Effects of the invasive plant< i> Lupinus polyphyllus</i> on vertical accretion of fine sediment and nutrient availability in bars of the gravel-bed Paloma river." Limnologica-Ecology and Management of Inland Waters 43.5 (2013): 381-387.	soil organic carbon	g/kg	riparian	7-72	woody riparian vegetation				9.7	30	1.314534138	7.2	74.226800412				Paloma River, wandering gravel-bed stream in Chilean Patagonia, 60 km south Coyhaigue		
565				riparian	0-33	woody riparian vegetation				2.5	18	0.542115199	2.3	92						

No	Citation	carbon type	soil carbon unit	landform	depth (cm)	vegetation	disturbance level/treatment	soil type/texture	age (year)	mean	n	SE	SD	CV (%)	bulk density	pH	water content	Site location/latitude, longitude	average annual temperature (° C)	average annual rainfall (mm)
566	Pinay, G., et al. "Control of C, N, P distribution in soils of riparian forests."Landscape Ecology 6.3 (1992): 121-132.	total organic carbon	mg/g	riparian	0-10	willow stand	erosional riparian site	loam		22.3	30	0.960340217	5.26	1.96		7.7	17.20%	Garonne River, downstream from city of Toulouse, southwest France.		
567				riparian		willow stand	depositional riparian site	silt loam		33.4	60	0.411827229	3.19	0.82		8	25.10%			
568	Cierjacks, Arne, et al. "Carbon stocks of soil and vegetation on Danubian floodplains." Journal of Plant Nutrition and Soil Science 173.5 (2010): 644-653.	carbon stocks of Ah horizon	t/ha	riparian	0-17	softwood riparian forest; canopy 39%	national park, in the past: straightened in the 19th century	Haplic Fluvisols, Gleysols/sand/loam		41	14	10	37.41657387	91.25993626				Donau-Auen National Park, Austria, part of national park; 48° 8' N, 16° 48' W - 48° 7' N, 16° 48' W	9.8	533
569				riparian	0-17	cottonwood forest; canopy 41%		Haplic Fluvisols, Gleysols/sand/loam		46	26	7	35.693136	77.59377521						
570				riparian	0-15	hardwood riparian forest; canopy 68%		Haplic Fluvisols, Gleysols/sand/loam		48	21	7	32.07802986	66.82922888						
571				riparian	0-20	reforestations; canopy 58%		Haplic Fluvisols, Gleysols/sand/loam		48	6	8	19.59591794	40.82482905						
572				riparian	0-16	meadows and reeds 0% (95% herb)		Haplic Fluvisols, Gleysols/sand/loam		58	9	13	39	67.24137931						
573		carbon stocks of OM horizons	t/ha	riparian	0-55	softwood riparian forest; canopy 39%		Haplic Fluvisols, Gleysols/sand/loam		113	14	14	52.38320341	46.35681718						
574				riparian	0-68	cottonwood forest; canopy 41%		Haplic Fluvisols, Gleysols/sand/loam		136	26	11	56.089214 65	41.2420696						
575				riparian	0-67	hardwood riparian forest; canopy 68%		Haplic Fluvisols, Gleysols/sand/loam		138	21	10	45.825756 95	33.20707025						
576				riparian	0-57	reforestations; canopy 58%		Haplic Fluvisols, Gleysols/sand/loam		128	6	24	58.787753 83	45.92793268						
577				riparian	0-70	meadows and reeds 0% (95% herb)		Haplic Fluvisols, Gleysols/sand/loam		154	9	15	45	29.22077922						
578	Norton, Jay B., et al. "Soil carbon and nitrogen storage in upper montane riparian meadows." Ecosystems 14.8 (2011): 1217-1231.	soil organic carbon	g/kg	riparian	0-10	properly functioning riparian; sedges & rushes	surface	sandy loam		113	5	19.7	44.05053916	38.98277801				upper montane riparian meadows in the Stanislaus National Forest, Sierra Nevada	2.7	1524
579				riparian	0-36.6		subsurface 1	sandy loam		39.2	5	12.5	27.95084972	71.30318806						
580				riparian	0-49.8		subsurface 2	sandy loam		29.4	5	8.14	18.20159334	61.91018142						

No	Citation	carbon type	soil carbon unit	landform	depth (cm)	vegetation	disturbance level/treatment	soil type/texture	age (year)	mean	n	SE	SD	CV (%)	bulk density	pH	water content	Site location/latitude, longitude	average annual temperature (° C)	average annual rainfall (mm)
581				riparian	0-11	functioning at risk riparian; sedges & rushes	surface	sandy loam		97.8	6	50.8	124.4340789	127.2332095						
582				riparian	0-58.7		subsurface 1	sandy loam		31.9	6	6.57	16.09314761	50.44873859						
583				riparian	0-49.8		subsurface 2	loam		13.8	6	8.01	19.62041284	142.1769046						
584				riparian	0-13.5	non functioning riparian; sedges & rushes	surface	sandy loam		41.3	6	10.7	26.20954025	63.461365653						
585				riparian	0-24.4		subsurface 1	sandy loam		48.5	6	17.4	42.62112152	87.878600108						
586				riparian	0-48.8		subsurface 2	sandy loam		20.1	6	5.93	14.52547417	72.266004067						
587	Bettez, Neil D., and Peter M. Groffman. "Denitrification potential in stormwater control structures and natural riparian zones in an urban landscape." Environmental science & technology 46.20 (2012): 10909-10917.	soil organic matter	g/kg	riparian	0-5	wet ponds, shallow marsh, permanent pool of water.	engineering structure to replace riparian zone function; decrease peak discharge			72	12	6	20.78460969	28.867513346			318 g/kg	Gwynns Falls Watershed		
588				riparian		dry detention pool, dry out between storms.	engineering structure			86	8	14	39.59797975	46.0441625			352 g/kg			
589				riparian		store runoff, drain over extended period	engineering structure			81	20	12	53.66563146	66.253866			302 g/kg			
590				riparian		infiltration basins and trenches	engineering structure			48	4	4	8	16.666666667			240 g/kg			
591				riparian		filtering practices, bioretention areas	engineering structure			74	6	19	46.54030511	62.892304021			325 g/kg			
592				riparian		Herbaceous 0%	natural			125	4	21	42	33.6			520 g/kg			
593				riparian		Herbaceous 32%	natural			40	4	13	26	65			271 g/kg			
594				riparian		Herbaceous 42%	natural			44	4	23	46	104.5454545			280 g/kg			
595				riparian		Forested 0%	natural			206	4	16	32	15.538058			552 g/kg			
596				riparian		Forested 32%	natural			98	4	35	70	71.427857143			334 g/kg			
597				riparian		Forested 42%	natural			76	4	30	60	78.946836842			315 g/kg			

No	Citation	carbon type	soil carbon unit	landform	depth (cm)	vegetation	disturbance level/treatment	soil type/texture	age (year)	mean	n	SE	SD	CV (%)	bulk density	pH	water content	Site location/latitude, longitude	average annual temperature (° C)	average annual rainfall (mm)
598	Cabezas, A., and Francisco A. Comín. "Carbon and nitrogen accretion in the topsoil of the Middle Ebro River Floodplains (NE Spain): Implications for their ecological restoration." Ecological Engineering 36.5 (2010): 640-652.	total organic carbon	g/m3	riparian	0-10	Highly flooded riparian	natural	silt loam	17.5	1573.3	15	243.66	943.6911221	59.98163873	1.2			Ebro River, discharging into Meditteranean Sea, NE Spain.		
599				riparian		Intermediate flooded riparian	natural	idem	38.5	2141.4	15	73.22	283.5798406	13.24273095	1.17					
600				riparian		Connected forest riparian	natural	idem	38.5	1903.3	12	187.23	648.5837454	34.07680058	1.03					
601				riparian		Mature forest riparian	natural	idem	68.5	3831.8	15	101.61	393.5338378	10.2702082	0.99					
602				riparian		Agriculture	agricultural site.	idem	68.5	1933.3	8	114.56	324.0246114	16.76018266	1.41					
603				riparian		Poplar grove	poplar grove	idem	68.5	2010.2	8	188.96	534.4595895	26.58738382	1.17					
604				riparian		Highly flooded riparian	natural	idem	17.5	1547.3	7	232.01	613.8407617	39.67173539	1.27					
605				riparian		Intermediate flooded riparian	natural	idem	38.5	2123.6	14	124.51	465.8737612	21.93792434	1.19					
606				riparian		Connected forest riparian	natural	idem	38.5	2022.4	15	131.07	507.6319272	25.10047108	1.13					
607				riparian		Mature forest riparian	natural	idem	>68.5	3015.4	13	104.8	377.8617737	12.53106632	1.05					
608				riparian		Agriculture	agricultural site.	idem	68.5	1715.9	8	181.45	513.2181018	29.90955777	1.3					
609				riparian		Poplar grove	poplar grove	idem	38.5	1632.3	9	82.65	247.95	15.19022239	1.27					
610				riparian		Highly flooded riparian	natural	idem	17.5	1882.1	8	277.78	785.6804867	41.74488533	1.17					
611				riparian		Intermediate flooded riparian	natural	idem	38.5	2771.7	15	106.43	412.2016175	14.87179772	1.17					
612				riparian		Connected forest riparian	natural	idem	38.5	1779.1	14	206.51	772.6896669	43.43149159	1.18					
613				riparian		Mature forest riparian	natural	idem	68.5	3131.1	15	161.2	624.3249154	19.93947544	1.07					

No	Citation	carbon type	soil carbon unit	landform	depth (cm)	vegetation	disturbance level/treatment	soil type/texture	age (year)	mean	n	SE	SD	CV (%)	bulk density	pH	water content	Site location/latitude, longitude	average annual temperature (° C)	average annual rainfall (mm)
614				riparian		Agriculture	agricultural site.	idem	68.5	996.1	7	107.72	285.0003312	28.61161843	1.35					
615				riparian		Poplar grove	poplar grove	idem	68.5	1943.8	8	98.99	279.9860011	14.40405397	1.28					
616	Huang, Wei, et al. "Dissolved Organic Carbon in Headwater Streams and Riparian Soil Organic Carbon along an Altitudinal Gradient in the Wuyi Mountains, China." PloS one 8.11 (2013): e78973.	soil organic carbon	g/kg	riparian	0-10	subtropical evergreen broadleaf forest	pristine	humic acrisols; sandy loam		0.47	3	0.0635085 3	0.11	23.40425532	0.87	4.54		27° 33'-27° 54' N, 117° 27'-117° 51' Wuyi Mountain National Nature Reserve;	15	2000
617				riparian		coniferous forest	pristine	humic alisols; sandy loam		0.47	3	0.01732050 8	0.03	6.382978723	0.64	4.64				
618				riparian		subalpine dwarf forest	pristine	dystric cambisols; sandy loam		0.68	3	0.0635085 3	0.11	16.17647059	0.61	4.59				
619				riparian		alpine meadow	pristine	cambric umbrisols; sandy loam		1.43	3	0.1096965 51	0.19	13.28671329	0.54	4.86				
620				riparian	10-25	subtropical evergreen broadleaf forest	pristine	humic acrisols; sandy loam		0.38	3	0.0346410 16	0.06	15.78947368	0.89	4.82				
621				riparian		coniferous forest	pristine	humic alisols; sandy loam		0.38	3	0.0230940 11	0.04	10.52631579	0.77	4.79				
622				riparian		subalpine dwarf forest	pristine	dystric cambisols; sandy loam		0.56	3	0.0461880 22	0.08	14.28571429	0.79	4.84				
623				riparian		alpine meadow	pristine	cambric umbrisols; silt loam		1.2	3	0.1443375 67	0.25	20.83333333	0.65	5.13				
624				riparian	25-40	subtropical evergreen broadleaf forest	pristine	humic acrisols; sandy loam		0.33	3	0.0346410 16	0.06	18.18181818	0.96	4.94				
625				riparian		coniferous forest	pristine	humic alisols; sandy loam		0.35	3	0.0346410 16	0.06	17.14285714	0.87	4.88				
626				riparian		subalpine dwarf forest	pristine	dystric cambisols; sandy loam		0.48	3	0.0230940 11	0.04	8.333333333	0.82	4.91				
627				riparian		alpine meadow	pristine	cambric umbrisols; silt loam		0.93	3	0.0750555 35	0.13	13.97849462	0.8	5.22				
628	Cardinali, Alessandra, et al. "Design of riparian buffer strips affects soil quality parameters." Applied Soil Ecology 80 (2014): 67-76.	dry soil organic carbon	%	riparian	0-15	maize cover: 0%	agricultural; maize crop as control	Combisols; silty loam	planted 1997, harvested April 2010	0.74	6	0.03	0.073484692	9.930363822		8.11	16.40%	Padua university experimental farm, Po Valley, NE Italy		

No	Citation	carbon type	soil carbon unit	landform	depth (cm)	vegetation	disturbance level/treatment	soil type/texture	age (year)	mean	n	SE	SD	CV (%)	bulk density	pH	water content	Site location/latitude, longitude	average annual temperature (° C)	average annual rainfall (mm)
629				riparian		without buffer: 0%	next to agricultural site; without buffer as control	Combisols; silty loam		0.74	6	0.03	0.073484692	9.930363822		8.11	18.80%			
630				riparian		grass cover 100%	next to agricultural site	Combisols; silty loam		1.13	6	0.02	0.048989795	4.335380076		8.11	18.50%			
631				riparian		grass cover and a shrub and tree row 86%	next to agricultural site	Combisols; silty loam		1.01	6	0.03	0.073484692	7.275712107		8.11	19.60%			
632				riparian		shrub and tree row 75%	next to agricultural site	Combisols; silty loam		0.94	6	0.01	0.024494897	2.605840152		8.11	18%			
633				riparian		two rows of trees and shrubs 63%	next to agricultural site	Combisols; silty loam		1.05	6	0.05	0.122474487	11.66423687		8.11	18.80%			
634				riparian		two rows of trees and shrubs 53%	next to agricultural site	Combisols; silty loam		1	6	0.01	0.024494897	2.449489743		8.11	20.40%			
635				riparian		two rows of trees and shrubs 48%	next to agricultural site	Combisols; silty loam		0.95	6	0.04	0.097979589	10.31364102		8.11	20.20%			
636				riparian		maize cover: 0%	agricultural; maize crop as control	Combisols; silty loam		0.77	6	0.01	0.024494897	3.181155551		8.11	17.90%			
637				riparian		without buffer: 0%	next to agricultural site; without buffer as control	Combisols; silty loam		0.74	6	0.01	0.024494897	3.310121274		8.11	18.80%			
638				riparian		grass cover only 88%	next to agricultural site	Combisols; silty loam		0.92	6	0.03	0.073484692	7.987466553		8.11	19.70%			
639				riparian		grass cover and a shrub and tree row 70%	next to agricultural site	Combisols; silty loam		0.99	6	0.03	0.073484692	7.422696619		8.11	19.20%			
640				riparian		shrub and tree row 71%	next to agricultural site	Combisols; silty loam		0.97	6	0.03	0.073484692	7.575741473		8.11	18.40%			
641				riparian		two rows of trees and shrubs 57%	next to agricultural site	Combisols; silty loam		0.88	6	0.03	0.073484692	8.350533214		8.11	19.90%			
642				riparian		two rows of trees and shrubs 51%	next to agricultural site	Combisols; silty loam		0.95	6	0.03	0.073484692	7.735230767		8.11	19.30%			
643				riparian		two rows of trees and shrubs 44%	next to agricultural site	Combisols; silty loam		0.93	6	0.04	0.097979589	10.53543975		8.11	19.90%			
	term: WETLAND																			

No	Citation	carbon type	soil carbon unit	landform	depth (cm)	vegetation	disturbance level/treatment	soil type/texture	age (year)	mean	n	SE	SD	CV (%)	bulk density	pH	water content	Site location/latitude, longitude	average annual temperature (° C)	average annual rainfall (mm)
644	Reisinger, Alexander J., et al. "Woody Vegetation Removal Stimulates Riparian and Benthic Denitrification in Tallgrass Prairie." Ecosystems 16.4 (2013): 547-560.	total soil carbon	mg/g	riparian	0-15	naturally grass dominated riparian, open canopy	ungrazed grass watershed, burned every 2 years.	Ivan Silt Loam	3	35.51	10	0.65	2.055480479	5.788455306				two separate branches of King's Creek, Konza Prairie Biological Station, Nature Conservancy and Kansas State University.		
645				riparian		naturally woody vegetated riparian, closed canopy	ungrazed woody watershed, burned every 2 years.	idem		38.7	10	0.75	2.371708245	6.128445078						
646				riparian		woody vegetation removed prior to study, open canopy	ungrazed removal watershed, burned every 2 years.	idem		41.21	10	0.94	2.972541001	7.213154575						
647				riparian		naturally grass dominated riparian, open canopy	grazed grass watershed (bison) burned every 4 years	idem		34.76	10	0.68	2.150348809	6.186273904						
648				riparian		naturally woody vegetated riparian, closed canopy	grazed woody watershed (bison), burned every 4 years	idem		40.92	10	0.39	1.233288287	3.013900996						
649				riparian		woody vegetation removed prior to study, open canopy	grazed removal watershed (bison), burned every 4 years	idem		42.34	10	0.72	2.276839915	5.377515152						
650	Naiman, Robert J., et al. "Beaver influences on the long-term biogeochemical characteristics of boreal forest drainage networks." Ecology (1994): 905-921.	soil organic matter	% soil dry mass	riparian		Grass	Moist meadow	Ochraqualf; silt loam		35	19	2	8.717797887	24.907996396	0.39	5.13	temporarily flooded	Kabetogama Peninsula of Voyageurs National Park, Minnesota, USA; 48° 34' N, 93° 23' W	1.4	
651				riparian		tuft grass	Wet meadow	Argiaquoll; silt loam		38	28	2	10.583008524	27.85000138	0.32	5.78	seasonally flooded			
652				riparian		tuft grass	Beaver pond	Haploquept		26	17	1	4.123105626	15.858009856	0.47	6.06	permanently flooded			
653		soil carbon	g/m2	riparian		Grass	Moist meadow	Typic Ochraqualf; silt loam		9619	19	658	2868.155505	29.817600583	0.39	5.13	temporarily flooded			
654				riparian		Grass	Wet meadow	Typic Argiaquoll; silt loam		5285	28	405	2143.058562	40.549830088	0.32	5.78	seasonally flooded			
655				riparian		Grass	Beaver pond	Typic Haploquept		5920	17	809	3335.592451	56.344406708	0.47	6.06	permanently flooded			

No	Citation	carbon type	soil carbon unit	landform	depth (cm)	vegetation	disturbance level/treatment	soil type/texture	age (year)	mean	n	SE	SD	CV (%)	bulk density	pH	water content	Site location/latitude, longitude	average annual temperature (° C)	average annual rainfall (mm)
656	Bruland, Gregory L., Matthew F. Hanchey, and Curtis J. Richardson. "Effects of agriculture and wetland restoration on hydrology, soils, and water quality of a Carolina bay complex." Wetlands Ecology and Management 11.3 (2003): 141-156.	total soil carbon	mg/cm3	riparian	0-40		agricultural/disturbed	Haplosaprist; poorly drained, organic soil		173	6	58.5	143.29515	82.829566645	0-31-1.67		poorly drained	Carolina bay complex, Cumberland County, North Carolina		
657				riparian		cypress, cedar, poplar, oak	restored wetland (riparian)	idem	2	111	16	16.6	66.4	59.81981982	0.31-1.67		poorly drained			
658				riparian		open shrub layer, closed tree canopy	non-riverine swamp forest; reference area	idem		131	6	34.3	84.01749818	64.13549479	0.1-1.37		poorly drained			
659				riparian		thick understory of bush, tree (Pine)	pocosin; reference area	idem		91.6	6	2.86	7.005540664	7.647970158	0.11-0.23		poorly drained			
660				riparian	40-100		agricultural/disturbed	idem		105	9	48.8	146.4	139.4285714	0-31-1.67		poorly drained			
661				riparian			restored wetland (riparian)	idem	2	51.1	24	7.77	38.06507 06	74.4913319	0-31-1.67		poorly drained			
662				riparian			non-riverine swamp forest; reference area	idem		130	9	47.5	142.5	109.6153846	0.1-1.37		poorly drained			
663				riparian			pocosin; reference area	idem		78.4	9	0.65	1.95	2.487244898	0.11-0.23		poorly drained			
664	Peralta, Rita M., Changwoo Ahn, and Patrick M. Gillevet. "Characterization of soil bacterial community structure and physicochemical properties in created and natural wetlands." Science of the Total Environment 443 (2013): 725-732.	soil organic matter	%	riparian	5-10	herbaceous, interspersed with young tree saplings and shrubs.	surface runoff from upland housing development and forested buffer; artificially created mitigation wetland		3	5.2	12	0.14	0.484974226	9.326427425		5.5	30.50%	39° 1' N, 77° 36' W		1090
665				riparian					3	3.7	12	0.1	0.346410162	9.362436798		4.7	15.70%			
666				riparian					3	3.9	12	0.05	0.173205081	4.441155917		5.3	16.70%			
667				riparian					7	3.6	12	0.29	1.004589468	27.906526301		4.7	30.50%	38° 51 N, 77° 32' W		
668				riparian		herbaceous wetland, few mature trees	natural wetland		~70	5.6	12	0.54	1.870614872	33.403837		5.1	42.10%	38° 49' N, 77° 30' W		

No	Citation	carbon type	soil carbon unit	landform	depth (cm)	vegetation	disturbance level/treatment	soil type/texture	age (year)	mean	n	SE	SD	CV (%)	bulk density	pH	water content	Site location/latitude, longitude	average annual temperature (° C)	average annual rainfall (mm)
669		total organic carbon	%	riparian		riparian wetland, herbaceous plants, some mature bottomland forest.	natural wetland			3.2	8	0.32	0.905096 68	28.28427125		4.6	30.70%	39° 1' N, 77° 35' W		
670				riparian		herbaceous, young tree saplings and shrubs.			3	2.1	12	0.22	0.762102 355	36.29058835		5.5	30.50%	39° 1' N, 77° 36' W		
671				riparian					3	1.1	12	0	0	0		4.7	15.70%	39° 1' N, 77° 37' W		
672				riparian					3	1.3	12	0.02	0.069282 032	5.3293871		5.3	16.70%	39° 1' N, 77° 38' W		
673				riparian					7	1.2	12	0.16	0.554256 258	46.188021 54		4.7	30.50%	38° 51 N, 77° 32' W		
674				riparian					~70	2.2	12	0.22	0.762102 355	34.641016 15		5.1	42.10%	38° 49' N, 77° 30' W		
675		soil organic matter	%	riparian		riparian wetland, herbaceous plants, some mature bottomland forest.				1.2	8	0.19	0.537401 154	44.78342948		4.6	30.70%	39° 1' N, 77° 35' W		
676				riparian		herbaceous, young tree saplings and shrubs.				5.6	12	0.6	2.078460 969	37.11537445		5.3	47.60%	39° 1' N, 77° 36' W		
677				riparian						3.8	12	0.01	0.034641 016	0.911605688		5.2	38%	39° 1' N, 77° 37' W		
678				riparian						3.9	12	0.05	0.173205 081	4.441155917		5.3	37.70%	39° 1' N, 77° 38' W		
679				riparian						3.6	12	0.28	0.969948 452	26.94301256		5.3	35.10%	38° 51 N, 77° 32' W		
680		total organic carbon	%	riparian		herbaceous wetland, few mature trees				5.5	12	0.56	1.939896 904	35.27085281		5.2	49.70%	38° 49' N, 77° 30' W		
681				riparian		riparian wetland, herbaceous plants, some mature bottomland forest.				3.3	8	0.25	0.707106 781	21.42747822		4.2	38.70%	39° 1' N, 77° 35' W		
682				riparian		herbaceous, young tree saplings and shrubs.				2	12	0.26	0.900666 42	45.033321		5.3	47.60%	39° 1' N, 77° 36' W		
683				riparian						1.1	12	0.16	0.554256 258	50.38693258		5.2	38%	39° 1' N, 77° 37' W		
684				riparian						1.5	12	0.004	0.013856 406	0.923760431		5.3	37.70%	39° 1' N, 77° 38' W		

No	Citation	carbon type	soil carbon unit	landform	depth (cm)	vegetation	disturbance level/treatment	soil type/texture	age (year)	mean	n	SE	SD	CV (%)	bulk density	pH	water content	Site location/latitude, longitude	average annual temperature (° C)	average annual rainfall (mm)
685				riparian						1.2	12	0.18	0.623538291	51.96152423		5.3	35.10%	38° 51 N, 77° 32' W		
686				riparian		herbaceous wetland, few mature trees				2.5	12	0.41	1.420281662	56.81126649		5.2	49.70%	38° 49' N, 77° 30' W		
687				riparian		riparian wetland, herbaceous plants, some mature bottomland forest.				1.7	8	0.24	0.678822 51	39.93073588		4.2	38.70%	39° 1' N, 77° 35' W		
688	Gift, Danielle M., et al. "Denitrification potential, root biomass, and organic matter in degraded and restored urban riparian zones." Restoration Ecology18.1 (2010): 113-120.	soil organic matter	g/g dry soil	riparian	0-10	Mature trees	restored riparian: 10-17% forested, 81-90% residential, 33-50% impervious surface		10	0.094	6	0.045	0.110227038	117.2628068				Baltimore City, Baltimore County, MD, USA; 76° 30' W, 39° 15' N		
689				riparian			suburban degraded riparian: 4-11% forested, 47-68% residential, 17-22% impervious surface			0.079	6	0.006	0.014696938	18.60371957						
690				riparian			natural forest riparian: 65-100% forested, 0-34% residential, 0-1% impervious surface			0.094	6	0.021	0.051439285	54.72264319						
691				riparian	10-30		restored riparian: 10-17% forested, 81-90% residential, 33-50% impervious surface			0.031	6	0.003	0.007348469	23.70473945						
692				riparian			suburban degraded riparian: 4-11% forested, 47-68% residential, 17-22% impervious surface			0.055	6	0.005	0.012247449	22.26808857						
693				riparian			natural forest riparian: 65-100% forested, 0-34% residential, 0-1% impervious surface			0.047	6	0.009	0.022045408	46.90512273						
694				riparian	30-70		restored riparian: 10-17% forested, 81-90% residential, 33-50% impervious surface			0.026	6	0.004	0.009797959	37.68445758						
695				riparian			suburban degraded riparian: 4-11% forested, 47-68% residential, 17-22% impervious surface			0.048	6	0.009	0.022045408	45.92793268						

No	Citation	carbon type	soil carbon unit	landform	depth (cm)	vegetation	disturbance level/treatment	soil type/texture	age (year)	mean	n	SE	SD	CV (%)	bulk density	pH	water content	Site location/latitude, longitude	average annual temperature (° C)	average annual rainfall (mm)
696				riparian			natural forest riparian: 65-100% forested, 0-34% residential, 0-1% impervious surface			0.034	6	0.008	0.019595918	57.63505277						
697				riparian	70-100		restored riparian: 10-17% forested, 81-90% residential, 33-50% impervious surface			0.023	6	0.009	0.022045408	95.849559863						
698				riparian			suburban degraded riparian: 4-11% forested, 47-68% residential, 17-22% impervious surface			0.047	6	0.015	0.036742346	78.175204560						
699				riparian			natural forest riparian: 65-100% forested, 0-34% residential, 0-1% impervious surface			0.019	6	0.005	0.012247449	64.460256639						